DEVELOPMENT OF CONJUGATED MONO- AND POLYNUCLEAR TUNGSTEN ORGANOMETALLIC COMPLEXES FOR POTENTIAL APPLICATION IN MOLECULAR ELECTRONICS

DISSERTATION

zur

Erlangung der naturwissenschaftlichen Doktorwürde

(Dr. sc. nat.)

vorgelegt der

Mathematisch-naturwissenschaftlichen Fakultät

der

Universität Zürich

von

Sergey N. Semenov

aus

Russland

Promotionskomitee

Prof. Dr. Heinz Berke (Vorsitz und Leitung)

Prof. Dr. Roger Alberto

Zürich 2010

"Chemistry creates its object. This creative faculty, akin to that of art, forms an essential distinction between chemistry and the other natural or historical science."

Marcellin Berthelot, 1876

ACKNOWLEDGEMENTS

I am indebted to many people who contributed in several ways to this Ph.D. work. I would like to thank particularly,

To my supervisor Prof. Dr. Heinz Berke, for having introduced me into an interesting research field and for his guidance, encouragement, which he provided through this work. I also wish to thank you for giving me the opportunity to work in your group.

I want to specially thank Ivan Timokhin for his huge support during my work.

I would like to extend my special thanks and appreciation to Dr. Koushik Venkatesan, for his continuous support during my dissertation and especially for correction of a lot of English texts.

All the X-ray structures presented in this thesis have been performed by Dr. Olivier Blacque, thanks a lot for your tireless effort and great patience on time consuming crystal structures which paved way for interesting breakthroughs. Also thanks to Dr. Thomas Fox and Dr. Ferdinand Wild for his contribution to this work through NMR and Raman measurements, respectively. All the elemental analyses for the different complexes were performed by Heinz and Barbara Spring, thanks a lot for all the analysis! Thanks to Stephen Weyeneth and Ferenc Muranyi from the physical institute for their help with the EPR and magnetic measurements. Thanks to Beatrice Schpihtig for a lot of help with financial things. And also many thanks to Susanna Sprokkereef, Nathalie Fichter and Tanja Spörri for their help with the administration work and for their extremely kindness. Thanks a lot for Hanspeter Stalder for technique support.

I would like to thank specially Shiva Taghipourian for a lot of help and advices and for her friendship conversation.

Also many thanks to all these people who have been working during these years with me, for his always helpful and kind attitude. Especially I would like to thank to Alexander Dybov, Samir Barman, Jai Anand, Gabriel Lancenet, Marcello Bertolli, Carolina Egler, Michael Koch and Yan Li.

I would like to extend my thanks and appreciation to Prof. Dr. Sergey I. Troyanov and Assoc. Prof. Dr. Andrey A. Drozdov from the “Lomonosov Moscow State University” for their help during all these years.

I would also like to thank my friends for their support during these years, which helped me through the (many) difficult times, and generally for their unconditional friendship. Without you all, everything would have been more difficult.

I especially thank Svetlana Eliseeva for the support and the motivation during these years.

Thanks also especially to my good friends from Moscow State University. Denis Savchenko, Alexander Mityaev, Alexander Tsirlin, Oxana Kotova, Katy Kondakova and Anna Shishkina.

I would also like to express particular gratitude to my parents, Tatiana Semenova and Nikolay Semenov, and my brother, Aleksey, who have always supported me and who have endured my absence and have put up with the little time I have had for them during these past years. Thank you so much for all the opportunities you have given me in my life and for believing in me.

CONTENT

LIST OF ABBREVIATIONS 8
I. INTRODUCTION 10
II. LITERATURE OVERVIEW 12
II.1. Molecular conductance 12
II.1.1. Methods for the single molecule conductance measurements 12
II.1.2. Anchor groups 13
II.1.3. Charge transport in single molecules 15
II.1.4. Single molecular study of metal containing compounds 18
II.2. Mixed–Valence complexes 20
II.2.1. Electronic interaction 21
II.2.2. Examples and classification 26
II.2.3. Electron transfer in MV complexes 27
II.3. Homo–metallic dinuclear complexes with C_n bridges and reversible redox properties ... 29
II.4. Tungsten complexes 33
II.4.1. Tungsten dinuclear complexes bridged by conjugated carbon chain 33
II.4.2. Synthetic methods 34
III. FORMULATION OF GOALS AND STRUCTURE OF WORK 39
IV. PUBLICATIONS 40
IV.1. Publication 1 40
IV.2. Publication 2 69
IV.3. Publication 3 97
IV.4. Publication 4 116
V. UNPUBLISHED RESULTS 133
V.1. Experimental part 133
V.1.1. General Procedures 133
V.1.2. Synthesis 133
V.1.3. X-Ray Diffraction Studies on 4, 5, 7 and 8 138
V.2. Results and discussion 140
V.2.1. A cross–conjugated system formula possessing anchor groups 140
V.2.2. Substitution of Iodine in the $[I(dppe)_2WC_4W(dppe)_2I]$ 141
V.2.3. Linear system with anchor groups 146
VI. SUMMARY 148
VII. CONCLUSIONS 156

VIII. REFERENCES 158
APPENDIX 168
List of prepared metal complexes 168
Abstract 170
Zusammenfassung 171
CURRICULUM VITAE 173

LIST OF ABBREVIATIONS

π^*	antibonding molecular orbital
χ	molar magnetic susceptibility
bipy	2,2'-Bipyridine
Cp	cyclopentadienyl
Cp*	pentamethylcyclopentadienyl
CV	cyclic voltammetry
depe	1,2-Bis(diethylphosphinoethane)
DMF	dimethylformamide
dmpe	1,2-Bis(dimethylphosphinoethane)
dppe	1,2-Bis(diphenylphosphinoethane)
dppm	1,2-Bis(diphenylphosphinomethane)
$\bar{e}$	electron
EPR	electron paramagnetic resonance
g	g factor
h	Planck constant
$\hbar$	reduced Planck constant
HOMO	highest occupied molecular orbital
IVCT	intervalence charge transfer
IR	infrared
J	exchange integral
K_c	comproportionation constant
LUMO	lowest unoccupied molecular orbital
MCBJ	mechanically controllable break junction
MV	mixed valence
NDR	negative differential resistance
NIR	near infrared
NMR	nuclear magnetic resonance
pic	4-methylpyridine
PZT	piezoelectric transducer
STM	scanning tunneling microscopy
STMBJ	scanning tunneling microscopy break junction
SQUID	superconducting quantum interference device
tpy	2,2';6'2''-terpyridine

Tp	hydridotrispyrazolylborate
Tp´	hydridotris(3,5-dimethylpyrazolyl)borate
THF	tetrahydrofuran
OTf	triflate
XPS	X-ray photoelectron spectroscopy

I. INTRODUCTION

Molecular electronics is a relatively new branch of science with the ultimate goal to utilize molecules as electronic elements in circuitry. The research in this field mainly comprises two directions. One direction concerns the investigation of separate single molecules and the other involves the development of methods to assemble those molecules into a logic circuit. During the last decade significant efforts were made in the first direction due to the development of methods such as scanning tunneling microscopy break junction (STMBJ) and mechanically controllable break junction (MCBJ). They allow evaluation of properties of individual molecules in two contact connection layout. The assembly of circuit seems to be a more difficult problem which so far has been realized only for two contact elements by cross bar method. The two contact connection circuit is suitable for memory element, which is a main applied goal in current state of molecular electronics. Fundamental investigations on a molecular level may be the most important outcome from the ongoing studies in molecular electronics other than applied goals. They allow investigation of matter on the level where quantum effects play domination role some times. It is clearly evident from the fact that the most well proved mechanism of molecular conductance is tunneling, a pure quantum effect. Several important effects have been observed in the molecular conductance studies. Most interesting of them are nonlinear differential resistance (NDR), Kondo resonance, Coulomb blockade and memory effect. They are observed also in macro systems, but an order of magnitude less pronounced. All of them are dependent on the ability of system to function as an electron reservoir. It especially belongs to the memory effect where switch of oxidation state looks the most rational way to control the current.

An introduction of a metal center seems a logical way to make the system able to keep charge and spin. It was proven by a preliminary experiment that introduction of metal enhances affects mentioned above and increases the conductivity. Metal centers could be introduced in different ways such as: porphyrins with metal ions; insertion of metal ion between polydentate ligands as in ferrocene and $[Ru(tpy)_2]$ (tpy - 2,2';6'2''-terpyridine) fragments; and insertion of the metal directly into conjugated chain via metal carbon bond. The latter approach has the advantage of the presence of metal directly on electron path due to the more pronounced influence of the metal to electron transfer process. In this context it is not surprising that many organometallic molecules consisting of metal centers bridged by conjugated chain were synthesized. However, for the single molecular measurements a molecule should be attached to the micro electrodes via chemical bond. Since gold electrodes are most commonly used, the molecule should have terminal groups with strong affinity to gold, which are called "anchor

groups". An integral problem of this concept is that the anchor groups would be reactive towards most metal centers. This makes the synthesis of the molecules especially challenging and it has been so far realized only for the metals with most predictable reactivity such as platinum and ruthenium. Platinum has irreversible electrochemistry making it a poor candidate for molecular conductor. Ruthenium seems an optimum choice but fundamental studies require tuning of properties by variation of the metal fragment and also ruthenium has relatively high oxidation potential. This could lead to far from optimum position of highest occupied molecular orbital (HOMO) relative to the Fermi levels of gold electrodes. Tungsten in $[W(dppe)_2]$ (1,2-Bis(diphenylphosphinoethane)) fragment is well protected from attack by reactive species and has reversible electrochemistry. In this project we thought to develop organometallic tungsten chemistry towards the direction of design of conjugated molecules bearing anchor groups, as well as to do preliminary investigation of the electron transfer in obtained molecules by a variety of physical methods.

II. LITERATURE OVERVIEW

II.1. Molecular conductance

The molecular conductance G is given by G = I/V where I – current and V – applied bias. It is presented in literature in macro units siemens (S) and in quantum units $G_0 = 2e^2/h$ where e and h is electron charge and Planck constant, respectively. G_0 is equal to 77 μS and it represents maximum theoretical conductance of single metal atom. Consequently molecule conductance in G_0 units shows us how conductive the molecule is in comparison with a metal atom.[1,2]

II.1.1. Methods for the single molecule conductance measurements

The evaluation of single molecule properties is a difficult experimental challenge, but several approaches were developed in the last 20 years.[2-6] They can be divided into two main groups: real single molecular measurements and methods based on data obtained from layer of many molecules. Methods which allow to measure "true" single molecule conductance are scanning tunneling microscopy break junction (STMBJ)[7,8] and mechanically controllable break junction (MCBJ).[9,10] The latter method will be discussed in more detail because the design of the molecules in our work is based on their suitability for investigations by MCBJ.

The principle of the STMBJ method is that scanning tunneling microscopy (STM) tip is moved into and out of contact with the substrate electrode in the presence of sample molecules. Molecules have two anchor groups and can strongly bind to substrate and STM tip. In a first step, the STM tip is in contact with the substrate and many junctions are formed. In the next step, the tip is pulled away from the substrate, and then the molecules break contact with one of the two electrodes individually (Figure 1).

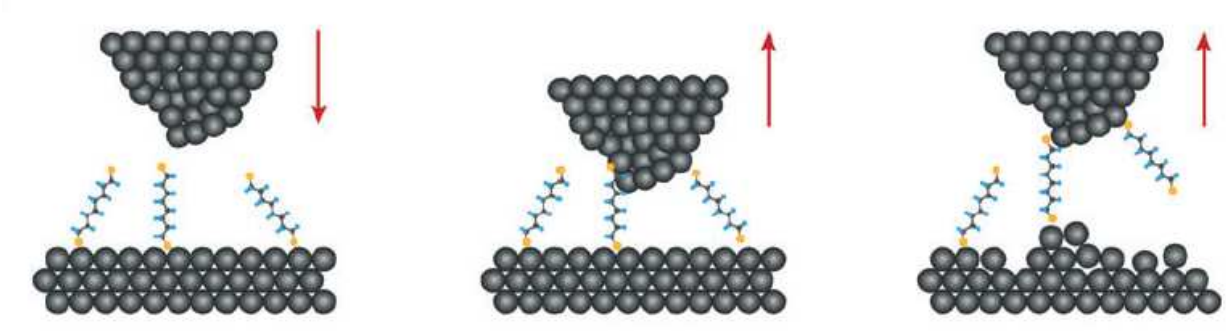

Figure 1. Principle of STM break junction method.[2]

This process generates current steps in the I/V curve. Repeating of procedure many times and subsequent statistical analysis allow evaluation of the single molecular conductance.

The basic principle of the MCBJ method is to break a thin metal wire supported on a solid substrate into a pair of facing electrodes.[11,12] Distance between the electrodes and the

breaking process are controlled by bending of the solid substrate. Bending is achieved by fixing two ends of the substrate while pushing the middle part of the substrate vertically (Figure 2).

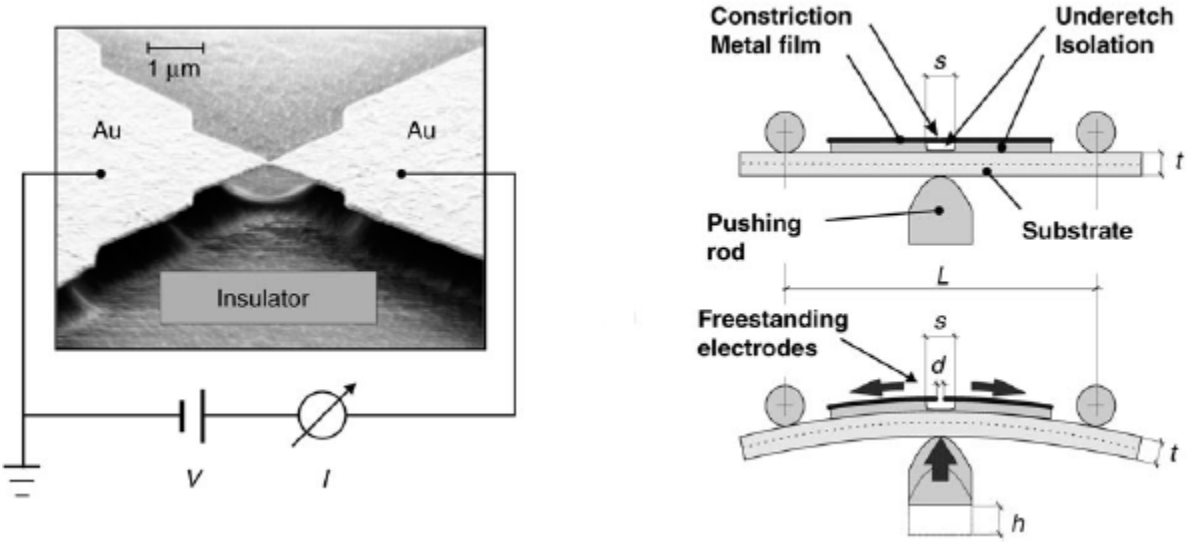

Figure 2. Principle of MCBJ method.[13]

A piezoelectric transducer (PZT) and a step motor are used for control of the bending. A simple calculation shows that vertical movement of the PZT is demagnified relative to the horizontal movement of electrodes in order of 1×10^5. It allows accurate control of the width of the gap. The device including metal wire with thick neck in the middle is built manually or using electron-beam lithography. During the experiment, the nanobridge breaks to form atomic size electrodes. A sample compound is immobilized on the electrodes using its diluted solution and solvent is removed under vacuum. Electrodes are slowly moved closer to each other and I/V curve is registered during this process. An additional advantage in this case is that electric field between two electrodes directs linear molecules along the line connecting two electrodes due to induced dipole moment. The movements of the electrodes are repeated many times which allows statistical analysis of the data.[14] The method was first applied to measure electron transport in molecules by Reed and coworkers.[10] Benzenedithiol molecules were investigated in this study. However, it was not clear how many molecules were involved in the conduction and whether the molecules were bound to both electrodes. Reichert *et al.* conducted an experiment where symmetrical and asymmetrical molecules were studied by the MCBJ setup.[15] The symmetrical molecules showed symmetrical I/V curve and unsymmetrical molecules had asymmetrical I/V dependence strongly confirming that only one molecule is involved in the measurements.

II.1.2. Anchor groups

As clearly evident from the previous part, methods for investigation of single molecule conductance strongly require a good contact with the electrodes. It could be achieved by chemical sorption. Since most common electrode material is gold, the end groups should have

strong affinity to it. Several anchor groups were tested. There are thiol,[16-19] thioacetyl,[8,20,21] isothiocyanate,[22-25] carbodithioate,[26] methyl sulfide,[27] fullerene,[28] isonitrile,[29-31] pyridyl,[7,32] dimethyl phosphine,[27] amine[19,27] and carboxylic acid groups[19] (Figure 3).

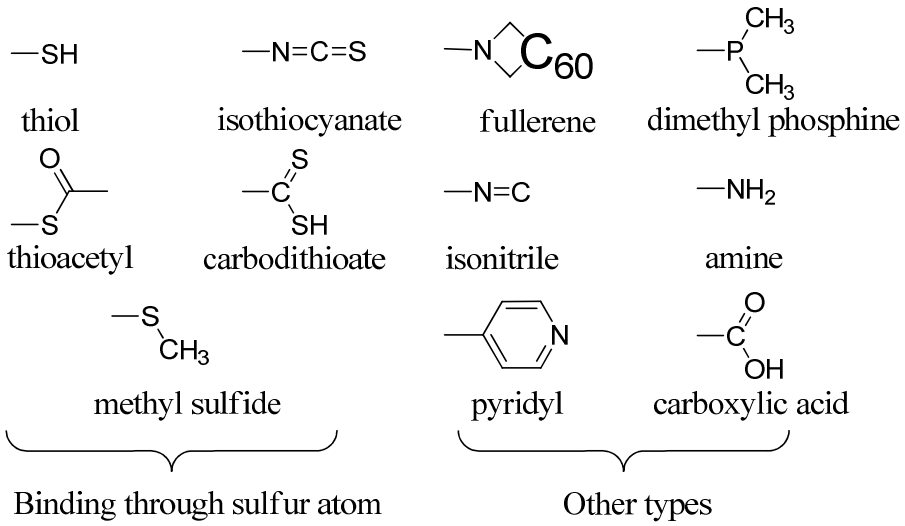

Figure 3. Examples of anchor groups.

Several factors reflect efficiency of anchor group for single molecular studies.[16,19,22,33] A strength of binding to electrode is probably the most important factor for experiment realization. It often correlates with contact conductivity, but there are some exceptions due to the different contribution of σ and π character to the bonding to the electrode.[22] Chemical compatibility with other functional groups in the molecule and synthetic accessibility are major factors during the preparation process. It is difficult to compare groups in long series since studies in identical conditions were done only for a short series. The results of some of these studies are summarized on figure 4.

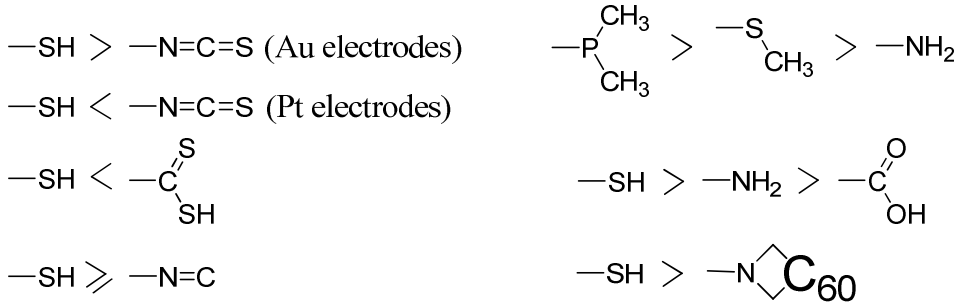

Figure 4. A comparison of contact conductance for different anchor groups *(The –SH group represents any groups forming –S– contact).*[19,22,23,26-28,30]

A sulfide contact is most experimentally proven and majority of data are available for this kind of anchor group. This contact is favorable as a first choice for the new molecules due to the possibility of comparison with the literature data. The sulfide bridge could be fabricated through the chemisorptions of –SH group or its protected form, the thioacetyl group. The former is especially important for the present work due to its relative low reactivity. It has been shown by

direct comparison that thioacetyl and thiol groups form contact with the same resistance and probably has the same nature.[34]

The isothiocyanate is also interesting for us because it is often connected to metal directly without -Ph-C≡C- fragment. It was successfully tested in SCN-(CH_2)n-NCS systems showing however higher resistance than analogous dithiols in the case of gold electrodes.[22,23] In the case of platinum electrodes –NCS group provided better contact than –SH group probably due to the stronger tendency to back donation.

II.1.3. Charge transport in single molecules

The design of organometallic molecular wires requires a deep understanding of basic mechanisms of charge transport in single molecules. A significant progress in the understanding of processes in single molecular conductors has been made in the last years.[35-38] Several good reviews were published[39-43] among which Ratner article in Materials Today is of special interest for synthetic chemists due to a clear qualitative explanation of main conductance mechanisms.[44]

In general, all mechanisms could be categorized into two groups: thermally activated processes and thermally independent processes.[45] The former group is presented by a tunneling mechanism. Its basis lies in the ability of an elementary particle to tunnel through energetic barrier with nonzero probability. In this case, the electron with energy not higher than Fermi level of the left electrode should transmit through the molecule to right electrode (Figure 5).

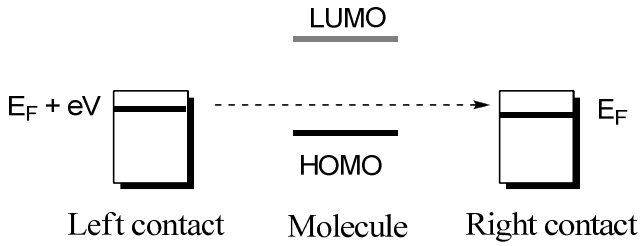

Figure 5. Schematic representation of tunneling process.

Because electrons in a molecule can occupy discrete energy levels, the height of the barrier would depend from the position of the highest occupied molecular orbital (HOMO) and the lowest unoccupied molecular orbital (LUMO) relative to the Fermi levels. The process could also be imagined in the way that if an electron was placed in one of the unoccupied orbitals, it would have a finite lifetime in it, before relocated on the metal. The lifetime associated with the molecular states is dependent from the mixing of the molecular states with the electrode. However, tunneling is a coherent process and it doesn't involve a real transition state.[46] Tunneling process can be coupled with molecular vibrations. An energy dissipation takes place in this case.[47] It is inelastic tunneling.[48,49] If the barrier is close to zero, electrons can move with maximum efficiency. Conductance should be then close to $G_0 = 2e^2/h$ and process is called

resonant tunneling. Direct non-resonant elastic tunneling is most well developed theoretical treatment of the molecular conductance, based on Landauer formula:[50]

$$G = \frac{2e^2}{h} T$$

Here T is a function that reflects the efficiency of electron transmission from one contact to the other. It can be divided into components:[40]

$$T = T_{lc} \cdot T_{rc} \cdot T_{mol}$$

where T_{lc} and T_{rc} gives the efficiency of change transport across the left and right contacts and T_{mol} reflects the charge transport through the molecule. In the approximation that molecule represents a barrier; transmission through the molecule will exponentially decay with the molecular length:

$$T_{mol} = e^{-\beta l}$$

where l is the length of molecule and β is the tunneling decay parameter. Former depends on molecular orbital energies by following equation:

$$\beta = 2 \frac{\sqrt{2m \cdot \alpha((E_{HOMO/LUMO} - E_F) - (eV/2))}}{\hbar^2}$$

Here $\hbar$ is the reduced Planck constant, $E_{HOMO/LUMO}$ is the position of HOMO or LUMO energy level dependent from the type (electron or hole) of conductance, E_F is the Fermi level of electrode, m is the effective electron mass, V is the applied bias and α is a parameter used to describe the asymmetry in the potential profile across the electrode-molecule-electrode junction. This relatively simple treatment brings a very important conclusion about the importance of the relative position of the electrode Fermi level and molecular levels. In general, smaller HOMO/LUMO gap will cause better alignment of levels and higher conductance.[45]

The tunneling mechanism is realized for molecules with enough higher barrier and relatively short length. It is the only confirmed conductance mechanism for alkane dithiol molecules and believed to be a dominant process also in short conjugated molecules.[19,45,51,52] Examples of molecules conducting by tunneling are presented on figure 6.[19,39,53-55] Tunneling conductance has strong length dependence. For the alkane dithiols the decay parameter β lies in the range 1 – 0.6 $Å^{-1}$.[19,39] The π – conjugated molecules show much less distance dependence of conductance with β in the range 0.6 – 0.1 $Å^{-1}$, as could be expected from their smaller HOMO/LUMO gap.[40,54,55] Experimental confirmation for tunneling mechanism is: temperature independence; exponential decay with length and linear I *vs* V dependence.[46]

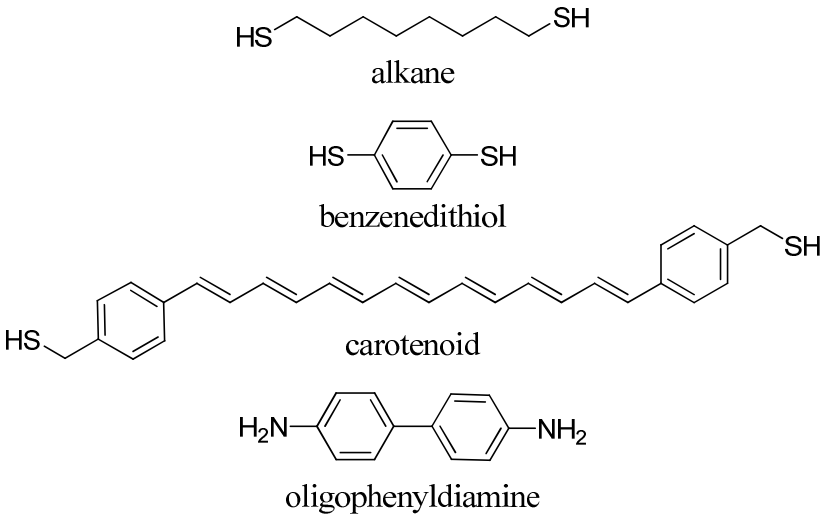

Figure 6. Examples of molecules where tunneling conductance dominates.

Hopping is the most important thermally activated conductance mechanism. Its principal difference from tunneling is that the system in this case has sufficient energy to cross the barrier because of thermal energy fluctuations. An electron path can include following steps (Figure 7).[39,42,44]

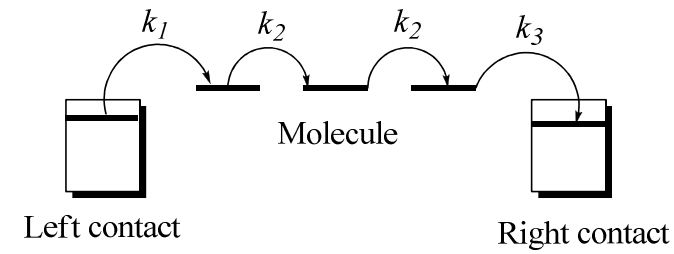

Figure 7. Schematic representation of the hopping process.

First step is a charge injection into the molecule. Second step is the hopping of the charge carrier along the molecule, which is essentially similar with an electron transfer in redox reactions. Finally, a charge carrier should be trapped on the opposite electrode. There are a few variations of this general mechanism such as direct thermionic emission (electron jumps directly from electrode to electrode by thermal activation), two step hopping (includes only steps 1 and 3) and processes with combination of tunneling with hopping steps. The hopping mechanism is characterized by low distance (inversely from the number of hopping steps) and strong thermal dependence of conductance.[46,56,57] It always dominates in conductive polymers; in molecular junctions it seems to plays an important role in long systems and high temperatures.[39,56,58] Two step thermally activated process was suggested for perylene tetracarboxylic diimides (Figure 8).[59]

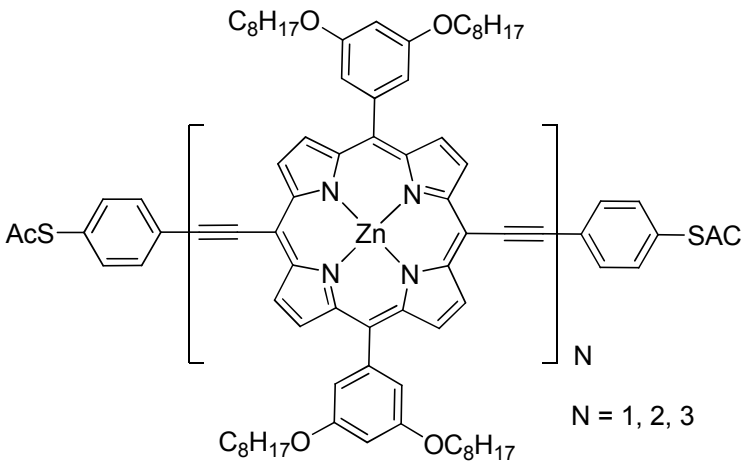

porphyrin oligomers

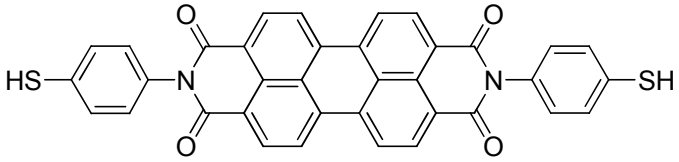

perylene tetracarboxylic diimides

Figure 8. Examples of molecules where hopping conductance is prevalent.

The hopping conductance probably plays an important role for conductance of porphyrin oligomers which show very weak length dependence of conductance with $\beta < 0.1$.[60] A low decay parameter ($\beta < 0.06$) allows the expected participation of the hopping electron transfer through polyyne bridged 4,4'-bipyridine molecules,[32] however it can be explained by only a tunneling process applying subsequent theoretical treatment. Salzer *et al.* showed a transition between tunneling and hopping conductance with increasing temperature.[61] Due to its low distance dependence hopping conduction is desirable for long molecular wires.

II.1.4. Single molecular study of metal containing compounds

As previously mentioned in the introduction, the synthesis of metal bearing conductive molecules with anchor groups is a challenging task. In this context it is not surprising that experimental data are available mainly for ruthenium and platinum derivatives as well as for ferrocene based molecules.

In the first studies, electric properties of a monolayer of $Fe(Cp)(C_5H_4(CH_2)_{11}SH)$ and of separated iron containing porphyrin molecules were investigated by STM.[62] This studies showed strong NDR behavior for the ferrocene derivative. The experiment with porphyrin molecules showed that molecular conductance can be controlled by the gate potential.[63] However, both of these studies are not true single molecule conductance experiments. Several molecular junctions are involved in a $Fe(Cp)(C_5H_4(CH_2)_{11}SH)$ measurements and conductance in perpendicular to π-system direction is obtained for the porphyrin molecule lying on the gold surface. Electrical

properties of a monolayer of [(AcSPhC$_2$)Ru(dppm)$_2$(C$_2$PhSAc)] were also studied.[64] An electron transfer rate through it appears to be higher than for identical thickness monolayer of AcSC$_2$PhC$_2$PhC$_2$PhSAc.

The structures of metal containing compounds studied by single molecular methods are listed on the figure 9.

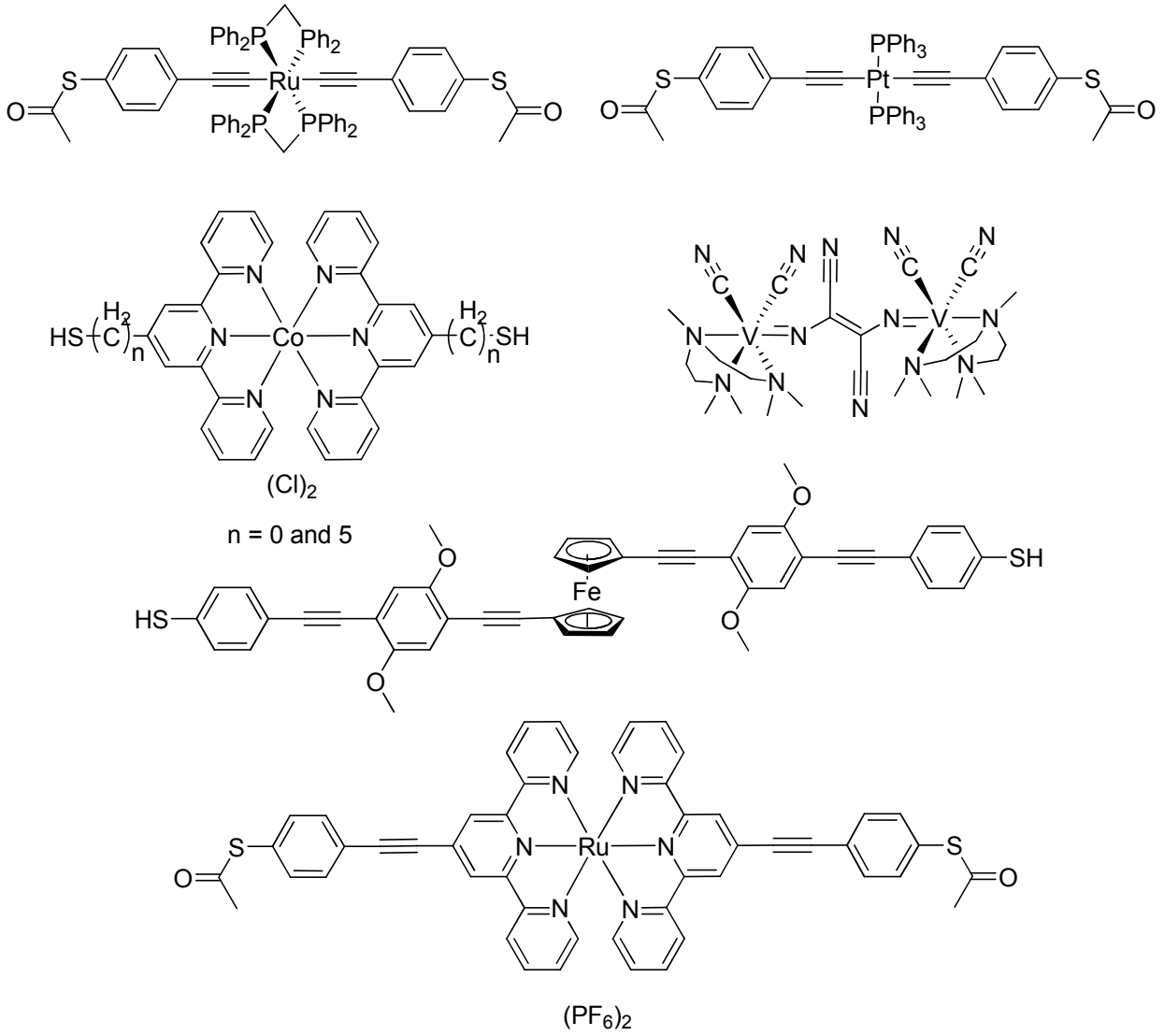

Figure 9. Structures of metal containing molecules investigated by single molecular techniques.

First single molecular studies were performed for the platinum complex.[65] It shows insulator behavior explained by the pure σ character of the platinum carbon bond. Subsequent studies of these type of molecules by the crossbar method affirmed no influence of phosphine ligands to their conductance.[66] It should be mentioned that there is a significant contradiction between two published reports. MCBJ measurements indicate a lower conductance than for conjugated organic molecules, while crossbars studies reveal a higher conductance. Two very interesting reports appeared simultaneously in Nature in 2002.[67,68] In the work from Park *et al.* Coulomb blockade and Kondo effect were observed for Co complexes between gold contacts.[68] The gate

bias required to remove a Coulomb blockade barrier is in good agreement with the electrochemical data. In the second work from Liang *et al.* the Kondo resonance was experimentally proven through the use of a magnetic field as an additional, tunable experimental parameter.[67] Outstanding work was published by Getty *et al*.[34] The conductance up to 70% of G_0 was reported for ferrocene containing molecules investigated by an electro-migration technique. However, an unusual character of these results requires confirmation by other experimental techniques. Molecules with a ferrocene unit connected to electrodes through peptide chains were tested by STMBJ. Results were quite unclear due to a strong fluctuation of the detected current.[69]

Recently, the break junction experiments were performed on ruthenium derivatives.[70,71] Two types of molecules were tested. The [(AcSPhC$_2$)Ru(dppm)$_2$(C$_2$PhSAc)] complex with acetylene chains directly bonded to the metal shows about five time lower resistance than 1,4-phenylene ethynylene derivative.[70] The effect is associated with a smaller HOMO-LUMO gap in the ruthenium compound than in aromatic compound. The [(AcSPhC$_2$tpy)Ru(tpyC$_2$PhSAc)] complex was tested by MCBJ experiment. I–V curves reveal reproducible characteristics with typical conductance peaks around 0.4 V. It was explained as a resonance transfer through the LUMO level at this potential.[71]

One of the motivations to introduce metal centers into molecular wires is for the promotion of the hopping type electron transfer which could result in lower decrease of the conductance as a function of distance. Redox active metal centers act in this case as charge carriers and short conjugated bridges mediate fast electron transfer between them. This simple concept was only recently experimentally tested on the monolayer formed by sequential stepwise coordination of metal ions by terpyridine-based ligands. Investigations showed that it is possible to make up to 40 nm length low-resistance molecular wires and that a metal oxidation potential has strong influence to the length decay constant.[72] Ruthenium mono-, di- and trinuclear complexes studied by cross bar method also have only weak length dependence of resistance.[73]

II.2. Mixed–Valence complexes

As could be seen from the previous chapter, a direct measurement of the electron transfer in organometallic complexes is a complicated task. However, important information about potential suitability of molecules as a conductor could be extracted from bulk physical methods. Objects of those studies ideally should comprise from redox active groups bridged by conjugated system (Figure 10).

Figure 10. System able to form mixed-valence complex.

Redox groups are metal centers in most cases but in some cases organic groups such as quinone and amine are also used.[74,75] If such a complex is oxidized or reduced by one electron, it forms species where the unpaired electron could be delocalized between centers to a different extent.[76-85] Such systems with the delocalized unpaired electron are called mixed-valence (MV) complexes because the oxidation state of the terminal atoms is a fractional number. A classical example of the MV complex is a Creutz–Taube ion (Figure 11).[86]

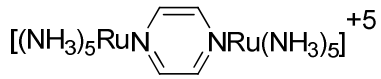

Figure 11. Structure of Creutz–Taube ion.

II.2.1. Electronic interaction

MV complexes are mostly discussed in the context of the interaction between terminal groups. The definition of "interaction" is a tricky question.[76,77] The most complete definition is based on quantum mechanical approximation where multi-electron wave function of the complex (Ψ) is determined on the basis of functions Ψ_A and Ψ_B.[76] Ψ_A is a wave function of complex with an electron localized on one center and Ψ_B represents a reversed situation. The "interaction" is represented then by $H_{AB} = \langle \Psi_A | H | \Psi_B \rangle$. A coupling between centers influences the electrochemical, spectroscopic and magnetic properties of a compound. A complete investigation of those properties gives comprehensive picture of the interaction between termini. A summary of the often used methods is provided in table 1.

Table 1.

Physical methods for investigation of metal centers interaction in [M]-(bridge)-[M].

Method	Form of [M]-(bridge)-[M] suitable for investigations	Key points in data analysis
X – Ray structural analysis	Mixed-Valence	Equivalence of bond lengths in coordination environment for metal centers.
Cyclic voltammetry	Any form	ΔE for reduction or oxidation waves, subsequent comproportionation constant.
EPR	Mixed-Valence	Identification where an unpaired electron is localized from hyperfine splitting and *g* anisotropy.
Magnetization measurements	Any form with $J \neq 0$	Presence of antiferromagnetic or ferromagnetic interactions between spins.
Near IR	Mixed-Valence	Presence of charge transfer band, its position and intensity.
IR	Mixed-Valence	Averaging of the characteristic signals from the ligands bounded to the metal centers and appearance of the forbidden vibrations.

The theoretical basis of all these methods starting from Near Infrared (NIR) will be discussed in more detail.

The MV complexes often show intensive absorption in NIR region of spectra. This absorption band often originates from a charge transfer transition.[87,88] Quantitative analysis of the NIR data is based on the semi-classical treatment by Sutin and Hush.[89-91] As mentioned above, the wave function of the interacting system (Ψ) is determined as combination of wave functions Ψ_A and Ψ_B of not interacting systems.[76] It is illustrated on potential energy surface diagram presented on figure 12.

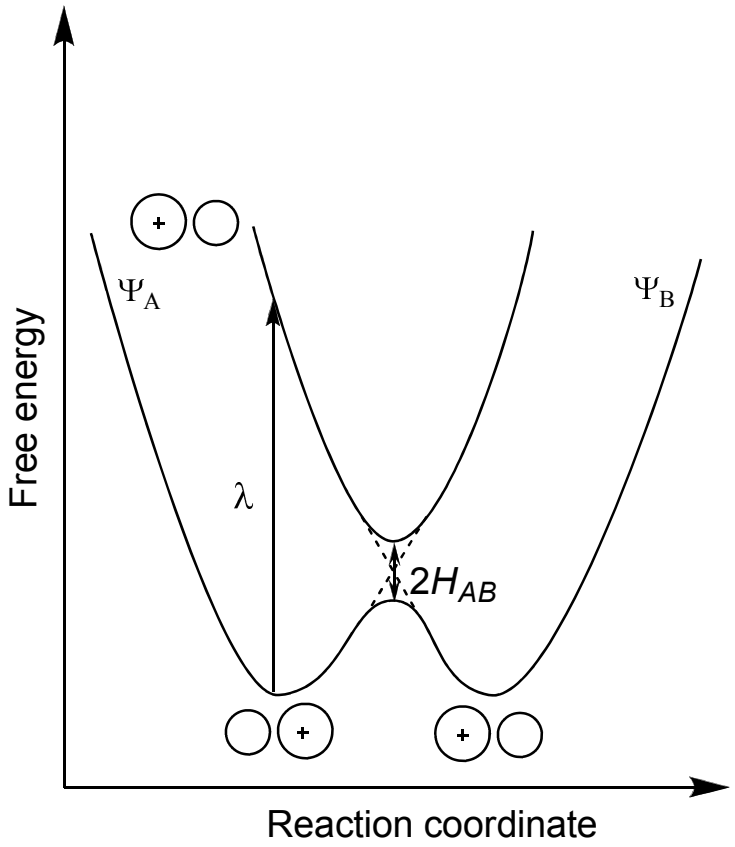

Figure 12. Energy-coordinate diagram for binuclear MV complex *(λ - position of intra valence charge transfer band; H_{AB} - electronic coupling).*

An application of a variational method results in the ground and exited states energies E_1 and E_2:

$$E_1 = (H_{AA} + H_{BB})/2 - \left\{\left[(H_{AA} - H_{BB})^2 + 4H_{AB}{}^2\right]^{1/2}\right\}/2$$

$$E_2 = (H_{AA} + H_{BB})/2 + \left\{\left[(H_{AA} - H_{BB})^2 + 4H_{AB}{}^2\right]^{1/2}\right\}/2$$

where for a symmetric molecule $H_{AA} = H_{BB} = \langle \Psi_A | H | \Psi_A \rangle = \langle \Psi_B | H | \Psi_B \rangle$

If we approximate that energies of initial states have harmonic dependence from nuclear coordinate:

$$H_{AA} = H^0_{AA} + fx^2/2$$

$$H_{BB} = H^0_{BB} + f(x-a)^2/2$$

where *f* is a force constant, the coordinate *x* is the displacement from the energy minimum at *x* = 0, *a* is the displacement difference between the minima before and after electron transfer.

The energies of ground and exited states would be expressed by:

$$E_1 = [\lambda(2X^2 - 2X + 1)]/2 - \{[\lambda(2X-1)]^2 + 4H_{AB}^2\}^{1/2}/2$$

$$E_1 = [\lambda(2X^2 - 2X + 1)]/2 - \{[\lambda(2X-1)]^2 + 4H_{AB}^2\}^{1/2}/2$$

where $\lambda = fa^2/2$ and $X = x/a$.

The ground state can have one or two maximum dependent from H_{AB}. Lowest energy transition in this case is a vertical transition between ground state in, for example, (0 +1) configuration to exited state with (+1 0) configuration and it is called intervalence charge transfer (IVCT) transition. The position, intensity and broadness of this band allows extracting information about mixing between states and barrier for electron transfer.

There is a following relation between IVCT band and H_{AB}.[92,93] The transition dipole between Ψ_1 (ground state) and Ψ_2 (exited state) is defined as:

$$M_{AB} = \langle \Psi_1 | \overline{\mu} | \Psi_2 \rangle$$

Hush pointed out that in the limit of small direct overlap between Ψ_1 and Ψ_2 this equation reduces to: $M_{AB} \cong e_0 \alpha r$.[89] Here, e_0 is the electron charge; *r* is the electron transfer distance and α is mixing parameter defined from:

$$\Psi_1 = \alpha\Psi_A + \sqrt{(1-\alpha^2)}\Psi_B$$

The oscillator strength *f* can be calculated from experiment as $f = 4.5 \cdot 10^{-9} \cdot \varepsilon_{\max} \Delta\nu_{1/2}$ and from theory as $f = 1.09 \cdot 10^{-5} \cdot M_{AB}^2 \cdot \overline{\nu}$ then $M_{AB} = 0.02 \cdot \sqrt{\varepsilon_{\max} \Delta\nu_{1/2} / \overline{\nu}}$ and it follows that:

$$\alpha^2 = 4.24 \cdot 10^{-4} \varepsilon_{\max} (\Delta\nu_{1/2}) / (\overline{\nu} r^2)$$

where $\overline{\nu}$ is a position of absorption maximum, ε_{max} – maximum extinction coefficient, $\Delta\nu_{1/2}$ - the width of the absorption band at half-height. Finally H_{AB} is defined by:

$$H_{AB}(cm^{-1}) \approx \alpha(E_1 - E_2) \cong \alpha\overline{\nu} = 2.05 \cdot 10^{-2} (\sqrt{\varepsilon_{\max} \Delta\nu_{1/2} \overline{\nu}}) / r$$

where $\overline{\nu}$, ε_{max} and $\Delta\nu_{1/2}$ are in cm^{-1} and *r* is in Å.

However, for very strongly coupled systems, with one energy minimum on the ground state, another equation should be used:[76,90] $H_{AB} = \overline{\nu}/2$

A most common electrochemical experiment is the Cyclic voltammetry (CV).[94-97] The complexes of the type discussed have two redox centers and should have at least two redox processes illustrated below (Figure 13):[84,98]

$$[L_xM^n(\mu\text{-}BL)M^nL_x] \rightleftharpoons [L_xM^{n+1}(\mu\text{-}BL)M^nL_x] \rightleftharpoons [L_xM^{n+1}(\mu\text{-}BL)M^{n+1}L_x]$$

Red (E_1) MV (E_2) Ox

Figure 13. Redox forms of binuclear metal complex *(M – metal; L –ligand; BL – bridging ligand; n – oxidation state of metal in reduced form).*

The stability of the MV complex is reflected by the comproportionation constant K_c which is readily calculated from the separation of the redox processes:[85,99]

$$K_c = \frac{[MV]^2}{[Ox][\mathrm{Re}d]} = e^{\Delta G_0 / RT}$$

$$\Delta G_0 = nF\Delta E, n = 1, \Delta E = E_1 - E_2$$

$$K_c = e^{F\Delta E / RT} = 10^{\Delta E / 59mV}$$

K_c qualitatively correlates with an interaction between metal centers and for strongly interacting systems it is normally a big number. However, ΔG_0 responsible for stabilization of MV complex consists of many contributions.[85,90,93]

$\Delta G_0 = \Delta G_{stat} + \Delta G_{coul} + \Delta G_{iduct} + \Delta G_{reson} + \Delta G_{af} + \Delta G_{ip}$

In this equation ΔG_{stat} represents the statistical distribution, ΔG_{coul} the electrostatic repulsion of the positively charged metal ions, ΔG_{iduct} an inductive factor related to the competitive coordination of the bridging ligand by the metal ions, especially to decrease of π acceptor properties of the bridging ligand in the reduced form of the complex, ΔG_{reson} the resonance exchange, ΔG_{af} the antiferromagnetic exchange stabilization, for example for biradical form, and ΔG_{ip} the ion-pairing effects depending on the charges of the complexes. Only ΔG_{reson} directly belongs to the interaction of metal centers in a MV complex.

It was shown by different studies that a solvation and an ion pairing have very often dominant contribution, and that K_c strongly depends from the solvent and the supporting electrolyte used in the experiment.[100,101]

Floriani *et al.* attempted to look for a quantitative relation between K_c and orbital coupling, but strong and badly defined solvation contribution makes those conclusions difficult in practical application.

Infrared (IR) spectroscopy can usually be utilized as a probe to measure the extent of the electron delocalization via the extent of averaging of the characteristic absorptions strongly affected by the oxidation state of the metal centre. Furthermore, in symmetry lowered systems with electron exchanges between the metal centers slow on the IR time scale (10^{-13} sec), one can often identify new absorptions forbidden to appear in a symmetrical system.[76,87,102] Systems containing metal center groups with intense IR bands, are suitable for a first approach, while

systems with IR active functional groups lying in the center of symmetry of molecule are well suited for the latter approach.

The electron paramagnetic resonance (EPR) method is a powerful tool to identify electron delocalization.[103] In certain cases it gives a direct information about the electron localization from hyperfine splitting and *g* anisotropy.[84] However, the method is very special to subject of study. An ideal situation for the study of electronic interactions between metal centers by EPR occurs when metal centers have nondegenerate ground states, and a suitable nuclei to which hyperfine coupling can be observed. Unfortunately, this situation often is not realized, from octahedral ions, Cr^{3+} and Mn^{2+} (high spin) ions have ideal electronic structure. The heavy elements in asymmetric environment also often have nondegenerate ground states, as for example [Re(Cp*)(NO)(PPh_3)] fragment in complexes investigated by Gladysz and coworkers.[104]

Measurements of the temperature dependence of sample magnetization could give important information about coupling of the electronic states for systems with more than one unpaired electron.[103] Experiments are normally carried out on SQUID device and the results could be easily transformed to temperature dependence of molar magnetic susceptibility χ_m. Analysis of χ_m *vs* T curve gives information about interaction of unpaired electrons in the system. Most important case for us is the binuclear complexes with one unpaired electron on each metal center. Such complexes can have antiferromagnetic or ferromagnetic interaction of spins, dependent on the electronic structure of the metal centers and bridge.

Nice systematic studies of the magnetic properties of complexes, consisting of [Mo(NO)(Tp´)Cl],[105] [Mo(O)(Tp´)Cl][106] and [W(O)(Tp´)Cl][107] centers bridged by bipyridyl and biphenol type ligands were performed by McCleverty and Ward showing importance of bridge-metal orbital overlap, as well as conjugation in the bridge to the type and energy of magnetic interactions.[82,108] The π-conjugated bridges with even number of atoms mostly provide the antiferromagnetic coupling while bridges with odd number of atoms mediate ferromagnetic coupling. Spin-polarization mechanism was used to explain these behaviors.

The antiferromagnetic coupling situation is much more common among usual bridges. Also, its energy is higher than that for ferromagnetic coupling. Systems with two unpaired electrons and only spin contribution to magnetic moment are described by the spin Hamiltonian $H = -J\boldsymbol{S_1}\cdot\boldsymbol{S_2}$. It results in the following equation for molar magnetic susceptibility:

$$\chi = \frac{2N_A g^2 \beta^2}{kT} \cdot \frac{1}{(3 + e^{J/kT})}$$

where N_A – Avogadro constant, *g* – g factor, β – electron Bohr magneton, k – Boltzmann constant, J – exchange integral. Such χ_m *vs* T curve shows a maximum at Neel temperature and drops considerably on going to higher temperature. The J is the most important parameter for data analysis which reflects the electronic coupling of magnetic centers. For dinuclear complexes it lies in a broad region from a few cm^{-1} to hundreds of cm^{-1} such that some complexes are diamagnetic at room temperature.

II.2.2. Examples and classification

Interaction of metal centers is a complex parameter that requires analysis by a variety of methods. First classification of MV species was carried out by Robin and Day.[109] It was a very general description involving multi and heterometallic systems and was based on the mixing parameter α described above. There are three types of MV complexes according to this classification. Class I is non-interacting systems with $\alpha \approx 0$. Class II is moderately interacting systems where two oxidation states are distinguishable $0 < \alpha < \sqrt{2}/2$. Class III is a fully delocalized system with $\alpha \approx \sqrt{2}/2$. An analysis could be done in more detail because we in particular deal with symmetrical dinuclear molecules. The H_{AB} is directly related to α and potential energy surfaces could be drawn.[76] Examples of the energy-coordinate curves for different H_{AB} are illustrated on figure 14.

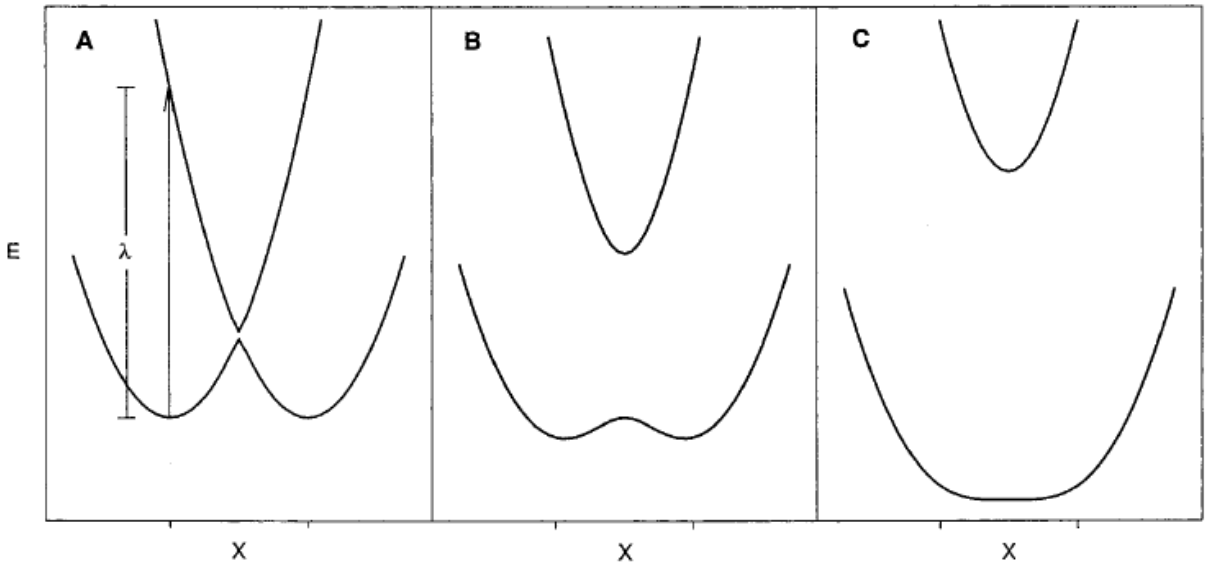

Figure 14. Energy-coordinate diagrams for ground and exited states calculated with λ = 8000 cm^{-1} and (A) H_{AB} = 100 cm^{-1}, (B) H_{AB} = 2000 cm^{-1}, and (C) H_{AB} = 4000 cm^{-1} *(The coordinate axis is the reduced coordinate X).*[76]

These three diagrams represent three principally different situation related to the Robin and Day classification. Figure A shows non-interacting centers with the electron localized on one of them. Figure B describes strongly interacting system, but still with two minimum for the ground state.

It means that in a static situation this system is also localized. The situation C is a fully delocalized system with only one minimum on the ground surface. Examples of complexes from different classes are depicted in figure 15. [79,99,102,110-112]

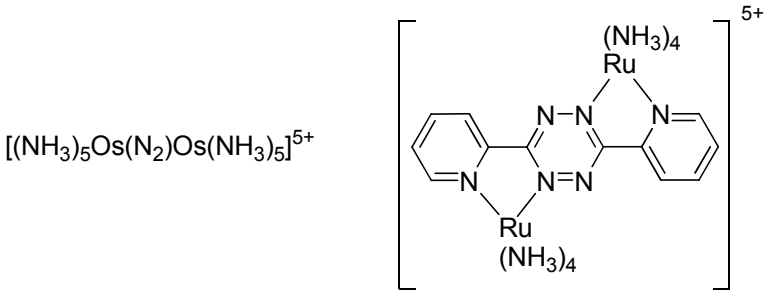

Class III (C)

Class II (B)

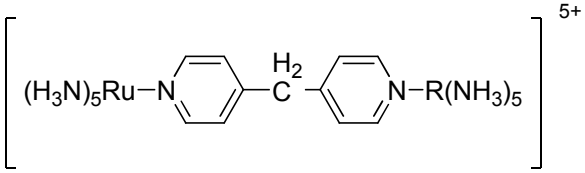

Class I (A)

Figure 15. Examples of MV molecules from different classes.

II.2.3. Electron transfer in MV complexes

Here in, we discuss the classical approach developed by Marcus, Hush and Sutin.[89,91,113] The electron transfer in MV complexes at room temperature is analogous to any redox reaction and it is analyzed in the same theoretical frame. This frame was already discussed in detail in the previous part concerning the analysis of the NIR data (Figure 12). The electron transfer is a switch between two minima of the ground state, consequently this description is applicable to class I and II systems, but not for class III systems. It is important to mention the relation of this electron transfer to single molecular conductance mechanisms discussed above. An electron movement in MV complex is a single hopping step in this context. Only thermally activated mechanism is normally discussed for electron transfer reactions and tunneling is considered as a minor component. There are two regimes for electron transfer dependent of the degree of electron coupling. Systems with weak coupling ($H_{AB} < 200$ cm^{-1}) would be described by a

nonadiabatic regime of the electron transfer.[90,91] The rate constant is calculated then from the following equation.

$$k = (2H^2{}_{AB} / h)(\pi^3 / \lambda k_b T)^{1/2} \exp(-G^* / k_b T)$$

The heights of the barrier could be calculated from the following equation:

$$G^* = \lambda(1 - 2H_{AB} / \lambda)^2 / 4$$

Here λ is called reorganization parameter and ideally should be equal to the energy of IVCT band. The λ depends from the structural changes upon oxidation (or reduction). The system where oxidation causes minimum structural changes should have small reorganization barrier. The H_{AB} can significantly reduce the barrier.

Strongly interacting systems have an adiabatic regime of electron transfer. This approximation means that there is a very high probability of switching between electron states in the intersection region. The rate constant is given by the following equation:

$$k = \nu_n \exp(-G^* / k_b T)$$

where ν_n is the nuclear frequency.

As could be seen from this summary, the rate constant for electron transfer doesn't directly correlate with the coupling of centers and for strongly interacting systems it more depends on the reorganization parameter.

An investigation of the electron transfer in MV complexes is based on quantitative analysis of NIR spectra as well as on averaging of signals for different metal centers in investigation by methods with different time scale. The summary of the time scales for different method is in table 2.

Table 2.

Time scales for different methods

Method	Time scale [s]
NMR	$1 - 1 \cdot 10^{-5}$
EPR	$10^{-5} - 10^{-9}$
Moessbauer	$10^{-6} - 10^{-9}$
IR	$10^{-11} - 10^{-15}$
XPS	10^{-17}

II.3. Homo–metallic dinuclear complexes with C_n bridges and reversible redox properties

Huge amount of literature concerning C_n bridged complexes is available due to the significant attention paid to areas of molecular electronics and electron transfer reactions. Here we discuss only complexes with reversible electrochemistry, since they were investigated by methods described above. There is only a few number of metal centers used for the synthesis.

A chemistry of complexes composed from [(NO)(PPh_3)(Cp*)Re] fragments was developed by Gladysz and coworkers.[104,114-123] They used complexes [(NO)(PPh_3)(Cp*)Re($C\equiv C)_nH$] (n = 1 and 2) as starting materials.[122,124] A sequence of hetero-couplings of [(NO)(PPh_3)(Cp*)Re($C\equiv C)_n$Cu] with Br($C\equiv C)_n$$SiEt_3$, followed by deprotection of the acetylene group with final oxidative homo-coupling forms a general strategy for the synthesis of [(NO)(PPh_3)(Cp*)Re(C_n)Re(NO)(PPh_3)(Cp*)] of different length up to n = 20.[114,115,117]

Iron containing compounds comprise mainly from [(dppe)(Cp*)Fe][125-130] and [$(CO)_2$(Cp*)Fe][131-133] building blocks. The former fragment was developed mainly by Lapinte and the bis-carbonyl fragment by Akita. The synthesis of long chain derivatives was done using the same strategy with rhenium derivatives. The [(dppe)(Cp*)Fe(C_4)Fe(dppe)(Cp*)] was obtained by deprotonation of bis-vinylidene derivative obtained by oxidative coupling.[125]
Compounds consisting of [$Mn(dmpe)_2$] end groups were obtained in our group using $Me_3SnC_4SnMe_3$ or by oxidative coupling.[134-136]

Two ruthenium based terminal groups were often used. A [$(PPh_3)_2$(Cp)Ru] fragment was explored by Bruce. A C_4 bridged complex as well as a long chain C_{14} derivative were obtained.[137,138] Dixneuf and coworkers explored chemistry of [$Cl(dppe)_2$Ru] block and showed that it can be used to build up versatile structures.[139,140] It is surprising in this context that simple C_n bridged complexes are quite unexplored. A nice example is a [$Cl(dppe)_2Ru(C_{12})Ru(dppe)_2Cl$] complex.[141,142]

From other metals, tungsten and molybdenum bis-carbyne complexes are of interest.[143] They were obtained via oxidative coupling and will be discussed in more detail at a later stage.

Some examples of the discussed complexes are presented in figure 16. It should be mentioned here that most of the used terminal metal centers are “dead end” and can not be further extended to longer linear systems. Exceptions are “bifunctional” manganese and ruthenium centers in square phosphine environment.

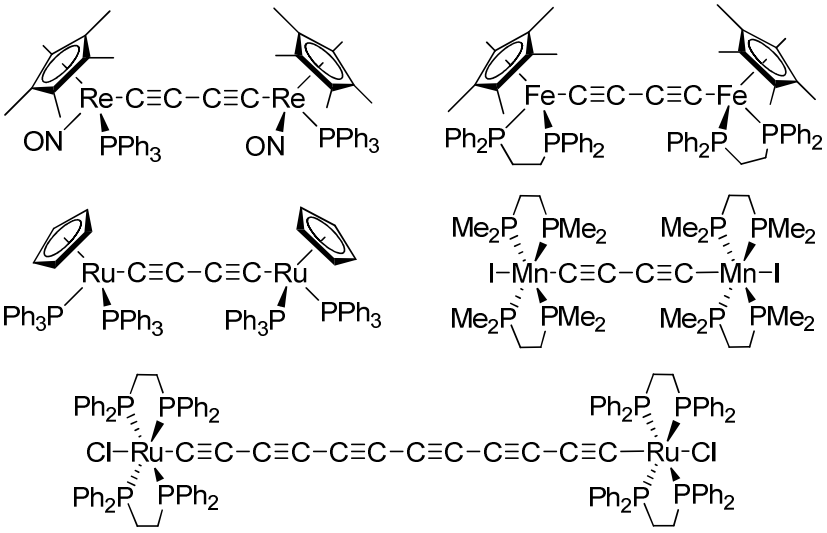

Figure 16. Examples of C_n bridged complexes.

Short C_2 bridged derivatives are rare. There are examples of tungsten and manganese complexes.[144-146] C_4 bridged complexes are most common. A C_4 chain can exist in three canonical forms (Figure 17).

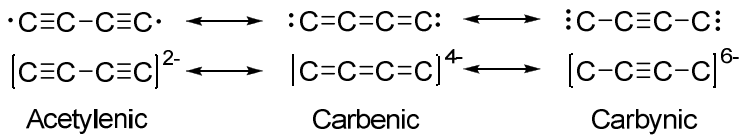

Figure 17. Canonical forms of a C_4 unit in [M]C_4[M] structures.

Two main tendencies could be observed based on these canonical forms:

- Firstly, in oxidation state +2 d^8 metals (Ru, Fe) have acetylenic bridges, d^7 metals (Mn) have a form of bridge close to cumulenic, while the d^6 metals (W, Mo) usually have carbynic bridges.
- Secondly, a stepwise oxidation of the complex in the acetylenic form causes its transformation first to the carbenic and latter to the carbynic forms. This type of transformation was put forward for $[RuC_4Ru]^{0\text{-}4+}$ (Ru = $[(PPh_3)_2(Cp)Ru]$ or $[(PPh_3)(PMe_3)(Cp)Ru]$) systems.[137]

A reason for both tendencies is probably that the metal centre normally adopts an 18ē configuration using electrons of the C_4 unit. It could also be seen from the analysis of population of Hückel orbitals as it was shown by Floriani.[147]

Many of the C_n bridged complexes were structurally characterized (see figure 18 for examples). The long C_n systems were subject of review;[148] where types of distortion from linearity of C_n chain were discussed.[149]

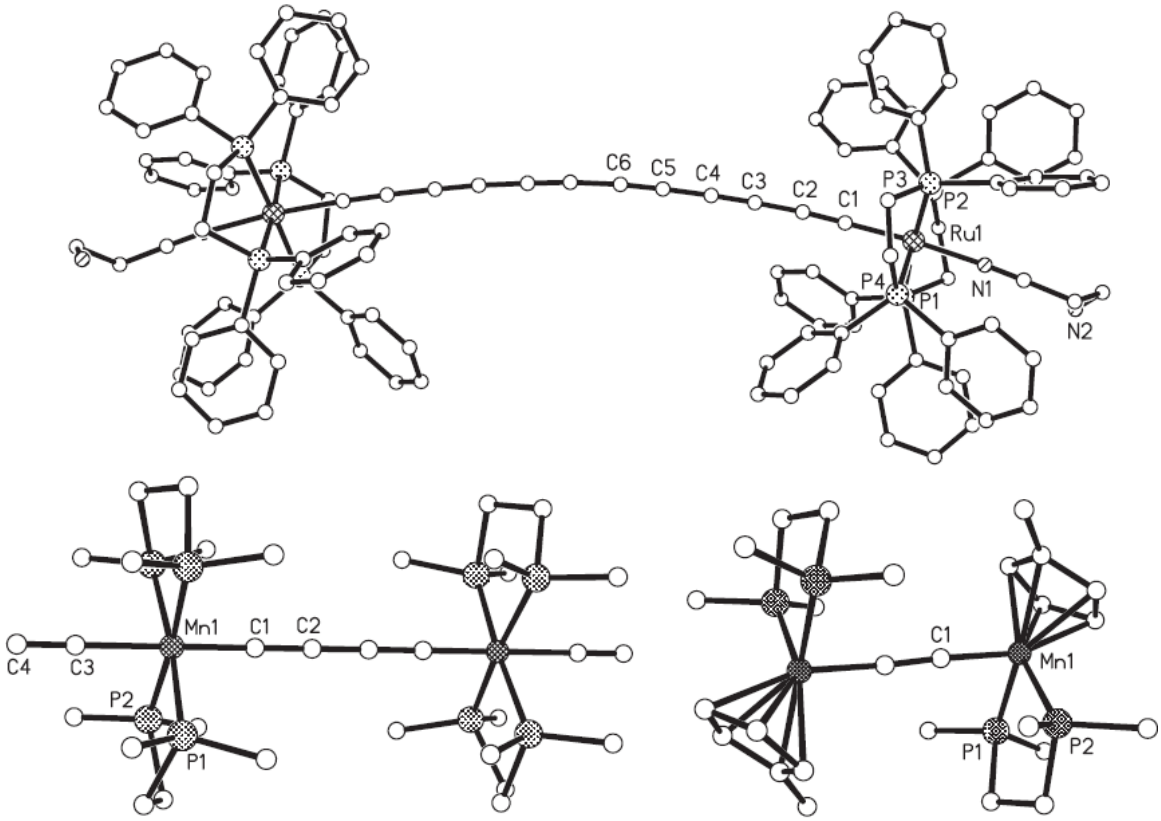

Figure 18. Examples of crystal structures of C_n bridged complexes. *(Counter-ions are omitted for clarity).*[136,142,146]

The C_n chains efficiently mediate communication between the terminal centers due to the presence of both strong σ – donating and π - acceptor interactions with the metals.[120,137,147] Molecular orbitals for the butadiyne dianion participating in the interaction with the metal orbitals are illustrated in figure 19. Many complexes are considered to be Class III species. The results of some investigation are summarized in table 3. Following conclusions could be drawn from the analysis of these data:

- Not only bridge, but also the metal centers have influence on the degree of coupling as seen from the comparison of rhenium, ruthenium and iron complexes with identical butadiyne bridges. The main reason is probably the different energy correlation between metal and bridge orbitals.
- Interaction decreases with increasing of chain length.
- The polyyne chain mediates stronger communication than polyene chain does.
- Carbyne systems show significantly less stabilization of MV species than acetylene bridged species.

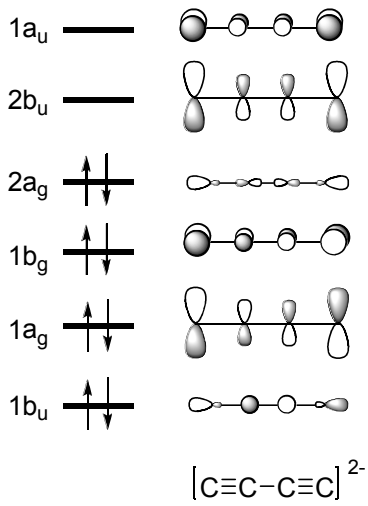

Figure 19. Orbital diagram for [C≡CC≡C]$^{2-}$. [120,137,147]

Table 3.

Comproportionation constants and coupling energies for selected binuclear metal complexes calculated from experimental data.

Compound	K_c	H_{AB} [eV] [a]	Reference
[(NO)(PPh$_3$)(Cp*)Re(C$_4$)Re(NO)(PPh$_3$)(Cp*)]	$1 \cdot 10^9$	0.18	104
[(NO)(PPh$_3$)(Cp*)Re(C$_6$)Re(NO)(PPh$_3$)(Cp*)]	$3 \cdot 10^6$	—	117
[(NO)(PPh$_3$)(Cp*)Re(C$_8$)Re(NO)(PPh$_3$)(Cp*)]	$59 \cdot 10^3$	—	117
[(dppe)(Cp*)Fe(C$_4$)Fe(dppe)(Cp*)]	$1.6 \cdot 10^{12}$	0.19	125
[(dppe)(Cp*)Fe(C$_8$)Fe(dppe)(Cp*)]	$2 \cdot 10^7$	0.32 [b]	126
[(dppe)(Cp*)Fe(CH=CHCH=CH)Fe(dppe)(Cp*)]	$1.5 \cdot 10^{10}$	0.23	150
[(dppe)(Cp*)Fe(C$_2$CH=CHC$_2$)Fe(dppe)(Cp*)]	$1.2 \cdot 10^8$	0.13	132
[(PPh$_3$)$_2$(Cp)Ru(C$_4$)Ru(PPh$_3$)$_2$(Cp)]	$1.8 \cdot 10^{11}$	0.7 [b]	137
[Cl(dppe)$_2$Ru(C$_{12}$)Ru(dppe)$_2$Cl]	$1 \cdot 10^4$	—	141
[I(dmpe)$_2$Mn(C$_4$)Mn(dmpe)$_2$I]	$5.4 \cdot 10^{10}$	—	134
[(HCC)(dmpe)$_2$Mn(C$_4$)Mn(dmpe)$_2$(CCH)]	$7.5 \cdot 10^9$	—	136
[(MeCp)(dmpe)Mn(C$_2$)Mn(dmpe)(MeCp)]	$8.6 \cdot 10^{16}$	—	146
[(Tp′)(CO)$_2$Mo≡CC≡CC≡Mo(Tp′)(CO)$_2$]	$1 \cdot 10^4$	—	151
[(Tp′)(CO)$_2$W≡CC≡CC≡W(Tp′)(CO)$_2$]	$5 \cdot 10^4$	—	151
[(dppe)(Cp*)Os(C$_4$)Os(dppe)(Cp*)]	$2 \cdot 10^{10}$	—	152

[a] Calculated by equation for Class II complex. [b] Calculated by equation for Class III complex.

It is important to mention that of course investigations of MV complexes only give an idea about the behavior of molecule as single molecular conductor. Important factors, such as contact conductance and tunneling processes are not considered in this approximation. The results should be analyzed critically taking into account specifics of the particular system.

II.4. Tungsten complexes

II.4.1. Tungsten dinuclear complexes bridged by conjugated carbon chain

Tungsten as well as molybdenum was never main targets in the fields of MV complexes and molecular wires, but some carbon bridged systems were synthesized. The most important published complexes are presented in figure 20.[143-145,153-163]

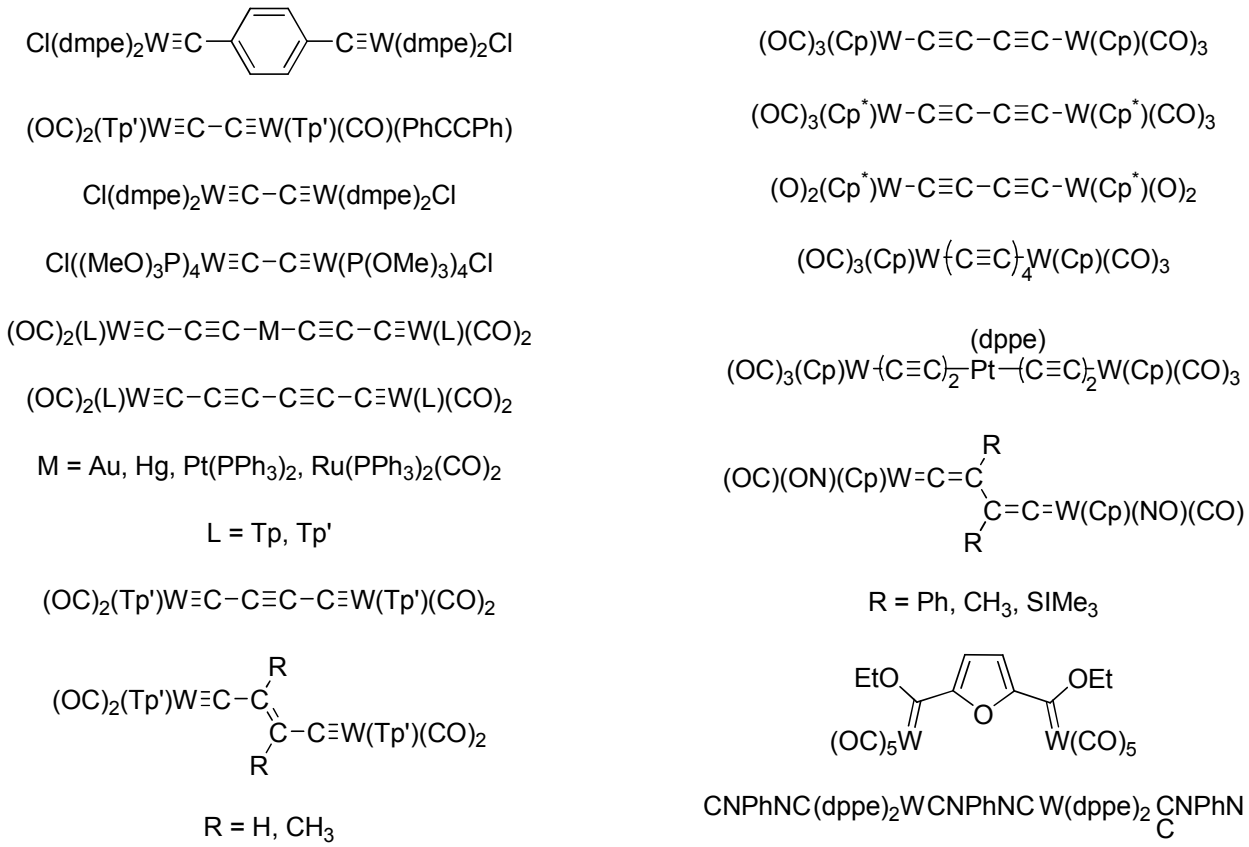

Figure 20. Tungsten dinuclear complexes bridged by a conjugated carbon chain.

Complexes can be distinguished into two main groups. The first group consists of carbyne type derivatives. The C_4 bridged carbyne complexes were synthesized by Templeton and coworkers via oxidative coupling of the $[(Tp')(CO)_2W{\equiv}C\text{-}CH_2R]$ (R = H, CH_3). Subsequent sequential of deprotonation and oxidation gave access to the systems with central unit varied from $\text{-}CH_2\text{-}CH_2\text{-}$ to -C≡C-.[143] Hill and coworkers used the $[(Tp')(CO)_2W{\equiv}CC{\equiv}CH]$ as starting material to gain access to different hetero-metallic complexs.[157] Reductive elimination of acetylene fragments from the mercury derivative resulted in the C_6 bridged compound.[156] Hopkins and coworkers obtained recently C_2 bridged complexes based on the $[W(PP)_2Cl]$ (PP = dmpe, 2 $P(OMe)_3$) terminal groups.[145] They used a principally different strategy based on $[(t\text{BuO})_3W{\equiv}CC{\equiv}W(t\text{BuO})_3]$ which was prepared in > 90% yield via triple-bond metathesis of $[W_2(O t\text{Bu})_6]$ and an internal diyne. The dinuclear germylidyne complex $[Cl(dppe)_2W{\equiv}GeGe{\equiv}W(dppe)_2Cl]$ published by Fillipou is also very close in its nature to the discussed compounds.[164]

The second group of compounds is represented by complexes with a single tungsten carbon bond obtained by Bruce and Low. The synthetic strategy was to apply metal acetylene coupling and oxidative homo-coupling to [(Cp or Cp^*)$(CO)_2$W-C≡CC≡CH] precursors.[154] The C_4 and C_8 bridged compounds were obtained by this way.[154,155]

In contrast to the significant synthetic work, the physical studies of metal···metal interaction in those complexes are very limited. The irreversible redox properties of many (for example (Cp or Cp^*)$(CO)_2$W) CO bearing compounds cause difficulties in generation of MV species. However, CV studies were carried out on some [(Tp)$(CO)_2$W≡C] based compounds and on [Cl$(PP)_2$W≡CC≡W$(PP)_2$Cl] (PP = dmpe, 2 $P(OMe)_3$) complexes (Table 4).[145,151] Magnetic studies of [Cl$(dmpe)_2$W≡CPhC≡W$(dmpe)_2$Cl][PF_6]$_2$ have been reported showing antiferromagnetic coupling with J equal to 26 cm^{-1}.[163]

Table 4.

Summary of CV data for tungsten dinuclear carbyne complexes (E *vs* $Fc^{0/+}$ [V]).

Compound	$E_{1/2}^{0/+}$	$E_{1/2}^{+/2+}$	$\Delta E_{1/2}$	K_c
[(Tp′)$(CO)_2$W≡CCH_2C≡W(Tp′)$(CO)_2$]	-0.21	-0.02	0.19	$6\cdot10^6$
[(Tp′)$(CO)_2$W≡CCH_2CH_2C≡W(Tp′)$(CO)_2$]	-0.20	-0.13	0.07	20
[(Tp′)$(CO)_2$W≡CCH=CHC≡W(Tp)$(CO)_2$]	-0.16	0.02	0.18	$1\cdot10^3$
[(Tp)$(CO)_2$W≡CC≡CC≡W(Tp)$(CO)_2$]	-0.14	0.14	0.28	$5\cdot10^4$
[Cl$(dmpe)_2$W≡CC≡W$(dmpe)_2$Cl]	-1.00	-0.60	0.40	$6\cdot10^6$
[Cl$(P(OMe)_3)_4$W≡CC≡W$(P(OMe)_3)_4$Cl]	-0.26	+0.22	0.48	$1.35\cdot10^7$

As could be seen from this chapter, the [W$(PP)_2$X] (PP = di- or monodentate phosphine; X = halogen) fragments are most promising containing tungsten metal centers due to the reversible electrochemistry and reactive terminal halogen atoms. However, the synthetic methodology for that type of polynuclear compound seems to be not very broadly explored.

II.4.2. Synthetic methods

There are a significant number of reactions which could be used for the synthesis of tungsten polynuclear rigid-rod complexes. They could be divided into five classes depending on the principal in their basis (see figure 21 for examples):

1. Reactions based on coordination of carbon donors to a vacant site. [165-174]
2. Halogen or triflate substitution reactions. [154,155,175-180]
3. Alkyne metathesis based reactions. [145,180-183]
4. Nucleophilic addition to coordinated CO ligand. [122,184-189]
5. Dehydrogenation or desilylation of vinyl and alkyl ligands. [190,191]

The first type of method requires a precursor with a labile ligand to form species with an open coordination site. Nitrogen (N_2) and weakly coordinated solvent molecules, such as THF or acetone can take over this function. There are two precursors based on the N_2 leaving group [*trans*-$W(dppe)_2(N_2)_2$][192,193] and [*trans*-$W(dppe)_2(CO)(N_2)$].[194,195] The first complex is well explored. It reacts with acetylenes (HC≡CR) forming dihydride acetylide complexes [*trans*-$W(dppe)_2(H)_2(C{\equiv}CR)_2$].[165,166] The respective chemistry of [*trans*-$W(dppe)_2(CO)(N_2)$] is expected to be more predictable due to the well defined position of the vacant site. Its synthetic potential was not explored, but an analogous [*trans*-$W(dppe)_2(CO)(DMF)$] complex reacts with acetylenes to form mono-hydride complexes [*trans*-$W(dppe)_2(H)(CO)(C{\equiv}CR)$] (R = Ph, CO_2Me) which could then be converted to carbynes [*cis*-$W(\equiv CCR)(dppe)_2(CO)][BF_4]$ by protonation.[167]

Carbonyl complexes [*fac*-$W(dppe)(CO)_3(L)$] (L = THF or acetone)[196] with labile solvent ligands also react with acetylenes, but the 1,2–H shift is observed instead of oxidative addition, presumably due to the electron-poor character of the tricarbonyl metal centers. Vinylidene complexes [*fac*-$W(dppe)(CO)_3(C{=}CRH)$] (R = Ph, CO_2Me), formed in this transformation, react with acids forming carbyne complexes.[168,169] If deprotonated acetylenes (LiC≡CR) (R = Ph, Me, *n*Bu) are reacted with these precursors, anionic complexes [*fac*-$W(dppe)(CO)_3(C{\equiv}CR)]^-$ were obtained.[173] They react stepwise with acids forming vinylidene and carbynes. The $[W(CO)_5(THF)]$ complex also reacts with lithiated acetylenes forming anionic complexes. This reaction was intensively used by Fischer and coworkers for the preparation of long cumulenes. Their strategy comprises of the cleavage of a NMe_2 group from $[W(CO)_5((C{\equiv}C)_nC(NMe_2)_3)]^-$ (n = 1,2 and 3) by BF_3. The C_3, C_5 and C_7 cumulenylidenes were generated in this way.[170-172]

The halogen replacement offers as a very general method for acetylide moieties. However, the W – Hal bond is very strong in compounds of low oxidation state. It does not easily dissociate in solution and prevents nucleophilic substitution at tungsten centre by a dissociative pathway. Precursors successfully used for this approach are [$W(Cp)(CO)_3Cl$] and $[W(CO)_5Cl]^-$.[154,155,175,176] The CO ligands probably have a double function in this case. They labilize the tungsten chlorine bond by π-acceptor effect and their small size makes the metal center more open for the nucleophilic attack required for associative substitution. Most of the binuclear tungsten complexes with polyyne bridges were obtained by this way and contain $[W(Cp)(CO)_3]$ terminal groups. There are a few reports claiming successful coupling of the $[W(Cp)(CO)_3I]$ with tributyltin acetylenes, but the purity of the obtained compounds and yields are not sufficient.[177] The problem of the strong W–Hal bond can be solved in some cases by changing of the halogen to a triflate substituent.[178] This was realized by Hopkins and coworkers on tungsten carbyne complexes [$(Cl(dmpe)_2W{\equiv}CR$] (R = H, $C_6H_4C{\equiv}CSi\mathit{i}Pr_3$).[179,180] The chlorine anion was substituted to the OTf^- using Me_3SiOTf. The triflate ligand was then substituted by the acetylide

moiety via the reaction with LiC≡CR (R = $SiMe_3$, Ph, C_6H_4Me, H, $C_6H_4MC_2Pr^n$). The AgOTf and TlOTf could also be used for halogen abstraction depending on the redox properties of the metal center.

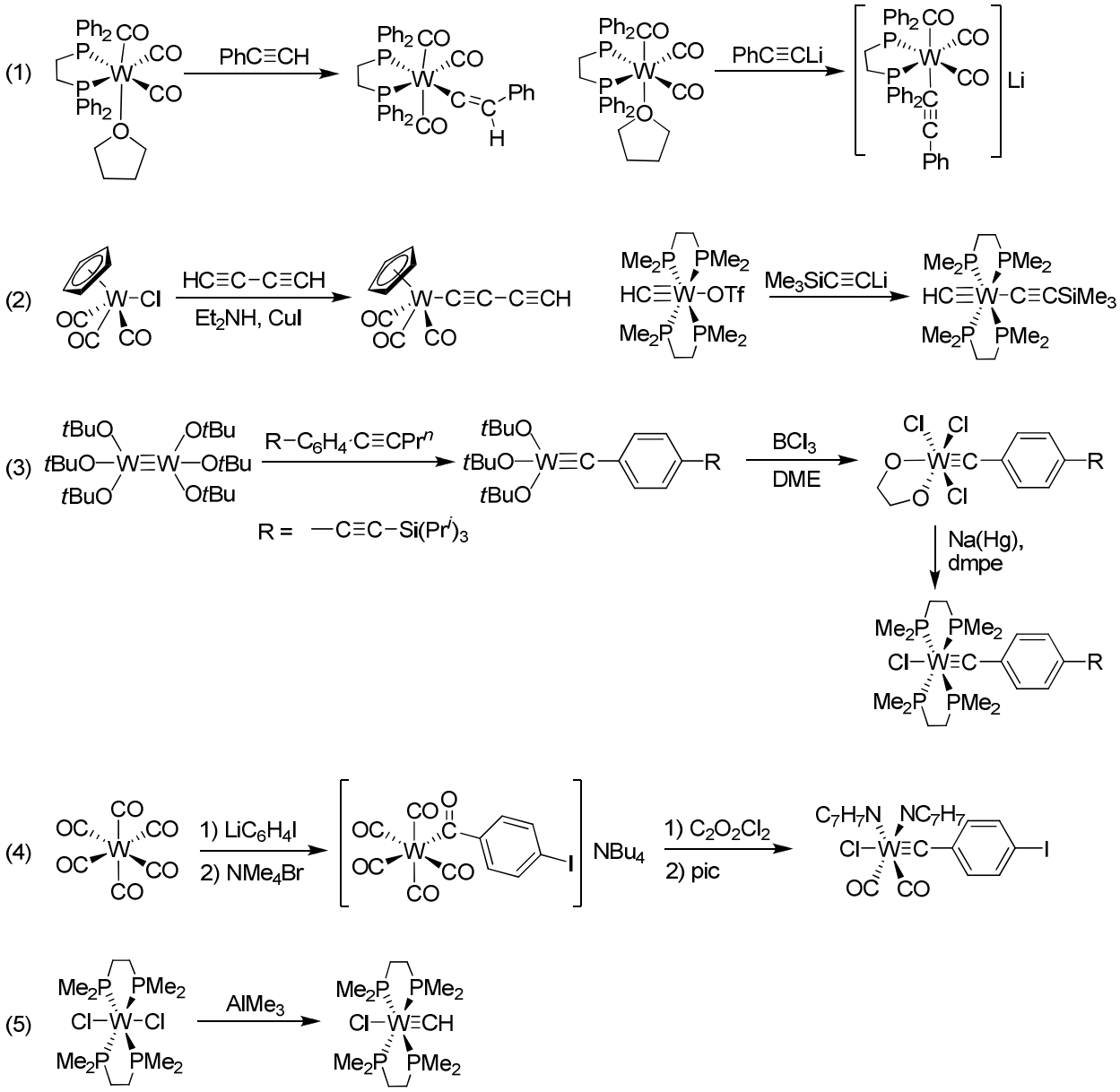

Figure 21. Examples of tungsten carbon bond formation methods

The alkyne metathesis is also a suitable approach to generate carbyne complexes with a desired net of substitutents. A dimeric $[(t\text{BuO})_3W{\equiv}W(O t\text{Bu})_3]$ starting material reacts with substrates containing C≡C or C≡N bonds. If di-substituted acetylenes ($R_1C{\equiv}CR_2$) are used, mononuclear carbynes $[(t\text{BuO})_3W{\equiv}CR_1]$ and $[(t\text{BuO})_3W{\equiv}CR_2]$ are formed. If the reaction is performed with di-substituted butadiynes ($R_1C{\equiv}CC{\equiv}CR_2$), a C_2 bridged complex $[(t\text{BuO})_3W{\equiv}CC{\equiv}W(O t\text{Bu})_3]$ can be obtained.[145] Finally aromatic nitriles were used for synthesis of $[(t\text{BuO})_3W{\equiv}CR]$ (R = $C_6H_4NMe_2$, C_6H_4SMe and 2,6 - $Me_2C_6H_2N$).[181,182] The complex $[(t\text{BuO})_3W{\equiv}CR]$ is converted to $[Cl(dmpe)_2W{\equiv}CR]$ via a sequence of chlorination with BCl_3 and simultaneous reduction and phosphine coordination.[180,183]

Reactions operating through nucleophilic attack at the CO ligand are an efficient tool to accomplish access to odd numbered carbon chains,[122] as well as to phenyl substituted carbynes.[184-187] Reaction of $W(CO)_6$ with LiC_6H_4R followed by $C_2O_2X_2$ (X = Cl and Br) and pic is a general way to obtain $[(X(CO)_2(pic)_2W{\equiv}CC_6H_4R]$ complexes.[185] The acetylene substituted carbynes $[(X(CO)_2(Pic)_2W{\equiv}CC{\equiv}CR]$ are normally prepared by the Fischer method. The $W(CO)_6$ reacts with $LiC{\equiv}CR$ to form $[(CO)_5W{=}C(OLi)C{\equiv}CR]$ which is converted to $[(CF_3CO)(CO)_4W{\equiv}CC{\equiv}CR]$ or $[(Cl)(CO)_4W{\equiv}CC{\equiv}CR]$ by $(CF_3CO)_2O$ or $C_2O_2Cl_2$ respectively.[188,189]

The $[W(PMe_3)_4Cl_2]$ forms carbynes directly from alkyl or vinyl derivatives. Subsequently the reaction with $AlMe_3$ generates complex with nonsubstituted methylidyne ligand.[190] Trioxymethylsilylethylene forms a $[(Cl)(PMe_3)_4W{\equiv}CCH_3]$ complex via $(MeO)_3SiCl$ abstraction.[191]

In order to synthesize rigid-rod complexes with desired electronic properties a most efficient strategy has to be applied, which combines above described metal–carbon coupling methods with carbon–carbon coupling reactions of metal containing building blocks. Design of the building blocks with predictable reactivity is especially important for the construction of long oligonuclear assemblies. Such long systems are target compounds for application in the field of molecular electronics. The most important published building blocks are listed in figure 22.[154,157,180,184,185,197,198]

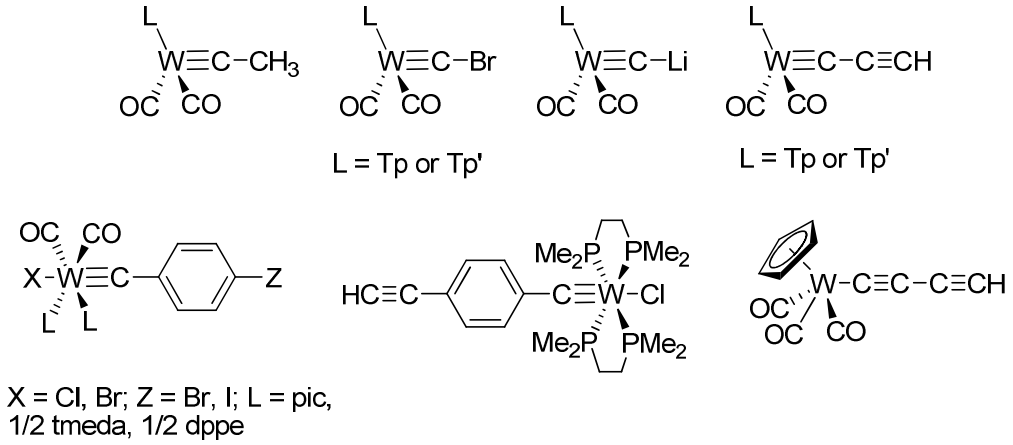

Figure 22. Building blocks for tungsten ridged-rod complexes.

None of these blocks seemed to be perfectly suitable for the construction of molecular wires. Blocks based on the $[(Tp')(CO)_2W{\equiv}C]$[157,184,197,198] fragment have "dead end" and can't be functionalized from both sides. The $[X(L)_2(CO)_2W{\equiv}C]$ (X = Cl, Br, I; L = Phosphine or amine) based compounds can be potentially elongated from both sides, but they are expected have irreversible redox properties.[185,199] The $[W(CO)_3(Cp)]$ fragment show both problems.[154,155] The block with $[Cl(dmpe)_2W{\equiv}C]$ fragments probably is suited best for the target combination of

properties.[180] However strongly donating dmpe ligands make them easily oxidizable. Based on all these finding, we can finally formulate the requirements for the ideal building blocks:

- Easy and controllable functionalization from both sides
- Reversible redox properties
- Maximum chemical and thermal stability

III. FORMULATION OF GOALS AND STRUCTURE OF WORK

As could be seen even from a short literature overview, molecular electronics is a fast growing field where metal containing compounds can play an important role. The metal centers could be attributed special functions to:

- increase of the tunneling efficiency by decrease of HOMO-LUMO gap;
- hopping type of conductance;
- appearance of such effects as Coulomb blockade, Kondo resonance and NDR.

It seems to be a rational way to control conductance by redox switching and switch of spin states. However, the number of metal complexes investigated in single molecule studies is very limited. Therefore the design and synthesis of new metal bearing single molecular conductors is a timely issue in molecular electronics especially with respect to the development of memory elements.

The main requirement for molecular wire to be studied by single molecular studies and to be introduced in circuitry is the presence of anchoring groups. Usually the high reactivity of anchor groups complicates the synthesis of metal containing molecular wires and limits the choice of the metal center. The main requirements for the applicability of metal center are:

- reversible redox properties;
- chemical inertness, especially with respect to anchor group properties.

As result, the yet published work concentrated more on ruthenium compounds, but they have the disadvantage of relatively low lyiring HOMOs, which makes them relatively hard to be oxidized.

Systematic studies of metal based molecular wires need variations of the metal center and in this work we thought to design systems based on a new metal centers, which preferably possess lower oxidation potential then the widely used ruthenium building blocks, but remain with similar chemical stability. The $W(dppe)_2$ fragment was chosen because compounds based on it usually have reversible redox properties at low potentials and the two bulky dppe ligands well protect the metal center from attack by reactive molecules. Realization of this idea was supposed to be carried out stepwise:

- development of the synthetic methods needed for the preparation of $W(dppe)_2$ based molecular wires;
- study of metal ··· metal interaction in the prepared compounds by electrochemical and spectroscopic methods;
- synthesis of molecules equipped by appropriate anchor groups;
- determination of single molecular conductivity.

IV. PUBLICATIONS

IV.1. Publication 1

Self-Coupling of a 4-H-Butatrienylidene Tungsten Complex

*Sergey N. Semenov, Olivier Blacque, Thomas Fox, Koushik Venkatesan, and Heinz Berke**

Department of Inorganic Chemistry, University of Zürich, Winterthurerstrasse 190, 8057 Zürich, Switzerland.

Angew. Chem. Int. Ed. **2009**, *48*, 5203-5206.

DOI: 10.1002/anie.200901914

Metallacumulenes

Self-Coupling of a 4-H-Butatrienylidene Tungsten Complex**

*Sergey N. Semenov, Olivier Blacque, Thomas Fox, Koushik Venkatesan, and Heinz Berke**

Organometallic complexes with cumulated π systems as bridges have gained importance in view of potential applications in the emerging field of molecular electronics.[1] Metallacumulenes by themselves are an interesting class of molecules that have been intensively investigated for their unique structural, reactive, and material properties.[2] Although metallacumulenes $[L_xM{=}C(=C)_nRR']$ (R, R′ = metal fragment or aromatic groups) with $n \geq 3$ have been isolated and characterized, cumulenes of the type $[L_xM{=}C(=C)_3HR]$, where R is an organic group, have not been isolated to date.[3] The terminal R groups apparently have significant influence on the stability of such systems, and this has triggered a search for such stable systems with simple terminal organic functionalities.[3a] Cumulenes bearing metal derived substituents at their terminal ends remain stable, but often display uncontrolled reactivity that is less suited for the preparation of new materials.[4] Herein we report the synthesis and characterization of a new stable and terminal secondary butatrienylidene complex of the type $[L_xM{=}C(=C)_3HR]$.

Organic cumulenes are known to undergo "self-coupling" by a [2+2] addition reaction.[5] Homocoupling reactions have been observed with metal vinylidene complexes, which have resulted in the formation of dinuclear complexes with π-conjugated bridges that have interesting electronic properties.[6] However, self-coupling reactions of metal allenylidenes and longer cumulenylidenes remain elusive. One of the reasons for the absence of such coupling reactions can be attributed to the lack of H-substituted cumulenylidenes of the type $[L_xM{=}C(=C)_nHR]$. Herein, we demonstrate the unprecedented reductive coupling of a butatrienyl complex.

We envisaged that tungsten butatrienyl complexes of the type $[W(CO)(dppe)_2\{C{=}C{=}C{=}C(SnMe_3)(R)\}]$ could be prepared by the reaction of a 1,3-butadiyne tin derivative with an electron-rich metal complex $[W(CO)(N_2)(dppe)_2]$ (**1**; dppe = tetraphenyl-1,2-diphosphinoethane) containing a labile N_2 ligand.[7] Intermediate formation of a but-1-en-3-ynylidene species was expected to be followed by migration of the tin group to the terminal position. To stabilize the cumulenic complex, the butadiyne $Me_3SnC{\equiv}CC{\equiv}C(p\text{-}C_6H_4t\text{Bu})$ was selected as the acetylenic precursor, as after subsequent deprotection of the ligand, a stable product was expected. Compound **1** indeed reacts with $Me_3SnC{\equiv}CC{\equiv}C(p\text{-}C_6H_4t\text{Bu})$ in an evacuated Young's tube at 55 °C for 6 h (Scheme 1; see the Supporting Information for details).

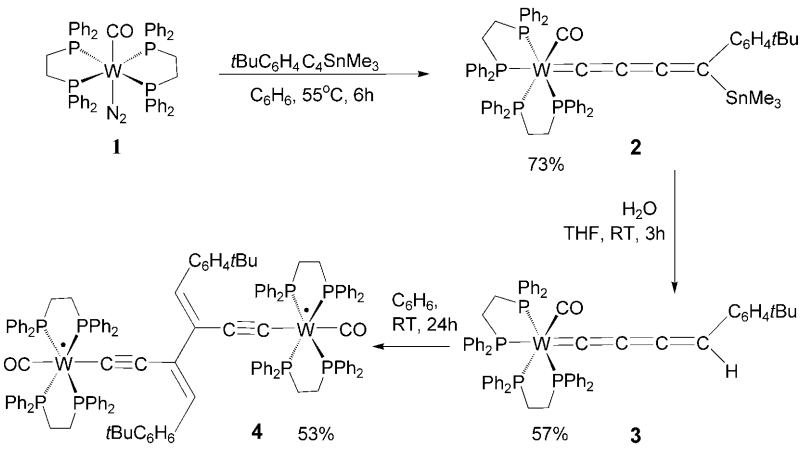

Scheme 1. Formation of compounds **2**–**4**.

The product $[W(CO)(dppe)_2\{C{=}C{=}C{=}C(SnMe_3)(p\text{-}C_6H_4t\text{Bu})\}]$ (**2**) was isolated as red crystals in 73% yield. The ^{31}P NMR spectrum revealed the *cis* position of the diphosphines, and the ^{13}C NMR spectrum showed four resonances for the C_4 cumulenic chain at $\delta = 267.6$ ($W{=}C_\alpha$), 162.6 ($=C_\beta=$), 140.0 ($=C_\gamma=$), and 70.7 ppm ($=C_\delta(SnMe_3)(p\text{-}C_6H_4t\text{Bu})$). These data are comparable to those obtained for MnC_4 derivatives.[3a] The C–Sn bond in **2** is very reactive, and removal of $SnMe_3$ was easily achieved with equimolar amounts of water in the form of a 0.01% THF solution. The deprotected compound $[W(CO)(dppe)_2\{C{=}C{=}C{=}CH(p\text{-}C_6H_4t\text{Bu})\}]$ (**3**) was fully characterized by NMR and IR spectroscopy and elemental analysis. The presence of the terminal $CH(p\text{-}C_6H_4t\text{Bu})$ group in **3** was confirmed by (^1H,^{13}C) correlation, ^{13}C-DEPT, and $^1H\{^{31}P\}$-decoupling NMR experiments. The $CH(p\text{-}C_6H_4t\text{Bu})$ protons appear at $\delta = 3.74$ ppm as a triplet with $^6J(^1H,^{31}P) = 4.0$ Hz. The solid-state structures of **2** (see the Supporting Information) and **3** (Figure 1) were confirmed by an X-ray diffraction study.[8] Both complexes have similar structural parameters. The

[*] S. N. Semenov, Dr. O. Blacque, Dr. T. Fox, Dr. K. Venkatesan, Prof. Dr. H. Berke
Department of Inorganic Chemistry, University of Zürich
Winterthurerstrasse 190, 8057 Zürich (Switzerland)
Fax: (+41) 44-635-6802
E-mail: hberke@aci.uzh.ch
Homepage: http://www.aci.uzh.ch

[**] We thank S. Weyeneth, F. Muranyi and A. Tsirlin for help with the magnetic measurements. Funding from the Swiss National Science Foundation (SNSF) and from the University of Zürich are gratefully acknowledged.

Supporting information for this article is available on the WWW under http://dx.doi.org/10.1002/anie.200901914.

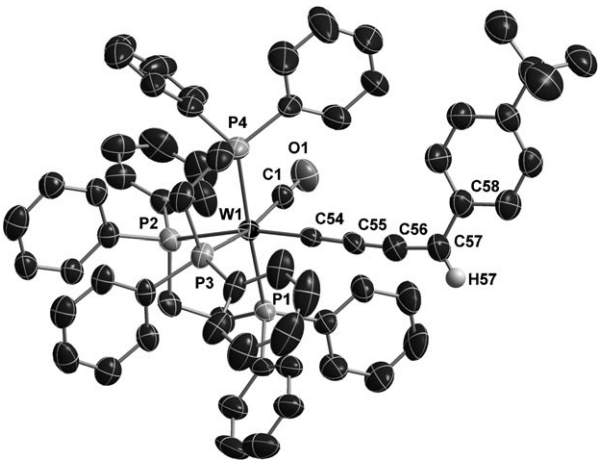

Figure 1. Molecular structure of **3** (ellipsoids set at 50% probability). Apart from H57, hydrogen atoms are omitted for clarity. Selected bond lengths [Å]: W1–C54 1.915(6), C54–C55 1.305(8), C55–C56 1.274(9), C56–C57 1.349(9).

unsaturated carbon chain deviates only slightly from linearity. The C54–C55 and C56–C57 bonds are both longer than the internal C55–C56 bond. This is in contrast to Ir-C_4 and Mn-C_4 cumulenic species.[3a,9] Prolonged storage of **3** in solution at room temperature resulted in [3,3′-bis{*trans*-(4-*p*-*tert*-butylphenylbuta-3-en-1-yl)bis(tetraphenyl-1,2-diphosphinoethane)carbonyltungsten}] (**4**; Scheme 1), and diffusion of pentane into a benzene solution of **3** gave brown crystals of the coupled molecule in 53% yield. Formation of **4** can be envisaged to occur by coupling at the C3 atom of **3** with subsequent rearrangement of the diphosphine ligands from *cis* to *trans*.[7] Such a dimerization process has only been observed for organic butatrienes to date;[10] however, the mechanism pertaining to the organic analogue cannot be applied to the reaction of **3**.

Among many pathways, a [2+2] cycloaddition process with the formation of a cyclobutane intermediate **A** is putatively preferred (Scheme 2), as it has been frequently observed with organic cumulenes and was also detected earlier for metal cumulenes.[5,11] Thus it could be rationalized that the reaction of **3** proceeds through a [2+2] cycloaddition between the terminal C_γ=C_δ double bonds, forming a intermediate **A**. Owing to the electron-accepting ability of the energetically very low-lying LUMO of the bisallenylidene system and the energetically high-lying d orbital of the metal, a two-electron metal-to-ligand redox process takes place. This process presumably occurs with stepwise electron transfers, forming a cyclobutene intermediate **B**, which subsequently opens by an electrocyclic reaction. DFT calculations of the LUMOs of allenylidene, butatrienylidene, and the bisallenylidene ligands revealed energies of −3.26, −2.98, and −4.99 eV, respectively, making clear that the bisallenylidene is the most susceptible system for the internal redox process.[12] Recently, such internal redox processes leading often to antiferromagnetic ground states have been more frequently observed.[13] The observed stereochemistry demands formation of mainly the *Z*,*Z* stereoisomer that originates from the sterically controlled *trans* position of the

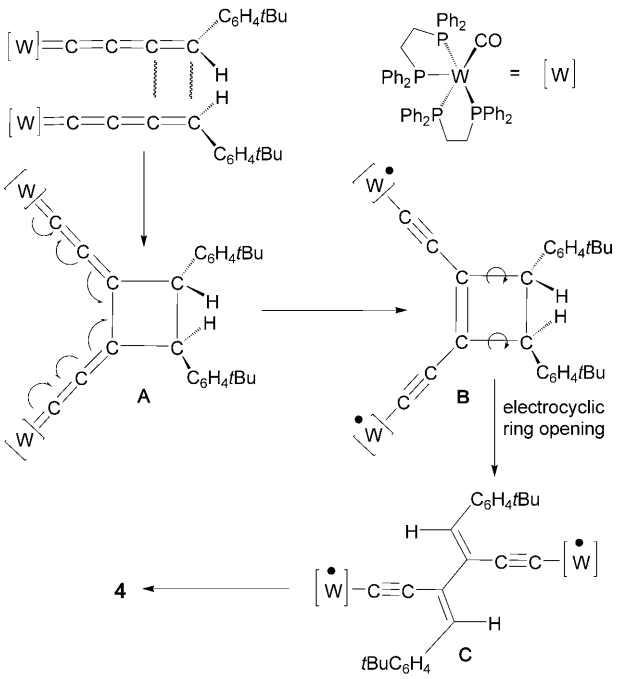

Scheme 2. Plausible mechanism for dimerization of **3**.

p-C_6H_4*t*Bu substituent in **A**. This formation is followed by stereoselective conrotatory electrocyclic ring-opening, leading to *E*,*E* or *Z*,*Z* stereoisomers of **C**, where *Z*,*Z* is sterically preferred. This mechanism is consistent with the stability of the tin derivative, in which the bulky $SnMe_3$ group prevents the initial approach of the double bonds.

The kinetics of the reaction were investigated by probing the concentration dependence of the dimerization reaction of **3**; the concentration was monitored by integration of the $C_\delta H$ proton signal in the ^{1}H NMR spectrum (Figure 2). The data

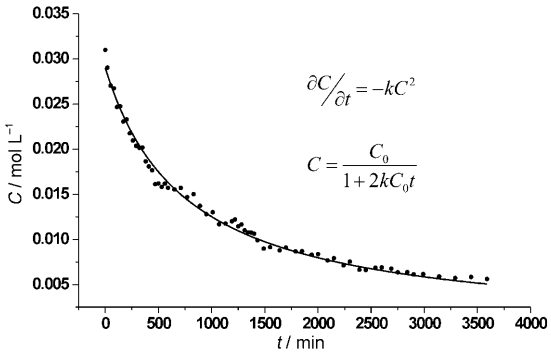

Figure 2. Time dependence of the concentration of **3** in the dimerization process at 25 °C. C_{start} = 0.031 mol L^{-1}.

could be fitted with second-order kinetics; the estimated rate constant *k* is 0.0227 L mol^{-1} min^{-1}. The second-order nature of the reaction additionally confirms that the rate-limiting step involves two parent molecules. The calculated value of ΔU from DFT calculations for the dimerization process is 22.3 kcal mol^{-1}.

The molecular structure (Figure 3) of **4** revealed an octahedral tungsten center with a squared phosphorus environment and an average W-P distance of 2.475(1) Å and mutually *trans* CO and alkynyl ligands.[8] The conjugated

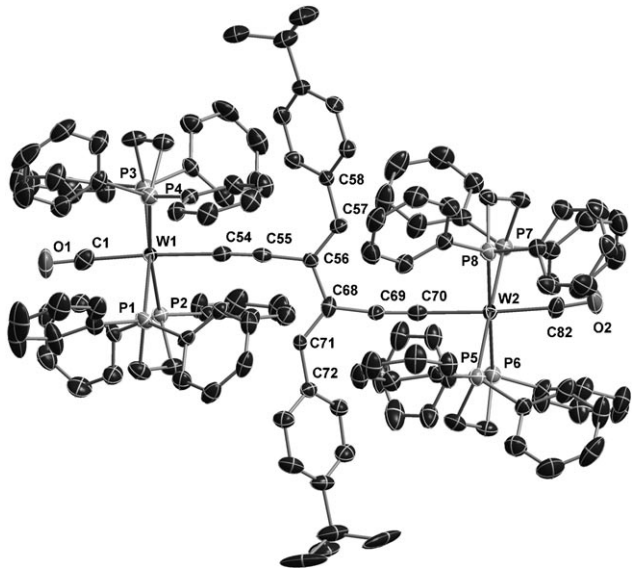

Figure 3. Molecular structure of **4** (ellipsoids set at 50% probability). Hydrogen atoms are omitted for clarity. Selected bond lengths [Å]: W1–C54 2.160(5), C54–C55 1.215(7), C55–C56 1.459(7), C56–C57 1.340(6), C56–C68 1.495(6), C71–C68 1.374 (7), C68–C69 1.444(7), C69–C70 1.233(7), W2– C70 2.176(5). Non-bonding and average distances [Å]: W1–W2 10.323(1), C(sp)≡C(sp) 1.224(7), C(sp^2)=C(sp^2) 1.357(6), C(sp)–C(sp^2) 1.452(6).

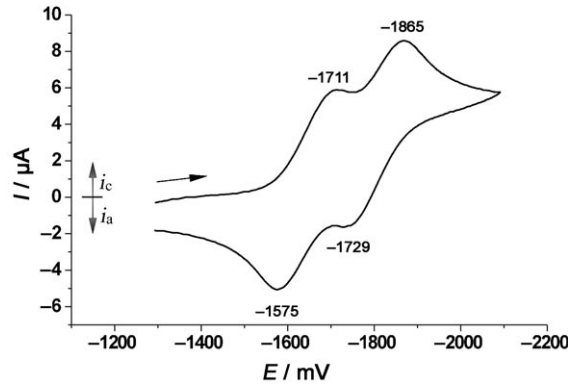

Figure 4. Cyclic voltammogram for **4** in 0.1 M [nBu$_4$N][PF$_6$]. Pt electrode, E versus Fc$^{0/+}$, scan rate = 50 mV s^{-1}, 20 °C.

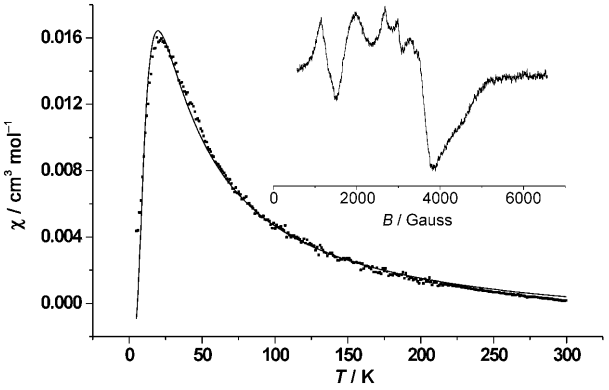

Figure 5. Temperature dependence of the molar magnetic susceptibility χ versus temperature T for **4**. The inset shows the EPR spectrum of solid **4** at 10 K.

part of the molecule is almost planar, with an average deviation of the atoms from the plane (C54–C58/C68–C72/W1/W2) of 0.14(1) Å. Based on the C–C bond lengths, compound **4** indeed possesses an 2,3-ethynyl substituted 1,3-butadiene bridge. The bridge in **4** is very reminiscent of the cross-conjugation of π systems, which is crucial to precisely control electron conduction along two different directions that would enable the creation of two-way molecular electronic switches. Metal centers with a d^5 low spin configuration as in **4** have interesting electrochemical and magnetic properties.

To probe the redox behavior of the open-shell molecule **4**, cyclic voltammetry studies were carried out, and show two reversible stepwise reductions filling the electronic holes at the tungsten centers (Figure 4). Furthermore, **4** undergoes an irreversible two-electron oxidation. The peak separation $\Delta E = 154$ mV for reversible reduction results in a comproportionation constant $K_c = 400$, which shows that it is a class II compound according to the Robin and Day classification,[14] which is quite reasonable for a C_6 bridge with a moderately delocalized π system.

The magnetic properties of **4** were established by variable-temperature magnetization measurements and by EPR spectroscopy (Figure 5). The magnetic susceptibility of **4** shows a maximum at 20 K (the Neel temperature), and it drops considerably on going to higher temperatures. Thus, the magnetic behavior of **4** is typical of an antiferromagnetically coupled spin dimer.

To obtain an estimate of the exchange coupling, we fitted the experimental data with equation for a spin-$^1/_2$ dimer model:

$$\chi = \frac{2N_A g^2 \beta^2}{kT} \cdot \frac{1}{(3 + e^{J/kT})} + \chi_0$$

with g, J, and χ_0 as parameters. The χ_0 accounts for core diamagnetism, van Vleck paramagnetism, and other temperature-independent contributions. The derived J indicates a singlet–triplet gap equal to -21 cm^{-1}, which is similar to that observed for tungsten(V) dinuclear μ-phenolate complexes.[15] The antiferromagnetic nature of the spin interactions can be explained by the spin-polarization mechanism involving six p orbitals of the bridge.[16]

A very broad signal centered about $g = 1.9$ was observed in EPR spectra. A more narrow signal at $g = 5.0$ is associated with transition having $\Delta m_s = 2$ (simultaneous flipping of two electron spins). A similar kind of behavior has been observed for compounds with two tungsten(V) centers.[15]

In conclusion, we have shown for the first time that a 4-H metal butatrienylidene, such as [W(CO)(dppe)$_2${C=C=C=C(H)(R)}], becomes stable when it has an aromatic organic terminal functionality. Under controlled reaction conditions, it was serendipitously found that this molecule undergoes an unusual coupling at the 3-position of the carbon chain to form a novel diethynyl butadiene bridged dimer **4** with interesting electrochemical and magnetic properties. The unique combination of a cross-conjugated π system and paramagnetic centers makes this type of molecule a unique model for the investigation of the Kondo effect on the molecular level.[17] The carbon framework in this transformation involves a complex sequence and comprises the three-step conversion of the butadiyne into the final diethynyl butadiene via a butatreienylidene species. We believe that this work opens interesting avenues in the field of organometallic cumulene chemistry and molecular electronics.

Received: April 9, 2009
Published online: June 12, 2009

Keywords: cumulenes · dimerization · molecular devices · tungsten · π-conjugation

[1] a) C. Joachim, J. K. Gimzewski, A. Aviram, *Nature* **2000**, *408*, 541 – 548; b) V. Balzani, A. Credi, M. Venturi, *Chem. Eur. J.* **2002**, *8*, 5524 – 5532; c) R. L. Carroll, C. B. Gorman, *Angew. Chem.* **2002**, *114*, 4556 – 4579; *Angew. Chem. Int. Ed.* **2002**, *41*, 4378 – 4400; d) N. J. Tao, *Nat. Nanotechnol.* **2006**, *1*, 173 – 181.

[2] For reviews, see: a) M. I. Bruce, *Chem. Rev.* **1998**, *98*, 2797 – 2858; b) M. I. Bruce, *Coord. Chem. Rev.* **2004**, *248*, 1603 – 1625; c) H. Fischer, N. Szesni, *Coord. Chem. Rev.* **2004**, *248*, 1659 – 1677.

[3] a) K. Venkatesan, F. J. Fernandez, O. Blacque, T. Fox, M. Alfonso, H. W. Schmalle, H. Berke, *Chem. Commun.* **2003**, 2006 – 2008; b) F. Coat, M. Guillemot, F. Paul, C. Lapinte, *J. Organomet. Chem.* **1999**, *578*, 76 – 84; c) M. I. Bruce, P. Hinterding, M. Z. Ke, P. J. Low, B. W. Skelton, A. H. White, *Chem. Commun.* **1997**, 715 – 716; d) R. F. Winter, F. M. Hornung, *Organometallics* **1999**, *18*, 4005 – 4014; e) R. F. Winter, *Eur. J. Inorg. Chem.* **1999**, 2121 – 2126.

[4] a) S. Kheradmandan, K. Heinze, W. H. Schmalle, H. Berke, *Angew. Chem.* **1999**, *111*, 2412 – 2415; *Angew. Chem. Int. Ed.* **1999**, *38*, 2270 – 2273; b) M. Brady, W. Weng, Y. Zhou, J. W. Seyler, A. J. Amoroso, A. M. Arif, M. Böhme, G. Frenking, J. A. Gladysz, *J. Am. Chem. Soc.* **1997**, *119*, 775 – 788.

[5] a) M. Iyoda, S. Tanaka, H. Otani, M. Nose, M. Oda, *J. Am. Chem. Soc.* **1988**, *110*, 8494 – 8500; b) Y. Kuwatani, G. Yamamoto, M. Oda, M. Iyoda, *Bull. Chem. Soc. Jpn.* **2005**, *78*, 2188 – 2208; c) N. Islam, T. Ooi, T. Iwasawa, M. Nishiuchi, Y. Kawamura, *Chem. Commun.* **2009**, 574 – 576.

[6] For example, see: a) K. Venkatesan, O. Blacque, T. Fox, M. Alfonso, H. W. Schmalle, H. Berke, *Organometallics* **2004**, *23*, 1183 – 1186; b) S. R. Iyer, J. P. Selegue, *J. Am. Chem. Soc.* **1987**, *109*, 910 – 911; c) J. P. Selegue, *J. Am. Chem. Soc.* **1983**, *105*, 5921 – 5923.

[7] a) G. Nakamura, Y. Harada, Y. Mizobe, M. Hidai, *Bull. Chem. Soc. Jpn.* **1996**, *69*, 3305 – 3315; b) T. Ishida, Y. Mizobe, T. Tanase, M. Hidai, *J. Organomet. Chem.* **1991**, *409*, 355 – 365.

[8] CCDC 726867 (**2**), 726868 (**3**), and 726869 (**4**) contain the supplementary crystallographic data for this paper. These data can be obtained free of charge from The Cambridge Crystallographic Data Centre via www.ccdc.cam.ac.uk/data_request/cif. The details of data collection and refinement are available in the Supporting Information.

[9] K. Ilg, H. Werner, *Angew. Chem.* **2000**, *112*, 1691 – 1693; *Angew. Chem. Int. Ed.* **2000**, *39*, 1632 – 1634.

[10] N. Suzuki, H. Tezuka, Y. Fukuda, H. Yoshida, M. Iwasaki, M. Saburi, M. Tezuka, T. Chihara, Y. Wakatsuki, *Chem. Lett.* **2004**, *33*, 1466 – 1467.

[11] a) S. Rigaut, L. L. Pichon, J.-C. Daran, D. Touchard, P. H. Dixneuf, *Chem. Commun.* **2001**, 1206 – 1207; b) M. I. Bruce, B. G. Ellis, B. W. Skelton, A. H. White, *J. Organomet. Chem.* **2005**, *690*, 1772 – 1783.

[12] See the Supporting Information for computational details.

[13] S. C. Bart, K. Chopek, E. Bill, M. W. Bouwkamp, E. Lobkovsky, F. Neese, K. Wieghardt, P. J. Chirik, *J. Am. Chem. Soc.* **2006**, *128*, 13901 – 13912.

[14] M. B. Robin, P. Day, *Adv. Inorg. Chem. Radiochem.* **1967**, *10*, 247 – 422.

[15] K. M. Stobie, Z. R. Bell, T. W. Munhoven, J. P. Maher, J. A. McCleverty, M. D. Ward, E. J. L. McInnes, F. Totti, D. Gatte, *Dalton Trans.* **2003**, 36 – 45.

[16] A. M. W. Cargill Thompson, D. Gatteschi, J. A. McCleverty, J. A. Navas, E. Rentschler, M. D. Ward, *Inorg. Chem.* **1996**, *35*, 2701 – 2703.

[17] W. Liang, M. P. Shores, M. Bockrath, J. R. Long, H. Park, *Nature* **2002**, *417*, 725 – 729.

Angewandte Chemie
Eine Zeitschrift der Gesellschaft Deutscher Chemiker

Supporting Information

69451 Weinheim, Germany

Supporting Information

Self-Coupling of a 4-H-Butatrienylidene Tungsten Complex

Sergey N. Semenov, Olivier Blacque, Thomas Fox, Koushik Venkatesan, and Heinz Berke

General Procedures: All the manipulations were carried out under a nitrogen atmosphere using Schlenk techniques or a drybox. Reagent grade benzene, toluene, hexane, pentane, diethyl ether, and tetrahydrofuran were dried and distilled from sodium benzophenone ketyl prior to use. Dichloromethane and acetonitrile were distilled from CaH_2. The literature procedures were used to prepare the following compounds: HC≡CC≡C(p-C_6H_4*t*Bu) [1], [(dppe)$_2$W(CO)(N_2)] [2]. The Me_3SnC≡CC≡C(p-C_6H_4*t*Bu) was obtained from HC≡CC≡C(p-C_6H_4*t*Bu) using general protocol from literature [3]. All other chemicals were used as obtained from commercial suppliers. IR spectra were obtained on a Bio-Rad FTS-45 instrument. NMR spectra were measured on a Varian Mercury spectrometer at 200 MHz for ^{1}H and 81 MHz for ^{31}P{1H} and on a Bruker-DRX-500 spectrometer at 500 MHz for ^{1}H and 125.8 MHz for ^{13}C{1H}. Chemical shifts for ^{1}H and ^{13}C are given in ppm relative to the solvent signals. X-band EPR spectra were obtained using Bruker EMX Electron Spin Resonance system. Magnetization measurements were done on the Quantum Design SQUID magnetometer, molar magnetic susceptibility was calculated according to the equation $\chi = (M \cdot Mw)/(m \cdot H)$, where M – experimental magnetization, Mw – molecular weight, m – sample weight, H – magnetic field. Cyclic Voltammetry data were obtained using BAS100B potentiostat connected to three electrode low volume cell. Measurements were done in THF solution ($1 \cdot 10^{-3}$ M) with 0.1M [nBu_4N][PF_6] as supporting electrolyte, Pt working electrode, scan rate = 50 mV/s, 20 ºC.

Me_3SnC≡CC≡C(p-C_6H_4*t*Bu). In a Schlenk tube equipped with a sintered-glass frit HC≡CC≡C(p-C_6H_4*t*Bu) (184 mg, 1 mmol) was dissolved in diethyl ether (3 mL). After the solution was cooled to -50 °C, a solution of *n*-BuLi in hexane (1 mmol) was added dropwise. The cooling bath was removed, and the mixture was allowed to reach room temperature. The resulting solution was stirred for an additional 30 min. This solution was again cooled to -30 °C, followed by addition of small portions of Me_3SnCl (200 mg, 1 mmol) as a solid. A white fluffy solid precipitated immediately. The resulting suspension was warmed to room temperature and stirred for an additional 1 h. The solvent was removed in vacuo until an oily suspension formed. This residue was extracted with pentane, and the extract was filtered through the glass frit. Evaporation of the solvent and recrystallisation from pentane gave the pure stannylated acetylene Me_3SnC≡CC≡C(p-C_6H_4*t*Bu). Yield: 300 mg (0.870 mmol, 87 %) Anal. Calcd. for $C_{17}H_{22}Sn$: C, 59.17; H, 6.23. Found: C, 59.28; H, 6.17. ^{1}H NMR (200 MHz, C_6D_6) δ = 7.35 (d, $^3J_{H-H}$ = 8.4 Hz, 2H, C_6H_4), 6.95 (d, $^3J_{H-H}$ = 8.4 Hz, 2H, C_6H_4), 1.038 (s, 9H, *t*Bu), 0.076 (t, $^2J_{H-Sn}$ = 61 Hz, 9H, $SnMe_3$); ^{119}Sn NMR (184.6 MHz, C_6D_6) δ = -59.1 (s, $SnMe_3$); ^{13}C (125 MHz, C_6D_6) 152.3 (s,

ipso-C_6H_4tBu), 132.8 (s, C_6H_4), 125.7 (s, C_6H_4), 119 (s, ipso-C_6H_4tBu), 91.1 (s, C≡C), 91.9 (s, C≡C), 75.3 (s, C≡C), 75.1 (s, C≡C), 34.6 (s, $C(CH_3)_3$), 31.0 (s, $C(CH_3)_3$), -8.2 (s, $Sn(CH_3)_3$).

[W(CO)(dppe)$_2$(C=C=C=C(SnMe$_3$)((p-C$_6$H$_4$*t*Bu)))]. (2) $W(CO)(N_2)(dppe)_2$ (150 mg, 0.145 mmol) and $Me_3SnC{\equiv}CC{\equiv}C(p\text{-}C_6H_4tBu)$ (60 mg, 0.174 mmol) were placed in an Young-Schlenk tube in 15 mL benzene. Three freeze-pump-thaw cycles was performed on the resulting solution to remove any dissolved nitrogen. The reaction mixture was heated under vacuum at 55 ºC for 6 hours. Resulting dark-red solution was concentrated to 1.5 mL under vacuo and layered with 10 ml of pentane. The complex **2** formed as red prisms in 10 hours. Yield: 143 mg (0.106 mmol, 73 %). Single crystals suitable for X-Ray diffraction were grown by layering a benzene solution of the title compound with pentane. Anal. Calcd. for $C_{70}H_{70}OP_4SnW$: C, 62.11; H, 5.21. Found: C, 62.28; H, 5.37. IR (cm^{-1}): ν = 1803 (CO), 1940 (CO). ^{1}H NMR (500 MHz, THF-d_8) δ = 8.25 – 8.14 (m, 3H, C_6H_5), 7.70 – 6.08 (m, 41H, C_6H_5 and C_6H_4), 3.21 – 1.92 (m, 8H, CH_2), 1.26 (s, 9H, *t*Bu), 0.04 (s, 9H, $Sn(CH_3)_3$); ^{119}Sn NMR (184.6 MHz, C_6D_6) δ = -37.7 (m, $Sn(CH_3)_3$); ^{31}P NMR (81 MHz, C_6D_6) δ = 48.7 (m, 1P), 44.3 (m, 1P), 29.5 (m, 1P), 26.2 (m, 1P); ^{13}C (125 MHz, THF d_8) 267.6 (m, Cα), 222.3 (d, $^2J_{C\text{-}P}$ = 35Hz, CO), 162.6 (s, Cβ), 145.1 (s, C_6H_4), 144.2 (s, C_6H_4), 143.4 (d, $^1J_{C\text{-}P}$ = 27Hz, ipso-C_6H_5), 141.8 (d, $^1J_{C\text{-}P}$ = 30Hz, ipso-C_6H_5), 141.0 (dd, $^1J_{C\text{-}P}$ = 48Hz, $^3J_{C\text{-}P}$ = 11Hz, ipso-C_6H_5), 140.4 (s, C_6H_4), 140.0 (s, Cγ), 138.3 (d, $^1J_{C\text{-}P}$ = 26Hz, ipso-C_6H_5), 137.2 (d, $^1J_{C\text{-}P}$ = 27Hz, ipso-C_6H_5), 136.3 (d, $^1J_{C\text{-}P}$ = 26Hz, ipso-C_6H_5), 135.4 (s, C_6H_4), 134.8 (d, $^{N*}J_{C\text{-}P}$ = 11Hz, C_6H_5), 133.7 (d, $^NJ_{C\text{-}P}$ = 10Hz, C_6H_5), 133.4 (s, C_6H_5), 132.9 (d, $^NJ_{C\text{-}P}$ = 11Hz, C_6H_5), 132.3 (m, C_6H_5), 130.0 (m, C_6H_5), 129.5 (m, C_6H_5), 128.7 (d, $^NJ_{C\text{-}P}$ = 11Hz, C_6H_5), 128.5 (d, $^NJ_{C\text{-}P}$ = 11Hz, C_6H_5), 128.1 (d, $^NJ_{C\text{-}P}$ = 11Hz, C_6H_5), 127.2 (s, C_6H_5), 125.4 (s, C_6H_5), 70.7 (s, Cδ), 35.15 (s, *t*Bu), 32.06 (s, *t*Bu), 29.5 (m, CH_2), 28.1 (m, CH_2), -7.9 (t, $^2J_{C\text{-}Sn}$ = 325Hz, $Sn(CH_3)_3$).

* N = 2 for *ortho* carbons, 3 for *meta* carbons, 4 for *para* carbons. Unfortunately, reliable assignment is difficult in this case.

[W(CO)(dppe)$_2$(C=C=C=C(H)((p-C$_6$H$_4$*t*Bu)))]·2(C$_5$H$_{12}$). (3) To a THF solution (4 mL) of **2** (80 mg, 0.059 mmol), a 1% solution of water in THF (120 μL) was added. The reaction mixture was stirred for 3 h at room temperature. Conversion was monitored by ^{1}H NMR. Resulting dark-red solution was evaporated to dryness under vacuo and extracted with 15 mL of Et_2O. The resulting solution was filtered, concentrated to 2 mL and 15 mL of pentane was added to give **3** as red powder. Single crystals suitable for X-Ray diffraction were grown by layering a benzene solution of the title compound with pentane at -30 ºC. Yield: 40 mg (0.034 mmol, 57 %). Anal. Calcd. for $C_{77}H_{86}OP_4W$: C, 69.26; H, 6.49. Found: C, 69.70; H, 6.25. IR (cm^{-1}): ν = 1805 (CO), 1952 (CO). ^{1}H NMR (200 MHz, C_6D_6) δ = 8.49 – 8.35 (m, 3H, C_6H_5), 7.68 – 6.02 (m, 41H,

C_6H_5), 3.74 (q, $^6J_{H-P}$ = 4Hz 1H, =CH(p-C_6H_4*t*Bu)), 3.05 – 2.04 (m, 8H, CH_2), 1.254 (s, 9H, *t*Bu); ^{31}P (81 MHz, C_6D_6) δ = 47.8 (m, 1P), 43.8 (m, 1P), 25.6 (m, 1P), 24.4 (m, 1P); ^{13}C (125 MHz, THF d_8) 275.6 (m, Cα), 221.4 (d, $^2J_{C-P}$ = 29Hz, CO), 158.0 (m, Cβ), 144.9 (s, C_6H_4), 142.9 (d, $^1J_{C-P}$ = 32Hz, ipso-C_6H_5), 142.6 (m, Cγ), 140.7 (d, $^1J_{C-P}$ = 32Hz, ipso-C_6H_5), 140.4 (d, $^1J_{C-P}$ = 26Hz, ipso-C_6H_5), 140.1 (s, C_6H_4), 139.7 (s, C_6H_4), 138.2 (dd, $^1J_{C-P}$ = 26Hz, $^3J_{C-P}$ = 5.5Hz, ipso-C_6H_5), 136.9 (dd, $^1J_{C-P}$ = 26Hz, $^3J_{C-P}$ = 2.2Hz, ipso-C_6H_5), 135.9 (dd, $^1J_{C-P}$ = 26Hz, $^3J_{C-P}$ = 2.2Hz, ipso-C_6H_5), 135.4 (s, C_6H_4), 134.6 (d, $^{N*}J_{C-P}$ = 11Hz, C_6H_5), 133.6 (d, $^NJ_{C-P}$ = 9Hz, C_6H_5), 133.45 (d, $^NJ_{C-P}$ = 8Hz, C_6H_5), 133.35 (d, $^NJ_{C-P}$ = 8Hz, C_6H_5), 132.7 (d, $^NJ_{C-P}$ = 7Hz, C_6H_5), 132.65 (d, $^NJ_{C-P}$ = 7Hz, C_6H_5), 132.35 (d, $^NJ_{C-P}$ = 11Hz, C_6H_5), 132.05 (d, $^NJ_{C-P}$ = 11Hz, C_6H_5), 130.0 (d, $^NJ_{C-P}$ = 10Hz, C_6H_5), 129.7 – 128.6 (m, C_6H_5), 128.15 (d, $^NJ_{C-P}$ = 8Hz, C_6H_5), 125.2 (d, $^NJ_{C-P}$ = 25Hz, C_6H_5), 73.6 (s, Cδ), 34.73 (s, tBu), 32.13 (s, tBu), 28.8 (m, CH_2), 27.3 (m, CH_2).

* N = 2 for *orto* carbons, 3 for *meta* carbons, 4 for *para* carbons. Unfortunately, reliable assignment is difficult in this case.

[(*trans*-W(CO)(dppe)$_2$(C≡C−C(=C(H)(PhtBu))))$_2$] (4). The **3** (40 mg, 0.034 mmol) of was solved in 2 mL of benzene and placed into test-tube. This solution was layered with 10 mL of pentane. The brown crystals of **4** were formed in 24 hours. They were washed with benzene and dried in vacuum to give pure **4**. These crystals were used for X-Ray diffraction studies. Yield: 21 mg (0.009 mmol, 53 %). Anal. Calcd. for $C_{134}H_{124}O_2P_8W_2$: C, 67.57; H, 5.25. Found: C, 67.83; H, 5.41. IR (cm^{-1}): ν = 1785 (CO). ^{1}H NMR (200 MHz, C_6D_6) δ = 14.44 (br, C_6H_5), 11.27 (br, C_6H_5), 8.03 (br, C_6H_5), 7.30 (br, C_6H_5), 3.02 (s, tBu), -7.02 (br, C_6H_5).

Full Cyclic Voltammetry data:

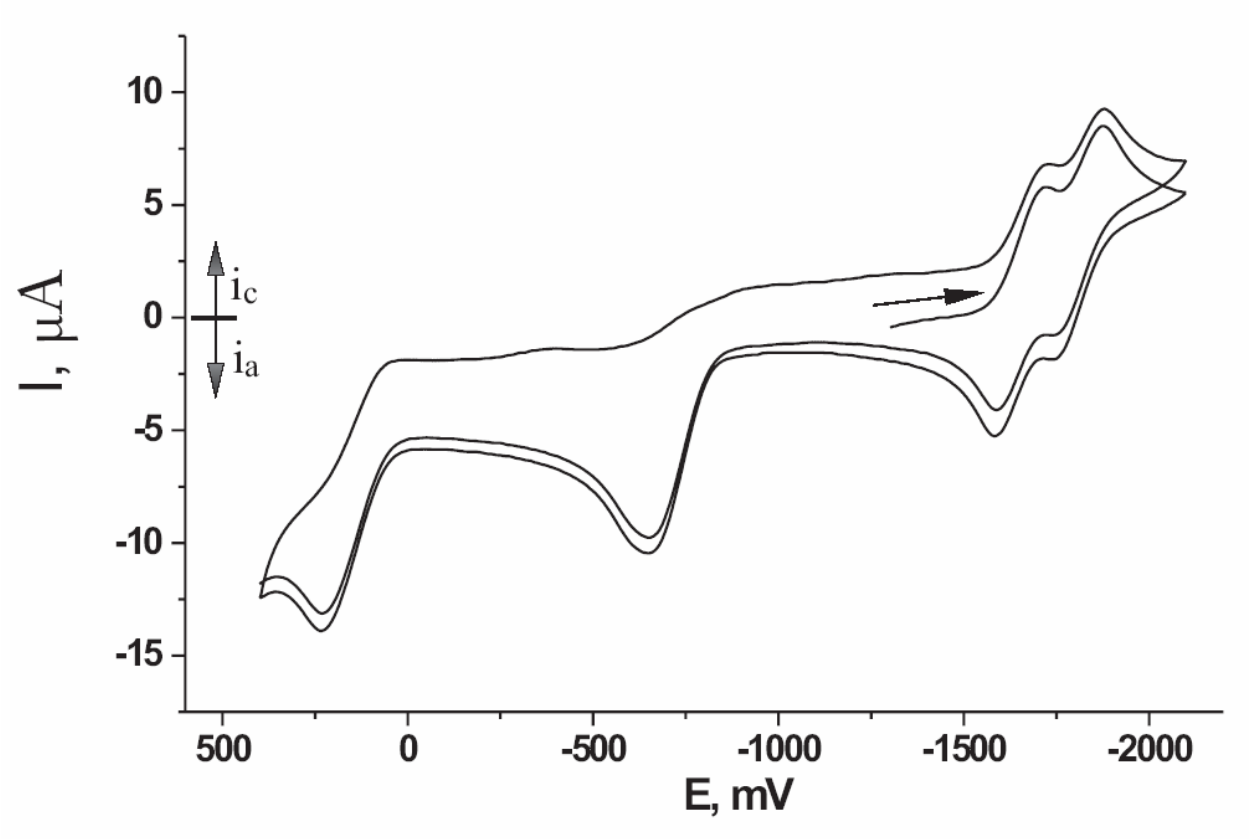

Figure 1S. Cyclic voltammogram for **4** in 0.1M $[nBu_4N][PF_6]$; Pt electrode; E *vs* $Fc^{0/+}$; scan rate = 50 mV/s; 20 ºC.

Kinetics experiment: The monomer **3** (24 mg, 0.02 mmol) was dissolved in 0.6 ml of C_6D_6 and placed into Young-Schlenk NMR tube. The NMR tube was inserted into Bruker-DRX-500 spectrometer. The ^1H NMR spectra were recorded every thirty minutes; temperature was seated at 25 °C. The concentration of **3** was monitored by integral intensity of Cδ***H*** proton (3.74 ppm) relatively intensity of ether CH_2 signal as reference. Dimerization reaction scheme is presented below:

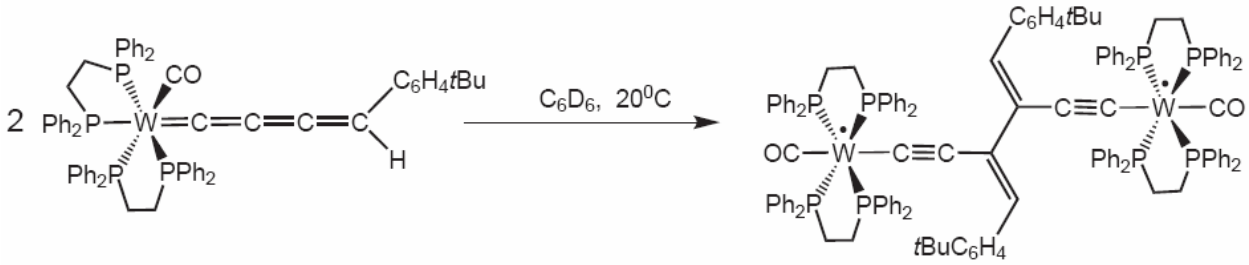

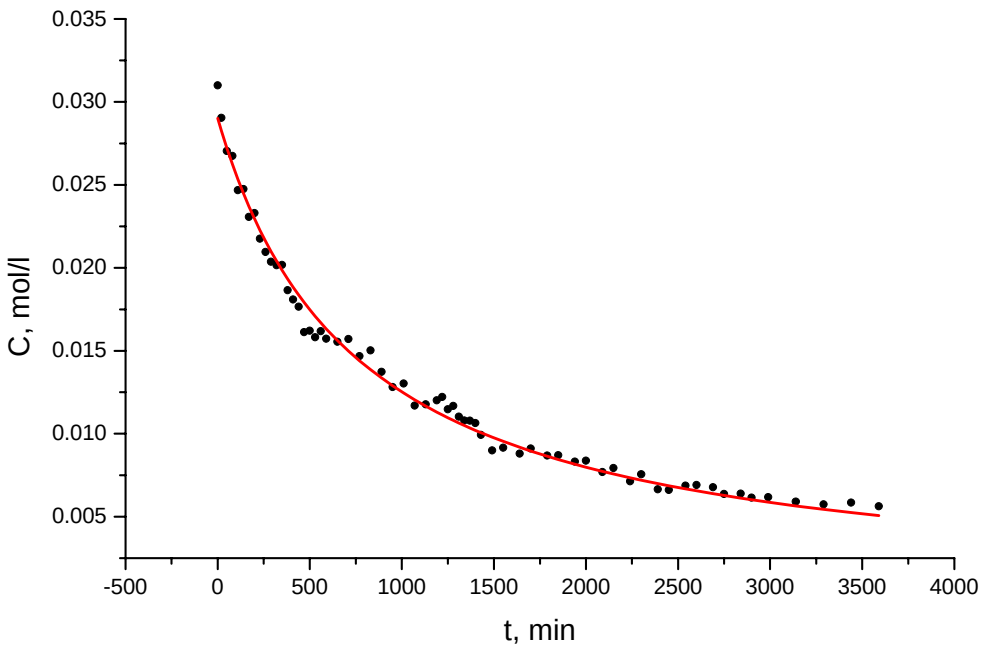

Figure 2S. Time dependence of **3** concentration in dimerization process at 25 °C, C_{start} = 0.031 mol/l

The data were attempted to fit by both first and second order reaction schemes. However, second order scheme gives much better results. Consequently, data were finally fitted by equations:

$$\partial C / \partial t = -kC^2$$

$$C = \frac{C_0}{1 + 2kC_0 t}$$

were C – concentration of monomer, t –time, k – rate constant, C_0 – initial concentration with minimized values:

$C_0 = 0.029$ *mol/l*

$k = 0.0227$ $l \cdot mol^{-1} min^{-1}$

$\chi = 4 \cdot 10^{-7}$

X-ray Diffraction: Crystallographic data were collected at 183(2) K on an Oxford Xcalibur diffractometer (4-circle kappa platform, Ruby CCD detector and a single wavelength Enhance X-ray source with MoK_α radiation, $\lambda = 0.71073$ Å).[1] The selected suitable single crystals were mounted using polybutene oil on the top of a glass fiber fixed on a goniometer head and immediately transferred to the diffractometer. Pre-experiment, data collection, face-indexing analytical absorption correction[2] and data reduction were performed with the Oxford program suite *CrysAlisPro*.[3] The structures were solved with the Patterson method and were refined by full-matrix least-squares methods on F^2 with SHELXL-97.[4] All programs used during the crystal structure determination process are included in the WINGX software.[5] The program PLATON[6] was used to check the result of the X-ray analyses. Compound **2** crystallizes with two benzene solvent molecules per asymmetric unit. The hydrogen positions were calculated after each cycle of refinement using a riding model with C-H distances in the range of 0.95 – 0.99 Å and their isotropic displacement parameters were constrained to 1.2 (aromatic C-*H* and C-H_2) or 1.5 times (C-H_3) the value of U_{eq} of the carbon atom it binds to. Compound **3** crystallizes with two ether solvent molecules. One ether molecule is positionally disordered over two positions in a ratio 0.71:0.29. The geometry of both solvent molecules was seriously restrained with DFIX / DANG commands and anisotropically refined with the help of the EADP command. All hydrogen positions were calculated after each cycle of refinement using a riding model with C-H distances in the range of 0.93 – 0.97 Å and their isotropic displacement parameters were constrained to 1.2 (aromatic C-*H* and C-H_2) or 1.5 times (C-H_3) the value of U_{eq} of the carbon atom it binds to. Compound **4** crystallizes with one pentane solvent molecule per asymmetric unit. One tertio-butyl group displays a rotational disorder in a ratio 0.48:0.52. The geometry of the pentane solvent molecule was seriously restrained and isotropically refined. Twenty-two restraints instructions were used for the final refinement using the following SHELXL-97 commands: SADI, EADP, DFIX and DANG. All hydrogen positions were calculated after each cycle of refinement using a riding model with C-H distances in the range of 0.93 – 0.97 Å and their isotropic displacement parameters were constrained t to 1.2 (aromatic C-*H* and C-H_2) or 1.5 times (C-H_3) the value of U_{eq} of the carbon atom it binds to. No classic hydrogen bonds were found in the three reported crystal structures.

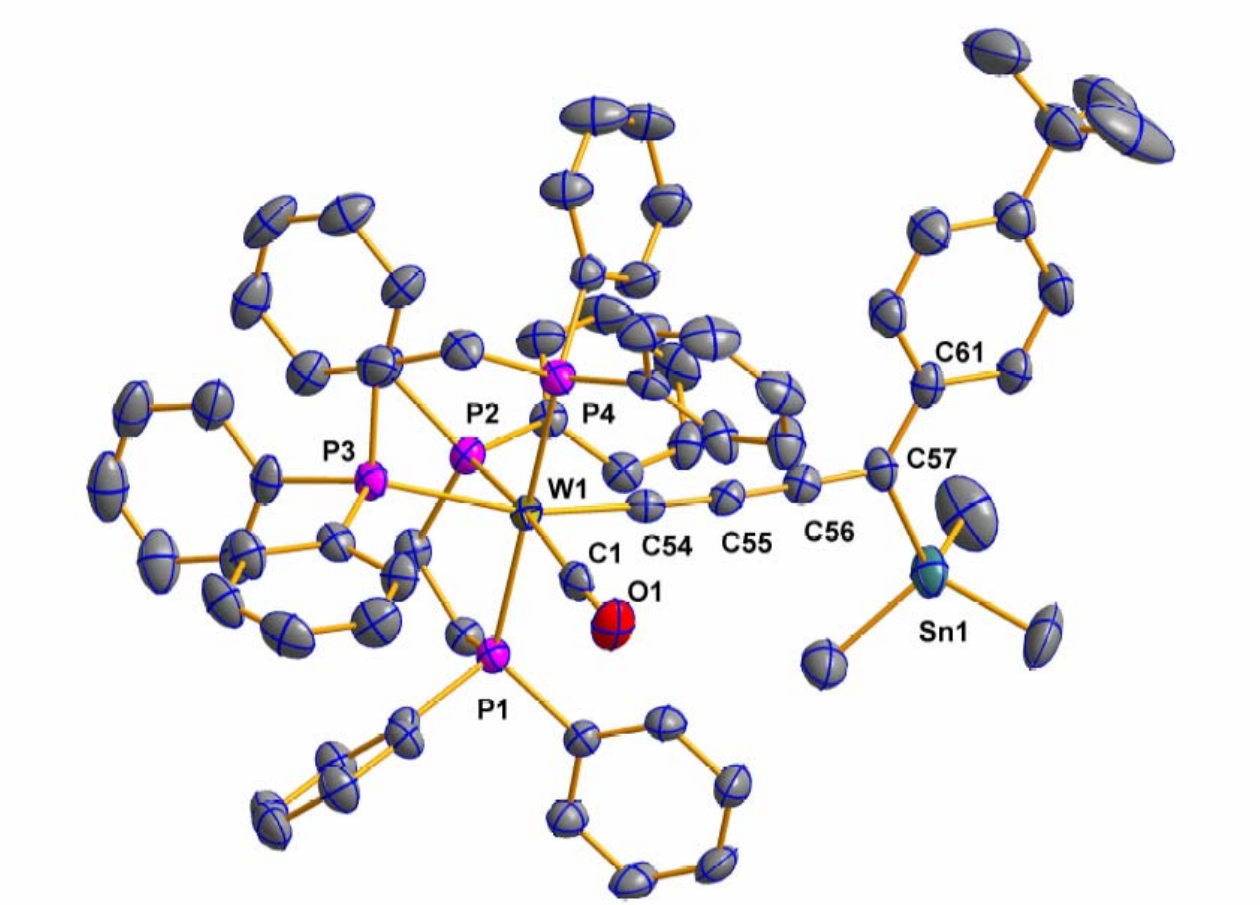

Figure 3S. ORTEP drawing of **2** (50% probability level of thermal ellipsoids). The hydrogen atoms are omitted for clarity. Selected bond lengths (Å): W1 – C54 1.923(3), C54 – C55 1.306(4), C55 – C56 1.273(4), C56 – C57 1.325(4).

Table 1S. Summary of the X-ray diffraction studies of compounds **2**, **3** and **4**.

	2	**3**	**4**
empirical formula	$C_{82}H_{82}OP_4SnW$	$C_{75}H_{82}O_3P_4W$	$C_{139}H_{136}O_2P_8W_2$
formula weight ($g \cdot mol^{-1}$)	1509.91	1339.14	2453.93
temperature (K)	183(2)	183(2)	183(2)
wavelength (Å)	0.71073	0.71073	0.71073
crystal system, space group	monoclinic, *C 2/c*	monoclinic, *P 2₁/n*	triclinic, *P -1*
a (Å)	44.6251(11)	16.2469(2)	15.3595(6)
b (Å)	12.4210(2)	18.6679(2)	19.5910(4)
c (Å)	32.1174(5) A	23.0449(2)	22.5407(6)
α (deg)	90	90	110.453(2)
β (deg)	127.559(1)	96.544(1)	93.152(3)
γ (deg)	90	90	110.950(3)
volume ($Å^3$)	14112.4(5)	6943.88(13)	5808.2(4)
Z, density (calcd) ($Mg \cdot m^{-3}$)	8, 1.421	4, 1.281	2, 1.403
abs coefficient (mm^{-1})	2.119	1.800	2.143
F(000)	6128	2760	2508
crystal size (mm^3)	0.26 x 0.14 x 0.05	0.51 x 0.39 x 0.10	0.22 x 0.17 x 0.05
θ range (deg)	2.53 to 28.28	2.36 to 26.37	2.23 to 25.68
reflections collected	62976	58686	57747
reflections unique	17479 [R(int) = 0.0528]	14123 [R(int) = 0.0491]	21988 [R(int) = 0.0477]
completeness to θ (%)	99.8	99.4 %	99.7
absorption correction	analytical	analytical	analytical
max/min transmission	0.9015 / 0.6088	0.891 / 0.579	0.919 / 0.719
data / restraints / parameters	17479 / 0 / 807	14123 / 21 / 749	21988 / 22 / 1342
goodness-of-fit on F^2	0.866	1.070	0.895
final *R1* and *wR2* indices [$I > 2\sigma(I)$]	0.0319, 0.0550	0.0533, 0.1383	0.0373, 0.0744
R1 and *wR2* indices (all data)	0.0700, 0.0599	0.0820, 0.1490	0.0748, 0.0800

The unweighted R-factor is $R_1 = \sum(Fo - Fc)/\sum Fo$; $I > 2\,\sigma(I)$ *and the weighted R-factor is* $wR2 = \{\sum w(Fo^2 - Fc^2)^2/\sum w(Fo^2)^2\}^{1/2}$.

Computational Details:

The geometry optimizations were performed with the Gaussian03 program package[9] using:

- for the organometallic species, the hybrid *m*PW1PW91 functional which includes modified Perdew-Wang exchange and Perdew-Wang 91 correlation,[10] in conjunction with the Stuttgart/Dresden double-ζ ECPs basis set (SDD)[11] for the W center and the extended 6-31G(d) basis set[12] for the remaining atoms
- for the organic species, the hybrid density functional BB1K[13] associated to the Dunning's correlation-consistent triple-zeta basis set augmented with the diffuse functions, aug-cc-pVTZ. [14]

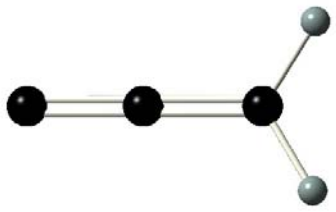

Gaussian03 - Method: BB1K – Basis set: aug-cc-pvtz

SCF Done: E(RB+HF-B95) = -115.303022773 A.U. after 6 cycles

Item	Value	Threshold	Converged?
Maximum Force	0.000007	0.000015	YES
RMS Force	0.000003	0.000010	YES
Maximum Displacement	0.000023	0.000060	YES
RMS Displacement	0.000011	0.000040	YES

Predicted change in Energy=-1.579962D-10
Optimization completed.
-- Stationary point found.

Center Number	Atomic Number	Atomic Type	Coordinates (Angstroms) X	Y	Z
1	6	0	0.000000	0.198749	0.000000
2	6	0	0.000325	-1.112534	0.000000
3	1	0	0.921875	-1.676108	0.000000
4	1	0	-0.920935	-1.676575	0.000000
5	6	0	-0.000481	1.472566	0.000000

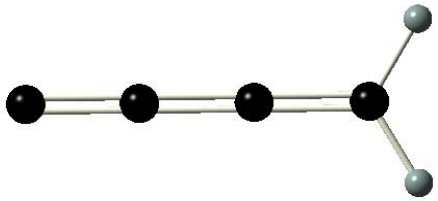

Gaussian03 - Method: BB1K – Basis set: aug-cc-pvtz

SCF Done: E(RB+HF-B95) = -153.383072286   A.U. after   6 cycles

Item	Value	Threshold	Converged?
Maximum Force	0.000002	0.000015	YES
RMS Force	0.000001	0.000010	YES
Maximum Displacement	0.000057	0.000060	YES
RMS Displacement	0.000030	0.000040	YES

Predicted change in Energy=-7.237427D-11
Optimization completed.
   -- Stationary point found.

Center Number	Atomic Number	Atomic Type	Coordinates (Angstroms) X	Y	Z
1	6	0	0.000000	0.446257	0.000000
2	6	0	0.000064	1.734489	0.000000
3	1	0	-0.928436	2.280708	0.000000
4	1	0	0.928648	2.280570	0.000000
5	6	0	-0.000030	-0.835406	0.000000
6	6	0	-0.000069	-2.105554	0.000000

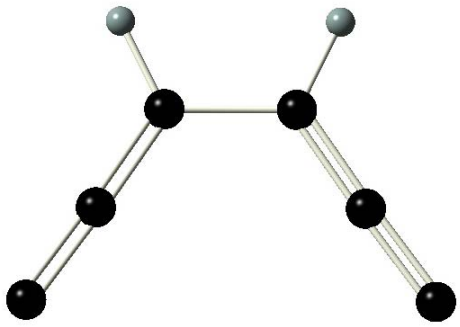

Gaussian03 - Method: BB1K – Basis set: aug-cc-pvtz

SCF Done: E(RB+HF-B95) = -229.421521898   A.U. after   8 cycles

	Item	Value	Threshold	Converged?
Maximum	Force	0.000009	0.000015	YES
RMS	Force	0.000004	0.000010	YES
Maximum	Displacement	0.000051	0.000060	YES
RMS	Displacement	0.000019	0.000040	YES

Predicted change in Energy=-3.010746D-10
Optimization completed.
   -- Stationary point found.

Center Number	Atomic Number	Atomic Type	Coordinates (Angstroms) X	Y	Z
1	6	0	0.031589	-3.139877	0.000000
2	6	0	-0.175275	-1.880307	0.000000
3	6	0	-0.437280	-0.585095	0.000000
4	1	0	-1.467106	-0.255402	0.000000
5	6	0	0.568886	0.458169	0.000000
6	1	0	0.202138	1.475388	0.000000
7	6	0	1.872732	0.243212	0.000000
8	6	0	3.138963	0.082070	0.000000

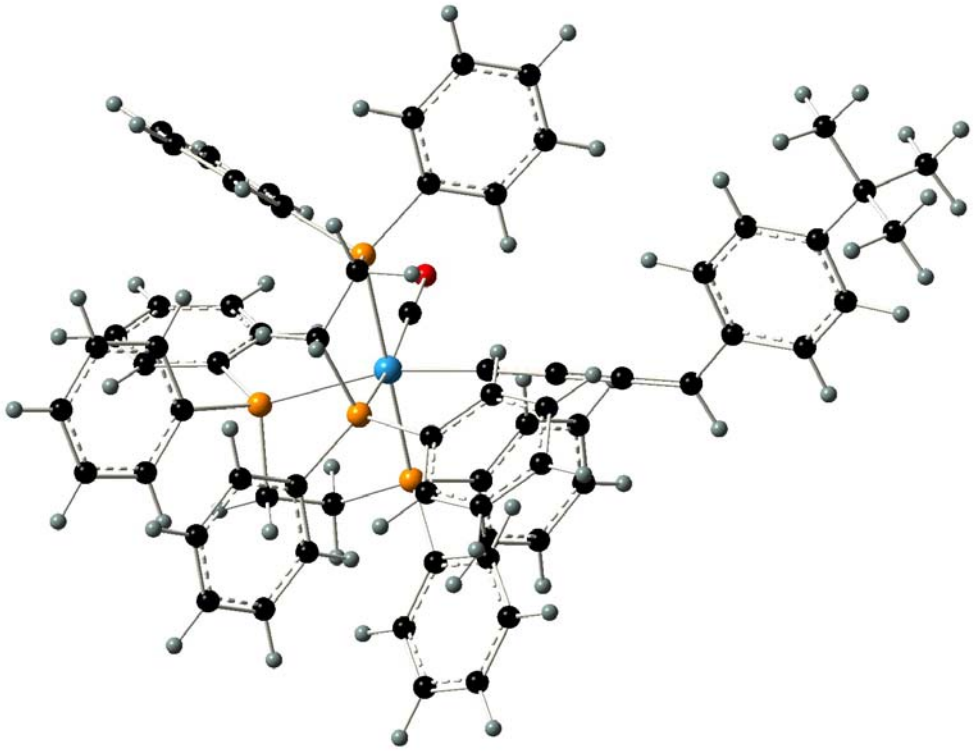

Gaussian03 - Method: mPW1PW91 – Basis set: SDD (W) and 6-31G(d) (remaining atoms)

Singlet state

SCF Done: E(RmPW+HF-PW91) = -4097.62875450   A.U. after   12 cycles

Item	Value	Threshold	Converged?
Maximum Force	0.000114	0.002500	YES
RMS Force	0.000010	0.001667	YES
Maximum Displacement	0.001445	0.010000	YES
RMS Displacement	0.000297	0.006667	YES

Predicted change in Energy=-2.396165D-07
Optimization completed.
   -- Stationary point found.

Center Number	Atomic Number	Atomic Type	Coordinates (Angstroms) X	Y	Z
1	1	0	-1.192427	-3.214117	6.732629
2	1	0	0.598333	-4.676869	5.824885
3	6	0	-0.742984	-2.990995	5.769994
4	6	0	0.263167	-3.811007	5.262242
5	1	0	-1.965532	-1.255882	5.414721
6	1	0	4.043456	2.224587	4.926007
7	6	0	-1.174380	-1.893577	5.034014
8	1	0	6.417923	2.842589	4.518617
9	6	0	0.834955	-3.526355	4.028109
10	6	0	4.515275	1.993359	3.976287
11	1	0	1.598722	-4.190118	3.634300
12	6	0	5.842997	2.339113	3.747631
13	6	0	-0.597319	-1.603599	3.798903
14	1	0	2.739330	1.108746	3.170493

15	1	0	3.123232	-1.432337	2.994163
16	6	0	0.419425	-2.411151	3.287818
17	6	0	3.776289	1.354916	2.982433
18	1	0	-0.948130	-0.756430	3.224934
19	1	0	3.324692	-3.096134	2.478015
20	8	0	0.401789	1.615804	3.230524
21	6	0	6.430085	2.035187	2.521915
22	6	0	3.013375	-2.104698	2.136271
23	1	0	7.466109	2.299598	2.333298
24	1	0	4.931551	-1.643736	1.223124
25	6	0	0.567381	1.017844	2.231617
26	6	0	4.354296	1.047209	1.746809
27	15	0	1.219934	-2.043911	1.665201
28	1	0	2.817631	-4.609939	1.219589
29	6	0	5.694880	1.392307	1.530823
30	1	0	-3.967298	3.120021	1.955792
31	6	0	3.866291	-1.629933	0.968662
32	1	0	-10.161446	1.869018	1.423100
33	6	0	1.845037	-4.701466	0.747603
34	1	0	-10.871354	0.279296	1.119971
35	1	0	3.623205	5.062745	1.811892
36	6	0	0.920292	-3.652897	0.805109
37	1	0	1.857445	3.361525	1.613451
38	1	0	-1.977005	1.808500	1.306265
39	1	0	3.709265	-2.278316	0.099559
40	6	0	-3.247795	3.545030	1.263416
41	6	0	-10.629851	1.241180	0.658590
42	1	0	6.169755	1.163605	0.583267
43	1	0	-4.966258	-2.609819	1.609478
44	1	0	-11.572387	1.713715	0.358318
45	1	0	-7.339245	-2.505623	1.329180
46	1	0	2.272878	-6.683481	0.034428
47	15	0	3.369095	0.101173	0.487380
48	6	0	1.541080	-5.881964	0.070619
49	6	0	-2.124618	2.802693	0.902087
50	1	0	-4.319070	5.395643	1.024473
51	6	0	-4.812123	-1.634540	1.148277
52	6	0	-3.559265	-1.199624	1.014118
53	6	0	-7.272071	-1.518961	0.878279
54	1	0	-9.380301	-1.378077	0.616286
55	6	0	-2.362192	-0.790791	0.876350
56	6	0	-0.319761	-3.816581	0.172004
57	6	0	3.171147	4.872429	0.844128
58	74	0	0.725872	0.109470	0.504450
59	6	0	-1.134033	-0.381539	0.671431
60	1	0	-1.045517	-3.009195	0.193326
61	6	0	-3.444379	4.818689	0.740817
62	6	0	2.174830	3.908563	0.732012
63	6	0	-8.429113	-0.873269	0.471287
64	6	0	-6.008368	-0.925443	0.719048
65	6	0	0.305883	-6.033693	-0.551243
66	1	0	5.303535	-1.558162	-1.157421
67	6	0	-0.624784	-4.998384	-0.494753
68	6	0	-5.974381	0.350274	0.134440
69	6	0	-8.399277	0.398890	-0.116748
70	1	0	-8.988555	3.139214	-0.453781
71	1	0	0.070122	-6.952572	-1.078637
72	1	0	-5.017295	0.847697	0.004726
73	6	0	-7.139442	0.989299	-0.270664
74	6	0	-9.700815	1.072711	-0.556070
75	6	0	-1.188509	3.330366	0.011116
76	1	0	-1.589564	-5.102544	-0.980332
77	6	0	4.403923	0.402565	-1.009207
78	1	0	-7.052089	1.974680	-0.715053

79	1	0	4.375812	6.325854	-0.193534
80	6	0	-2.510958	5.355294	-0.143857
81	6	0	5.251786	-0.557860	-1.569133
82	6	0	3.594243	5.577897	-0.280246
83	1	0	1.797162	-3.152812	-1.456826
84	6	0	-9.462072	2.456924	-1.167194
85	15	0	0.266013	2.340916	-0.543837
86	1	0	-10.419029	2.899431	-1.462989
87	6	0	1.580556	3.634190	-0.507424
88	1	0	-2.653785	6.351757	-0.550332
89	1	0	-10.635173	-0.796437	-1.220649
90	6	0	-1.388729	4.618117	-0.503555
91	1	0	3.446069	-4.604499	-2.556691
92	1	0	3.749564	2.452752	-1.148254
93	6	0	-10.400397	0.198168	-1.611084
94	1	0	-11.340318	0.661723	-1.932429
95	6	0	4.378842	1.682490	-1.578788
96	6	0	2.316118	-2.795141	-2.338502
97	6	0	6.047935	-0.247983	-2.670049
98	1	0	-8.831615	2.403636	-2.060659
99	1	0	-0.658694	5.055625	-1.177742
100	1	0	6.696476	-1.010115	-3.090007
101	6	0	3.245174	-3.619432	-2.966113
102	6	0	3.009788	5.317456	-1.515705
103	15	0	0.703573	-0.540342	-2.008783
104	1	0	-2.150672	-0.078411	-1.594762
105	6	0	2.009021	4.353359	-1.628595
106	1	0	-9.764563	0.068381	-2.492590
107	6	0	2.018640	-1.525561	-2.848681
108	6	0	-2.071111	-0.814388	-2.383628
109	6	0	5.174300	1.991448	-2.676754
110	6	0	6.013211	1.025375	-3.227610
111	6	0	-0.810917	-1.282789	-2.776817
112	6	0	-0.123823	2.114359	-2.344986
113	1	0	3.330007	5.864406	-2.397319
114	1	0	-1.164838	1.780010	-2.384784
115	1	0	-4.197663	-0.947738	-2.626275
116	6	0	-3.233724	-1.315821	-2.962472
117	1	0	1.576986	4.163560	-2.605087
118	6	0	3.900072	-3.185894	-4.116298
119	1	0	5.142307	2.993423	-3.093200
120	6	0	0.797777	1.069257	-2.956761
121	1	0	1.840473	1.405029	-2.903039
122	1	0	-0.085544	3.058877	-2.896745
123	6	0	-0.747531	-2.272367	-3.765976
124	1	0	4.623089	-3.827859	-4.609964
125	1	0	6.637839	1.265331	-4.082363
126	1	0	0.210950	-2.657838	-4.093054
127	6	0	-3.157032	-2.299877	-3.942883
128	6	0	2.679969	-1.103751	-4.006980
129	6	0	-1.911102	-2.775358	-4.341602
130	1	0	-4.062939	-2.698184	-4.388999
131	6	0	3.615090	-1.925643	-4.631978
132	1	0	0.540852	0.895770	-4.006821
133	1	0	-1.839167	-3.543685	-5.105518
134	1	0	2.474506	-0.131684	-4.438628
135	1	0	4.118450	-1.576647	-5.528156

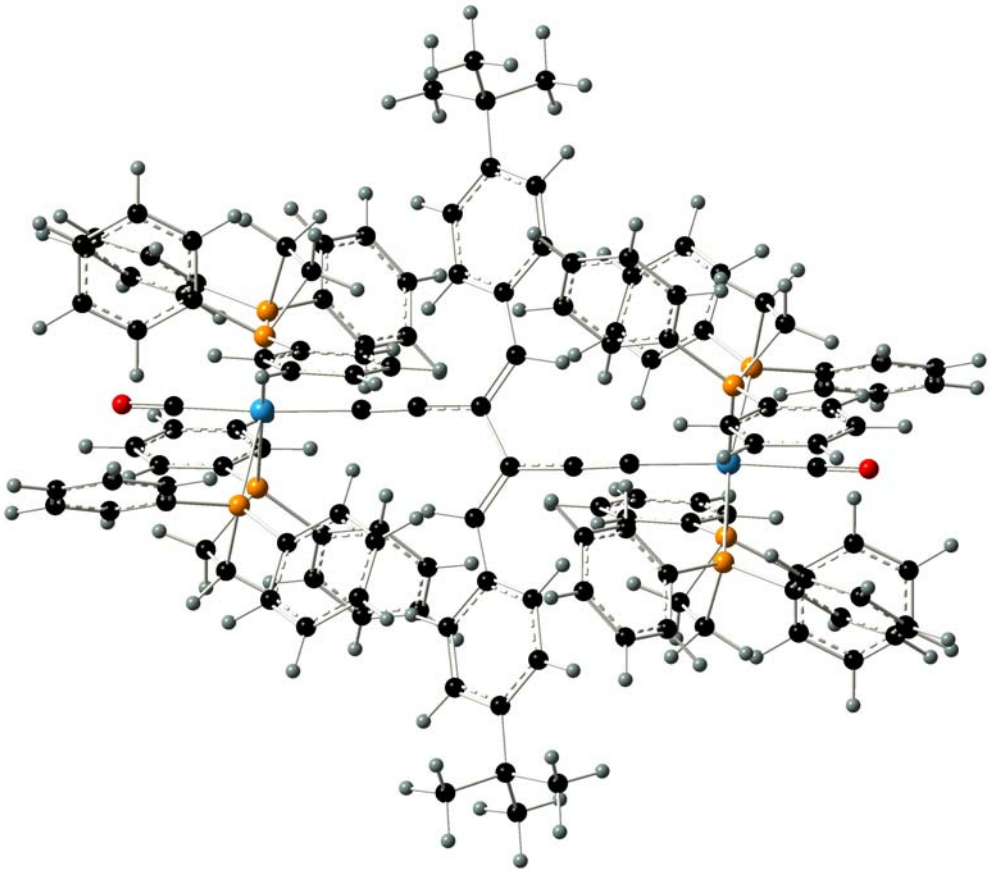

Gaussian03 - Method: mPW1PW91 – Basis set: SDD (W) and 6-31G(d) (remaining atoms)

Triplet state

SCF Done: E(UmPW+HF-PW91) = -8195.29304175 A.U. after 14 cycles

Item	Value	Threshold	Converged?
Maximum Force	0.000200	0.002500	YES
RMS Force	0.000017	0.001667	YES
Maximum Displacement	0.009155	0.010000	YES
RMS Displacement	0.001581	0.006667	YES

Predicted change in Energy=-1.823690D-06
Optimization completed.
-- Stationary point found.

Center Number	Atomic Number	Atomic Type	Coordinates (Angstroms) X	Y	Z
1	6	0	0.549006	0.516912	-0.030287
2	6	0	0.180288	1.886033	-0.207068
3	6	0	-0.549006	-0.516912	0.030287
4	6	0	-0.180288	-1.886033	0.207068
5	6	0	0.210034	-3.064644	0.290704
6	6	0	-0.210034	3.064644	-0.290704
7	74	0	0.838931	-5.161705	0.341079
8	74	0	-0.838931	5.161705	-0.341079
9	8	0	1.508203	-8.236611	0.725446
10	8	0	-1.508203	8.236611	-0.725446
11	6	0	-1.835814	-0.088675	-0.138083

12	1	0	-1.936579	0.974064	-0.335816
13	6	0	1.835814	0.088675	0.138083
14	1	0	1.936579	-0.974064	0.335816
15	6	0	-1.252580	7.103097	-0.559908
16	6	0	1.252580	-7.103097	0.559908
17	6	0	-3.108445	-0.790994	-0.068830
18	6	0	-3.322317	-1.996536	0.611615
19	6	0	-4.237881	-0.176926	-0.642787
20	6	0	-4.595060	-2.550953	0.713846
21	1	0	-2.487330	-2.485052	1.097417
22	6	0	-5.496439	-0.747650	-0.558843
23	1	0	-4.115887	0.768134	-1.163068
24	6	0	-5.713147	-1.951177	0.127476
25	1	0	-4.703911	-3.462056	1.290705
26	1	0	-6.331005	-0.231777	-1.025078
27	6	0	3.108445	0.790994	0.068830
28	6	0	4.237881	0.176926	0.642787
29	6	0	3.322317	1.996536	-0.611615
30	6	0	5.496439	0.747650	0.558843
31	1	0	4.115887	-0.768134	1.163068
32	6	0	4.595060	2.550953	-0.713846
33	1	0	2.487330	2.485052	-1.097417
34	6	0	5.713147	1.951177	-0.127476
35	1	0	6.331005	0.231777	1.025078
36	1	0	4.703911	3.462056	-1.290705
37	15	0	-2.150578	5.126001	-2.463809
38	15	0	-3.137063	4.848267	0.578509
39	15	0	0.404891	5.226444	1.838063
40	15	0	1.434097	5.862258	-1.077709
41	15	0	-0.404891	-5.226444	-1.838063
42	15	0	-1.434097	-5.862258	1.077709
43	15	0	2.150578	-5.126001	2.463809
44	15	0	3.137063	-4.848267	-0.578509
45	6	0	-7.123614	-2.534590	0.227299
46	6	0	7.123614	2.534590	-0.227299
47	6	0	7.671306	2.798740	1.185763
48	1	0	7.040594	3.516445	1.720082
49	1	0	7.714073	1.883241	1.782945
50	1	0	8.685821	3.209965	1.131884
51	6	0	7.154689	3.854219	-1.004577
52	1	0	6.801815	3.729505	-2.033250
53	1	0	6.539754	4.622364	-0.524131
54	1	0	8.181379	4.232356	-1.049068
55	6	0	8.041321	1.532108	-0.948473
56	1	0	9.059558	1.930655	-1.024362
57	1	0	8.093646	0.577129	-0.417762
58	1	0	7.676787	1.330606	-1.960777
59	6	0	-8.041321	-1.532108	0.948473
60	1	0	-8.093646	-0.577129	0.417762
61	1	0	-9.059558	-1.930655	1.024362
62	1	0	-7.676787	-1.330606	1.960777
63	6	0	-7.154689	-3.854219	1.004577
64	1	0	-6.539754	-4.622364	0.524131
65	1	0	-6.801815	-3.729505	2.033250
66	1	0	-8.181379	-4.232356	1.049068
67	6	0	-7.671306	-2.798740	-1.185763
68	1	0	-7.714073	-1.883241	-1.782945
69	1	0	-7.040594	-3.516445	-1.720082
70	1	0	-8.685821	-3.209965	-1.131884
71	6	0	4.380844	-4.930169	0.823455
72	1	0	5.330685	-5.341139	0.465686
73	1	0	4.563931	-3.890042	1.115103
74	6	0	3.861393	-5.715791	2.020885
75	1	0	3.790131	-6.780787	1.786414

76	1	0	4.532650	-5.605314	2.878815
77	6	0	-2.696051	-5.656258	-0.302098
78	1	0	-3.612492	-5.228907	0.113716
79	1	0	-2.947377	-6.644800	-0.695154
80	6	0	-2.152350	-4.763376	-1.408201
81	1	0	-2.098322	-3.729787	-1.057477
82	1	0	-2.801799	-4.777619	-2.288729
83	6	0	2.696051	5.656258	0.302098
84	1	0	3.612492	5.228907	-0.113716
85	1	0	2.947377	6.644800	0.695154
86	6	0	2.152350	4.763376	1.408201
87	1	0	2.098322	3.729787	1.057477
88	1	0	2.801799	4.777619	2.288729
89	6	0	-4.380844	4.930169	-0.823455
90	1	0	-4.563931	3.890042	-1.115103
91	1	0	-5.330685	5.341139	-0.465686
92	6	0	-3.861393	5.715791	-2.020885
93	1	0	-4.532650	5.605314	-2.878815
94	1	0	-3.790131	6.780787	-1.786414
95	6	0	-0.611606	-6.848754	-2.697471
96	6	0	-1.720625	-7.112413	-3.513350
97	6	0	0.364154	-7.838909	-2.556792
98	6	0	-1.858960	-8.341408	-4.150279
99	1	0	-2.480521	-6.352741	-3.664486
100	6	0	0.234449	-9.064738	-3.206517
101	1	0	1.230248	-7.651936	-1.934044
102	6	0	-0.880487	-9.322006	-3.997370
103	1	0	-2.729406	-8.531238	-4.770803
104	1	0	1.007793	-9.816077	-3.085338
105	1	0	-0.987951	-10.280338	-4.496097
106	6	0	0.611606	6.848754	2.697471
107	6	0	-0.364154	7.838909	2.556792
108	6	0	1.720625	7.112413	3.513350
109	6	0	-0.234449	9.064738	3.206517
110	1	0	-1.230248	7.651936	1.934044
111	6	0	1.858960	8.341408	4.150279
112	1	0	2.480521	6.352741	3.664486
113	6	0	0.880487	9.322006	3.997370
114	1	0	-1.007793	9.816077	3.085338
115	1	0	2.729406	8.531238	4.770803
116	1	0	0.987951	10.280338	4.496097
117	6	0	3.679753	-6.217668	-1.695896
118	6	0	3.575490	-6.059802	-3.083667
119	6	0	4.150136	-7.436212	-1.195901
120	6	0	3.928991	-7.094046	-3.944685
121	1	0	3.221786	-5.119262	-3.492679
122	6	0	4.507345	-8.469840	-2.058301
123	1	0	4.234907	-7.594097	-0.127157
124	6	0	4.396381	-8.302978	-3.435508
125	1	0	3.843222	-6.951330	-5.017522
126	1	0	4.872501	-9.406613	-1.648941
127	1	0	4.675774	-9.108123	-4.107827
128	6	0	-3.679753	6.217668	1.695896
129	6	0	-4.150136	7.436212	1.195901
130	6	0	-3.575490	6.059802	3.083667
131	6	0	-4.507345	8.469840	2.058301
132	1	0	-4.234907	7.594097	0.127157
133	6	0	-3.928991	7.094046	3.944685
134	1	0	-3.221786	5.119262	3.492679
135	6	0	-4.396381	8.302978	3.435508
136	1	0	-4.872501	9.406613	1.648941
137	1	0	-3.843222	6.951330	5.017522
138	1	0	-4.675774	9.108123	4.107827
139	6	0	-0.086732	-4.119920	-3.282061

140	6	0	0.503350	-4.618293	-4.449848
141	6	0	-0.404022	-2.756488	-3.220076
142	6	0	0.770240	-3.778584	-5.527744
143	1	0	0.748851	-5.672425	-4.523008
144	6	0	-0.140555	-1.921022	-4.302541
145	1	0	-0.837880	-2.337388	-2.319180
146	6	0	0.446664	-2.427341	-5.458756
147	1	0	1.225260	-4.186146	-6.425461
148	1	0	-0.393470	-0.867420	-4.238201
149	1	0	0.649869	-1.772382	-6.300299
150	6	0	0.086732	4.119920	3.282061
151	6	0	0.404022	2.756488	3.220076
152	6	0	-0.503350	4.618293	4.449848
153	6	0	0.140555	1.921022	4.302541
154	1	0	0.837880	2.337388	2.319180
155	6	0	-0.770240	3.778584	5.527744
156	1	0	-0.748851	5.672425	4.523008
157	6	0	-0.446664	2.427341	5.458756
158	1	0	0.393470	0.867420	4.238201
159	1	0	-1.225260	4.186146	6.425461
160	1	0	-0.649869	1.772382	6.300299
161	6	0	3.791950	-3.412276	-1.523180
162	6	0	2.922073	-2.418067	-1.968418
163	6	0	5.154977	-3.321451	-1.840707
164	6	0	3.404154	-1.345341	-2.717965
165	1	0	1.870423	-2.481102	-1.713745
166	6	0	5.634406	-2.247771	-2.579984
167	1	0	5.842646	-4.100852	-1.525835
168	6	0	4.757073	-1.257149	-3.021074
169	1	0	2.717288	-0.574641	-3.049747
170	1	0	6.692297	-2.184045	-2.816300
171	1	0	5.132105	-0.414592	-3.593468
172	6	0	-3.791950	3.412276	1.523180
173	6	0	-2.922073	2.418067	1.968418
174	6	0	-5.154977	3.321451	1.840707
175	6	0	-3.404154	1.345341	2.717965
176	1	0	-1.870423	2.481102	1.713745
177	6	0	-5.634406	2.247771	2.579984
178	1	0	-5.842646	4.100852	1.525835
179	6	0	-4.757073	1.257149	3.021074
180	1	0	-2.717288	0.574641	3.049747
181	1	0	-6.692297	2.184045	2.816300
182	1	0	-5.132105	0.414592	3.593468
183	6	0	1.683039	-6.247956	3.855968
184	6	0	0.891596	-5.752761	4.901576
185	6	0	2.044965	-7.599289	3.880166
186	6	0	0.484199	-6.579409	5.943409
187	1	0	0.599679	-4.708412	4.909476
188	6	0	1.641854	-8.425177	4.927000
189	1	0	2.629323	-8.028233	3.075994
190	6	0	0.863598	-7.919748	5.963096
191	1	0	-0.125748	-6.171539	6.743524
192	1	0	1.937603	-9.469530	4.925474
193	1	0	0.554510	-8.564076	6.780362
194	6	0	-1.683039	6.247956	-3.855968
195	6	0	-0.891596	5.752761	-4.901576
196	6	0	-2.044965	7.599289	-3.880166
197	6	0	-0.484199	6.579409	-5.943409
198	1	0	-0.599679	4.708412	-4.909476
199	6	0	-1.641854	8.425177	-4.927000
200	1	0	-2.629323	8.028233	-3.075994
201	6	0	-0.863598	7.919748	-5.963096
202	1	0	0.125748	6.171539	-6.743524
203	1	0	-1.937603	9.469530	-4.925474

204	1	0	-0.554510	8.564076	-6.780362
205	6	0	-1.655042	-7.634691	1.543129
206	6	0	-1.570182	-8.031853	2.882233
207	6	0	-1.802442	-8.621954	0.562283
208	6	0	-1.669891	-9.375160	3.231476
209	1	0	-1.423648	-7.292010	3.661514
210	6	0	-1.904235	-9.964507	0.913392
211	1	0	-1.812494	-8.358271	-0.489943
212	6	0	-1.846375	-10.345693	2.250110
213	1	0	-1.603384	-9.659271	4.276863
214	1	0	-2.020258	-10.712212	0.135050
215	1	0	-1.927181	-11.393071	2.524066
216	6	0	1.655042	7.634691	-1.543129
217	6	0	1.802442	8.621954	-0.562283
218	6	0	1.570182	8.031853	-2.882233
219	6	0	1.904235	9.964507	-0.913392
220	1	0	1.812494	8.358271	0.489943
221	6	0	1.669891	9.375160	-3.231476
222	1	0	1.423648	7.292010	-3.661514
223	6	0	1.846375	10.345693	-2.250110
224	1	0	2.020258	10.712212	-0.135050
225	1	0	1.603384	9.659271	-4.276863
226	1	0	1.927181	11.393071	-2.524066
227	6	0	-2.262790	-5.025395	2.501883
228	6	0	-3.508376	-5.462685	2.973690
229	6	0	-1.648956	-3.939385	3.127984
230	6	0	-4.119928	-4.829229	4.050359
231	1	0	-3.994205	-6.315397	2.508493
232	6	0	-2.264081	-3.300585	4.204081
233	1	0	-0.698033	-3.580565	2.747616
234	6	0	-3.496811	-3.745663	4.668735
235	1	0	-5.081494	-5.183279	4.409344
236	1	0	-1.776031	-2.452473	4.674513
237	1	0	-3.974396	-3.251186	5.509028
238	6	0	2.262790	5.025395	-2.501883
239	6	0	1.648956	3.939385	-3.127984
240	6	0	3.508376	5.462685	-2.973690
241	6	0	2.264081	3.300585	-4.204081
242	1	0	0.698033	3.580565	-2.747616
243	6	0	4.119928	4.829229	-4.050359
244	1	0	3.994205	6.315397	-2.508493
245	6	0	3.496811	3.745663	-4.668735
246	1	0	1.776031	2.452473	-4.674513
247	1	0	5.081494	5.183279	-4.409344
248	1	0	3.974396	3.251186	-5.509028
249	6	0	2.596835	-3.608708	3.424805
250	6	0	2.207499	-2.351578	2.963419
251	6	0	3.383935	-3.692323	4.583047
252	6	0	2.602274	-1.196358	3.640579
253	1	0	1.590099	-2.282903	2.073163
254	6	0	3.772691	-2.542191	5.259141
255	1	0	3.682564	-4.663352	4.967032
256	6	0	3.382982	-1.288792	4.787132
257	1	0	2.309507	-0.225771	3.253796
258	1	0	4.381216	-2.622709	6.154786
259	1	0	3.690311	-0.389169	5.311296
260	6	0	-2.596835	3.608708	-3.424805
261	6	0	-3.383935	3.692323	-4.583047
262	6	0	-2.207499	2.351578	-2.963419
263	6	0	-3.772691	2.542191	-5.259141
264	1	0	-3.682564	4.663352	-4.967032
265	6	0	-2.602274	1.196358	-3.640579
266	1	0	-1.590099	2.282903	-2.073163
267	6	0	-3.382982	1.288792	-4.787132

268	1	0	-4.381216	2.622709	-6.154786
269	1	0	-2.309507	0.225771	-3.253796
270	1	0	-3.690311	0.389169	-5.311296

References:

[1] W. B. Wan, M. M. Haley, *J. Org. Chem.* **2001,** *66,* 3893-3901.

[2] T. Ishida, Y. Mizobe, T. Tanase, M. Hidai, *J. Organomet. Chem,* **1991**, *409*, 355-365.

[3] D. Unseld, V. V. Krivykh, K. Heinze, F. Wild, G. Artus, H. Schmalle, H. Berke, *Organometallics* **1999,** *18,* 1525-1541.

[4] R.C. Clark, J. S. Reid, *Acta Cryst.* **1995**, *A51*, 887-897.

[5] *CrysAlisPro* (Version 1.171.31.8), Oxford Diffraction Ltd, Abingdon, Oxfordshire, England.

[6] G. M. Sheldrick, *Acta Cryst.* **2008**, *A64*, 112-122.

[7] L. J. Farrugia, *J. Appl. Cryst.* **1999***, 32,* 837-838

[8] A. L. Spek, *J. Appl. Cryst.* **2003**, *36*, 7-13.

[9] Gaussian 03, Revision C.01, M. J. Frisch, G. W. Trucks, H. B. Schlegel, G. E. Scuseria, M. A. Robb, J. R. Cheeseman, J. A. Montgomery, T. Vreven, K. N. Kudin, J. C. Burant, J. M. Millam, S. S. Iyengar, J. Tomasi, V. Barone, B. Mennucci, M. Cossi, G. Scalmani, N. Rega, G. A. Petersson, H. Nakatsuji, M. Hada, M. Ehara, K. Toyota, R. Fukuda, J. Hasegawa, M. Ishida, T. Nakajima, Y. Honda, O. Kitao, H. Nakai, M. Klene, X. Li, J. E. Knox, H. P. Hratchian, J. B. Cross, V. Bakken, C. Adamo, J. Jaramillo, R. Gomperts, R. E. Stratmann, O. Yazyev, A. J. Austin, R. Cammi, C. Pomelli, J. W. Ochterski, P. Y. Ayala, K. Morokuma, G. A. Voth, P. Salvador, J. J. Dannenberg, V. G. Zakrzewski, S. Dapprich, A. D. Daniels, M. C. Strain, O. Farkas, D. K. Malick, A. D. Rabuck, K. Raghavachari, J. B. Foresman, J. V. Ortiz, Q. Cui, A. G. Baboul, S. Clifford, J. Cioslowski, B. B. Stefanov, G. Liu, A. Liashenko, P. Piskorz, I. Komaromi, R. L. Martin, D. J. Fox, T. Keith, M. A. Al-Laham, C. Y. Peng, A. Nanayakkara, M. Challacombe, P. M. W. Gill, B. Johnson, W. Chen, M. W. Wong, C. Gonzalez, J. A. Pople, Gaussian, Inc., Wallingford CT 2004.

[10] C. Adamo, V. Barone, *J. Chem. Phys.* **1998**, *108*, 664-675.

[11] (a) T. H. Dunning Jr. and P. J. Hay, in *Modern Theoretical Chemistry*, Ed. H. F. Schaefer III, Vol. 3 (Plenum, New York, 1976) 1-28; (b) P. Fuentealba, H. Preuss, H. Stoll, and L. v. Szentpaly, *Chem. Phys. Lett.* **1982**, *89*, 418-422.

[12] R. Ditchfield, W. J. Hehre, and J. A. Pople, *J. Chem. Phys.* **1971**, *54*, 724-728.

[13] Y. Zhao, B. J. Lynch, D. G. Truhlar *J. Phys. Chem. A* **2004**, *108*, 2715-2719.

[14] (a) T. H. Dunning, Jr, *J. Chem. Phys.* **1989**, *90*, 1007-1023; (b) R. A. Kendall, T. H. Dunning, Jr and R. J. Harrison, *J. Chem. Phys.* **1992**, *96*, 6796-6806; (c) D. E. Woon and T. H. Dunning, Jr, *J. Chem. Phys.* **1993**, *98*, 1358-1371.

IV.2. Publication 2

Electronic Communication in Dinuclear C_4 – Bridged Tungsten Complexes

*Sergey N. Semenov, Olivier Blacque, Thomas Fox, Koushik Venkatesan, and Heinz Berke**

Department of Inorganic Chemistry, University of Zürich, Winterthurerstrasse 190, 8057 Zürich, Switzerland.

J. Am. Chem. Soc. **2010**, *132*, 3115-3127.

J|A|C|S ARTICLES

Published on Web 02/10/2010

Electronic Communication in Dinuclear C_4-Bridged Tungsten Complexes

Sergey N. Semenov, Olivier Blacque, Thomas Fox, Koushik Venkatesan, and Heinz Berke*

Department of Inorganic Chemistry, University of Zürich, Winterthurerstrasse 190, 8057 Zürich, Switzerland

Received November 17, 2009; E-mail: hberke@aci.uzh.ch

Abstract: The dinuclear tungsten carbyne $[X(CO)_2(dppe)WC_4W(dppe)(CO)_2X]$ (dppe = 1,2-bis(diphenylphosphino)ethane; X = I (**3**), Cl (**7**)) complexes were prepared from the bisacetylide precursor $Li_2[(CO)_3(dppe)WC_4W(CO)_3(dppe)]$ (**2**) via oxidative replacement of one CO group at each tungsten center with a halide substituent. The iodide ligand in **3** could be substituted with isothiocyanate or triflate resulting in $[X(CO)_2(dppe)WC_4W(dppe)(CO)_2X]$ complexes (X = NCS (**8**), OTf (**9**)). Substitution of two and all four CO ligands in **3** was achieved via subsequent photolytic or thermal activation with dppe. The "half-substituted" complex $[I(CO)_2(dppe)WC_4W(dppe)_2I]$ **(11)** allows reversible one-electron oxidation which results in the monocationic species $[I(CO)_2(dppe)WC_4W(dppe)_2I][PF_6]$ **(11[PF$_6$])**. The "all-dppe substituted" complex $[I(dppe)_2WC_4W(dppe)_2I]$ (**10**) possesses two reversible redox states leading to the stable monocationic $[I(dppe)_2WC_4W(dppe)_2I][PF_6]$ (**10[PF$_6$]**) and the dicationic $[I(dppe)_2WC_4W(dppe)_2I][PF_6]_2$ (**10[PF$_6$]$_2$**) compounds. The complexes **2**, **3**, $[W(CO)_3(dppe)(C{\equiv}CPh)(I)]$ (**4**), $[X(CO)_2(dppe)W{\equiv}C{-}C(Me){=}C(Me){-}C{\equiv}W(dppe)(CO)_2X]$ (X = I (**5**), Cl (**6**)), **7**, **8**, **10**, **11** and **11[PF$_6$]** were characterized by single crystal X-ray diffraction. The electronic properties of complexes **10**, **10[PF$_6$]**, **10[PF$_6$]$_2$**, as well as of compounds **11** and **11[PF$_6$]**, were investigated using cyclic voltammetry (CV), EPR, IR, near-IR spectroscopy, and magnetization measurements. These studies showed that the [W]≡C−C≡C−C≡[W] canonical form of the bridged system with strong tungsten−carbon interaction contributes significantly to the electronic coupling in the mixed-valent species **10[PF$_6$]** (comproportionation constant $K_c = 7.5 \times 10^4$) and to the strong antiferromagnetic coupling in the dicationic complex **10[PF$_6$]$_2$** (exchange integral $J = -167$ cm^{-1}). In addition, the rate for electron transfer between the tungsten centers in **10[PF$_6$]** was evaluated by near-IR and IR studies.

Introduction

Organometallic dinuclear metal complexes of the type $[L_nMC_xML_n]$ (M = metal; L = ligand) are thought to have great potential for their application as devices in molecular electronics. Among other aspects these abilities are based on their basic function of "single-electron" conductance across the linear, unsaturated carbon bridge and on their redox-active end groups lending electrons for through-bridge travel. Such type of compounds in particular can potentially function as a molecular wire. Molecular wires constitute the basis for the construction of field-effect transistors and diodes. In addition to this their mixed valent states are exceptional models for electron transfer studies.[1−5] The complexes with $n = 4$ are the most ubiquitous of these series of complexes and have been reported for Mn,[6] Fe,[7,8] Re,[9] Ru,[10,11] Pt,[12] W and Mo centers.[13,14] The electronics and structures of the C_4 chain correspond for most complexes to the acetylenic butadiynediyl canonical form, but for rarer other cases they correspond to the cumulenic butatrienebisylidene form (Scheme 1).

There are only two examples of a carbyne-type butynebis(triyl) bridge reported for related W and Mo complexes.[13] The C_4 chain has been demonstrated as one of the most efficient bridges for electronic communication between metal centers due to the presence of two transmitting π-systems and their propensity for polarization.[8] These complexes therefore often show high degrees of electron delocalization resulting in efficient stabilization of mixed-valence species. Various such complexes possess low thermal and air stability, which would limit their application in molecular electronics and hinder also attempts for further buildup of oligonuclears based on such systems. The most common and well-documented end groups are the

Scheme 1. Canonical Forms of a C_4 Unit in $[M]C_4[M]$ Structures

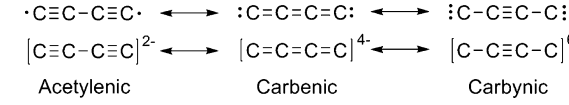

(1) (a) Carroll, L. R.; Gorman, B. C. *Angew. Chem., Int. Ed.* **2002**, *41*, 4378–4400. (b) Joachim, C.; Gimzewski, J. K.; Aviram, A. *Nature* **2000**, *408*, 541–548. (c) Chen, F.; Hihath, J.; Huang, Z. F.; Li, X. L.; Tao, N. J. *Annu. Rev. Phys. Chem.* **2007**, *58*, 535–564. (d) Tao, N. J. *Nature Nanotechnol.* **2006**, *1*, 173–181. (e) Nitzan, A.; Ratner, M. A. *Science* **2003**, *300*, 1384–1389. (f) Zhirnov, V. V.; Cavin, R. K. *Nat. Mater.* **2006**, *5*, 11–12. (g) Park, J.; Pasupathy, A. N.; Goldsmith, J. I.; Chang, C.; Yaish, Y.; Petta, J. R.; Rinkoski, M.; Sethna, J. P.; Abruna, H. D.; McEuen, P. L.; Ralph, D. C. *Nature* **2002**, *417*, 722–725. (h) Liang, W. J.; Shores, M. P.; Bockrath, M.; Long, J. R.; Park, H. *Nature* **2002**, *417*, 725–729. (i) Tuccitto, N.; Ferri, V.; Cavazzini, M.; Quici, S.; Zhavnerko, G.; Licciardello, A.; Rampi, M. A. *Nat. Mater.* **2009**, *8*, 41–46. (j) Low, P. J. *Dalton Trans.* **2005**, 2821–2824. (k) Paul, F.; Lapinte, C. *Coord. Chem. Rev.* **1998**, 178–180, 431−509.

[Re(NO)(Cp)(PPh_3)] and [Fe(dppe)(Cp*)] moieties.[15] These units, however, represent stopper functions that provide no functionality for a hook-up to electrodes or for further extension of these systems to form oligonuclears. The acetylenic or cumulenic chemistry of platinum has been extensively reported;[16,17] however, Pt compounds do not normally provide suitable redox properties for single-electron conductance. Moreover, in π-delocalized Pt(II) systems, delocalization is often interrupted at the metal center, which may hinder the electron travel in single-molecule junctions.[18] Ruthenium complexes with fragments [$Ru(P_2)_2$], P_2 = dppe and dppm (dppm = 1,2-bis(diphenylphosphino)methane) seem to offer the right balance between electronic delocalization and redox properties, and stability required for applications.[19] Such complexes were therefore used in single-layer capacity studies and recently also in single-electron conductance measurements.[20] However, the absence of new metal end groups with an appropriate combination of properties seems to currently impede further progress in the field.

Bridged complexes with emphasis on the carbyne canonical forms [$L_nM]C_4[ML_n$] are expected to possess higher stability and the possibility for facile synthetic modifications.[21−25] Carbyne-type canonical forms promise strong involvement of metal orbitals in the π-conjugated systems with the possibility for a tuning of spectroscopic, in particular NLO (nonlinear optical), properties.[25−29] Organometallic polymers based on such type of building blocks connected by bisacetylides have great implications, since these compounds retain conjugation along the backbone.[25,27] Mononuclear tungsten Fischer-type carbyne complexes are relatively common species, and several preparative methods were developed for their synthesis.[22,23,27,30−32] However, dinuclear C_4-bridged complexes with emphasis on the carbyne structure are rare except for [W]C_4[W] and [Mo]C_4[Mo] systems.[13] These compounds were synthesized using relatively complex procedures starting from mononuclear precursors utilizing the oxidative coupling of C_2 units to build the C_4 bridges. Physical characterization of these complexes have been limited to CV studies.[33] Moreover, these complexes have stopper-type termini not prone to further chemical func-

(2) Brunschwig, B. S.; Sutin, N. *Coord. Chem. Rev.* **1999**, *187*, 233–254.
(3) Demadis, D. D.; Hartshorn, C. M.; Meyer, T. J. *Chem. Rev.* **2001**, *101*, 2655–2685.
(4) Ward, M. D.; McCleverty, J. A. *Dalton Trans.* **2002**, 275.
(5) Kaim, W.; Klein, A.; Glockle, M. *Acc. Chem. Res.* **2000**, *33*, 755–763.
(6) (a) Kheradmandan, S.; Heinze, K.; Schmalle, H. W.; Berke, H. *Angew. Chem., Int. Ed.* **1999**, *38*, 2270–2273. (b) Venkatesan, K.; Fox, T.; Schmalle, H. W.; Berke, H. *Organometallics* **2005**, *24*, 2834–2847. (c) Venkatesan, K.; Fernandez, F. J.; Blacque, O.; Fox, T.; Alfonso, M.; Schmalle, H. W.; Berke, H. *Chem. Commun.* **2003**, 2006–2008.
(7) Lenarvor, N.; Toupet, L.; Lapinte, C. *J. Am. Chem. Soc.* **1995**, *117*, 7129–7138.
(8) Jiao, H. J.; Costuas, K.; Gladysz, J. A.; Halet, J. F.; Guillemot, M.; Toupet, L.; Paul, F.; Lapinte, C. *J. Am. Chem. Soc.* **2003**, *125*, 9511–9522.
(9) (a) Brady, M.; Weng, W. Q.; Zhou, Y. L.; Seyler, J. W.; Amoroso, A. J.; Arif, A. M.; Bohme, M.; Frenking, G.; Gladysz, J. A. *J. Am. Chem. Soc.* **1997**, *119*, 775–788. (b) Zhou, Y. L.; Seyler, J. W.; Weng, W. Q.; Arif, A. M.; Gladysz, J. A. *J. Am. Chem. Soc.* **1993**, *115*, 8509–8510. (c) Yam, V. W. W.; Lau, V. C. Y.; Cheung, K. K. *Organometallics* **1996**, *15*, 1740–1744.
(10) Paul, F.; Meyer, W. E.; Toupet, L.; Jiao, H. J.; Gladysz, J. A.; Lapinte, C. *J. Am. Chem. Soc.* **2000**, *122*, 9405–9414.
(11) Bruce, M. I.; Low, P. J.; Costuas, K.; Halet, J. F.; Best, S. P.; Heath, G. A. *J. Am. Chem. Soc.* **2000**, *122*, 1949–1962.
(12) Onitsuka, K.; Ose, N.; Ozawa, F.; Takahashi, S. *J. Organomet. Chem.* **1999**, *578*, 169–177.
(13) Woodworth, B. E.; White, P. S.; Templeton, J. L. *J. Am. Chem. Soc.* **1997**, *119*, 828–829.
(14) Roberts, R. L.; Puschmann, H.; Howard, J. A. K.; Yamamoto, J. H.; Carty, A. J.; Low, P. J. *Dalton Trans.* **2003**, 1099–1105.
(15) (a) Ibn Ghazala, S.; Paul, F.; Toupet, L.; Roisnel, T.; Hapiot, P.; Lapinte, C. *J. Am. Chem. Soc.* **2006**, *128*, 2463–2476. (b) Coat, F.; Lapinte, C. *Organometallics* **1996**, *15*, 477–479. (c) Bartik, T.; Bartik, B.; Brady, M.; Dembinski, R.; Gladysz, J. A. *Angew. Chem., Int. Ed. Engl.* **1996**, *35*, 414–417. (d) Dembinski, R.; Bartik, T.; Bartik, B.; Jaeger, M.; Gladysz, J. A. *J. Am. Chem. Soc.* **2000**, *122*, 810–822.
(16) (a) Zheng, Q. L.; Gladysz, J. A. *J. Am. Chem. Soc.* **2005**, *127*, 10508–10509. (b) Farley, R. T.; Zheng, Q. L.; Gladysz, J. A.; Schanze, K. S. *Inorg. Chem.* **2008**, *47*, 2955–2963.
(17) Zhuravlev, F.; Gladysz, J. A. *Chem.—Eur. J.* **2004**, *10*, 6510–6522.
(18) (a) Mayor, M.; von Hanisch, C.; Weber, H. B.; Reichert, J.; Beckmann, D. *Angew. Chem., Int. Ed.* **2002**, *41*, 1183–1186. (b) Schull, T. L.; Kushmerick, J. G.; Patterson, C. H.; George, C.; Moore, M. H.; Pollack, S. K.; Shashidhar, R. *J. Am. Chem. Soc.* **2003**, *125*, 3202–3203.
(19) (a) Rigaut, S.; Perruchon, J.; Le Pichon, L.; Touchard, D.; Dixneuf, P. H. *J. Organomet. Chem.* **2003**, *670*, 37–44. (b) Touchard, D.; Haquette, P.; Guesmi, S.; LePichon, L.; Daridor, A.; Toupet, L.; Dixneuf, P. H. *Organometallics* **1997**, *16*, 3640–3648. (c) Rigaut, S.; Massue, J.; Touchard, D.; Fillaut, J. L.; Golhen, S.; Dixneuf, P. H. *Angew. Chem., Int. Ed.* **2002**, *41*, 4513–4517. (d) Rigaut, S.; Le Pichon, L.; Daran, J. C.; Touchard, D.; Dixneuf, P. H. *Chem. Commun.* **2001**, 1206–1207. (e) Rigaut, S.; Olivier, C.; Costuas, K.; Choua, S.; Fadhel, O.; Massue, J.; Turek, P.; Saillard, J. Y.; Dixneuf, P. H.; Touchard, D. *J. Am. Chem. Soc.* **2006**, *128*, 5859–5876.
(20) (a) Qi, H.; Gupta, A.; Noll, B. C.; Snider, G. L.; Lu, Y. H.; Lent, C.; Fehlner, T. P. *J. Am. Chem. Soc.* **2005**, *127*, 15218–15227. (b) Liu, K.; Wang, X. H.; Wang, F. S. *ACS Nano* **2008**, *2*, 2315–2323.
(21) (a) Frank, K. G.; Selegue, J. P. *J. Am. Chem. Soc.* **1990**, *112*, 6414–6416. (b) Dewhurst, R. D.; Hill, A. F.; Willis, A. C. *Organometallics* **2009**, *28*, 4735–4740. (c) Schrock, R. R. *Chem. Rev.* **2002**, *102*, 145–179. (d) Herndon, J. W. *Coord. Chem. Rev.* **2009**, *253*, 86–179. (e) Jeffery, J. C.; Weller, A. S. *J. Organomet. Chem.* **1997**, *548*, 195–203. (f) Dewhurst, R. D.; Hill, A. F.; Rae, A. D.; Willis, A. C. *Organometallics* **2005**, *24*, 4703–4706. (g) Dewhurst, R. D.; Hill, A. F.; Smith, M. K. *Organometallics* **2005**, *24*, 5576–5580. (h) Atagi, L. M.; Critchlow, S. C.; Mayer, J. M. *J. Am. Chem. Soc.* **1992**, *114*, 9223–9224. (i) Bannwart, E.; Jacobsen, H.; Furno, F.; Berke, H. *Organometallics* **2000**, *19*, 3605–3619. (j) Furno, F.; Fox, T.; Schmalle, H. W.; Berke, H. *Organometallics* **2000**, *19*, 3620–3630. (k) Mayr, A.; Dorries, A. M.; Mcdermott, G. A.; Vanengen, D. *Organometallics* **1986**, *5*, 1504–1506.
(22) (a) Mcdermott, G. A.; Dorries, A. M.; Mayr, A. *Organometallics* **1987**, *6*, 925–931. (b) Zhang, L.; Gamasa, M. P.; Gimeno, J.; Carbajo, R. J.; López-Ortiz, F.; Lanfranchi, M.; Tiripicchio, A. *Organometallics* **1996**, *15*, 4274–4284.
(23) Yu, M. P. Y.; Cheung, K. K.; Mayr, A. *J. Chem. Soc., Dalton Trans.* **1998**, 2373–2378.
(24) Yu, M. P. Y.; Yam, V. W. W.; Cheung, K. K.; Mayr, A. *J. Organomet. Chem.* **2006**, *691*, 4514–4531.
(25) Manna, J.; Geib, S. J.; Hopkins, M. D. *J. Am. Chem. Soc.* **1992**, *114*, 9199–9200.
(26) Powell, C. E.; Humphrey, M. G. *Coord. Chem. Rev.* **2004**, *248*, 725–756.
(27) John, K. D.; Hopkins, M. D. *Chem. Commun.* **1999**, 589–590.
(28) (a) Mayr, A.; Yu, M. P. Y.; Yam, V. W. W. *J. Am. Chem. Soc.* **1999**, *121*, 1760–1761. (b) Da Re, R. E.; Hopkins, M. D. *Coord. Chem. Rev.* **2005**, *249*, 1396–1409.
(29) Xu, Z. H.; Mayr, A.; Butler, I. S. *J. Organomet. Chem.* **2002**, *648*, 93–98.
(30) (a) Pollagi, T. P.; Geib, S. J.; Hopkins, M. D. *J. Am. Chem. Soc.* **1994**, *116*, 6051–6052. (b) Mayr, A.; Asaro, M. F.; Kjeisberg, M. A.; Lee, K. S.; Van Engen, D. *Organometallics* **1987**, *6*, 432–434. (c) Mayr, A.; Mcdermott, G. A. *J. Am. Chem. Soc.* **1986**, *108*, 548–549. (d) Birdwhistell, K. R.; Burgmayer, S. J. N.; Templeton, J. L. *J. Am. Chem. Soc.* **1983**, *105*, 7789–7790. (e) Sharp, P. R.; Holmes, S. J.; Schrock, R. R.; Churchill, M. R.; Wasserman, H. J. *J. Am. Chem. Soc.* **1981**, *103*, 965–966. (f) Atagi, L. M.; Critchlow, S. C.; Mayer, J. M. *J. Am. Chem. Soc.* **1992**, *114*, 1483–1484.
(31) Schwenzer, B.; Schleu, J.; Burzlaff, N.; Karl, C.; Fischer, H. *J. Organomet. Chem.* **2002**, *641*, 134–141.
(32) Birdwhistell, K. R.; Tonker, T. L.; Templeton, J. L. *J. Am. Chem. Soc.* **1985**, *107*, 4474–4483.
(33) Frohnapfel, D. S.; Woodworth, B. E.; Thorp, H. H.; Templeton, J. L. *J. Phys. Chem. A* **1998**, *102*, 5665–5669.

Scheme 2

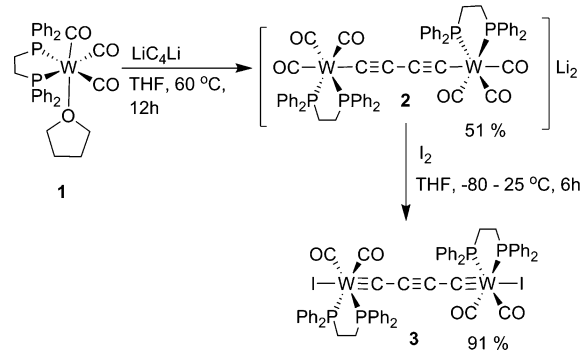

tionalization. In this paper we demonstrate facile synthetic access to tungsten complexes with delocalized, preferably carbyne-type [W]C_4[W] structures where [W] is [(X)W(dppe)$(CO)_2$], [(X)W$(dppe)_2$], and replaceable X groups. A thorough study is sought to unravel the physical properties of these complexes for proper pre-evaluation prior to measurements of single-electron conductance.

Results and Discussion

Synthesis and Characterization of Complexes. Substitution reactions of *fac*-W$(CO)_3$(dppe)(L) (L = acetone, THF) complexes with lithium acetylides were explored earlier as routes to access the corresponding tungsten acetylide species.[32,34] In these studies the *fac*-W$(CO)_3$(dppe)(acetone) intermediate could not be used, since it was necessary to avoid acetone in the reaction mixture; instead the *fac*-W$(CO)_3$(dppe)(THF) complex (**1**) turned out to be more feasible because the released THF does not have any impact on the reaction. It was isolated in 55% yield after two steps starting from $W(CO)_6$ and could be stored at −30 °C over long periods of time.[35] As depicted in Scheme 2, subsequent reaction of **1** with solid [$Li_2C_4(THF)_n$][36] gave the key compound Li_2[$(CO)_3$(dppe)W(C≡CC≡C)W(dppe)$(CO)_3$] (**2**) in 51% yield upon precipitation with benzene. Attempts to use *in situ* generated lithium salt, Li_2C_4, obtained from $Me_3SiC{\equiv}CC{\equiv}CSiMe_3$ and MeLi·LiBr produced side reactions and thus gave lower yields in comparison with the utilization of solid [$Li_2C_4(THF)_n$]. The ^{13}C NMR spectrum of **2** showed two resonances for the C_4 chain at 106.2 (C_α) and 106.9 (C_β) ppm. In the IR spectra typical ν(C≡O) bands were observed at 1892, 1814, and 1727 cm^{-1}. The band positions were similar to those of the previously reported M[W(dppe)$(CO)_3$(C≡CR)] (M = Li, Na; R = Ph, Me, H) series.[32]

Conversion of **2** into the [I$(CO)_2$(dppe)WC_4W(dppe)$(CO)_2$I] complex **3** as indicated in Scheme 2 was effected by oxidation with 2 equiv of I_2. The reaction from **2** to **3** was anticipated to involve single-electron oxidation steps, loss of CO, and coordination of iodide or I^+ transfer at each tungsten center. **3** was obtained as air-stable violet crystals in 80% yield and was fully characterized by NMR, IR spectroscopy, and elemental analysis. A carbyne-type structure was presumed. The C_α and C_β resonances appear as triplets at 225.2 and 87.5 ppm with $^2J(^{13}C,^{31}P)$ = 11.1 Hz and $^3J(^{13}C,^{31}P)$ = 3.7 Hz, respectively.

Scheme 3

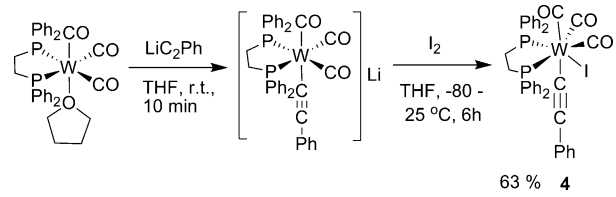

Scheme 4

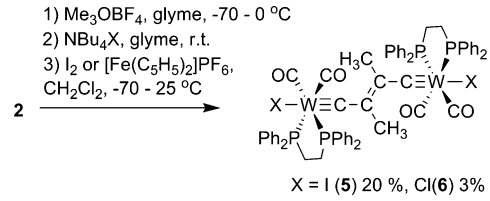

Scheme 5

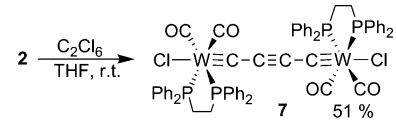

The C_α resonances were shifted high field in comparison with many of the reported mononuclear tungsten carbyne complexes, indicating changes in the electronic structure.[24,25,32] The ^{31}P NMR spectrum showed a superimposed singlet (W nucleus not magnetically active) and doublet at 29.3 ppm with $^1J(^{31}P,^{183}W)$ = 228 Hz. The oxidative transformation to **3** is unprecedented. A related type of transformation was put forward for $[RuC_4Ru]^{0-4+}$ systems, but was never clearly confirmed.[11] In order to trace the intermediates of the conversion of **2** to **3**, a "model" reaction between Li[W$(CO)_3$(dppe)(C≡CPh)] and one equivalent of I_2 was carried out, which was found to proceed via a seven-coordinated [W$(CO)_3$(dppe)(C≡CPh)(I)] complex (**4**) (Scheme 3). On the basis of these observations the formation of [$(CO)_3$(dppe)(I)WC_4W(I)(dppe)$(CO)_3$] is invoked as a primary intermediate in the formation of **3**.

According to Scheme 4, compound **2** was reacted with electrophiles. Treatment of **2** with Me_3OBF_4 in the presence of NBu_4X (X = Cl, I) with subsequent oxidation by I_2 or [$FeCp_2$][PF_6] gave the neutral complexes **5** and **6**. This reaction is thought to involve the intermediate [$X(CO)_2$(dppe)W≡C−C(Me)=C(Me)−C≡W(dppe)$(CO)_2$X][NBu_4]$_2$ presumably resulting from a sequence of electrophilic attacks by Me_3O^+ followed by rearrangement of the bridge to the carbyne form and subsequent substitution of CO activated by the *trans* effect of carbyne as was found in mononuclear complexes.[32,37]

A chloride derivative [$Cl(CO)_2$(dppe)WC_4W(dppe)$(CO)_2$Cl] (**7**) analogous to **3** was obtained in 15% yield upon treatment of **2** with chloroform or in 51% yield applying chlorination with C_2Cl_6 (Scheme 5).

We then sought to utilize **3** and **7** for variation of the axial groups by substitution with labile anionic ligands. The best results were achieved using silver salts due to concomitant enforcement of the halogen abstraction (Scheme 6). Since N-bound isothiocyanate ligands could principally be used for the anchoring of such molecules via sulfur coordination to gold surfaces as required for measurements of single-electron-

(34) Roth, G.; Fischer, H. *Organometallics* **1996**, *15*, 1139–1145.
(35) Birdwhistell, K. R.; Dema, A. C.; Li, X.; Lukehart, C. M.; Owen, M. D. *Inorg. Synth.* **1992**, *29*, 141–146.
(36) Werz, D. B.; Gleiter, R.; Rominger, F. *J. Am. Chem. Soc.* **2002**, *124*, 10638–10639.
(37) Mayr, A.; Schaefer, K. C.; Huang, E. Y. *J. Am. Chem. Soc.* **1984**, *106*, 1517–1518.

Scheme 6

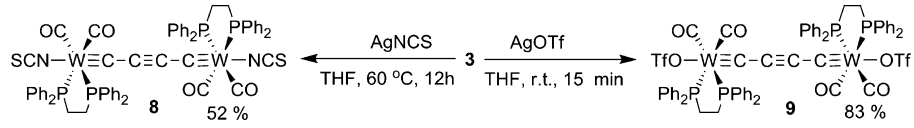

Scheme 7

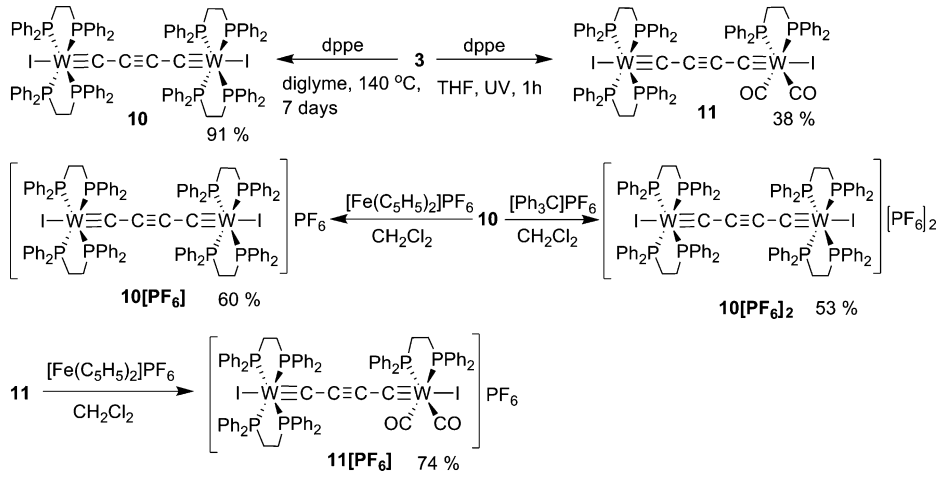

conductivities,[38] the heterogeneous reaction of a THF solution of **3** with AgSCN was carried out, which indeed afforded the isothiocyanate derivative [SCN(CO)$_2$(dppe)WC$_4$W(dppe)-(CO)$_2$NCS] (**8**). The N-coordination was assigned on the basis of υ (NCS) observed at 2034 cm^{-1}. Bands lower than 2100 cm^{-1} are more typical for isothiocyanates (N-coordination) derivatives,[39] and the structure was further confirmed by X-ray analysis. The reaction with silver triflate gave the corresponding substituted product [(OTf)(CO)$_2$(dppe)WC$_4$W-(dppe)(CO)$_2$(OTf)] (**9**) in 83% yield.

The spectroscopic properties of **7**−**9** overall resemble those of **3**. For instance the ^{31}P NMR shifts are similar to those of mononuclear tungsten carbynes, and the $^1J_{W-P}$ coupling constants were only slightly affected by the new substituent in the axial positions.[25,27,32] The C$_\beta$ resonances of the symmetrical molecules **3** and **7**−**9** shift monotonically downfield with a decreasing size of the ligand *trans* to the C$_4$ chain. This behavior is consistent with an increase of the WC$_\alpha$ bond lengths from **3** to **8** and might be related to an increase in the π-acceptor property on going from I$^-$ to NCS$^-$. A similar behavior was observed in the [XW(PMe$_3$)$_4$(CH)] series.[40] The C$_\beta$ resonances of **3** and **7**−**9** shift monotonically highfield from I$^-$ to OTf$^-$.

The IR spectra exhibit two characteristic absorptions for the C≡O vibrations in the range of 2000−1925 cm^{-1}. These ν(C≡O) are shifted to lower energies with respect to the comparable mononuclear compounds [(X)(CO)$_2$(dppe)WC−R],[23,29,31] which might be due to a increase in electron density on the metal center and a concomitant weaker tungsten-to-carbon bond in **3** and **7**−**9**. The ν(C≡O) bands of **3** show a slight high energy shift upon substitution of the iodine ligands by chlorides and by about 15 cm^{-1} upon substitution with the OTf.

CV studies on the complexes **3** and **7**−**9** revealed irreversible oxidation behavior, which was thought to be due to the presence of the CO ligands becoming labile in higher oxidation states of the tungsten centers. Indeed, CO-containing carbyne compounds of the type [W(CR)(CO)$_n$L$_{4-2n}$X] typically showed electrochemically irreversible behavior.[24] However, mononuclear "all-phosphine"-substituted complexes of the type [W(CR)(PP)$_2$X] possess reversible redox processes.[41]

In order to fine-tune the electrochemical properties of such types of compounds to the requirements of the redox wires, the substitution of the CO ligands of **3** with dppe was attempted by thermal and photolytic activation (Scheme 7). UV irradiation of **3** produced the unsymmetrically substituted complex [I(CO)$_2$(dppe)WC$_4$W(dppe)$_2$I] (**11**), which showed four different ^{13}C NMR signals for the carbon chain at 230.3, 212.3, 93.9, and 83.0 ppm. However, approaching exhaustive CO substitution of **3** by extended UV irradiation led to degradation of **11**. Substitution of all four CO molecules could eventually be effected by heating compound **3** to 140 °C in diglyme with intermittent removal of the evolved CO applying vacuum. The desired product [I(dppe)$_2$WC$_4$W(dppe)$_2$I] (**10**) precipitated during the course of the reaction as large dark-green crystals in 85−90% yield. In contrast to the previously discussed complexes, **10** furnished a broad ^{31}P NMR signal at around 45 ppm. The ^{13}C NMR spectrum revealed sharp signals for the C$_\alpha$ and C$_\beta$ nuclei, but broad lines for *ipso*-C$_6$H$_5$ carbon atoms. The broadening was attributed to ligand dynamics confirmed by variable-temperature ^{31}P NMR studies as shown in Figure 1. The initially broad ^{31}P NMR signal splits upon lowering the temperature into four doublets, two of which overlap. Phosphorus nuclei in *trans* positions are known to couple more strongly than the nuclei in *cis* positions. Hence, the coupling constants of $^2J_{P-P} \approx 120$ Hz can be attributed to the phosphorus nuclei in the *trans* position. We assume an arrangement of four inequivalent "in-plane" phosphorus nuclei due to the tilting distortion of the square pyramid formed by the four phosphorus nuclei and the C$_\alpha$. This could be attributed from the crystal structure, where the P$_4$ plane is not fully perpendicular to the

(38) Han, W. H.; Durantini, E. N.; Moore, T. A.; Moore, A. L.; Gust, D.; Rez, P.; Leatherman, G.; Seely, G. R.; Tao, N. J.; Lindsay, S. M. *J. Phys. Chem. B* **1997**, *101*, 10719–10725.
(39) Sabatini, A.; Bertini, I. *Inorg. Chem.* **1965**, *4*, 1665–1667.
(40) Holmes, S. J.; Schrock, R. R.; Churchill, M. R.; Wasserman, H. J. *Organometallics* **1984**, *3*, 476–484.
(41) van der Eide, E. F.; Piers, W. E.; Parvez, M.; McDonald, R. *Inorg. Chem.* **2007**, *46*, 14–21.

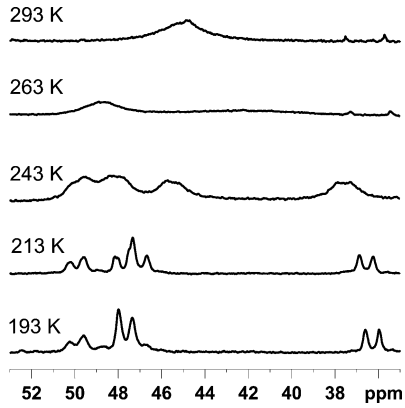

Figure 1. Temperature-dependent ^{31}P NMR shifts of **10** in a toluene-d_8/CD_2Cl_2 (4:1) mixture.

W≡C bond vector (for more details see crystal structure discussion below), making all four phosphorus atoms inequivalent. At higher temperatures upcoming dynamic processes average the phosphorus positions within the NMR time scale, giving rise to the observed broad signal.

In contrast to **3**, complexes **10** and **11** could be oxidized in facile reactions with $[FeCp_2][PF_6]$, leading to the corresponding monocationic products **10[PF$_6$]** and **11[PF$_6$]** (Scheme 7). **10** could be oxidized further to the dicationic species **10[PF$_6$]$_2$** upon reaction with $[Ph_3C][PF_6]$. It is important to mention at this point that **11** failed the oxidation to a dicationic form, which is in constrast to **10**, where both mono- and dicationic derivatives were isolated. This confirms that only CO-free units of the type $[W(CR)(PP)_2X]$ can undergo reversible oxidation. The third diphosphine substitution forming **11** had only little effect on the ν(C≡O) position in comparison to **3**. In contrast to this, the oxidation of **11** to **11[PF$_6$]** induced a larger shift of the ν(C≡O) bands of about 15 cm^{-1} to higher energies.

Complex **10** is stable in air in solid state and only slowly decomposes in solution. It was also found that the complex is stable toward strong bases and acids such as HBF_4 and MeLi. **10** reacts with thallium triflate showing iodine substitution with the formation of thallium iodide precipitate. This reaction is currently being investigated to exploit for substitution of iodine to acetylenes.

Structural Studies of Complexes 2−8, 10, 11, 11[PF$_6$]. All compounds except **9**, **10[PF$_6$]**, and **10[PF$_6$]$_2$** were structurally characterized. The ORTEP plots of **2**, **3**, **10**, **11** are presented in Figures 2 and 3. The plots for structures of **4**−**8** and **11[PF$_6$]** are presented in the Supporting Information. Selected bond distances are summarized in Table 1.

The structure of **2** revealed a dianionic complex along with two lithium cations, which are in tetrahedral environment coordinating two THF molecules and one acetylenic bond of the C_4 bridge. The anionic part comprises two octahedral tungsten fragments, and the structure of the C_4 bridge is close to a butadiynyl form. Structures **3**, **7**, and **8** consist of a C_4 chain with pseudo-square pyramidal [*trans*-$W(CO)_2$(dppe)X] end groups (X = I (**3**), Cl (**7**), NCS (**8**)). The W−C_α bond lengths are close to the size of a triple bond.[23] The C_α−C_β bonds are longer than the central C_β−C_β', clearly indicating that the oxidation of **2** causes the structure of the C_4 bridge to transform from an acetylenic to a biscarbynic canonical form. The C_4 bridge acts as a flexible electron reservoir, which switches upon oxidation of the tungsten centers from one-electron donation (acetylenic) at each side in **2** to three-electron donation in **3**, **7**, and **8**. This indeed is the first example of related complexes to clearly document a redox-induced structural switch from an acetylene to a carbyne form of bridge. The axial ligands lead to tightening of the W≡C carbyne bonds via π donation with increasing influence from NCS to I. A related structural trend was observed in mononuclear species.[42] The π-donor effect also affects the C_α−C_β bond distances, which get longer, and the central C_β−C_β' bonds, which shorten upon going from I to NCS. The bond length alternation in the bridge (C_α−C_β vs C_β−C_γ) of **3**, **7**, **8** resembles qualitatively that of a metal-capped C_6 system.[43]

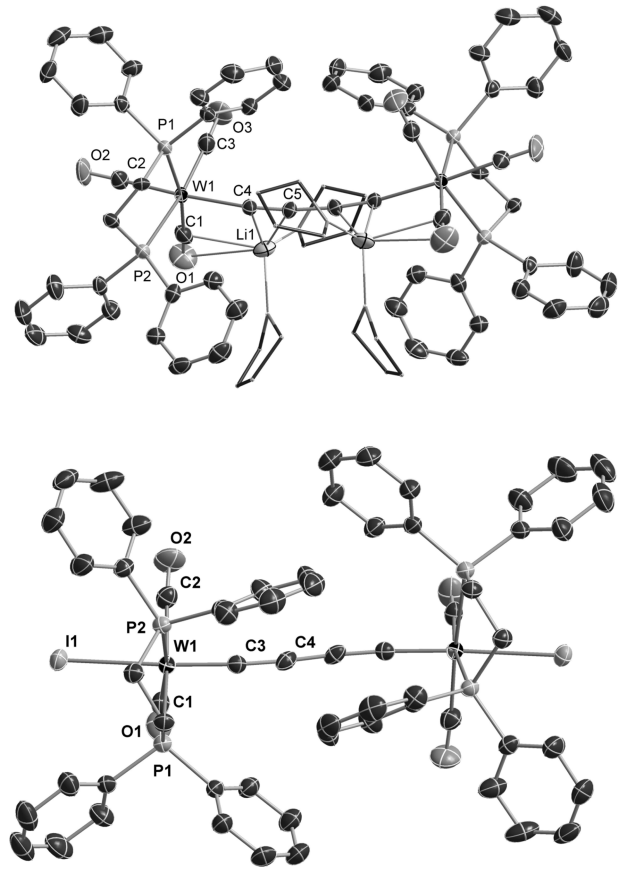

Figure 2. ORTEP-like drawing of **2** (top) and **3** (bottom) (50% probability level of thermal ellipsoids). Hydrogen atoms and solvent molecules are omitted for clarity. Coordinated THF molecules are shown in wire style.

All of the [W]C_4[W] structures display distortions from linearity. Complexes **3**, **7**, **8**, and **10** show S-shape distortion (transoid), compounds **2** and **11** have bow-shaped distortion (cisoid). For complexes containing [*trans*-$W(CO)_2$(dppe)X], the ($WC_\alpha C_\beta$) and ($C_\alpha C_\beta C_\beta'$) angles contribute approximately equally to the deviation from linearity. However, for **10** and **11** constructed from [*trans*-$W(dppe)_2X$] centers, the ($WC_\alpha C_\beta$) angles of ∼172° contribute a large portion to the total deviation more than the ($C_\alpha C_\beta C_\beta'$) angles (∼176°). Gladysz et al. have shown by DFT calculations for platinum-capped polyynes that the energetic barrier for bow-shaped distortions in [M]C_n[M] systems is quite small (about 2 kcal/mol), which is indeed in

(42) (a) Carriedo, G. A.; Riera, V.; Gonzalez, J. M. R.; Sanchez, M. G. *Acta Crystallogr., Sect. C: Cryst. Struct. Commun.* **1990**, *46*, 581–584. (b) Zhang, L.; Gamasa, M. P.; Gimeno, J.; da Silva, M. F.; C, G.; Pombeiro, A. J. L.; Graiff, C.; Lanfranchi, M.; Tiripicchio, A. *Eur. J. Inorg. Chem.* **2000**, 1707–1715.
(43) Dewhurst, R. D.; Hill, A. F.; Willis, A. C. *Organometallics* **2005**, *24*, 3043–3046.

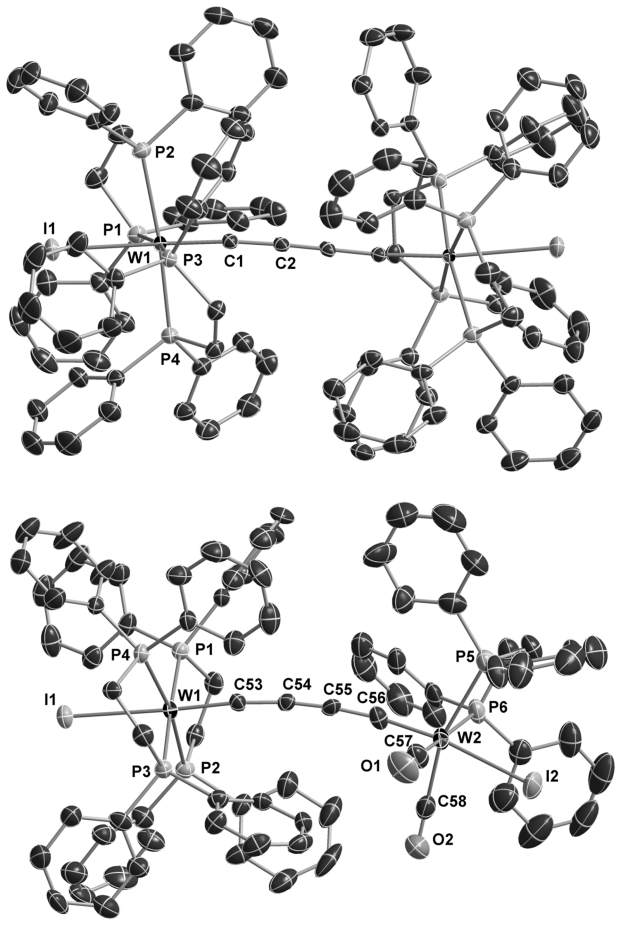

Figure 3. ORTEP-like drawing of **10** (top) and **11** (bottom) (50% probability level of thermal ellipsoids). Hydrogen atoms and solvent molecules are omitted for clarity.

Table 1. Selected Average Bond Lengths of Compounds **2**, **3**, **5**−**8**, **10**, **11**, and **11[PF$_6$]**; Assignment of the Bond Lengths in the C_4 Bridge According to the Following Notation: [W]$C_\alpha C_\beta C_\beta' C_\alpha'$[W]

bond	W−P	W−X	W−CO	W−C_α W−C_α'	C_α−C_β C_α'−C_β'	C_β−C_β'
2	2.500(2)		1.987(7)	2.189(5)	1.228(8)	1.40(1)
3	2.5382(9)	2.8610(3)	2.025(4)	1.844(3)	1.320(5)	1.299(7)
5	2.514(2)	2.9121(7)	2.028(1)	1.850(9)	1.420(2)	1.38(2)
6	2.527(2)	2.519(2)	2.026	1.816(6)	1.48(2)	1.36(3)
7	2.5349(8)	2.5037(7)	2.024(3)	1.849(3)	1.346(4)	1.242(6)
8	2.533(1)	2.181(4)	2.026(5)	1.857(5)	1.352(7)	1.231(7)
10	2.4741(6)	2.8618(2)		1.847(2)	1.370(3)	1.244(4)
11	2.492(2), 2.533(2)	2.8776(6), 2.8573(7)	2.03(1)	1.849(8), 1.840(8)	1.34(1), 1.36(1)	1.27(1)
11[PF$_6$]	2.569(2), 2.525(2)	2.8291(5), 2.8500(5)	2.034(9)	1.827(6), 1.838(6)	1.359(9), 1.345(9)	1.255(9)

the range of crystal packing effects.[17,44] In accord with this observation and with the fact that **10** and **11** with bulky [*trans*-W(dppe)$_2$X] fragments are more distorted than complexes with [*trans*-W(CO)$_2$(dppe)X] units, we attribute the deviation from linearity to steric and crystal packing effects.

A comparison of **3** with **11** revealed that the "asymmetric" diphosphine substitution has only little effect on the CO bond distances of both sides. The average W−P distance at the [*trans*-W(dppe)$_2$I] center is shorter than in the [*trans*-W(CO)$_2$(dppe)X]. Also the bond alternation of the bridge is more pronounced in **3** than in **11**. The oxidized [*trans*-W(dppe)$_2$I] center of **11[PF$_6$]** shows elongated W−P bonds and a contraction of the W−I bond in comparison with the corresponding bond lengths of **11**. In general, changes of the bond lengths upon oxidation were found to be less prominent. The structural changes upon oxidation are the basis of the application of the Franck−Condon model, which would reflect the barrier for the electron transfer between the tungsten centers of dinuclear complex.

Structure **10** consists of two symmetrically arranged [*trans*-W(dppe)$_2$X] fragments bridged by a C_4 system resembling a carbynic structure [W]≡C−C≡C−C≡[W]. As previously mentioned, a comparison of **10** and **3** reveals that the W−P bonds contract upon CO substitution, and the C_4 chain shows a more pronounced [W]≡C−C≡C−C≡[W] alternation. Two important points to note for further discussion of the through-bridge metal····metal interaction for **10**: there is distortion of the [W]C_4[W] from linearity and distortion of the [*trans*-C≡W(dppe)$_2$I] fragment from C_{4v} symmetry. The S-shape of **10** is reflected by the deviation of the angle between the mean plane (P1, P2, P3, P4) and the W····W axis, which is equal to 15°. In this view the otherwise symmetrized structure of **10** would be closer to C_{2h} than to C_{4h} or D_{4d}. The coordination environment of the tungsten center is also distorted with an angle between the perpendicular of the mean plane (P1, P2, P3, P4) and the W−C axis of about 10°. Furthermore the W−P distances in **10** are significantly different, W−P3 and W−P4 (both about 2.44 Å) are shorter than the W−P1 and W−P2 distances, which are about 2.51 Å. The structural parameters of the inner coordination sphere of the tungsten centers in **5** and **6** are almost identical to those in **3** and **7** except for separations in the bridge. The W≡C bond distances reflect typical triple bond lengths. A tungsten dinuclear complex with an analogous $C_4(CH_3)_2$ bridge was structurally characterized by Templeton and co-workers.[13]

Spectroscopic Studies with Emphasis on the Characterization of the C_4 Bridges. Raman and UV−Vis Studies. Selected Raman, NMR, and UV−vis spectroscopic data are listed in Table 2. They will be discussed for the sake of a structural and electronic characterization mainly of the [W]C_4[W] unit and for the characterization of the through-bridge [W]····[W] interactions.

The Raman spectra of **3**, **6**−**11**, **10[PF$_6$]**, **10[PF$_6$]$_2$**, **11[PF$_6$]** showed strong bands around 1150 and 1930 cm^{-1} that can be attributed to the ν(WC) and symmetrical $\nu(C_4)$ vibrations, respectively (Table 2). Related carbynic structures of the complexes with substantial M≡C triple bond character were found to possess in their ν(MC) vibrations strong dependence on the nature of the carbyne substituents and only little variation with respect to the type of *trans*-carbyne ligand.[29,45] The ν(WC) vibrations of complexes **2**, **3**, **7**−**11**, **10[PF$_6$]**, **10[PF$_6$]$_2$**, **11[PF$_6$]** appear at significantly lower wavenumbers than those of mononuclear complexes of the type [(X)(CO)$_2$(dppe)W≡C−R] (∼1300 cm^{-1}) indicating electronic delocalization presumably with contribution from the carbenic form of the bridge. Similarly, ν(CC) bands of these compounds were observed around 1930 cm^{-1} at significantly lower energies than ν(C≡C) vibrations of related mononuclear tungsten carbyne complexes in conjugation with C≡C bonds.[31] Those modes were observed in the range of 2050−2100 cm^{-1}. For the dinuclear [{Cp*(PPh$_3$)(NO)Re}$_2$(μ-C_4)] complex, the $\nu(C_4)$ vibration was located at 2056 cm^{-1}. The strong shifts of the $\nu(C_4)$ Raman bands of complexes **2**, **3**, **7**−**11**, **10[PF$_6$]**, **10[PF$_6$]$_2$**, **11[PF$_6$]** also indicate

(44) Szafert, S.; Gladysz, J. A. *Chem. Rev.* **2003**, *103*, 4175–4206.

(45) Dao, N. Q. *J. Organomet. Chem.* **2003**, *684*, 82–90.

Table 2. Raman, NMR and UV−Vis Data of Complexes **2**, **3**, **5**-**11**, **10[PF$_6$]**, **10[PF$_6$]$_2$** and **11[PF$_6$]**

	Raman [cm^{-1}]		NMR [ppm]			absorption [nm]	
	ν(C$_4$)	ν(WC)	^{31}P{^{1}H} ($^1J_{W-P}$ (d, satellite) [Hz])	^{13}C (C$_\alpha$ (C$_\alpha$′))	^{13}C (C$_\beta$ (C$_\beta$′))	λ_1 (ε/1000 [M^{-1} cm^{-1}])	λ_2[a] (ε/1000 [M^{-1} cm^{-1}])
2[b]	2080		34.4 (202)	106.2	106.9	274 (45)	460 (3.2)
3	1947	1149, 1109	29.3 (228)	225.2	87.5	407 (340)	533 (5.6)
5[b,c]	1474	1067	28.0 (225)			462 (39)	
6[b,c]			38.2 (230)			450 (30)	
7	1936	1149, 1113	37.5 (226)	228.4	85.8	382 (190)	517 (3)
8	1923	1114, 1082	39.9 (234)	232.1	82.1	412 (330)	543 (4.7)
9	1964	1173, 1127	44.8 (236)		82.1	367 (400)	524 (2.5)
10	1892	1084	45	213.1	86.5	412 (290)	668 (2.3)
10[PF$_6$]	1894	1082				410 (300)	702 (1.8), 470 (6)
10[PF$_6$]$_2$	1895	1078				413 (160)	520 (7.8), 660 (1.7)
11[d]	1916	1141, 1100	38.7 (230), (32.3) (268)	230.3 (212.3)	93.9 (83.0)	416 (300)	780 (1), 480 (4.5)
11[PF$_6$]	1936	1143, 1096				406 (280)	503 (7), 620 (2.7)

[a] For the unsymmetrical complexes two absorptions of lower intensity are present. [b] **2**, **5**, **6** have an electronic structure deviating from those of the other compounds; therefore, the classification of the UV−vis absorption bands differs from those of the other complexes. [c] In the first column ν(C═C). [d] The NMR chemical shifts in brackets belong to the [(I)(dppe)$_2$W≡C−] fragment.

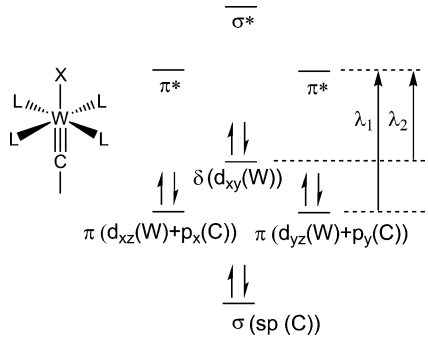

Figure 4. Qualitative molecular orbital diagram for a tungsten carbyne complex of the type discussed.

reduced bond orders in agreement with contribution from the biscarbenic form of [W]C$_4$[W] π-system.

It should be mentioned at this point that differences of the ancillary ligand sphere of complexes **3** and **7**−**12** also influence the ν(C$_4$) Raman bands. For instance, the triflate derivative **9** shows a high-energy shift of the ν(C$_4$) vibration by about 30 cm^{-1}, the dppe-substituted complex **10** shows significant shifts (30−100 cm^{-1}) of both ν(C$_4$) and ν(WC) to lower energies with respect to the corresponding band of **3**.

The UV−vis spectra of the symmetrical complexes **3**, **7**−**10** show two main absorptions λ_1 and λ_2. The best approximation for the electronic description of the [W]C$_4$[W] systems is a formulation with the bridge in the carbynic form (Figure 4).[28]

Indeed for the complexes described in this paper, two electronic transitions were found with one quite intense absorption at about 400 nm assigned to a $\pi \rightarrow \pi^*$ (λ_1) transition, while the weaker absorption is anticipated to be associated with a d$_{xy}$ $\rightarrow \pi^*$ (λ_2) transition. Figure 4 comprises a qualitative MO scheme showing that the position of λ_1 should be in a first-order approximation affected only by the axial ligands, while λ_2 is mainly influenced by the equatorial ligands due to changes in the energy of the d$_{xy}$ orbital being of δ-type with ideally no or only little orbital interaction with the bridge π-orbitals. The experiments confirmed the qualitative picture of Figure 4. The position of the $\pi \rightarrow \pi^*$ (λ_1) transition is indeed changing with the axial ligand X, as observed for complexes **3**, **7**−**9**. However, significant changes in the equatorial ligand patterns on going from **3** to **10** did not influence λ_1 but strongly shifted λ_2 from 533 to 668 nm. The decreasing energy of λ_2 is in agreement with a decrease in the π-acceptor properties of the dppe relative to the CO ligand resulting in an energetic increase of d$_{xy}$. The spectra of the unsymmetrical complexes **11**, **11[PF$_6$]**, **10[PF$_6$]** show one strong and two weak absorptions.

Electronic Communication between the Tungsten Centers. The interaction between the metal centers in the [W]C$_4$[W] systems was evaluated on the basis of the stabilization energy of the mixed-valence complex, electronic delocalization, electron-transfer capability, and ordering in the spin system.[3−5,46−48]

CV Evidence for Stabilization of Mixed-Valence Complexes. As expected, the unsymmetrical complex **11** has only one reversible redox step with an $E_{1/2}$ value of −435 mV *vs* Fc$^{0/+}$ (Figure 5). This is explained on the basis that only the pure phosphine-substituted tungsten center has reversible redox properties. The unpaired electron is therefore expected to be localized in the d$_{xy}$ orbital of the [(I)(dppe)$_2$WC−] unit.[49−51] The given $E_{1/2}$ value is, however, found at significantly higher potential than those of the mononuclear carbyne complexes ([ClW(dmpe)$_2$(CH)] −880 mV and [ClW(PMe$_3$)$_4$(CH)] −910 mV), indicating direct influence of the P$_4$ framework in-plane with the HOMO of such systems (Figure 4). This lower reduction potential is assumed to be due to lower σ-donating and higher π-accepting properties of the dppe ligand. For the symmetric complex **10** two oxidation waves were found at −543 mV and −253 mV revealing that both tungsten centers are involved in the redox process. But a relatively small peak separation of **10** was observed witnessing only moderate electronic coupling of the tungsten centers.

Under rigorous symmetry conditions, i.e. molecular distortions or pseudo-symmetries excluded, the HOMO is of δ-type

(46) Astruc, D. *Acc. Chem. Res.* **1997**, *30*, 383–391.
(47) McCleverty, J. A.; Ward, M. D. *Acc. Chem. Res.* **1998**, *31*, 842–851.
(48) Barlow, S.; O'Hare, D. *Chem. Rev.* **1997**, *97*, 637–669.
(49) Salaymeh, F.; Berhane, S.; Yusof, R.; de la Rosa, R.; Fung, E. Y.; Matamoros, R.; Lau, K. W.; Zheng, Q.; Kober, E. M.; Curtis, J. C. *Inorg. Chem.* **1993**, *32*, 3895–3908.
(50) Richardson, D. E.; Taube, H. *Coord. Chem. Rev.* **1984**, *60*, 107–129.
(51) (a) Gagne, R. R.; Spiro, C. L.; Smith, T. J.; Hamann, C. A.; Thies, W. R.; Shiemke, A. D. *J. Am. Chem. Soc.* **1981**, *103*, 4073–4081. (b) Moore, K. J.; Lee, L.; Mabbott, G. A.; Petersen, J. D. *Inorg. Chem.* **1983**, *22*, 1108–1112.

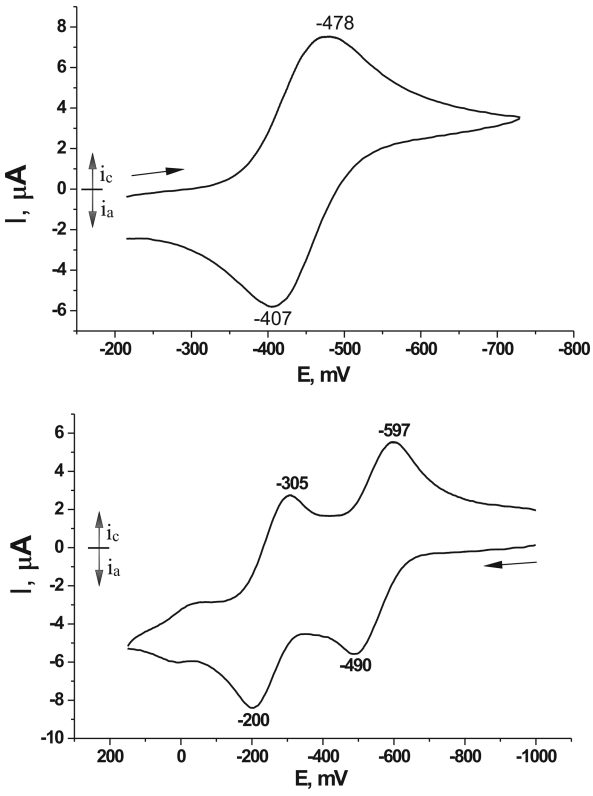

Figure 5. Cyclic voltammogram for **11[PF$_6$]** (top) and **10** (bottom) in CH_2Cl_2 with 0.1 M [nBu$_4$N][PF$_6$]; Au electrode; E vs $Fc^{0/+}$; scan rate = 100 mV/s; 20 °C.

(Figure 4) not allowing interactions with the halogens or the bridge system, which possess σ- or π-type orbitals. Due to this, orbital overlap between the HOMO or SOMO and the bridge can not occur. In a C_{4h} or D_{4d} structure this would prevent π-orbital influence of the axial ligands on the redox properties of such species.[41] Nevertheless a through-bridge electronic coupling was observed, which is thought to originate from symmetry lowering allowing with just "approximate" orthogonality of the π-type orbitals of the bridge and the *axial* ligands with the HOMO or SOMO of δ-type symmetry. As we have seen, a symmetry lowering to C_{2h} in the solid-state structure of **10** is evident. It is also prevailing in solution as confirmed by ^{31}P NMR. Symmetry lowering induces mixing of the δ-orbital with the d_{xz} and d_{yz} orbitals and consequently electronic communication depending on the extent of the mixing. A spin−orbital coupling may be another important factor for tungsten contributing mixing between orbitals of different symmetry.

The ΔE value for **10** of 290 mV ($K_c = 7.5 \times 10^4$) is similar to that reported for another related C_4-bridged system with low-symmetry end groups (250 mV).[33] It is indicative of a borderline class II-/III-type system according to the Robin−Day classification.[52] The peak separation is also solvent dependent, since in THF a ΔE value of 250 mV was found (see Supporting Information). Another explanation for this small but significant peak splitting was reported in the literature.[49] In accordance with this, the oxidation of the [M]C_4[M] system would lead to enhancement of the π-acceptor properties of the C_4 chain to stabilize the system and consequently to increase the second oxidation potential.

(52) Robin, M. B.; Day, P. *Adv. Inorg. Chem. Radiochem.* **1967**, *10*, 247–422.

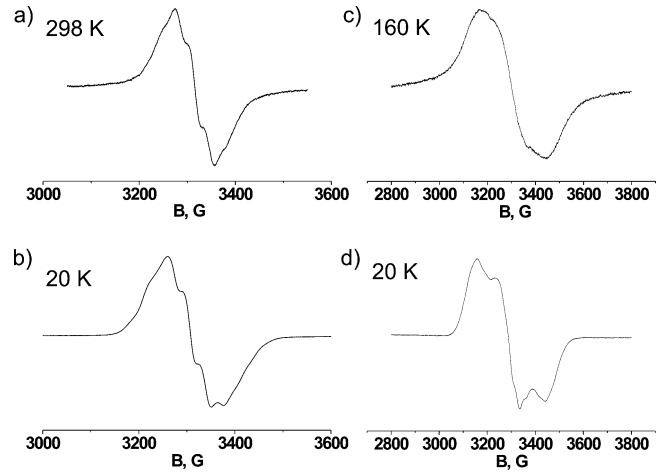

Figure 6. EPR spectra of (a) **11[PF$_6$]** at 298 K in CH_2Cl_2 solution; (b) **11[PF$_6$]** at 20 K in CH_2Cl_2 glass; (c) **10[BAr$^f_4$]** at 160 K in toluene solution; (d) **10[PF$_6$]** at 20 K in CH_2Cl_2/toluene glass.

EPR Study for Through-Bridge Electron Transfer in the Dinuclear Complexes. Localization or delocalization of an electron becomes evident through signal averaging at metal centers using different methods, such as EPR and IR.[3,5] Therefore, EPR measurements were carried out for **11[PF$_6$]**, **10[PF$_6$]**, **10[BAr$^f_4$]**, and **10[PF$_6$]$_2$** (Figure 6). **10[BAr$^f_4$]** (BAr$^f_4$-tetrakis[(3,5-trifluoromethyl)phenyl]borate) was used instead of **10[PF$_6$]** due to its solubility in toluene, which was required as a solvent to obtain a good signal-to-noise ratio in 100−200 K temperature interval. Compound **10[BAr$^f_4$]** was prepared *in situ* by anion exchange between Na[BAr$^f_4$] and **10[PF$_6$]**. The EPR spectra of **10[PF$_6$]** and **10[BAr$^f_4$]** in frozen CH_2Cl_2 at 20 K are completely identical. No clear signal was detected for **10[PF$_6$]$_2$**, apparently due to strong antiferromagnetic interactions.

Compound **11[PF$_6$]** showed one signal with $g = 2$ at room temperature and in frozen toluene solution, confirming electron localization on the [*trans*-W(dppe)$_2$I] center. The signal is fully symmetrical at room temperature and revealed only slight asymmetry in glass, which reflects only small spin−orbit coupling as expected from the molecular orbital diagram with the unpaired electron localized in the energetically rather isolated d_{xy} orbital (see Figure 4). A hyperfine coupling is detected due to coupling with the four phosphorus nuclei. Thus, the solution spectra of **11[PF$_6$]** could be modeled with a hyperfine ^{31}P coupling constant of 31 G and a line broadness of 20 G. The EPR spectrum of the mixed-valence complex **10[PF$_6$]** did not show any signal at room temperature. A signal of reasonable intensity was observed only below 160 K. The line broadness was then almost twice that of the signal of **11[PF$_6$]** which prevented observation of hyperfine coupling. The spectrum in frozen toluene solution at 20 K showed stronger anisotropy than in the case of **11[PF$_6$]**.

The broadness of the signal of **10[PF$_6$]** is interpreted in terms of electron dynamics with intramolecular transfer between the remote metal ends or with a stronger spin−orbit coupling.

IR Investigation of Through-Bridge Electron Transfer in the Dinuclear Complexes. IR can usually be utilized as a probe to measure the extent of the electron delocalization via the extent of averaging of the characteristic absorptions strongly affected by the oxidation state of the metal center. Furthermore, in symmetry-lowered systems with electron exchanges between the metal centers slow on the IR time scale (10^{-13} s), one can often identify new absorptions forbidden to appear in a

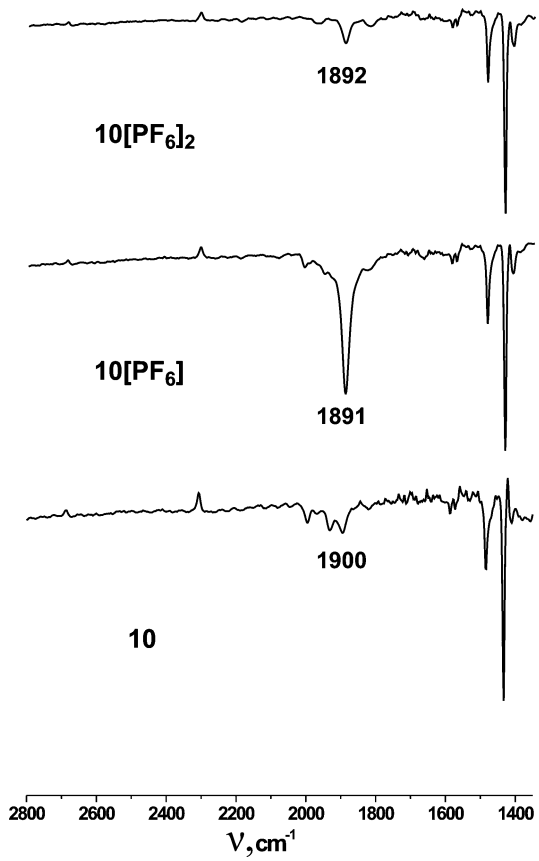

Figure 7. $\nu(C_4)$ absorptions in the IR spectra of **10**, **10[PF$_6$]**, and **10[PF$_6$]$_2$** (CH_2Cl_2, room temperature, 5×10^{-3} M).

symmetrical system.[3,53] In the spectra of the mixed-valence complex we did not find shifts for any absorption that might originate from oxidation of the metal center; however, our system seemed to be well suited for the latter approach, because of the highly symmetric C_4 bridge and the IR forbidden central ν(CC) vibration. The appearance of an intense ν(CC) band in the IR spectrum of **10[PF$_6$]** indicates that this vibration is no longer forbidden, because on the IR time scale the centered symmetry of the molecule is apparently broken by tungsten centers of different electron counts. The IR spectra of the complexes **10**, **10[PF$_6$]** and **10[PF$_6$]$_2$** are presented in Figure 7.

The IR spectra of the symmetrical complexes **10** and **10[PF$_6$]$_2$** are presented for comparison in Figure 7 demonstrating the presence of only weak $\nu(C_4)$ bands. In contrast to **10** and **10[PF$_6$]$_2$**, **10[PF$_6$]** possesses an intense band at 1981 cm^{-1} corresponding to a symmetric $\nu(C_4)$ vibration. As mentioned previously, the presence of strong symmetrical ν(CC) vibration is an indicator of localization in the IR time scale. It should be mentioned that delocalization in such a short time regime would be characteristic of full delocalization and typically observed only for strongly interacting systems.[48]

NIR Evidence for Through-Bridge Electron Transfer in the Dinuclear Complexes. The electron transfer between the metal centers is sketched in the schematic energy diagram in Figure 8.[2]

Near-IR spectroscopy allows direct measurement of the reorganization parameter λ and approximation of the electronic coupling energy H_{ab} via the following equations:[3]

$$H_{ab}(cm^{-1}) = [(4.2 \times 10^{-4})\varepsilon\Delta\bar{\nu}_{1/2}E_{IT}]^{1/2}/d;\ \lambda = E_{IT}$$

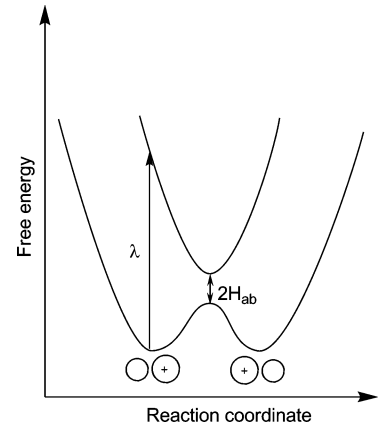

Figure 8. Schematic energy diagram explaining the origin of the charge transfer bands in the near-IR range.

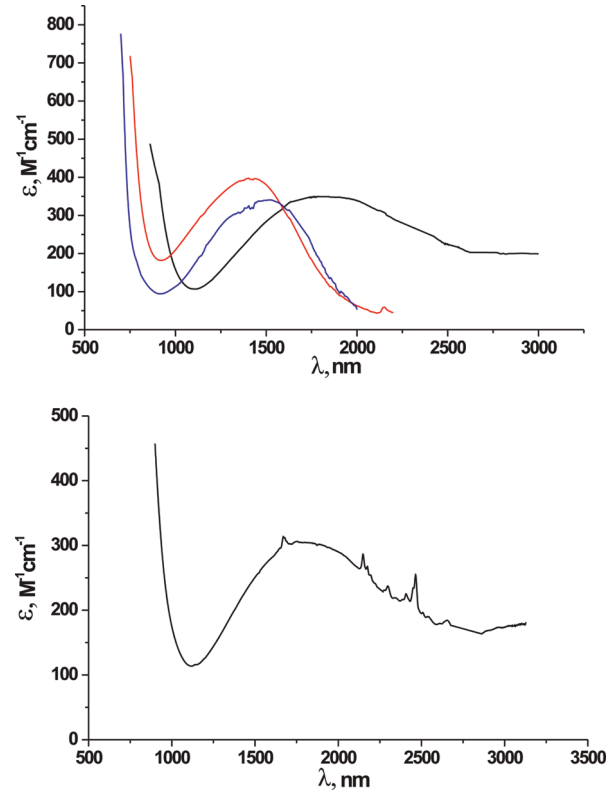

Figure 9. NIR spectra for **10[PF$_6$]** (black), **11[PF$_6$]** (blue), and **10[PF$_6$]$_2$** (red) in CH_2Cl_2. Regions with high noise due to solvent absorptions were linearly approximated. The bottom spectrum shows the NIR absorption of **10[PF$_6$]** in $CDCl_3$, where the solvent background is less than that in CH_2Cl_2.

where ε is the absorption coefficient in M^{-1} cm^{-1}, $\Delta\nu_{1/2}$ the width of the absorption band at half-height in cm^{-1}, E_{IT} the energy of the band maximum in cm^{-1}, and d the electron transfer distance in Å. The spectra for **11[PF$_6$]**, **10[PF$_6$]**, and **10[PF$_6$]** are presented in Figure 9.

All spectra are of relatively low intensity and broad especially that of **10[PF$_6$]**. The bands of **11[PF$_6$]** and **10[PF$_6$]$_2$** are centered at significantly higher energies than those of **10[PF$_6$]**. The fact that **11[PF$_6$]** and **10[PF$_6$]$_2$** have a similar absorption in the NIR supports the idea that this absorption is a result of a $\pi \rightarrow d_{xy}$ transition (see Figure 4). The spectrum of **10[PF$_6$]** can be explained as a superposition of a $\pi \rightarrow d_{xy}$ transition and a charge-transfer transition, Figure 9. Calculations with overlapping bands

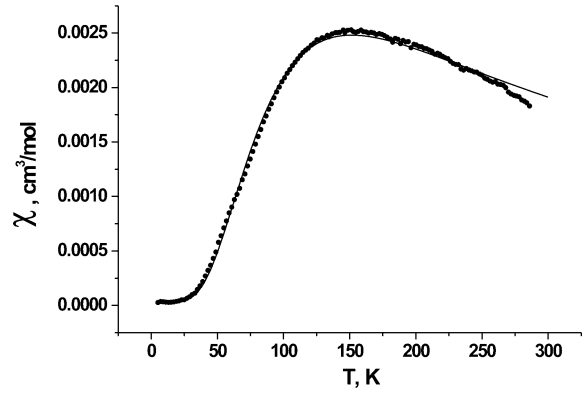

Figure 10. Temperature dependence of χ vs T for **10[PF$_6$]$_2$**. The data are corrected for core diamagnetism, van Vleck paramagnetism, and other temperature-independent contributions. Contribution from a small (on the level of 2%) paramagnetic impurity has been compensated. The uncorrected data are presented in the Supporting Information.

must possess tentative character. We estimated by using the right edge of the plateau of the given band as the center of the charge transfer band in the calculations. An estimate of the reorganization parameter λ for **10[PF$_6$]** from this absorption band amounts to 2000 nm (5000 cm^{-1}). This value is significantly smaller in energy than those of the majority of published systems detected in the range of 1000 to 1500 nm.[3,48,50,54] The low value would indicate a small reorganization energy, which is in agreement with the derived structural data, where only small changes in bond distances were detected upon oxidation. Approximation of H_{ab} leads to an energy of about 250 cm^{-1}. Within the nonadiabatic limit, the rate constant for electron transfer is given by the following equation:[2,55]

$$k = (2H_{ab}^2/\hbar)(\pi^3/\lambda k_b T)^{1/2}\exp(-\lambda(1 - 2H_{ab}/\lambda)^2/4k_b T)$$

From this equation we calculated a value of 1.5×10^{11} s^{-1} for our system, which is consistent with electron localization on the IR time scale and with a borderline case between localized behavior and an averaging situation for the EPR exchange.

Magnetic Measurements to Characterize Through-Bridge Electronic Interaction in the Dinuclear Complexes. The magnetic properties of **11[PF$_6$]**, **10[PF$_6$]**, and **10[PF$_6$]$_2$** were established by variable-temperature magnetization measurements. The magnetic susceptibilities of **11[PF$_6$]** and **10[PF$_6$]** showed a typical paramagnetic behavior, as could be expected from the presence of one unpaired electron in these molecules (Figures 8S and 9S in the Supporting Information). The magnetic susceptibility of **10[PF$_6$]$_2$** shows a maximum at 150 K (Neel temperature) and drops considerably on going to higher temperatures (Figure 10).

Thus, the magnetic behavior of **10[PF$_6$]$_2$** is typical of a strongly antiferromagnetically coupled spin dimer. To obtain an estimate of the exchange coupling, we fitted the experimental data with the equation for a spin-$^1/_2$ dimer model (spin Hamiltonian: $H = -J\mathbf{S_1}\cdot\mathbf{S_2}$):

$$\chi = \frac{2N_A g^2\beta^2}{kT}\cdot\frac{1}{(3 + e^{J/kT})}$$

with g and J as parameters. The minimized value for the g-factor is close to a free electron value of 2. The derived J indicates a singlet−triplet gap equal to 167 cm^{-1}, which is significantly more than 26 cm^{-1} observed for related bis-carbyne complex and than J for dinuclear W and Mo complexes in low spin d^5 and d^1 configurations.[47,56,57] Comparable values of exchange energies were obtained for dinuclear ruthenium complexes.[58] The antiferromagnetic nature of the spin interactions could be explained by a spin-polarization mechanism involving eight p-orbitals of the bridge.[57] The presence of strong antiferromagnetic coupling provides additional evidence for the interaction of metal orbitals with the π-orbitals of the bridge required for the mediation of magnetic ordering over long distance. The original data showed also presence of small paramagnetic impurities. The amount of these impurities was estimated using a fitting procedure of the sum of the antiferromagnetic and paramagnetic contributions on the level of 2% (see Supporting Information for details). This paramagnetic contribution was subtracted from the presented curve.

Conclusion

A versatile synthetic route to C$_4$-bridged tungsten complexes of the type [W]C$_4$[W] ([W] = [(X)W(dppe)(CO)$_2$] and [(X)W(dppe)$_2$]) was developed. The structures of the W(0) complexes were found to be close to a diacetylenic canonical form [W(0)]−C≡C−C≡C−[W(0)], while the structures with W(II) centers could be ascribed with biscarbynic bridge structures [W(II)]≡C−C≡C−C≡[W(II)]. The termini could be functionalized with reactive triflate substituents to eventually enable expansion of these dinuclear systems to polynuclear complexes. The mixed-valent complex **10[PF$_6$]** was found to reflect a class II system of the Robin−Day classification[52] possessing medium M····M "electronic communication" with barrier between the remote metal termini. The rate of electron transfer in this system was found to be in the same range as the EPR time scale, but appeared localized on the IR time scale. The remarkable stability, along with the ease of functionalization of the metal termini makes these complexes suitable candidates for "with barrier" organometallic wires to build complex single-electron devices.

Experimental Section

General Procedures. All the manipulations were carried out under a nitrogen atmosphere using Schlenk techniques or a drybox. Reagent grade benzene, toluene, hexane, pentane, diethyl ether, and tetrahydrofuran were dried and distilled from sodium benzophenone ketyl prior to use. Dichloromethane and acetonitrile were distilled from CaH_2, and chloroform was dried by P_2O_5. The modified literature procedures were used to prepare the following compounds: W(CO)$_3$(dppe)(THF),[35] Li$_2$C$_4$(THF)$_x$,[36] see Supporting Information

(53) Demadis, K. D.; El-Samanody, E. S.; Coia, G. M.; Meyer, T. J. *J. Am. Chem. Soc.* **1999**, *121*, 535–544.
(54) Ward, M. D. *Chem. Soc. Rev.* **1995**, 121–134.
(55) Sutin, N. *Prog. Inorg. Chem.* **1983**, *30*, 441–498.
(56) (a) Hu, J. S.; Sun, J. B.; Hopkins, M. D.; Rosenbaum, T. F. *J. Phys.: Condens. Matter* **2006**, *18*, 10837–10841. (b) Thompson, A. M. W. C.; Gatteschi, D.; McCleverty, J. A.; Navas, J. A.; Rentschler, E.; Ward, M. D. *Inorg. Chem.* **1996**, *35*, 2701–2703. (c) Stobie, K. M.; Bell, Z. R.; Munhoven, T. W.; Maher, P. J.; McCleverty, J. A.; Ward, M. D.; McInnes, E. J. L.; Totti, F.; Gatteschi, D. *Dalton Trans.* **2003**, 36–45.
(57) Ung, V. A.; Thompson, A. M. W. C.; Bardwell, D. A.; Gatteschi, D.; Jeffery, J. C.; McCleverty, J. A.; Totti, F.; Ward, M. D. *Inorg. Chem.* **1997**, *36*, 3447–3454.
(58) Aquino, M. A. S.; Lee, F. L.; Gabe, E. J.; Bensimon, C.; Greedan, J. E.; Crutchley, R. J. *J. Am. Chem. Soc.* **1992**, *114*, 5130–5140.

for details. All other chemicals were used as obtained from commercial suppliers. IR spectra were obtained on a Bio-Rad FTS-45 instrument and Bio-Rad Excalibur FTS-3500. NMR spectra were measured on a Varian Mercury spectrometer at 200 MHz for ^{1}H and 81 MHz for ^{31}P{^{1}H}, Varian Gemini-2000 spectrometer at 300 MHz for ^{1}H and 75 MHz for ^{13}C{^{1}H} and on a Bruker-DRX-500 spectrometer at 500 MHz for ^{1}H, 125.8 MHz for ^{13}C{^{1}H} and 202.5 MHz for ^{31}P{^{1}H}. Chemical shifts for ^{1}H and ^{13}C are given in ppm relative to TMS and those for ^{31}P relative to phosphoric acid. The UV−vis and near-IR spectra were recorded on a Varian CARY 50 Scan UV−visible and on a Varian CARY 500 Scan UV−visible−near-IR spectrometers. CHN elemental analyses were performed with a LECO CHN-932 microanalyzer. Raman spectra were recorded on a Renishaw Ramanscope spectrometer (633 nm). Cyclic voltammograms were obtained with BAS 100W voltammetric analyzer equipped with the low volume cell. The cell was equipped with an Au working and a Pt counter electrode, and a non-aqueous reference electrode. All sample solutions (CH_2Cl_2) were approximately 5×10^{-3} M in substrate and 0.1 M in Bu_4NPF_6, and were prepared under nitrogen. Ferrocene was subsequently added and the calibration of voltammograms recorded. BAS 100W program was employed for data analysis. X-band EPR spectra were obtained using Bruker EMX Electron Spin Resonance system. To measure spectrum of $\mathbf{10}^+$ at different temperatures toluene solution was required. Due to insolubility of **10[PF$_6$]** in toluene, the **[PF$_6$]**$^-$ counter-ion was exchanged to **[BAr$^f_4$]**$^-$ by treatment of **10[PF$_6$]** with Na[BAr$^f_4$] in CH_2Cl_2. The spectra of **10[PF$_6$]** and **10[BAr$^f_4$]** in frozen solution at 20 K are fully identical. A solution spectrum of **11[PF$_6$]** was modeled with help of Bruker WIN EPR Simfonia software. Magnetization measurements were carried out on a Quantum Design SQUID magnetometer, molar magnetic susceptibility was calculated according to the equation $\chi = (M \cdot M_w)/(m \cdot H)$, where M = experimental magnetization, M_w = molecular weight, m = sample weight, H = magnetic field.

X-ray Diffraction Studies on 2−8, 10, 11, 11[PF$_6$]. Data collection for crystals of **2** and **6**, were carried out on Stoe IPDS diffractometer (Imaging Plate Detector System with graphite-monochromated Mo K_α radiation, $\lambda = 0.71073$ Å)[59] and for others on Oxford Diffraction Xcalibur R diffractometer (4-circle kappa platform, Ruby CCD detector and a single wavelength Enhance X-ray source with Mo K_α radiation, $\lambda = 0.71073$ Å) at 183(2) K using a cold N_2-gas stream from an Oxford Cryogenic System. Pre-experiment, data collection, and data reduction (unit cell determination, intensity data integration, and empirical absorption correction) for for **3**−**8**, **10**, **11**, **11[PF$_6$]**: were carried out with the Oxford *CrysAlisPro* software.[60] The structures were solved with the unique data sets using the Patterson method of the program SHELXS-97. The structure refinement was performed with the program SHELXL-97.[61] Non-hydrogen atoms were refined anisotropically by full-matrix least-squares techniques based on F^2. The hydrogen atoms of the organic groups were placed in calculated positions and refined with a riding model with a fixed temperature factor. The program PLATON[62] was used to check the result of the X-ray analysis. The disorders observed for one THF molecule in **1**, for the positions of the $-CH_2-CH_2-$ units of the dppe ligand and for the C_4 bridge between the transition metals in **7** and **8**, were treated with the EADP and PART instructions of SHELXL-97 and anisotropically refined. Further details on all structures are provided in Tables 1Sa and 1Sb, and in the form of cif files available as part of the Supporting Information or from the CCDC under deposition numbers 754637−754645 and 755094.

Li$_2$[(CO)$_3$(dppe)WC$_4$W(CO)$_3$(dppe)] (THF)$_3$(C$_6$H$_6$)$_2$ (2). Solid $Li_2C_4(THF)_x$ (150 mg) was added to a solution of W(CO)$_3$(dppe)(THF) (1 g, 1.35 mmol) in 80 mL of THF. This mixture was stirred during 18 h at 55 °C. The resulting brown suspension was filtered and concentrated to 20 mL *in vacuo*. Complex **2** was obtained as a powder after addition of benzene (60 mL) to the THF solution. The product was recrystallized from a glyme/ether mixture. Yield: 610 mg (0.346 mmol, 51%). Single crystals suitable for X-ray diffraction were grown by addition of ether to the THF solution of **2**. Anal. Calcd for $C_{86}H_{84}Li_2O_9P_4W_2$: C, 58.45; H, 4.79. Found: C, 58.24; H, 4.69. IR (cm^{-1}): 2050 (C≡C), 1892 (CO), 1814 (CO), 1726 (CO). ^{1}H NMR (200 MHz, THF-d_8) δ = 7.99−7.71 (m, 15H, C_6H_5), 7.38−7.22 (m, 25H, C_6H_5), 2.83 (m, 4H, CH_2), 2.35 (m 4H, CH_2). ^{31}P NMR (81 MHz, THF-d_8) δ = 34.40 (s, $^1J_{W-P}$ (d, satellite) = 202 Hz). ^{13}C NMR (125 MHz, THF-d_8) δ = 218.5 (dd, $^2J_{C-P(cis)}$ = 7.3 Hz, $^2J_{C-P(trans)}$ = 34.5 Hz, CO (equatorial)), 213.5 (s, CO (axial)), 140.7 (d, $^1J_{C-P}$ = 37.5 Hz, *ipso*-C_6H_5), 140.0 (d, $^1J_{C-P}$ = 37.5 Hz, *ipso*-C_6H_5), 129.2 (s, C_6H_5), 128.7 (s, C_6H_5), 128.1 (m, C_6H_5), 106.9 (s, C_β), 106.2 (t, $^2J_{C-P}$ = 12.5 Hz, C_α), 32.3 (dd, $^1J_{C-P}$ = 18.5 Hz, $^2J_{C-P}$ = 18.0 Hz, CH_2).

[I(CO)$_2$(dppe)WC$_4$W(CO)$_2$(dppe)I] (3). Ten milliliters of a THF solution of iodine (121 mg, 0.47 mmol) was added dropwise to a solution of **2** (400 mg, 0.23 mmol) in glyme/THF (10/15 mL) at −60 °C. After stirring the reaction mixture for 20 min, the cooling bath was removed, and the mixture was additionally stirred for 6 h at room temperature. The resulting brown-violet solution was evaporated to dryness *in vacuo*. Addition of acetonitrile (5 mL) resulted in the formation of violet crystals of **3** (300 mg, 0.19 mmol) which were filtered and washed with acetonitrile (10 mL). A second crystallization from the filtrate afforded an additional 30 mg (0.019 mmol) of the desired product **3**. Yield: 330 mg (0.21 mmol, 91%). Single crystals suitable for X-ray diffraction were grown by cooling a dichloromethane solution of **3**. Anal. Calcd for $C_{60}H_{48}I_2O_4P_4W_2$: C, 45.66; H, 3.07. Found: C, 45.76; H, 3.20. IR (cm^{-1}): 1990 (CO), 1929 (CO). ^{1}H NMR (500 MHz, CD_2Cl_2) δ = 7.68−7.58 (m, 16H, C_6H_5), 7.46−7.42 (m, 8H, C_6H_5) 7.41−7.37 (m, 4H, C_6H_5), 7.27−7.23 (m, 4H, C_6H_5), 7.18−7.13 (m, 8H, C_6H_5), 3.1 (m, 4H, CH_2), 2.6 (m, 4H, CH_2). ^{31}P NMR (81 MHz, CD_2Cl_2) δ = 29.32 (s, $^1J_{W-P}$ (d, satellite) = 228 Hz). ^{13}C NMR (125 MHz, CD_2Cl_2) δ = 225.2 (t, $^2J_{C-P}$ = 11.1 Hz, C_α), 211.2 (dd, $^2J_{C-P(cis)}$ = 6.9 Hz, $^2J_{C-P(trans)}$ = 43,0 Hz, CO), 134.7 (d, $^1J_{C-P}$ = 25.1 Hz, *ipso*-C_6H_5), 134.3 (d, $^1J_{C-P}$ = 25.2 Hz, *ipso*-C_6H_5), 133.3 (d, $^2J_{C-P}$ = 11.9 Hz, *ortho*-C_6H_5), 132.5 (d, $^2J_{C-P}$ = 9.8 Hz, *ortho*-C_6H_5), 130.7 (d, $^4J_{C-P}$ = 62.5 Hz, *para*-C_6H_5), 128.7 (t, $^3J_{C-P}$ = 10.5 Hz, *meta*-C_6H_5), 87.5 (t, $^3J_{C-P}$ = 3.7 Hz, C_β) 38.4 (dd, $^1J_{C-P}$ = 28.1 Hz, $^2J_{C-P}$ = 11.9 Hz, CH_2).

[IW(CO)$_3$(dppe)(CCPh)] (4). A solution of lithium phenylacetylide (7.5 mg, 0.068 mmol) in THF (2 mL) was slowly added to a solution of W(CO)$_3$(dppe)(THF) (60 mg, 0.068 mmol) in 5 mL of THF. This mixture was stirred during 20 min at room temperature. To the resulting yellow solution of Li[W(CO)$_3$(dppe)(CCPh)] was added dropwise a THF solution of iodine (17 mg, 0.068 mmol) at −20 °C. The resulting brown-yellow solution was evaporated to dryness *in vacuo*. Addition of acetonitrile (2 mL) to the remaining solid led to the formation of orange crystals of **4**, which were filtered and washed with acetonitrile (5 mL). Single crystals suitable for X-ray diffraction were grown by layering a CH_2Cl_2 solution with acetonitrile. Yield: 38 mg (0.043 mmol, 63%). Anal. Calcd for $C_{37}H_{29}IO_3P_2W$: C, 49.58; H, 3.49. Found: C, 49.50; H, 3.41. IR (cm^{-1}): 2024 (CO), 1955 (CO), 1896 (CO). ^{1}H NMR (200 MHz, CD_2Cl_2) δ = 7.67 (br, 15H, PC_6H_5), 7.46 (m, 25H, PC_6H_5), 7.04 (m, 3H, CCC_6H_5), 6.55 (m, 2H, CCC_6H_5), 2.85−2.65 (m, 4H, CH_2). ^{31}P NMR (81 MHz, CD_2Cl_2) δ = 28−22 br. ^{13}C NMR (125 MHz, CD_2Cl_2) δ = 133.1 (s, C_6H_5), 130.7 (s, C_6H_5), 130.1 (s, C_6H_5), 128.5 (s, C_6H_5), 127.6 (s, C_6H_5), 126.7 (s, C_6H_5), 126.0 (s, C_6H_5), 26.6 (br, CH_2).

[X(CO)$_2$(dppe)WCC(Me)C(Me)CW(CO)$_2$(dppe)X] (5 (X = I), 6 (X = Cl)). Solid $[Me_3O]BF_4$ (7 mg, 0.046 mmol) was slowly added to the solution of **2** (40 mg, 0.023 mmol) and NBu_4I or

(59) *Stoe IPDS Software*, Version 2.87 5/1998 ed.; Stoe & Cie: Darmstadt, Germany, 1998.
(60) *CrysAlisPro*, Version 1.171.32.5 ed.; Oxford Diffraction Ltd.: Abingdon, Oxfordshire, England, 2007.
(61) Sheldrick, G. M. *Acta Crystallogr.* **2008**, *A64*, 112–122.
(62) Spek, A. L. *J. Appl. Crystallogr.* **2003**, *36*, 7–13.

NBu_4Cl (25 or 19 mg, 0.069 mmol) in glyme (2 mL) at −20 °C. Stirring of this mixture for 6 h led to the formation of a pale-orange precipitate (15 mg for I and 5 mg for Cl), which was filtered and dispersed in CH_2Cl_2 (8 mL). To this solution was added iodine (3 mg, 0.012 mmol) or $[FeCp_2]PF_6$ (2.6 mg, 0.008 mmol) in 2 mL of CH_2Cl_2. After stirring the reaction mixture for 1 h, the solvent was removed *in vacuo*, and the red-brown product obtained was crystallized from CH_2Cl_2/acetonitrile to give **5** and **6** as red crystals, respectively. Single crystals of **5** and **6** suitable for X-ray diffraction were grown by slow evaporation of CH_2Cl_2 from CH_2Cl_2/acetonitrile mixture. For **5**: Yield: 7 mg (0.0044 mmol, 20%). Anal. Calcd for $C_{62}H_{54}I_2O_4P_4W_2$: C, 46.30; H, 3.38. Found: C, 46.28; H, 3.60. IR (cm^{-1}): 1976 (CO), 1918 (CO). ^1H NMR (200 MHz, CD_2Cl_2) δ = 7.85−7.57 (m, 15H, C_6H_5), 7.44−7.34 (m, 25H, C_6H_5), 3.15 (m, 4H, CH_2), 2.75 (m, 4H, CH_2), 0.56 (s, 6H, CH_3). ^{31}P NMR (81 MHz, CD_2Cl_2) δ = 28.04. ^{13}C NMR (125 MHz, CD_2Cl_2) δ = 133.0 (s, C_6H_5), 132.3 (s, C_6H_5), 129.0 (m, C_6H_5), 128.5 (m, C_6H_5), 30.0 (m, CH_2), 10.7 (s, CH_3). For **6**: Yield: 1 mg (0.0007 mmol, 3%). Anal. Calcd for $C_{62}H_{54}Cl_2O_4P_4W_2$: C, 52.24; H, 3.82. Found: C, 52.47; H, 3.97. IR (cm^{-1}): 1983 (CO), 1921 (CO). ^1H NMR (200 MHz, CD_2Cl_2) δ = 7.82−7.57 (m, 15H, C_6H_5), 7.45−7.32 (m, 25H, C_6H_5), 2.97 (m, 4H, CH_2), 2.70 (m, 4H, CH_2), 0.53 (s, 6H, CH_3). ^{31}P NMR (81 MHz, CD_2Cl_2) δ = 38.19 (s, $^1J_{W-P}$ (d, satellite) = 230 Hz). ^{13}C NMR (125 MHz, CD_2Cl_2) δ = 132.7 (m, C_6H_5), 130.7 (s, C_6H_5), 130.0 (m, C_6H_5), 128.6 (m, C_6H_5), 26.3 (m, CH_2), 16.7 (s, CH_3).

[Cl(CO)$_2$(dppe)WC$_4$W(CO)$_2$(dppe)Cl] (7). Method 1: Chloroform (1 mL) was added to the solution of **2** (40 mg, 0.023 mmol) in diglyme (2 mL). The reaction mixture was kept at room temperature until a color change to dark violet was observed. After that the solvent was removed *in vacuo*. The reaction mixture was adsorbed onto silica gel and subjected to column chromatography using benzene as eluent to isolate a red band to give 6 mg (0.0034 mmol, 15%) of **7**. A pink powder was isolated after removal of the solvent and subsequent washing with acetonitrile and drying *in vacuo*. Method 2: A solution of C_2Cl_6 (12.15 mg, 0.053 mmol) in THF (1 mL) was added dropwise to a solution of **2** (40 mg, 0.023 mmol) in glyme (1 mL) at room temperature. After stirring the reaction mixture for 6 h, the solvent was removed *in vacuo*, and the red-brown product obtained was washed three times with 1 mL of acetonitrile and dried *in vacuo*. Single crystals suitable for X-ray diffraction were grown by layering a benzene solution with pentane. Yield: 17 mg (0.012 mmol, 51%). Anal. Calcd for $C_{60}H_{48}Cl_2O_4P_4W_2$: C, 51.64; H, 3.47. Found: C, 51.81; H, 3.71. IR (cm^{-1}): 1992 (CO), 1934 (CO). ^1H NMR (200 MHz, C_6D_6) δ = 7.75−7.54 (m, 15H, C_6H_5), 7.06−6.89 (m, 25H, C_6H_5), 2.55 (m, 4H, CH_2), 2.15 (m, 4H, CH_2); ^{31}P NMR (81 MHz, C_6D_6) δ = 37.46 (s, $^1J_{W-P}$ (d, satellite) = 226 Hz); ^{13}C NMR (125 MHz, C_6D_6) δ = 228.4 (s, C_α), 215.0 (dd, $^2J_{C-P(cis)}$ = 7.2 Hz, $^2J_{C-P(trans)}$ = 48.0 Hz, CO), 135.3−135.0 (d, $^1J_{C-P}$ = 42.5 Hz, *ipso*-C_6H_5), 133.5−133.2 (m, C_6H_5), 130.7−130.4 (d, $^3J_{C-P}$ = 40.4 Hz, *para*-C_6H_5), 128.7−128.6 (m, C_6H_5), 85.8 (s, C_β) 27.8 (dd, $^1J_{C-P}$ = 26 Hz, $^2J_{C-P}$ = 12.5 Hz, CH_2).

[(SCN)(CO)$_2$(dppe)WC$_4$W(CO)$_2$(dppe)(NCS)] (8). An excess of the AgSCN (50 mg, 0.16 mmol) was added to a THF solution (5 mL) of **3** (50 mg, 0.032 mmol). The reaction mixture was stirred for 18 h at 50 °C. The resulting brown suspension was filtered, and solvent was removed *in vacuo*. Complex **8** formed as violet needles after crystallization from CH_2Cl_2/pentane. Single crystals suitable for X-ray diffraction were grown by layering benzene solution with pentane. Yield: 24 mg (0.017 mmol, 52%). Anal. Calcd for $C_{62}H_{48}N_2O_4P_4S_2W_2$: C, 51.69; H, 3.36; N, 1.94. Found: C, 51.75; H, 3.46; N, 1.96. IR (cm^{-1}): 2034 (NCS), 1988 (CO), 1931 (CO). ^1H NMR (500 MHz, CD_2Cl_2) δ = 7.62−7.52 (m, 15H, C_6H_5), 7.49 (m, 10H, C_6H_5), 7.35−7.15 (m, 15H, C_6H_5), 2.88 (m, 4H, CH_2), 2.62 (m, 4H, CH_2). ^{31}P NMR (81 MHz, C_6D_5Cl) δ = 39.88 (s, $^1J_{W-P}$ = (d, satellite) 234 Hz). ^{13}C NMR (125 MHz, C_6D_5Cl)[63] δ = 232.1 (s, C_α), 210.8 (dd, $^2J_{C-P(cis)}$ = 7.1 Hz, $^2J_{C-P(trans)}$ = 50.0 Hz, CO), 143.8 (s, NCS), 134.0 (d, $^1J_{C-P}$ = 49.5 Hz, *ipso*-C_6H_5), 133.1 (d, $^NJ_{C-P}$ = 18.5 Hz, C_6H_5), 132.6 (d, $^NJ_{C-P}$ = 18.4 Hz, C_6H_5), 131.2 (s, C_6H_5), 130.9 (s, C_6H_5), 129.5 (d, $^NJ_{C-P}$ = 16.5 Hz, C_6H_5), 128.9 (d, $^NJ_{C-P}$ = 16.6 Hz, C_6H_5), 82.1 (s, C_β) 24.9 (dd, $^1J_{C-P}$ = 36 Hz, $^2J_{C-P}$ = 16.5 Hz, CH_2).

[(TfO)(CO)$_2$(dppe)WC$_4$W(CO)$_2$(dppe)(OTf)] (9). A solution of silver triflate (17 mg, 0.064 mmol) in THF (3 mL) was added dropwise to a solution of **3** (50 mg, 0.032 mmol) in THF (3 mL) at room temperature. After stirring the reaction mixture for 20 min, the solution was filtered and cooled to −30 °C to give **9** as pale-violet needles. Yield: 43 mg (0.026 mmol, 83%). Anal. Calcd for $C_{62}H_{48}F_6O_{10}P_4S_2W_2$: C, 45.89; H, 2.98; N. Found: C, 45.81; H, 3.07; IR (cm^{-1}): 2000 (CO), 1945 (CO). ^1H NMR (200 MHz, THF-d_8) δ = 7.68−7.59 (m, 15H, C_6H_5), 7.42−7.34 (m, 25H, C_6H_5), 2.96−2.85 (m, 8H, CH_2). ^{31}P NMR (81 MHz, THF-d_8) δ = 44.82 (s, $^1J_{W-P}$ = (d, satellite) 236 Hz). ^{19}F NMR (188 MHz, THF-d_8) δ = −79.31 (s, SO_3CF_3). ^{13}C NMR (125 MHz, CD_2Cl_2) 215.7 (dd, $^2J_{C-P(cis)}$ = 7 Hz, $^2J_{C-P(trans)}$ = 50.5 Hz, CO), 135.6 (d, $^1J_{C-P}$ = 45.6 Hz, *ipso*-C_6H_5), 133.8 (d, $^NJ_{C-P}$ = 11.7 Hz, C_6H_5), 133.4 (d, $^NJ_{C-P}$ = 11.5 Hz, C_6H_5), 131.6 (d, $^1J_{C-P}$ = 40.6 Hz, *ipso*-C_6H_5), 131.7 (s, C_6H_5), 129.9 (d, $^NJ_{C-P}$ = 10.2 Hz, C_6H_5), 129.6 (d, $^NJ_{C-P}$ = 10.5 Hz, C_6H_5), 82.1 (s, C_β) 28.2 (dd, $^1J_{C-P}$ = 29.0 Hz, $^2J_{C-P}$ = 11.2 Hz, CH_2).

[I(dppe)$_2$WC$_4$W(dppe)$_2$I] (10). 3 (300 mg, 0.192 mmol) and diphenylphosphinoethane (dppe) (450 mg, 1.13 mmol) in diglyme (21 mL) were placed into a Young−Schlenk tube. The mixture was heated at 140 °C for 7 days. The tube was evacuated three times during this time. Large dark-green crystals of **10** separated as the solution became more transparent. Single crystals suitable for X-ray diffraction were grown by layering a CH_2Cl_2 solution with pentane. Yield: 395 mg (0.174 mmol, 91%). Anal. Calcd for $C_{108}H_{96}I_2P_8W_2$: C, 57.32; H, 4.28. Found: C, 57.12; H, 4.14. IR (cm^{-1}): 1900 (C≡C). ^1H NMR (200 MHz, CD_2Cl_2): δ = 7.85 (br, 15H, C_6H_5), 7.26−6.76 (m, 65H, C_6H_5), 2.81 (m, 8H, CH_2), 1.82 (m, 8H, CH_2). ^{31}P NMR (81 MHz, C_6D_6): δ = 45 br. ^{13}C NMR (125 MHz, CD_2Cl_2) δ = 213.1 (m, C_α), 141.7 (br, *ipso*-C_6H_5), 139.9 (br, *ipso*-C_6H_5), 135.5 (s, C_6H_5), 134.0 (s, C_6H_5), 129.4 (s, C_6H_5), 126.8 (s, C_6H_5), 86.5 (s, C_β) 36.0 (m, CH_2).

[I(dppe)$_2$WC$_4$W(dppe)$_2$I][PF$_6$] (10[PF$_6$]). To a solution of **10** (40 mg, 0.0177 mmol) in 8 mL of dichloromethane was added dropwise a solution of $[FeCp_2][PF_6]$ (5.9 mg, 0.0177 mmol). The reaction mixture was stirred for 1 h, and the solvent was removed *in vacuo*. The resulting solid was washed with benzene to remove ferrocene and recrystallized by layering the CH_2Cl_2 solution with ether to give **10[PF$_6$]**. Yield: 25.5 mg (0.0106 mmol, 60%). Anal. Calcd for $C_{108}H_{96}I_2F_6P_9W_2$: C, 53.86; H, 4.02. Found: C, 53.97; H, 4.21. IR (cm^{-1}): 1891 (C≡C). ^1H NMR (200 MHz, CD_2Cl_2): δ = 8.54−7.03 (m, C_6H_5), 1.26 (br), 0.2 (br), −2.6 (br), −3.4 (br), −4.8 (br).

[I(dppe)$_2$WC$_4$W(dppe)$_2$I][PF$_6$]$_2$ (10[PF$_6$]$_2$). A solution of $[Ph_3C][PF_6]$ (14.3 mg, 0.0354 mmol) was added dropwise at −20 °C to a solution of **10** (40 mg, 0.0177 mmol) in 8 mL of dichloromethane. The reaction mixture was stirred for 10 min at room temperature, and the solvent was removed *in vacuo*. The resulting solid was washed with benzene and recrystallized by layering a CH_2Cl_2 solution with ether to give **10[PF$_6$]$_2$**. Yield: 24 mg (0.0094 mmol, 53%). Anal. Calcd for $C_{108}H_{96}I_2F_{12}P_{10}W_2$: C, 50.81; H, 3.79. Found: C, 50.69; H, 3.86. IR (cm^{-1}): 1892 (C≡C). ^1H NMR (200 MHz, CD_2Cl_2): δ = 9.12−7.2 (m, C_6H_5), 1.35 (br), −0.64 (br), −5.82 (br), −6.82 (br).

[I(dppe)$_2$WC$_4$W(dppe)(CO)$_2$I] (11). 3 (50 mg, 0.032 mmol) and diphenylphosphinoethane (dppe) (40 mg, 0.1 mmol) were placed into Young−Schlenk tube and dissolved in a mixture of 3 mL of THF with 0.3 mL of CH_3CN. This tube was irradiated by a 125 W

(63) The NMR ^{13}C signals of the phenyl groups of dppe were determined separately in CD_2Cl_2 solution. N = 2 for ortho carbons, 3 for meta carbons, 4 for para carbons. Unfortunately, reliable assignment is difficult in this case.

medium pressure UV lamp (six intervals, 10 min each). The reaction was monitored by ^{31}P NMR and stopped when the signal of **3** had disappeared. The reaction mixture was evaporated, washed with pentane, and subsequently subjected to flash chromatography (silica gel, benzene) to give 23 mg of **11**. It was recrystallized from benzene. Single crystals suitable for X-ray diffraction were grown by layering a benzene solution with pentane. Yield: 23 mg (0.012 mmol, 38%). Anal. Calcd for $C_{84}H_{72}I_2O_2P_6W_2$: C, 52.52; H, 3.78. Found: C, 52.37; H, 3.92. IR (cm^{-1}): 1987 (CO), 1922 (CO). ^1H NMR (200 MHz, C_6D_6): δ = 7.72−7.58 (m, 16H, C_6H_5), 7.27 (m, 8H, C_6H_5), 7.08 (m, 17H, C_6H_5), 6.95 (m, 15H, C_6H_5), 6.78 (m, 4H, C_6H_5), 2.91 (m, 6H, CH_2), 2.36 (m, 6H, CH_2). ^{31}P NMR (81 MHz, C_6D_6): δ = 31.74 (s, 2P, $^1J_{W-P}$ (d, satellite) = 230 Hz), 32.33 (s, 4P, $^1J_{W-P}$ = (d, satellite) 268 Hz). ^{13}C NMR (125 MHz, CD_2Cl_2) δ = 230.3 (s, C_α W(dppe)$(CO)_2$), 212.8 (dd, $^2J_{C-P(cis)}$ = 6.7 Hz, $^2J_{C-P(trans)}$ = 42.0 Hz, CO), 212.3 (s, C_α W$(dppe)_2$) 140.9−139.6 (m, *ipso*-C_6H_5), 136.1−134.9 (m, C_6H_5), 134.2 (s, C_6H_5), 133.8 (d, J_{C-P} = 12 Hz, C_6H_5), 132.7 (d, $^NJ_{C-P}$ = 10 Hz, C_6H_5), 130.1 (s, C_6H_5), 129.7 (s, C_6H_5), 128.9−128.7 (m, C_6H_5), 127.5 (s, C_6H_5), 93.9 (s, $C_{\beta1}$), 83.0 (s, $C_{\beta2}$), 36.0 (m, CH_2 W$(dppe)_2$), 28.6 (dd, $^1J_{C-P}$ = 27.7 Hz, $^2J_{C-P}$ = 11.9 Hz, CH_2 W(dppe)$(CO)_2$).

[I(dppe)$_2$WC$_4$W(dppe)(CO)$_2$I][PF$_6$] (11[PF$_6$]). A solution of $[FeCp_2][PF_6]$ (4.3 mg, 0.013 mmol) was added dropwise to a solution of **11** (25 mg, 0.013 mmol) in 5 mL of dichloromethane. The reaction mixture was stirred for 1 h, and the solvent was removed *in vacuo*. The resulting solid was washed with benzene to remove ferrocene and redissolved in 1 mL of THF. The solution was placed at −30 °C. Brown crystals of **11[PF$_6$]** appeared after one day. Yield: 20 mg (0.0097 mmol, 74%). Anal. Calcd for $C_{84}H_{72}I_2F_6O_2P_7W_2$: C, 48.84; H, 3.51. Found: C, 49.01; H, 3.65. IR (cm^{-1}): 2000 (CO), 1938 (CO). ^1H NMR (200 MHz, CD_2Cl_2): δ = 9.1−6.75 (br, C_6H_5), 2.81 (br, CH_2), 2.29 (br, CH_2).

Acknowledgment. We thank S. Weyeneth, F. Muranyi, and A. Tsirlin for help with the magnetic measurements. Funding from the Swiss National Science Foundation (SNSF) and from the University of Zürich are gratefully acknowledged.

Supporting Information Available: Details of X-ray experiments, crystallographic information files, ORTEP-like plots of **4**−**8**, **11[PF$_6$]**, CV of **10** in THF, temperature dependence of χ vs T for **10[PF$_6$]**, **11[PF$_6$]**, and **10[PF$_6$]$_2$**. This material is available free of charge via the Internet at http://pubs.acs.org.

JA909764X

Supporting Information

Electronic Communication in Dinuclear C_4 – Bridged Tungsten Complexes

Sergey N. Semenov, Olivier Blacque, Thomas Fox, Koushik Venkatesan, and Heinz Berke

Synthesis

(1) **[W(dppe)(CO)$_3$(THF)]** A solution of **[W(dppe)(CO)$_4$] (**2.5 g, 3.6 mmol) in 300 mL in dry THF was irradiated with 500 W ultraviolet lamp with regular monitoring of the ^{31}P signal of **[W(dppe)(CO)$_4$]** until the presence of only 5% of **[W(dppe)(CO)$_3$(THF)]** in signal intensity. The temperature of reaction mixture was not allowed to exceed 20 ^{o}C and was kept in the range of 0 – 10 ^{o}C to avoid formation of side products and polymerization of THF. The CO formed during the reaction was removed continuously during the reaction time by purging with a flow of N_2 gas through solution. After completion of the reaction, the reaction mixture was concentrated to 10 mL in *vacuo*. Subsequent cooling and addition of Et_2O (10 mL) resulted in crystallization of the compound. The crystals was filtered and washed twice with Et_2O (20 mL). Yield 2.2 g (2.98 mmol, 83%) ^{1}H NMR (200 MHz, C_6D_6) δ 7.70 – 7.07 (m, 20H, C_6H_5), 3.62 (br, 4H, THF), 2.15 (m, 4H, CH_2), 1.50 (m 4H, THF); ^{31}P NMR (81 MHz, THF-d_8) δ = 41.7 ($^{1}J_{W\text{-}P}$ = 234 Hz).

(2) **[Li$_2$C$_4$(THF)n]** 1.01 g of $Me_3SiC{\equiv}CC{\equiv}CSiMe_3$ (5.2 mmol) were solved in 100 mL of dry THF in Schlenk flask under N_2. The solution was cooled to -20 ^{o}C and 7.6 mL of 1.5 M Methyllithium solution in ether (11.4 mmol, 2.2 equiv.) was added dropwise by a syringe. The cooling bath was than removed and the reaction mixture was stirred for 4 h at room temperature. The white precipitate formed during this time was filtered, washed with THF and dried in *vacuo* for 30 min to yield 1 g of [Li_2C_4(THF)n].

Table 1Sa. Summary of the X-ray diffraction studies of compounds **2-6**.

	2	**3**	**4**	**5**	**6**
empirical formula	C78 H80 Li2 O10 P4 W2	C60 H48 I2 O4 P4 W2, 2(C H2 Cl2)	C37 H29 I O3 P2 W	C62 H54 I2 O4 P4 W2	C62 H54 Cl2 O4 P4 W2, C2 H3 N
formula weight ($g \cdot mol^{-1}$)	1682.88	1748.20	894.29	1608.41	1466.57
temperature (K)	183(2)	183(2)	183(2)	183(2)	183(2)
wavelength (Å)	0.71073	0.71073	0.71073	0.71073	0.71073
crystal system, space group	monoclinic, C 2/c	monoclinic, C 2/c	triclinic, P -1	monoclinic, P 2_1/n	monoclinic, C 2/c
a (Å)	28.184(4)	24.5678(2)	9.5159(2)	11.6313(5)	19.357(3)
b (Å)	11.7485(11)	13.6187(1)	9.9084(2)	8.9452(4)	11.0318(10)
c (Å)	21.651(3)	20.6625(1)	18.0985(1)	27.3906(10)	30.138(4)
α (deg)	90	90	79.654(2)	90	90
β (deg)	97.261(18)	92.2971(6)	84.718(2).	94.231(4)	107.685(14)
γ (deg)	90	90	75.752(2)	90	90
volume ($Å^3$)	7111.4(17)	6907.74(8)	1625.03(5)	2842.1(2)	6131.6(14)
Z, density (calcd) ($Mg \cdot m^{-3}$)	4, 1.572	4, 1.681	2, 1.828	2, 1.880	4, 1.589
abs coefficient (mm^{-1})	3.381	4.510	4.639	5.290	3.987
F(000)	3368	3352	864	1544	2888
crystal size (mm^3)	0.13 x 0.07 x 0.05	0.18 x 0.16 x 0.075	0.47 x 0.17 x 0.12	0.12 x 0.05 x 0.02	0.33 x 0.22 x 0.15
θ range (deg)	2.6 to 25.0	2.5 to 30.5	2.4 to 30.5	2.4 to 29.0	2.2 to 25.0
reflections collected	26472	72801	42682	42915	26034
reflections unique	5964 [R(int) = 0.0936]	10537 [R(int) = 0.0345]	11813 [R(int) = 0.0276]	7509 [R(int) = 0.0811]	5379 [R(int) = 0.0780]
completeness to θ (%)	95.2	100.0	99.9 %	99.5	99.6
absorption correction	numerical	semi-empirical from equivalents	analytical	Semi-empirical from equivalents	numerical
max/min transmission	0.856 / 0.759	1.000 and 0.698	0.795 and 0.492	0.900 and 0.718	0.575 and 0.287
data / restraints / parameters	5964 / 0 / 437	10537 / 4 / 379	11813 / 0 / 397	7509 / 4 / 332	5379 / 0 / 366
goodness-of-fit on F^2	0.872	1.108	1.026	0.986	1.057
final R_1 and wR_2 indices [$I > 2\sigma(I)$]	0.0326, 0.0658	0.0246, 0.0809	0.0194, 0.0446	0.0505, 0.1203	0.0388, 0.1022
R_1 and wR_2 indices (all data)	0.0591, 0.0710	0.0388, 0.0857	0.0233, 0.0452	0.1029, 0.1564	0.0438, 0.1052

Table 1Sb. Summary of the X-ray diffraction studies of compounds **7**, **8**, **10**, **11** and **11[PF_6]**.

	7	**8**	**10**	**11**	**11[PF_6]**
empirical formula	C60 H48 Cl2 O4 P4 W2, C6 H6	C62 H48 N2 O4 P4 S2 W2, C5 H12, C6 H6	4(C108 H96 I2 P8 W2), 2(C H2 Cl2)	2(C84 H72 I2 O2 P6 W2), C H2 Cl2	2(C84 H72 I2 O2 P6 W2), 4(C4 H8 O), C H2 Cl2, 2(F6 P)
formula weight ($g \cdot mol^{-1}$)	1473.55	1590.98	9222.28	3926.37	4504.72
temperature (K)	183(2)	183(2)	183(2)	183(2)	183(2)
wavelength (Å)	0.71073	0.71073	0.71073	0.71073	0.71073
crystal system, space group	monoclinic, C 2/c	triclinic, P -1	monoclinic, C 2/c	monoclinic, P 2_1/n	monoclinic, P 2_1/c
a (Å)	24.9296(2)	13.1172(2)	34.7541(3)	18.7529(6)	16.9627(2)
b (Å)	12.9619(2)	13.7047(3)	13.28420(10)	23.9809(7)	16.7625(2)
c (Å)	20.4535(2)	22.2271(5)	20.1653(2)	19.4363(7)	36.0870(1)
α (deg)	90	103.552(2)	90	90	90
β (deg)	92.782(1)	92.316(2)	96.467(1)	115.899(4)	118.139(1)
γ (deg)	90	116.301(2)	90	90	90
volume ($Å^3$)	6601.5(1)	3434.31(14)	9250.68(14)	7862.9(5)	9048.11(18)
Z, density (calcd) ($Mg \cdot m^{-3}$)	4, 1.483	2, 1.539	1, 1.655	2, 1.658	2, 1.653
abs coefficient (mm^{-1})	3.703	3.550	3.370	3.911	3.438
F(000)	2896	1580	4556	3828	4424
crystal size (mm^3)	0.29 x 0.21 x 0.09	0.21 x 0.07 x 0.04	0.33 x 0.22 x 0.10	0.26 x 0.17 x 0.05	0.30 x 0.23 x 0.11
θ range (deg)	2.5 to 30.5	2.2 to 30.5	2.3 to 30.5	2.3 to 27.0 deg	2.3 to 30.5
reflections collected	65770	58428	68273	89489	96018
reflections unique	10007 [R(int) = 0.0357]	20927 [R(int) = 0.0503]	14124 [R(int) = 0.0383]	17145 [R(int) = 0.0588]	27192 [R(int) = 0.0725]
completeness to θ (%)	99.3	99.8	100.0	99.9	98.5
absorption correction	analytical	analytical	analytical	analytical	analytical
max/min transmission	0.793 and 0.460	0.897 and 0.575	0.799 and 0.490	0.861 and 0.516	0.714 and 0.391
data / restraints / parameters	10007 / 0 / 337	20927 / 4 / 705	14124 / 1 / 557	17145 / 2 / 892	27192 / 4 / 1048
goodness-of-fit on F^2	1.038	0.951	1.100	1.117	0.934
final R_1 and wR_2 indices [$I > 2\sigma(I)$]	0.0288, 0.0804	0.0404, 0.0804	0.0254, 0.0675	0.0462, 0.1017	0.0583, 0.1331
R_1 and wR_2 indices (all data)	0.0440, 0.0849	0.0849, 0.0928	0.0328, 0.0690	0.1012, 0.1371	0.1383, 0.1621

The unweighted R-factor is $R_1 = \sum(Fo - Fc)/\sum Fo$; I > 2 σ(I) and the weighted R-factor is $wR2 = \{\sum w(Fo^2 - Fc^2)^2/\sum w(Fo^2)^2\}^{1/2}$.

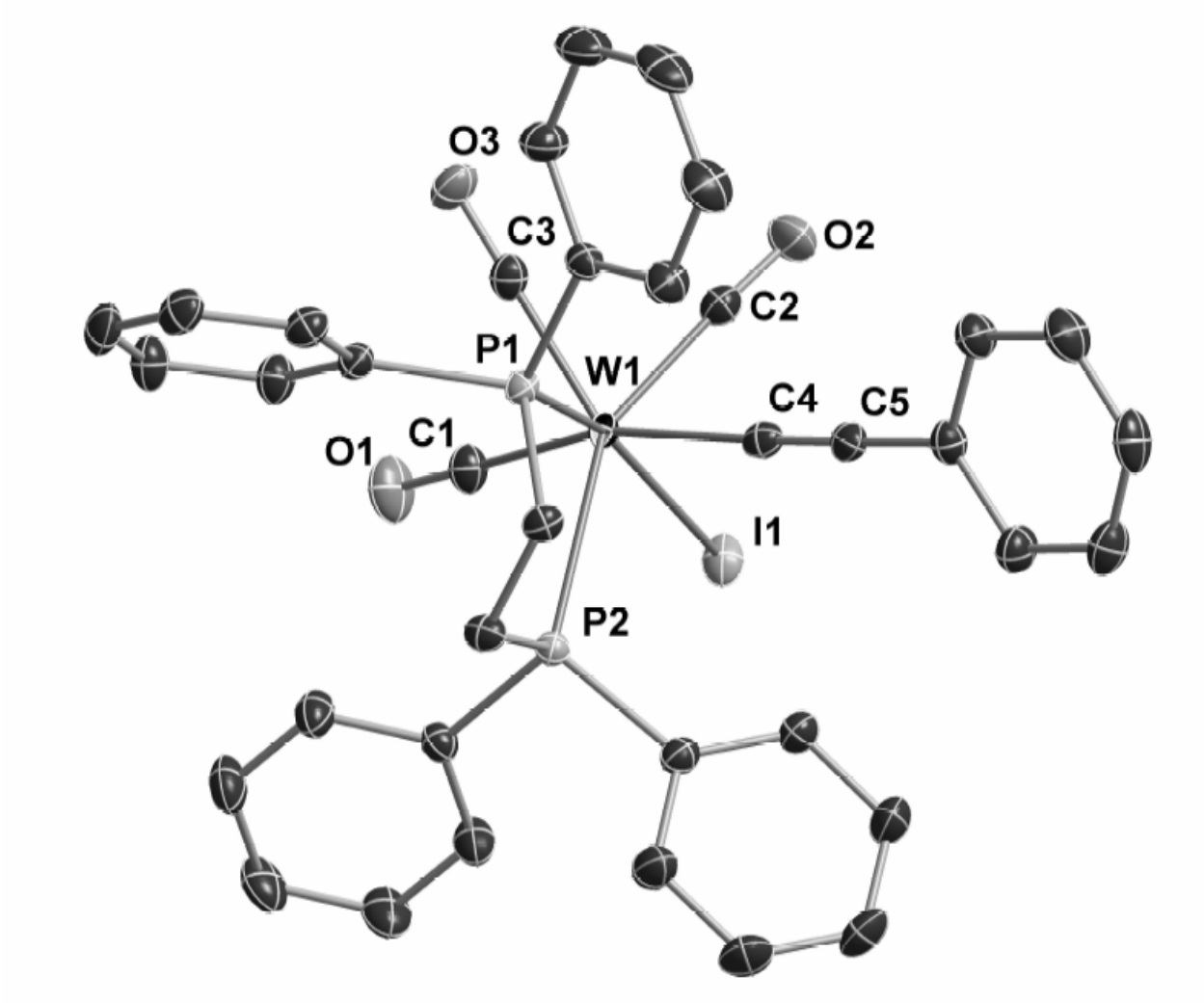

Figure 1S. ORTEP like drawing of **4** (50% probability level of thermal ellipsoids). Hydrogen atoms and solvent molecules are omitted for clarity.

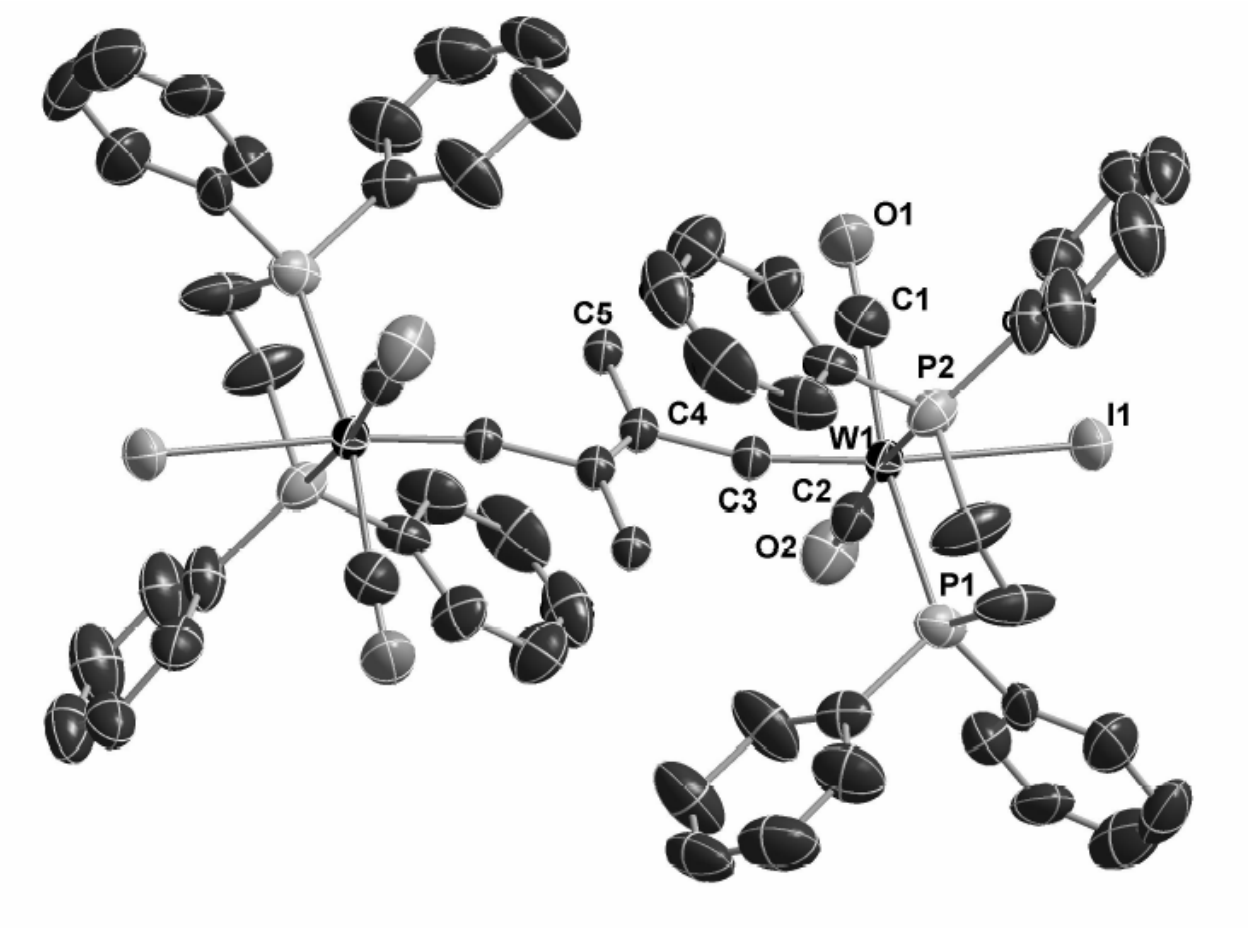

Figure 2S. ORTEP like drawing of **5** (50% probability level of thermal ellipsoids). Hydrogen atoms and solvent molecules are omitted for clarity. Only one component of disordered part is shown.

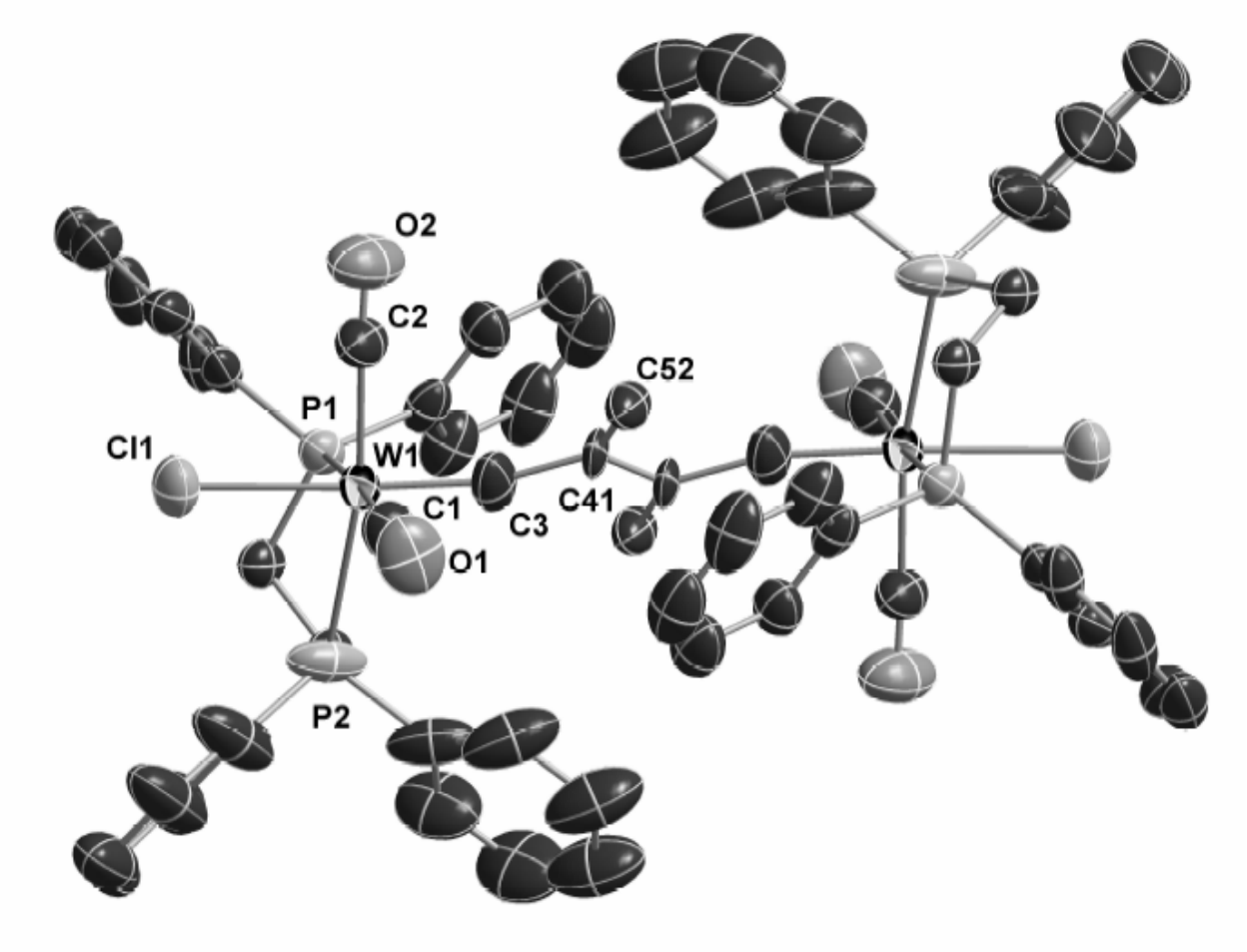

Figure 3S. ORTEP like drawing of **6** (50% probability level of thermal ellipsoids). Hydrogen atoms and solvent molecules are omitted for clarity. Only one component of disordered part is shown.

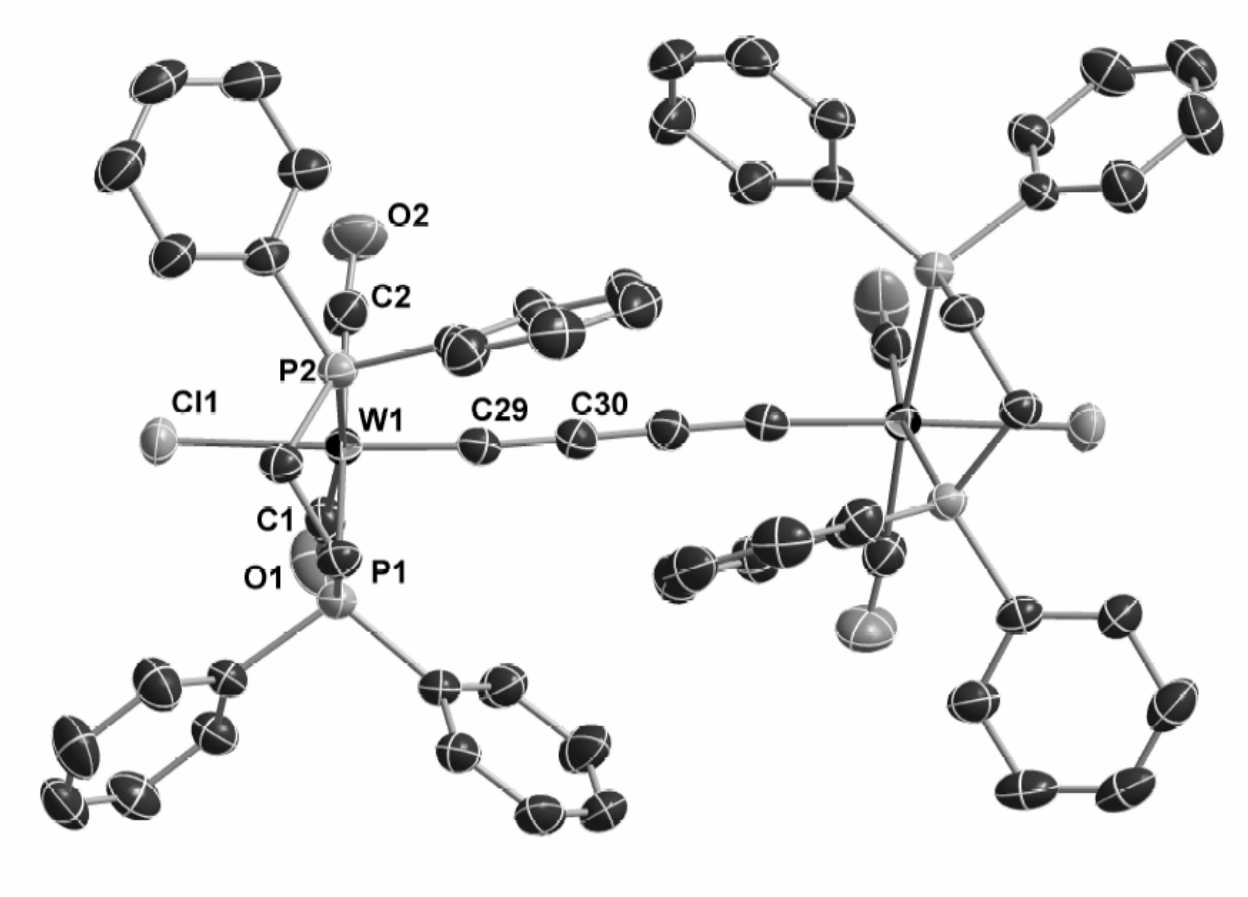

Figure 4S. ORTEP like drawing of **7** (50% probability level of thermal ellipsoids). Hydrogen atoms and solvent molecules are omitted for clarity.

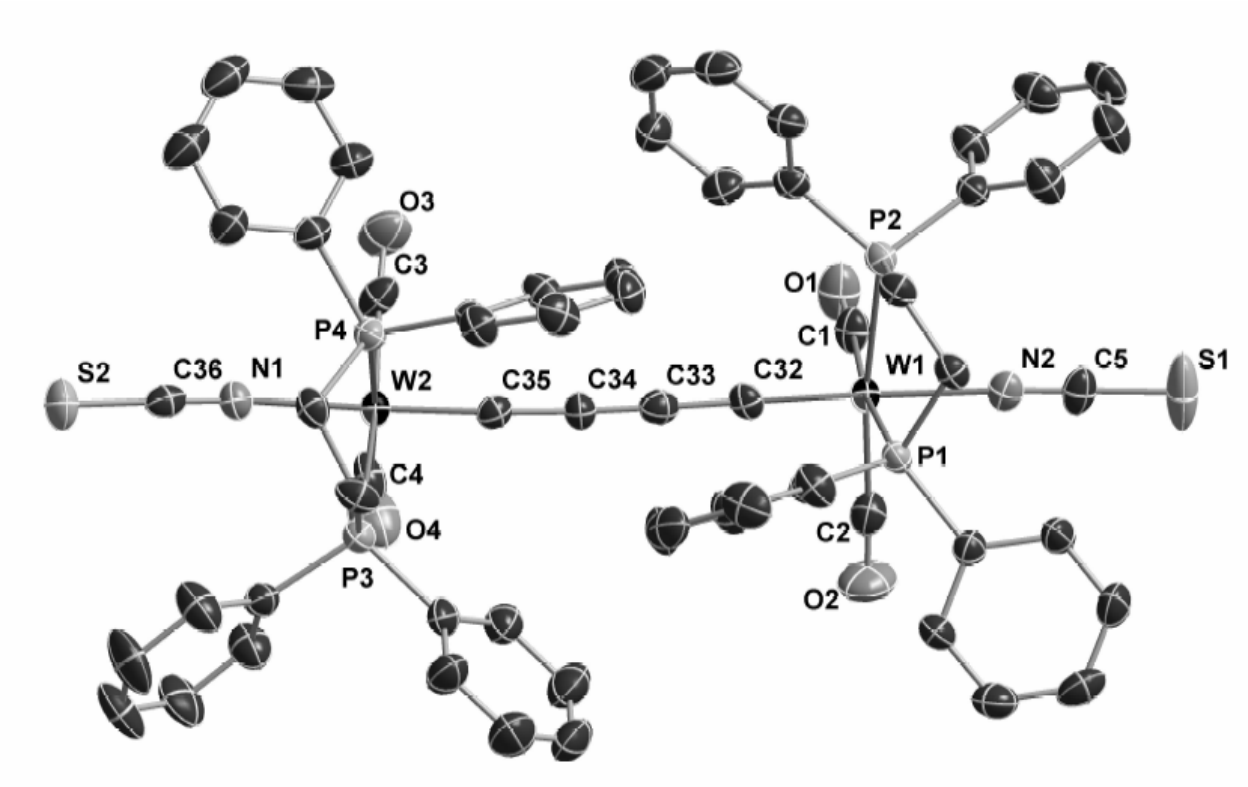

Figure 5S. ORTEP like drawing of **8** (50% probability level of thermal ellipsoids). Hydrogen atoms and solvent molecules are omitted for clarity.

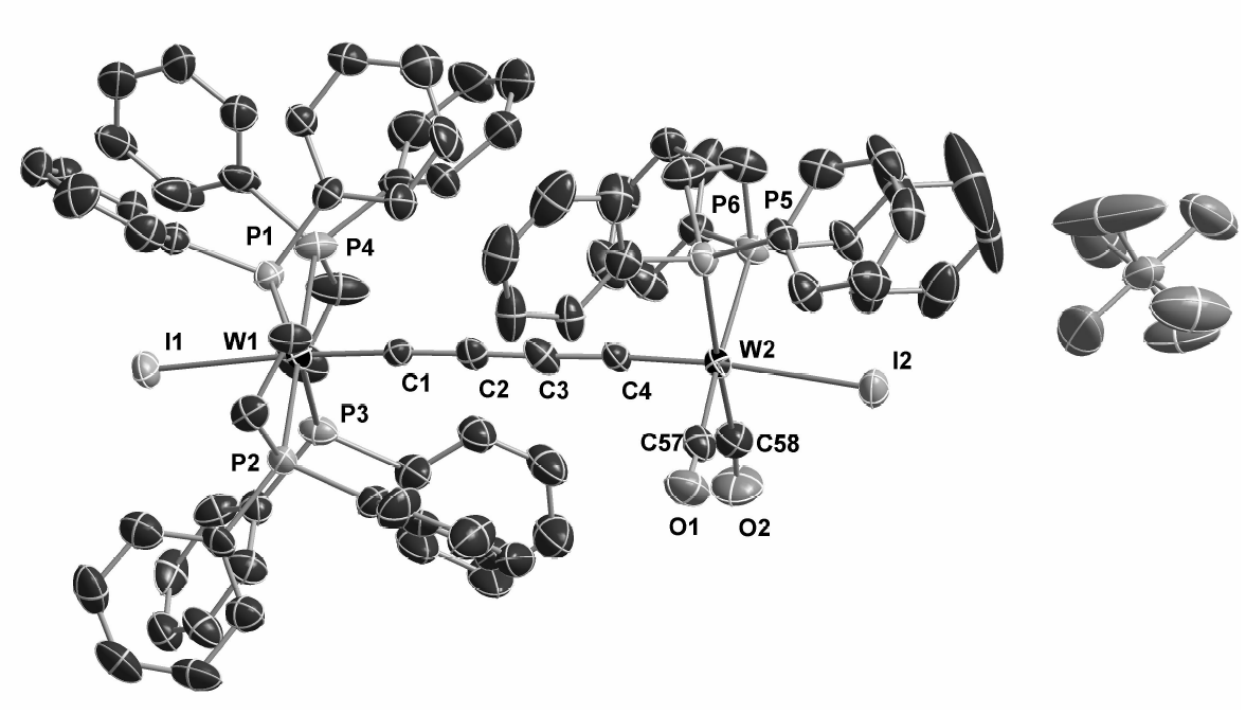

Figure 6S. ORTEP like drawing of **11[PF_6]** (50% probability level of thermal ellipsoids). Hydrogen atoms and solvent molecules are omitted for clarity.

Cyclic votammetry studies

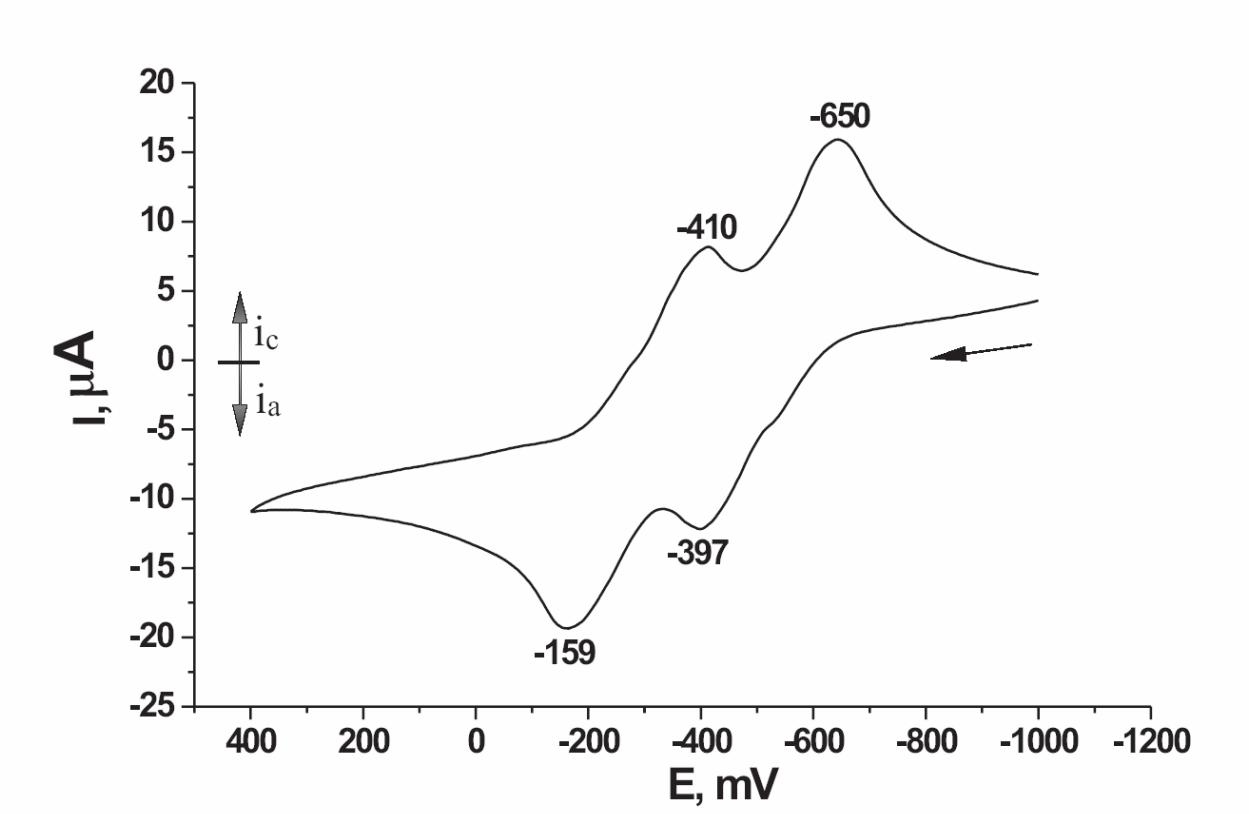

Figure 7S. Cyclic voltammogram for **10** in THF with 0.1M $[nBu_4N][PF_6]$; Au electrode; E *vs* $Fc^{0/+}$; scan rate = 100 mV/s; 20 ºC.

Magnetization measurements

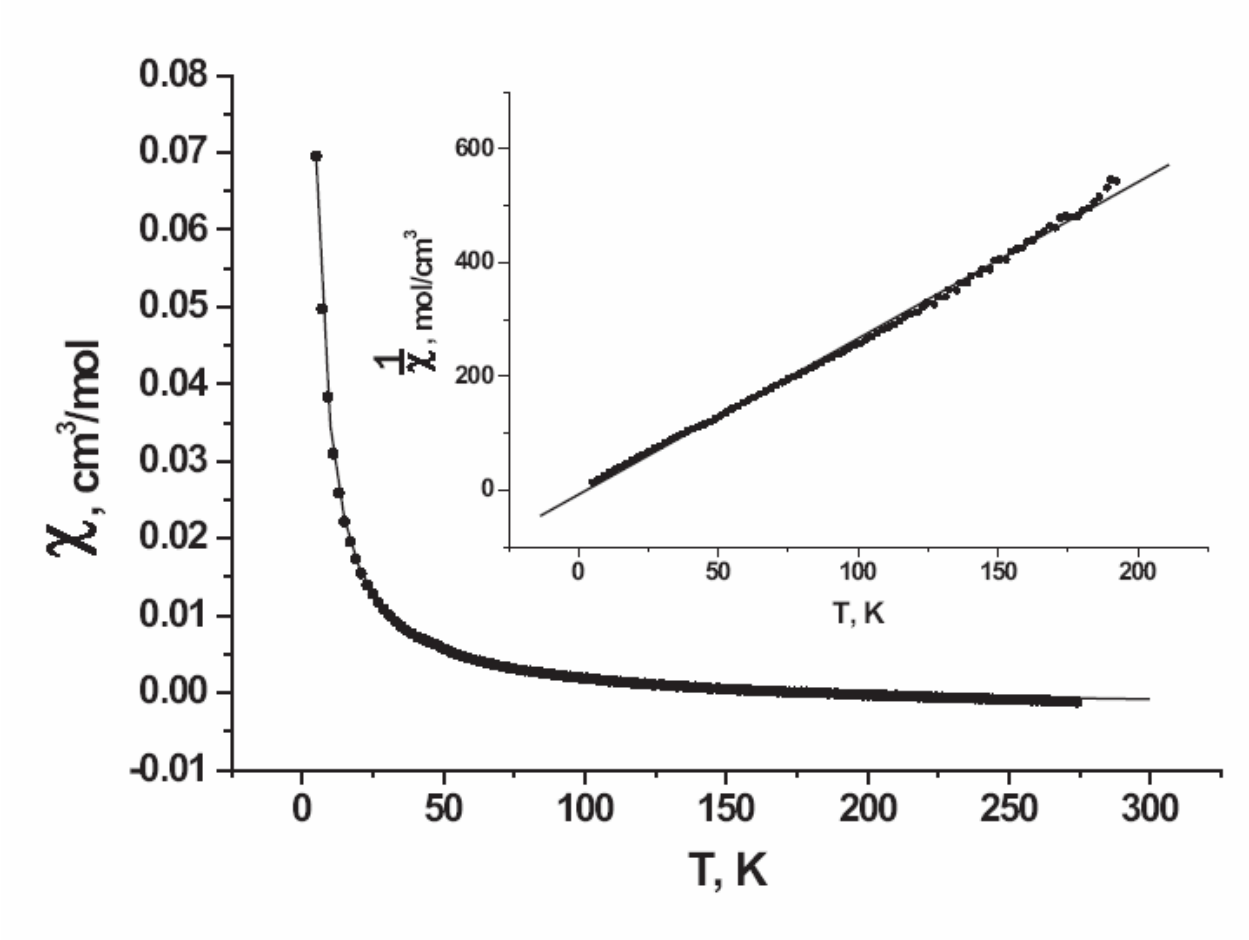

Figure 8S. Temperature dependence of χ *vs* T for **11[PF_6]**. The inset shows 1/χ *vs* T.

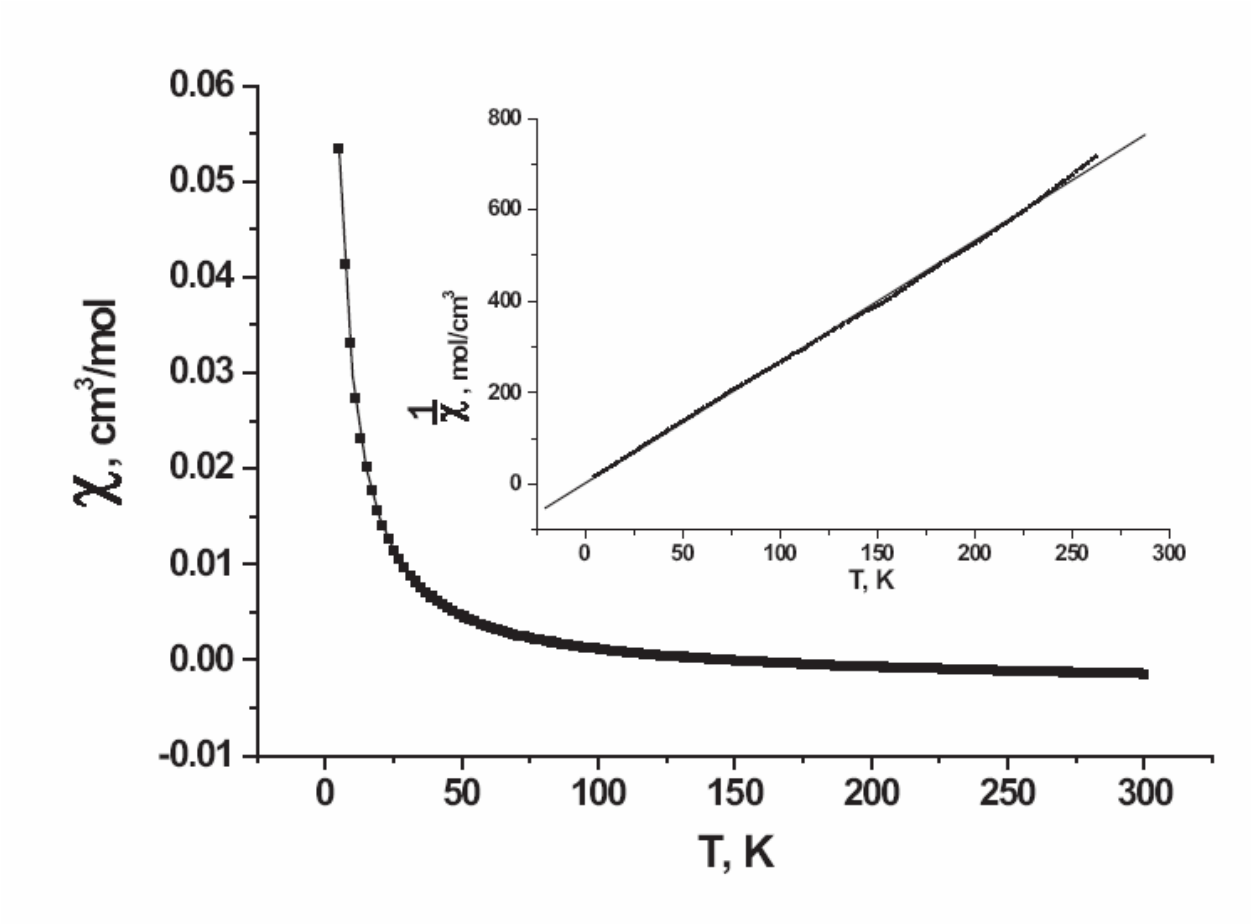

Figure 9S. Temperature dependence of χ *vs* T for **10[PF_6]**. The inset shows 1/χ *vs* T.

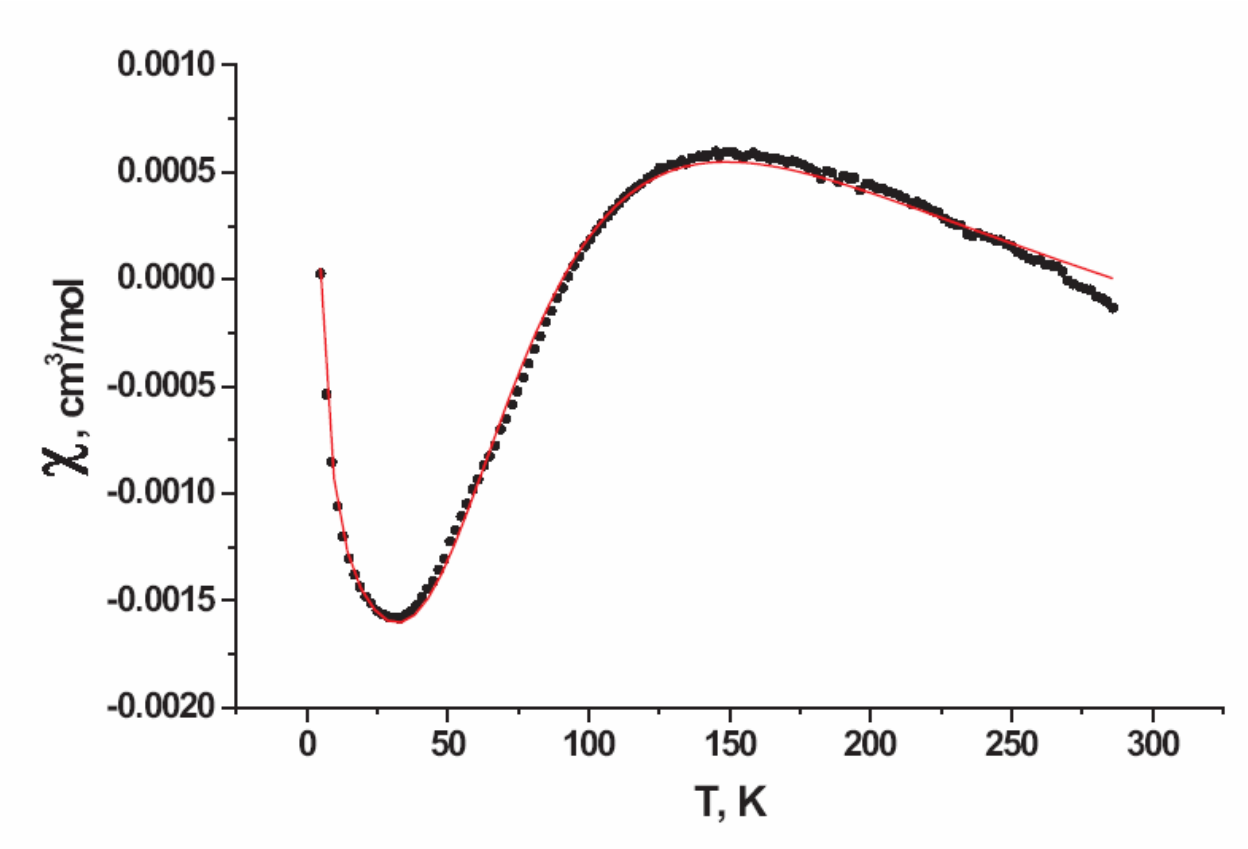

Figure 10S. Temperature dependence of χ *vs* T for **10[PF_6]$_2$**. The data are fitted with equation for a spin-1/2 dimer model with paramagnetic contribution:

$\chi = \frac{2N_A g^2 \beta^2}{kT} \cdot \frac{1}{(3 + e^{J/kT})} + \chi_0 + C/T$, where N_A – Avogadro constant, g – g factor, β – electron Bor magneton, k – Bolzman constant, J – exchange integral, χ_0 - core diamagnetism, van Vleck paramagnetism, and other temperature-independent contributions, C – Curie constant for paramagnetic contribution. The g, J, χ_0 and C were refined as parameters. The minimized values are: g – 1.98; J - -167 cm^{-1} , χ_0 – -0.002 cm^3/mol and C – 0.01 cm^3K/mol.

IV.3. Publication 3

An Iron Capped Metalorganic Polyyne

{[Fe](C≡C)$_2$[W]≡CC≡CC≡[W](C≡C)$_2$[Fe]}

*Sergey N. Semenov, Shiva F. Taghipourian, Olivier Blacque, Thomas Fox, Koushik Venkatesan, and Heinz Berke**

Department of Inorganic Chemistry, University of Zürich, Winterthurerstrasse 190, 8057 Zürich, Switzerland.

J. Am. Chem. Soc. **2010**, *132*, 7584-7585.

J|A|C|S COMMUNICATIONS

Published on Web 05/13/2010

An Iron-Capped Metal−Organic Polyyne: {[Fe](C≡C)$_2$[W]≡CC≡CC≡[W](C≡C)$_2$[Fe]}

Sergey N. Semenov, Shiva F. Taghipourian, Olivier Blacque, Thomas Fox, Koushik Venkatesan, and Heinz Berke*

Department of Inorganic Chemistry, University of Zürich, Winterthurerstrasse 190, 8057 Zürich, Switzerland

Received March 26, 2010; E-mail: hberke@aci.uzh.ch

One of the long-standing fundamental challenges in the field of molecular electronics is the accomplishment of nanometer-sized low-resistivity rigid-rod-type molecules.[1] Compounds bearing redox-active metal ends seemed particularly suited for high single-electron conductivity, and one approach to enhanced conductivity, termed the "relay" approach, was based on the idea that higher rates of electron transfer between the remote ends could eventually be accomplished by creating linked sections of alternating metal centers and short bridges of "conducting" organic moieties.[2] In contrast to organic single-electron-conducting molecules, metal-containing redox wires are expected to possess low work functions and strong d_π/p_π interactions, allowing the metal centers to become intrinsic constituents of the electronic conjugation.[3,4] We reasoned that organometallic p_π/d_π-conjugated complexes of the type {H(C≡C)$_n$[M]≡C(C≡C)$_n$C≡[M](C≡C)$_n$H}[5] constitute unique building blocks for the construction of polymetallic "molecular wires", and on the basis of a tungsten compound with the given structural motif, we approached the preparation of a tetranuclear polyyne of the type {[Fe](C≡C)$_2$[W]≡C(C≡C)C≡[W](C≡C)$_2$[Fe]}. Such systematic build-up of oligomers can also afford tunable systems for the development of bulk-conductive, nonlinear optical, luminescent, and magnetic materials.[4,6,7]

Scheme 1. Reaction Path for **1**−**5**

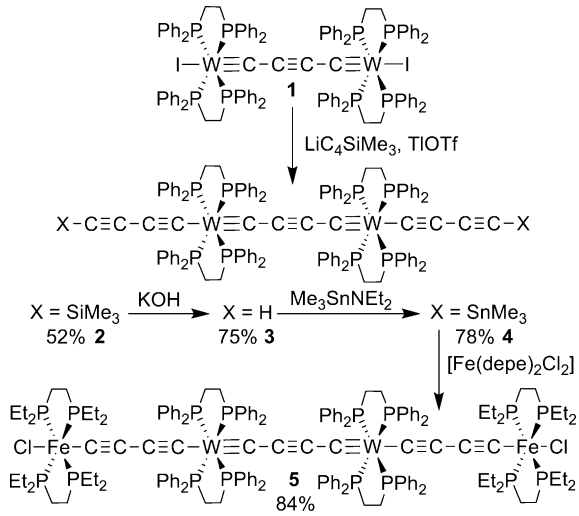

Our first preparative goal was to achieve access to the {(HC$_4$)[W](C$_4$)[W](C$_4$H)} polyyne. The starting material utilized for this approach was the [I(dppe)$_2$W(C$_4$)W(dppe)$_2$I] complex [**1**, dppe = 1,2-bis(diphenylphosphino)ethane] obtained recently in our group.[8] A controlled way of substituting the iodide ligands was the key to further functionalization of this dinuclear complex. Quite strong tungsten−iodine bonds combined with the possibility for trans → cis rearrangement rendered all standard strategies unsuccessful. The conversion of **1** to **2** was eventually achieved using a 3-fold excess of a 1:1 mixture of TlOTf with LiC≡CC≡CSiMe$_3$ in the presence of a catalytic amount of copper iodide (Scheme 1; also see the Supporting Information). The mechanism of this transformation is unclear, but it seems reasonable to infer the involvement of a putative Tl(III) intermediate formed by disproportionation of the unstable Tl(I) acetylide to metallic thallium as one of the observed reaction products. The desired product [(Me$_3$SiC$_4$)(dppe)$_2$W(C$_4$)W(dppe)$_2$(C$_4$SiMe$_3$)] (**2**) was separated by low-temperature chromatography on alumina followed by crystallization from ether in 52% yield. Complex **2** was fully characterized by ^{1}H, ^{13}C, and ^{31}P NMR spectroscopy, and its structure was confirmed by X-ray diffraction (XRD) analysis (see the Supporting Information). Removal of the SiMe$_3$ protecting group was achieved using excess KOH in a mixture of THF, methanol, and water. The desilylated compound [(HC$_4$)(dppe)$_2$W(C$_4$)W(dppe)$_2$(C$_4$H)] (**3**) is stable in both solution and the solid state in the absence of light and oxygen.

X-ray structural analysis of **3** revealed a biscarbyne-type bridged [(dppe)$_2$W≡C(C≡C)C≡W(dppe)$_2$] moiety coupled with C$_4$H chains (Figure 1). The crystal structure shows alternation of the W≡C and C≡C triple bonds and W−C and C−C single bonds, affirming that the bridge can be viewed to consist of a ditungstenatetradecaheptayne unit analogous in structure to the HC$_{14}$H parent compound. Introduction of the tungsten fragments makes the compound much more stable than any polyyne H$_2$C$_n$ (n > 4) molecule. **3** was converted to the corresponding stannylated derivative [(Me$_3$SnC$_4$)(dppe)$_2$W(C$_4$)W(dppe)$_2$(C$_4$SnMe$_3$)] (**4**) via reaction with excess Me$_3$SnNEt$_2$ in order to obtain a stable precursor with controllable reactivity.

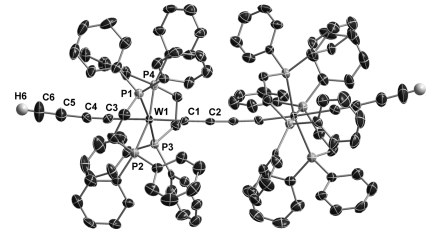

Figure 1. Thermal ellipsoid plot of the structure of **3** (50% probability level).

Finally, we wanted to perform preliminary investigations on the suitability of the {(C≡C)$_2$[W]≡C(C≡C)C≡[W](C≡C)$_2$} building block for electron transfer. For this purpose, the conjugated bridge had to be capped with redox-active groups. An iron-containing group was chosen as the terminal metal center on the basis of the fast electron transfer observed earlier in dinuclear FeC$_n$Fe systems.[9] Indeed the [Fe(PP)$_2$X] fragment (PP = chelate phosphine; X =

10.1021/ja102570f

halogen) allows reversible redox properties to be combined with the possibility of further functionalization by halogen substitution for the attachment of anchor groups,[6,10,11] a key requirement for single-molecule conductivity measurements.[12] On the basis of our previous work, the reaction of **4** with $[Fe(depe)_2Cl_2]$ [depe = 1,2-bis(diethylphosphino)ethane] was carried out at 60 °C, giving $\{[Cl(depe)_2Fe]C_4[(dppe)_2W]C_4[W(dppe)_2]C_4[Fe(depe)_2Cl]\}$ (**5**) in 84% yield after 6 h. Compound **5** is stable in the solid state and solution in the absence of air. **5** consists of a bridging $\{(C{\equiv}C)_2[W]{\equiv}C(C{\equiv}C)C{\equiv}[W](C{\equiv}C)_2\}$ fragment essentially identical in structure to **3** that is end-capped with $[Fe(depe)_2Cl]$ units (Figure 2). The added iron units induce an S-shaped distortion of the ditungstenatetradecaheptayne axis from linearity, with the main deviations from 180° at the C_α atoms of the tungsten centers being similar to other complexes with polyyne bridges.[8,13] The Fe−Fe distance in **5** is 23.5 Å.

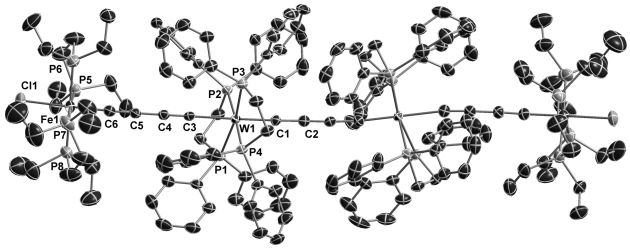

Figure 2. Thermal ellipsoid plot of the structure of **5** (50% probability level).

The redox properties of **5** were evaluated by cyclic voltammetry (CV) in dichloromethane (Figure 3) and THF (see the Supporting Information). The assignment of redox waves to oxidation processes was based on the fact that the oxidation potentials of **1** are higher than those for the iron in $[Cl(depe)_2Fe(C_2R)]$-type complexes.[11] As a consequence, the first two oxidation waves belong to the iron centers. The stabilization of the mixed-valence complex in dichloromethane solution is reflected by a peak separation of $\Delta E = 188$ mV with a comproportionation constant (K_c) of 1500.

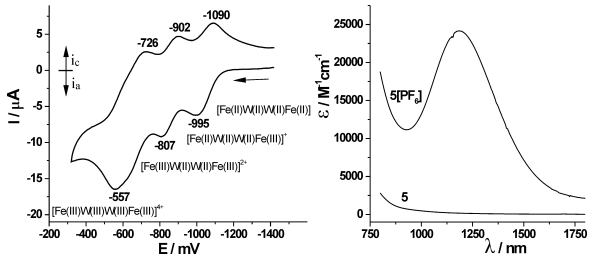

Figure 3. (left) Cyclic voltammogram of **5** in 0.1 M $[nBu_4N][PF_6]$ (Au electrode; E vs $Fc^{0/+}$; scan rate = 100 mV/s; 20 °C; CH_2Cl_2). (right) NIR spectrum of **5[PF$_6$]** in CH_2Cl_2 solution. The background spectrum of **5** is shown for comparison.

On the basis of electrochemical studies, **5** was oxidized with 1 equiv of $[Fe(Cp)_2][PF_6]$ in dichloromethane solution to give the mixed-valence complex **5[PF$_6$]**. The communication between the iron centers was additionally probed by IR, near-IR (NIR), and electron paramagnetic resonance (EPR) studies (Figure 3; also see the Supporting Information). The mixed-valence complex **5[PF$_6$]** shows a strong Gaussian-shaped band in the NIR spectrum. Data were analyzed using the Hush approximation.[14] It results in electronic coupling energy (H_{ab}) of 680 cm^{-1}, implying that the electron transfer should be described by an adiabatic regime with an estimated rate constant on the order of 10^9 s^{-1}.[15] The EPR spectra show a relatively sharp signal with $g = 2$ at both room and liquid helium temperatures. Moreover, only weak anisotropy was noticed for the resonance in frozen solution. This could be the result of partial delocalization of the electron into the ligands due to the covalent nature of the bonds.[16] However, the IR spectrum of **5[PF$_6$]** shows additional $\nu(C{\equiv}C)$ absorptions relative to **5**, suggesting localization of the unpaired electron on the IR time scale and favoring the Hush approximation.

In summary, we have developed long linear tungsten complexes with a continuous conjugated system. This building block efficiently mediates communication between two metal centers over a 24 Å distance, as shown by investigation of the tetranuclear complex **5** with redox-active termini. Fast electron transfer in combination with reversible oxidation of all four metal centers, the presence of terminal reactive sites for further functionalization, and the suitability for surface attachment because of its cylindrical shape and stability makes **5** a unique and promising system for long-range electron transfer, particularly in the field of metal-based molecular wires. This work shows great potential for the development of organometallic d_π/p_π-conjugated materials in general. In particular, further functionalization of **3** and **5** by anchor groups could lead to an investigation of single-molecule conductivity in these oligonuclear complexes; that investigation is currently in progress.

Acknowledgment. Funding from the Swiss National Science Foundation (SNSF) and the University of Zürich is gratefully acknowledged.

Supporting Information Available: Synthesis of all compounds; details of single-crystal X-ray diffraction studies; CIF files; thermal ellipsoid plot of **2**; EPR, CV, and IR data for **5[PF$_6$]**; and detailed analysis of NIR, IR, and EPR data. This material is available free of charge via the Internet at http://pubs.acs.org.

References

(1) (a) Heath, J. R. *Annu. Rev. Mater. Res.* **2009**, *39*, 1. (b) Carroll, L. R.; Gorman, B. C. *Angew. Chem., Int. Ed.* **2002**, *41*, 4378.
(2) Tuccitto, N.; Ferri, V.; Cavazzini, M.; Quici, S.; Zhavnerko, G.; Licciardello, A.; Rampi, M. A. *Nat. Mater.* **2009**, *8*, 41.
(3) (a) John, K. D.; Hopkins, M. D. *Chem. Commun.* **1999**, 589. (b) Manna, J.; Geib, S. J.; Hopkins, M. D. *J. Am. Chem. Soc.* **1992**, *114*, 9199.
(4) Pollagi, T. P.; Geib, S. J.; Hopkins, M. D. *J. Am. Chem. Soc.* **1994**, *116*, 6051.
(5) Shaner, S. E.; Sun, J.; Hopkins, M. D. *Polym. Prepr.* **2009**, *50*, 346.
(6) Field, L. D.; Turnbull, A. J.; Turner, P. *J. Am. Chem. Soc.* **2002**, *124*, 3692.
(7) (a) Powell, C. E.; Humphrey, M. G. *Coord. Chem. Rev.* **2004**, *248*, 725. (b) Brison, H. A.; Pollagi, T. P.; Stoner, T. C.; Geib, S. J.; Hopkins, M. D. *Chem. Commun.* **1997**, 1263. (c) Da Re, R. E.; Hopkins, M. D. *Coord. Chem. Rev.* **2005**, *249*, 1396. (d) Hu, J. S.; Sun, J. B.; Hopkins, M. D.; Rosenbaum, T. F. *J. Phys.: Condens. Matter* **2006**, *18*, 10837. (e) Zheng, Q. L.; Hampel, F.; Gladysz, J. A. *Organometallics* **2004**, *23*, 5896. (f) Manners, I. *Synthetic Metal-Containing Polymers*; Wiley-VCH: Weinheim, Germany, 2004. (g) Kingsborough, R. P.; Swager, T. M. *Prog. Inorg. Chem.* **1999**, *48*, 123. (h) Wolf, M. O.; Zhu, Y. B. *Adv. Mater.* **2000**, *12*, 599.
(8) Semenov, S. N.; Blacque, O.; Fox, T.; Venkatesan, K.; Berke, H. *J. Am. Chem. Soc.* **2010**, *132*, 3115.
(9) Lenarvor, N.; Toupet, L.; Lapinte, C. *J. Am. Chem. Soc.* **1995**, *117*, 7129.
(10) (a) Field, L. D.; George, A. V.; Malouf, E. Y.; Slip, I. H. M.; Hambley, T. W. *Organometallics* **1991**, *10*, 3842. (b) Colbert, M. C. B.; Lewis, J.; Long, N. J.; Raithby, P. R.; Younus, M.; White, A. J. P.; Williams, D. J.; Payne, N. N.; Yellowlees, L.; Beljonne, D.; Chawdhury, N.; Friend, R. H. *Organometallics* **1998**, *17*, 3034.
(11) Field, L. D.; George, A. V.; Laschi, F.; Malouf, E. Y.; Zanello, P. *J. Organomet. Chem.* **1992**, *435*, 347.
(12) (a) Reed, M. A.; Zhou, C.; Muller, C. J.; Burgin, T. P.; Tour, J. M. *Science* **1997**, *278*, 252. (b) Reichert, J.; Ochs, R.; Beckmann, D.; Weber, H. B.; Mayor, M.; von Lohneysen, H. *Phys. Rev. Lett.* **2002**, *88*, 176804.
(13) Zhuravlev, F.; Gladysz, J. A. *Chem.—Eur. J.* **2004**, *10*, 6510.
(14) Hush, N. S. *Prog. Inorg. Chem.* **1967**, *8*, 391.
(15) (a) Sutin, N. *Prog. Inorg. Chem.* **1983**, *30*, 441. (b) Demadis, D. D.; Hartshorn, C. M.; Meyer, T. J. *Chem. Rev.* **2001**, *101*, 2655.
(16) Desimone, R. E. *J. Am. Chem. Soc.* **1973**, *95*, 6238.

JA102570F

Supporting Information

An Iron-Capped Metal-Organic Polyyne

{[Fe](C≡C)$_2$[W]≡CC≡CC≡[W](C≡C)$_2$[Fe]}

Sergey N. Semenov, Shiva F. Taghipourian, Olivier Blacque, Thomas Fox, Koushik Venkatesan, and Heinz Berke

Experimental

General Procedures: All the manipulations were carried out under a nitrogen atmosphere using Schlenk techniques or a drybox. Reagent grade benzene, toluene, hexane, pentane, diethyl ether, and tetrahydrofuran were dried and distilled from sodium benzophenone ketyl prior to use. Dichloromethane was distilled from CaH_2. Literature procedures were used to prepare the following compounds: depe (depe = 1,2-Bis(diethylphosphinoethane)),[1] $HC{\equiv}CC{\equiv}CSiMe_3$,[2] $[I(dppe)_2WC(CC)CW(dppe)_2I]$ (dppe = 1,2-Bis(diphenylphosphinoethane)).[3] For $[Fe(depe)_2Cl_2]$ the procedure analogous to literature protocol for, $[Fe(dmpe)_2Cl_2]$ (dmpe = 1,2-Bis(dimethylphosphinoethane)) was used.[4] The $HC{\equiv}CC{\equiv}CSiMe_3$ was lithiated by BuLi in Et_2O at -40 ^oC. All other chemicals were used as obtained from commercial suppliers. IR spectra were obtained on a Bio-Rad FTS-45 instrument and Bio-Rad Excalibur FTS-3500. NMR spectra were measured on a Varian Mercury spectrometer at 200 MHz for ^1H and 81 MHz for $^{31}P\{^1H\}$, and on a Bruker-DRX-500 spectrometer at 500 MHz for ^1H, 125.8 MHz for $^{13}C\{^1H\}$ and 202.5 MHz for $^{31}P\{^1H\}$. Chemical shifts for ^1H and ^{13}C are given in ppm relative to TMS and those for ^{31}P relative to phosphoric acid. The Near-IR spectra were recorded on a Varian CARY 500 Scan UV-visible/near-IR spectrometer. CHN elemental analyses were performed with a LECO CHN-932 microanalyzer. Cyclic voltammograms were obtained with BAS 100W Voltammetric Analyzer equipped with the low volume cell. The cell was equipped with an Au working electrode and a Pt counter electrode, and a nonaqueous reference electrode. All sample solutions (CH_2Cl_2) were approximately $5{\cdot}10^{-3}$M in substrate and 0.1M in Bu_4NPF_6, and were prepared under nitrogen. Ferrocene was subsequently added and the calibration of voltammograms recorded. BAS 100W program was employed for data analysis. X-band EPR spectra were obtained using Bruker EMX Electron Spin Resonance system.

$[(Me_3SiC_4)(dppe)_2W(C_4)W(dppe)_2(C_4SiMe_3)]$ (2) The crystalline compound **1** is sparingly soluble in THF, the following procedure was performed to improve its solubility. **1** (200 mg, 0.088 mmol) was dissolved in approximately 20 mL of CH_2Cl_2. This solution was evaporated to dryness in *vacuo* and the residue was dissolved in 5 mL of benzene. The benzene solution was freeze-dried. Amorphous **1** was then dissolved in 30 mL of THF, placed into a 250 mL Schlenk flask and mixed with a solution of LiC_4SiMe_3 (68 mg, 0.531 mmol) in 20 mL of THF. A solution of TlOTf (210 mg, 0.595 mmol) in 30 ml of THF was added dropwise to the reaction mixture. The solution turned cloudy at the end of the addition. The reaction was stirred for 6 h at room temperature. The resulting green-yellow solution was evaporated to dryness in *vacuo*. Solid residue was extracted with benzene (3 × 10 mL), filtered and again dried in *vacuo*. Resulting mixture was chromatographed at low temperature (-10 ^oC) on Al_2O_3 (Merck, activity II, neutral. The use of Merck Al_2O_3 is important for this reaction. Merck, activity I, basic aluminum oxide also could be used) with toluene as eluent. The first dark green fraction was collected and evaporated. Recrystallization from a mixture Et_2O and toluene gave crystals of **2** in a few minutes. They were separated from solution and washed with two portions (1 ml each) of Et_2O. Single crystals suitable for X-

Ray diffraction were grown by layering a benzene solution with acetonitrile. Yield (104 mg, 0.046 mmol, 52%) Anal. Calcd. for $C_{122}H_{114}P_8Si_2W_2$: C, 65.07; H, 5.10. Found: C, 65.03; H, 5.13. IR (cm^{-1}): ν = 2111 (C≡C). ^{1}H NMR (500 MHz, C_6D_6): δ = 8.05 (br, 15H, C_6H_5), 7.00 (m, 50H, C_6H_5), 6.80 (br, 15H, C_6H_5), 2.76 (m, 8H, CH_2), 2.03 (m, 8H, CH_2), 0.21 (s, 18H, $Si(CH_3)_3$). ^{31}P NMR (81 MHz, C_6D_6): δ = 51.0 (s, (d, satellite, $^1J_{P\text{-}W}$ = 269 Hz)); ^{13}C NMR (125 MHz, C_6D_6) δ = 223.2 (m, C_α (WC_4W chain)), 140.6 (m, C_6H_5 – ipso), 139.2 (m, C_6H_5 – ipso), 138.7 (pent, $^2J_{C\text{-}P}$ = 13.2 Hz, C_α (WC_4Si chain)), 135.1 (s, C_6H_5), 133.2 (s, C_6H_5), 129.2 (s, C_6H_5), 128.3 (s, C_6H_5), 127.2 (s, C_6H_5), 104.9 (s, C_β (WC_4Si chain)), 94.3 (s, C_γ (WC_4Si chain)), 91.4 (s, C_β (WC_4W chain)), 74.0 (s, C_δ (WC_4Si chain)), 36.0 (m, CH_2), 0.8 (s, $Si(CH_3)_3$).

[(HC$_4$)(dppe)$_2$W(C$_4$)W(dppe)$_2$(C$_4$H)] (3) Complex **2** (64 mg, 0.028 mmol) was dissolved in 2.8 mL of THF containing 5% of water. A solution of KOH (20 mg, 0.36 mmol) in 1.2 mL of MeOH was added dropwise. The mixture was stirred for 1 h in dark at room temperature. After the reaction mixture was evaporated to dryness, it was extracted with benzene (3 mL), filtered through Al_2O_3 (Merck, activity II, neutral) plug and again evaporated. Solid residue was dissolved in 0.8 mL of THF and 4 mL of Et_2O was further added to precipitate polymeric byproducts. This solution was filtered and evaporated to give pure **3**. It should be mentioned that all manipulations should be done with minimum light quickly since the product **3** is light sensitive especially in the solid-state. Yield (44 mg, 0.021 mmol, 75%) Anal. Calcd. for $C_{116}H_{98}P_8W_2$: C, 66.11; H, 4.69. Found: C, 65.97; H, 4.75. IR (cm^{-1}): ν = 2108 (C≡C), 3293 (≡CH). ^{1}H NMR (500 MHz, C_6D_6): δ = 8.07 (br, 15H, C_6H_5), 7.98 (m, 50H, C_6H_5), 6.82 (br, 15H, C_6H_5), 2.81 (m, 8H, CH_2), 2.07 (m, 8H, CH_2), 1.41 (s, 2H, CH). ^{31}P NMR (81 MHz, C_6D_6): δ = 51.1 (s, (d, satellite, $^1J_{P\text{-}W}$ = 269 Hz)); ^{13}C NMR (125 MHz, C_6D_6) δ = 222.6 (m, C_α (WC_4W chain)), 140.8 (m, C_6H_5 – ipso), 139.3 (m, C_6H_5 – ipso), 135.1 (s, C_6H_5), 134.0 (m, C_α (WC_4H chain)), 133.1 (s, C_6H_5), 129.2 (s, C_6H_5), 128.8 (s, C_6H_5), 128.7 (s, C_6H_5), 127.2 (s, C_6H_5), 103.6 (s, C_β (WC_4H chain)), 90.9 (s, C_β (WC_4W chain)), 72.9 (s, C_γ (WC_4H chain)), 57.8 (s, C_δ (WC_4H chain)), 35.7 (m, CH_2).

[(Me$_3$SnC$_4$)(dppe)$_2$W(C$_4$)W(dppe)$_2$(C$_4$SnMe$_3$)] (4) Complex **3** (44 mg, 0.021 mmol) was dissolved in 0.8 mL of THF and Et_2NSnMe_3 (30 mg, 0.126 mmol) was added dropwise at -20 ^{o}C. The reaction mixture was allowed to stay at room temperature for 24 h. Solvent was removed in *vacuo* and solid residue was dissolved in benzene (1 mL) and freeze-dried. The resulting product was crystallized from 2 mL of Et_2O to give pure **4**. Yield (40 mg, 0.016 mmol, 78%) Anal. Calcd. for $C_{122}H_{114}P_8Sn_2W_2$: C, 60.22; H, 4.72. Found: C, 60.48; H, 4.81. IR (cm^{-1}): ν = 2101 (C≡C). ^{1}H NMR (500 MHz, C_6D_6): δ = 8.06 (br, 15H, C_6H_5), 7.00 (m, 50H, C_6H_5), 6.83 (br, 15H, C_6H_5), 2.80 (m, 8H, CH_2), 2.07 (m, 8H, CH_2), 0.19 (s, (d, satellite, $^2J_{H\text{-}Sn}$ = 55 Hz), 18H, $Sn(CH_3)_3$). ^{119}Sn NMR (186.5 MHz, C_6D_6) δ = -67.7 (pent, $^6J_{Sn\text{-}P}$ = 7.3 Hz, $SnMe_3$); ^{31}P NMR (81 MHz, C_6D_6): δ = 51.0 (s, (d, satellite, $^1J_{P\text{-}W}$ = 269 Hz)); ^{13}C NMR (125 MHz, C_6D_6) δ = 222.3 (m, C_α (WC_4W chain)), 140.8 (m, C_6H_5 – ipso), 139.3 (m, C_6H_5 – ipso), 135.1 (s, C_6H_5), 134.0 (m, C_α (WC_4Sn chain)), 133.3 (s, C_6H_5), 129.1 (s, C_6H_5), 127.2 (s, C_6H_5), 105.4 (s, C_β (WC_4Sn

chain)), 98.0 (s, C_γ (WC_4Sn chain)), 91.3 (s, C_β (WC_4W chain)), 74.0 (s, C_δ (WC_4Sn chain)), 35.7 (m, CH_2), -7.6 (s, (d, satellite, $^1J_{C\text{-}Sn}$ = 381 Hz), $Sn(CH_3)_3$).

[Cl(depe)$_2$Fe(C$_4$)(dppe)$_2$W(C$_4$)W(dppe)$_2$(C$_4$)Fe(depe)$_2$Cl] (5) A mixture of **4** (20 mg, 0.0082 mmol) and [Fe(depe)$_2$Cl$_2$] (16.5 mg, 0.03 mmol) in 0.5 mL of THF was placed into Young- Schlenk tube. The reaction mixture was heated at 60 ^{o}C for 6h and after the solvent was removed in *vacuo*. The solid residue was washed with Et_2O (3 × 2:1:1 ml) to give **5**. Single crystals suitable for X-Ray diffraction were grown by diffusion of Et_2O vapor into CH_2Cl_2 solution of **5** at -25 ^{o}C. Yield (21.5 mg, 0.0069 mmol, 84%) Anal. Calcd. for $C_{156}H_{192}Cl_2Fe_2P_{16}W_2$: C, 60.19; H, 6.22. Found: C, 60.04; H, 6.35. IR (cm^{-1}): ν = 2010 (C≡C). ^{1}H NMR (500 MHz, C_6D_6): δ = 7.91 (br, 16H, C_6H_5), 7.09 (br, 12H, C_6H_5), 7.01 (m, 36H, C_6H_5), 6.93 (t, $J_{H\text{-}H}$ = 8 Hz, 16H, C_6H_5), 2.83 (m, 8H, CH_2 (dppe)), 2.39 (m, 8H, PCH_2CH_2P (depe)), 2.33 (m, 8H, CH_2 (dppe)), 2.17 (m, 8H, PCH_2 (Et from depe)), 1.75 (m, 24H, PCH_2CH_2P (depe) + PCH_2 (Et from depe)), 1.64 (m, 8H, PCH_2 (Et from depe)), 1.11 (m, 48H, CH_3). ^{31}P NMR (202 MHz, C_6D_6): δ = 72.8 (s, 8P, depe), 49.6 (s, (d, satellite, $^1J_{P\text{-}W}$ = 270 Hz), 8P, dppe). ^{13}C NMR (125 MHz, C_6D_6) δ = 211.8 (pent, $^2J_{C\text{-}P(dppe)}$ = 15 Hz, C_α (WC_4W chain)), 141.9 (m, C_6H_5 – ipso), 141.5 (m, C_6H_5 – ipso), 134.9 (s, C_6H_5), 133.9 (s, C_6H_5), 128.5 (s, C_6H_5), 127.4 (s, C_6H_5), 126.7 (s, C_6H_5), 111.8 (pent, $^2J_{C\text{-}P(depe)}$ = 28.9 Hz, C_δ (WC_4Fe chain)), 111.0 (s, C_γ (WC_4Fe chain)), 109.1 (s, C_β (WC_4Fe chain)), 108.2 (m, C_α (WC_4Fe chain)), 91.0 (s, C_β (WC_4W chain)), 35.2 (m, CH_2, (dppe)), 20.7 (pent, $^2J_{C\text{-}P(depe)}$ = 10.3 Hz, PCH_2 (Et from depe)), 10.1 (d, $^3J_{C\text{-}P(depe)}$ = 41.6 Hz, CH_3).

[Cl(depe)$_2$Fe(C$_4$)(dppe)$_2$W(C$_4$)W(dppe)$_2$(C$_4$)Fe(depe)$_2$Cl][PF$_6$] (5[PF$_6$]) To a solution of **5** (10 mg, 0.00321 mmol) in 2 mL of CH_2Cl_2, a solution of [Fe(C$_5$H$_5$)$_2$][PF$_6$] (1.06 mg, 0.320 mmol) was added at -20 ^{o}C. Reaction mixture was stirred for 3 min and solvent was removed in vacuo. The solid residue was washed with Et_2O and hexane and dried to give **6**. Yield (10 mg, 0.003 mmol, 96%). Anal. Calcd. for $C_{156}H_{192}Cl_2F_6Fe_2P_{17}W_2$: C, 57.51; H, 5.94. Found: C, 57.68; H, 6.09. IR (cm^{-1}): ν = 1984 (C≡C), 1914 (C≡C). ^{1}H NMR (200 MHz, CD_2Cl_2): δ = 7.28 (br), 2.01 (br), 1.15 (br), 0.76 (br)

X-Ray Diffraction Studies on 2, 3 and 5

Crystallographic data were collected at 183(2) K on an Oxford Xcalibur diffractometer (4-circle kappa platform, Ruby CCD detector and a single wavelength Enhance X-ray source with MoK_α radiation, λ = 0.71073 Å).[5] The selected suitable single crystals were mounted using polybutene oil on the top of a glass fiber fixed on a goniometer head and immediately transferred to the diffractometer. Pre-experiment, data collection, analytical absorption correction,[6] and data reduction were performed with the Oxford program suite *CrysAlisPro*.[7] The structures were solved with the Patterson method and were refined by full-matrix least-squares methods on F^2 with SHELXL-97.[8] All programs used during the crystal structure determination process are included in the WINGX software.[9] The program PLATON[10] was used to check the result of the X-ray analyses. CCDC 759377 (**2**), 759378 (**3**) and 759379 (**5**) contain the supplementary crystallographic data for this paper. These data can be obtained free of charge from The Cambridge Crystallographic Data Centre via www.ccdc.cam.ac.uk/data_request/cif. The details of data collection and refinement are available in supporting information

Compound **2** crystallizes in the centrosymmetric space group C2/c. The dinuclear species lie on a two-fold axis, which led to refine only one half of the molecule. All non-hydrogen atoms were anisotropically refined. All hydrogen positions were calculated after each cycle of refinement using a riding model, with C-H = 0.93Å and $U_{iso}(H) = 1.2U_{eq}(C)$ for aromatic H atoms, with C-H = 0.97Å and $U_{iso}(H) = 1.2U_{eq}(C)$ for methylene H atoms, and with C-H = 0.96Å and $U_{iso}(H) = 1.5U_{eq}(C)$ for methyl H atoms.

Compound **3** crystallizes in the centrosymmetric space group C2/c. The dinuclear species lie on a two-fold axis, which led to refine only one half of the molecule. All non-hydrogen atoms were anisotropically refined. All hydrogen positions were calculated after each cycle of refinement using a riding model, with C-H = 0.93Å and $U_{iso}(H) = 1.2U_{eq}(C)$ for aromatic and acetylenic H atoms, and with C-H = 0.97Å and $U_{iso}(H) = 1.2U_{eq}(C)$ for methylene H atoms.

Compound **5** crystallizes in the centrosymmetric space group C2/c. The tetranuclear species lie on a two-fold axis, which led to refine only one half of the molecule. The asymmetric unit contains one solvent molecule of dichloromethane (disordered over three positions) for one half of the tetranuclear species. Two ethyl groups are disordered over two positions. A total of 20 distance restraints were used to correct the geometry of the disordered groups. All non-hydrogen atoms were anisotropically refined. All aromatic hydrogen positions were calculated after each cycle of refinement using a riding model, with C-H = 0.93Å and $U_{iso}(H) = 1.2U_{eq}(C)$ for aromatic H atoms, with C-H = 0.97Å and $U_{iso}(H) = 1.2Ueq(C)$ for methylene H atoms, and with C-H = 0.96Å and $U_{iso}(H) = 1.5U_{eq}(C)$ for methyl H atoms.

Table 1S. Summary of the X-ray diffraction studies of compounds **2**, **3** and **5**.

	2	**3**	**5**
empirical formula	$C_{122}H_{114}P_8Si_2W_2$	$C_{116}H_{98}P_8W_2$	$C_{156}H_{192}Cl_2Fe_2P_{16}W_2$, $2(CH_2Cl_2)$
formula weight ($g \cdot mol^{-1}$)	2251.76	2107.39	3282.61
temperature (K)	183(2)	183(2)	183(2)
wavelength (Å)	0.71073	0.71073	0.71073
crystal system, space group	monoclinic, *C* 2/c	monoclinic, *C* 2/c	monoclinic, *C* 2/c
a (Å)	37.6605(8)	36.6258(11)	46.1875(7)
b (Å)	12.54627(17)	13.1143(4)	19.2094(3)
c (Å)	25.9227(5)	20.2917(5)	17.5800(3)
α (deg)	90	90	90
β (deg)	120.282(3)	103.530(3)	93.679(1)
γ (deg)	90	90	90
volume ($Å^3$)	10577.2(5)	9476.1(5)	15565.4(4)
Z, density (calcd) ($Mg \cdot m^{-3}$)	4, 1.414	4, 1.477	4, 1.401
abs coefficient (mm^{-1})	2.37	2.612	1.972
F(000)	4568	4248	6745.8
crystal size (mm^3)	0.44 x 0.28 x 0.12	0.14 x 0.10 x 0.04	0.36 x 0.23 x 0.08
θ range (deg)	2.5 to 32.7	2.6 to 25.7	2.5 to 26.4
reflections collected	40935	35043	61631
reflections unique	16138 [R(int) = 0.040]	8990 [R(int) = 0.082]	15883 [R(int) = 0.041]
completeness to θ (%)	99.9	99.9	99.9
absorption correction	analytical	analytical	analytical
max/min transmission	0.830 and 0.559	0.933 and 0.796	0.884 and 0.650
data / restraints / parameters	16138 / 0 / 606	8990 / 0 / 568	15883 / 20 / 882
goodness-of-fit on F^2	0.914	0.752	0.968
final R_1 and wR_2 indices [$I > 2\sigma(I)$]	0.0262, 0.0518	0.0376, 0.0446	0.0379, 0.0951
R_1 and wR_2 indices (all data)	0.0394, 0.0531	0.0896, 0.0494	0.0598, 0.0997
Largest diff. peak and hole (e. $Å^{-3}$)	1.16 / -1.11	1.54 / -0.81	1.64 / -0.83

The unweighted R-factor is $R_1 = \sum(Fo - Fc)/\sum Fo$; $I > 2\,\sigma(I)$ *and the weighted R-factor is* $wR2 = \{\sum w(Fo^2 - Fc^2)^2/\sum w(Fo^2)^2\}^{1/2}$.

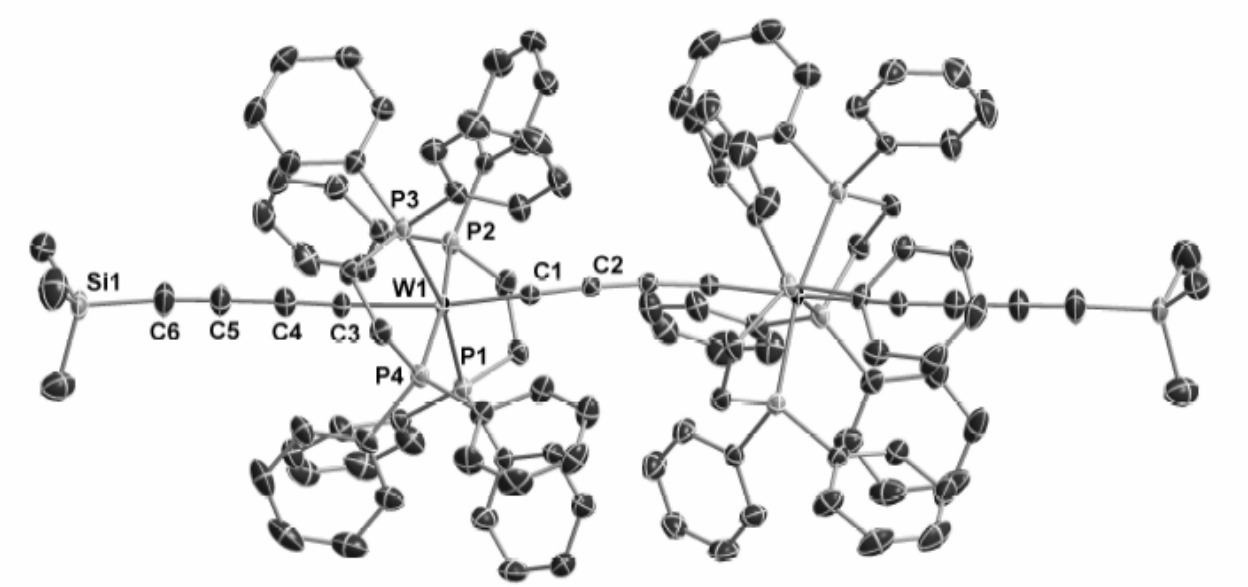

Figure 1S. Thermal ellipsoid plot of the structure of **2** (50% probability level). All hydrogen atoms are omitted for clarity

Additional NMR studies.

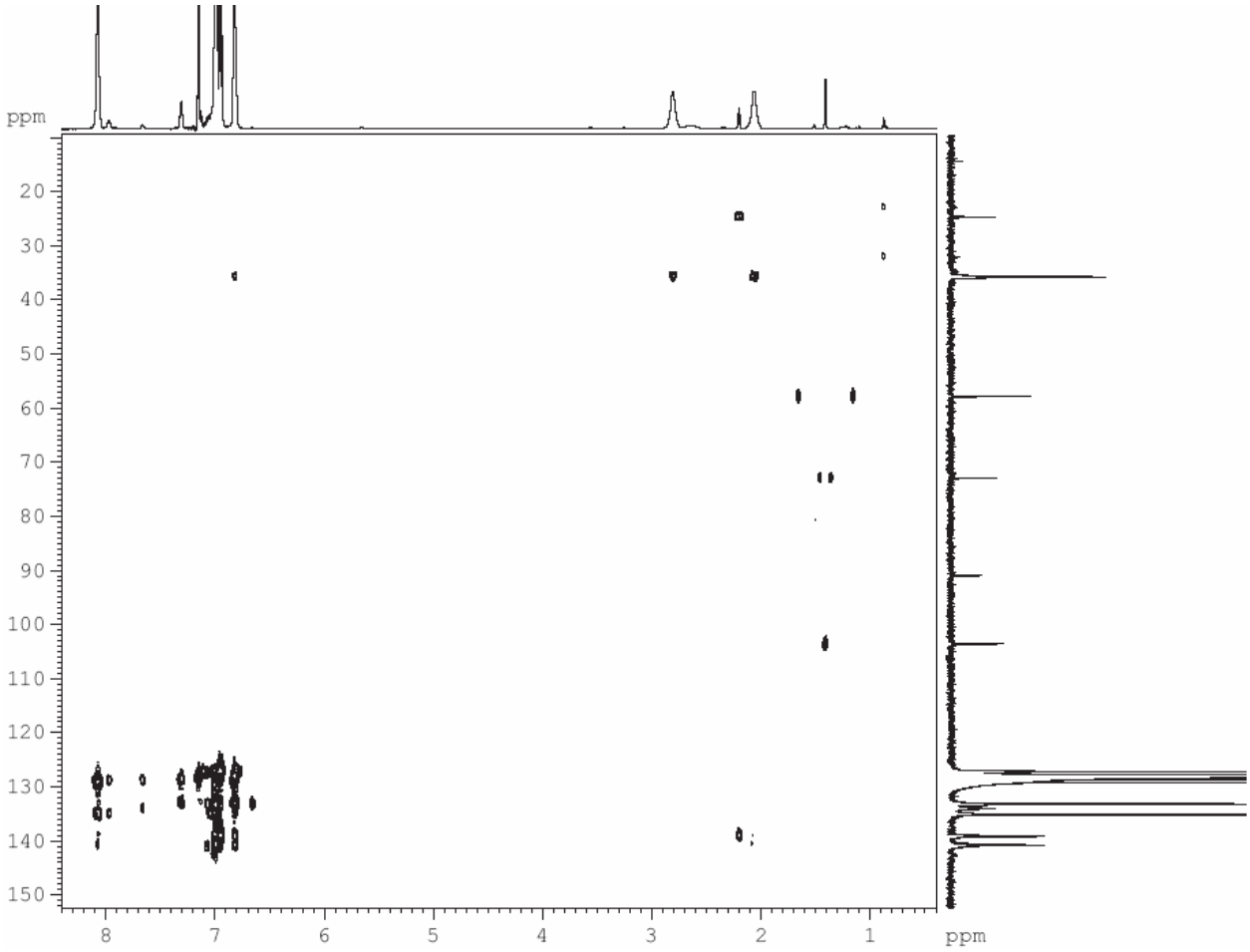

Figure 2S. Long range C – H correlation for **3**.

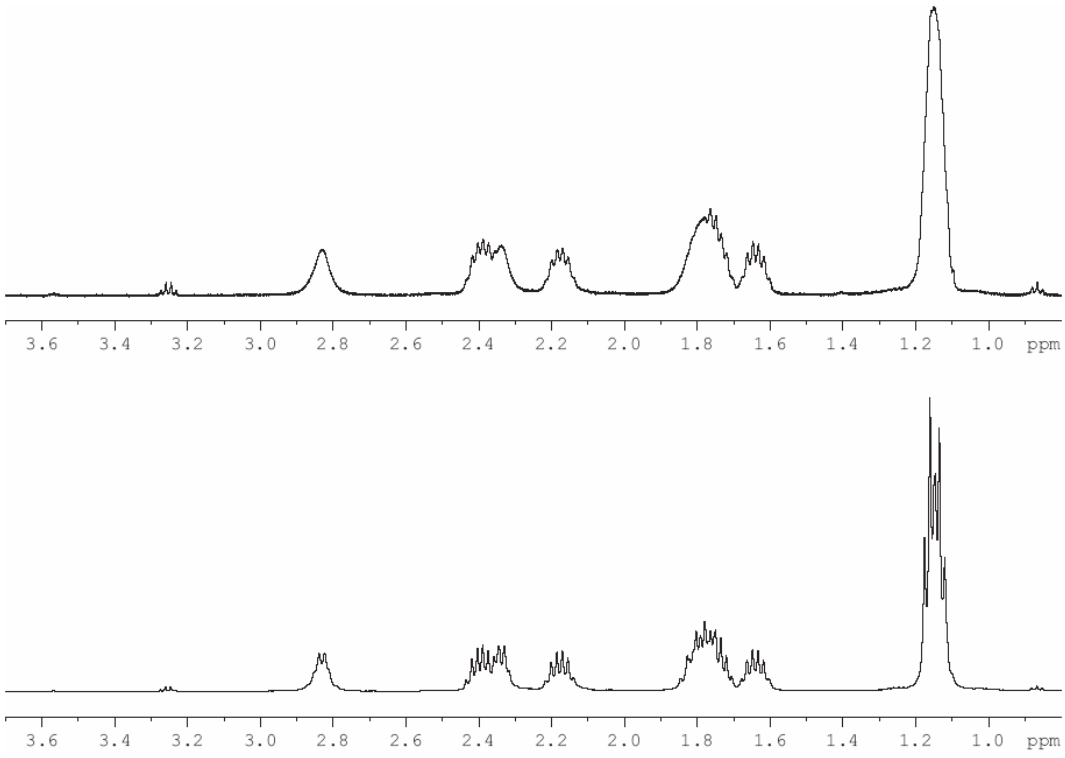

Figure 3S. The comparison of phosphor decoupled (bottom) and non phosphor decoupled ^{1}H NMR for **5**.

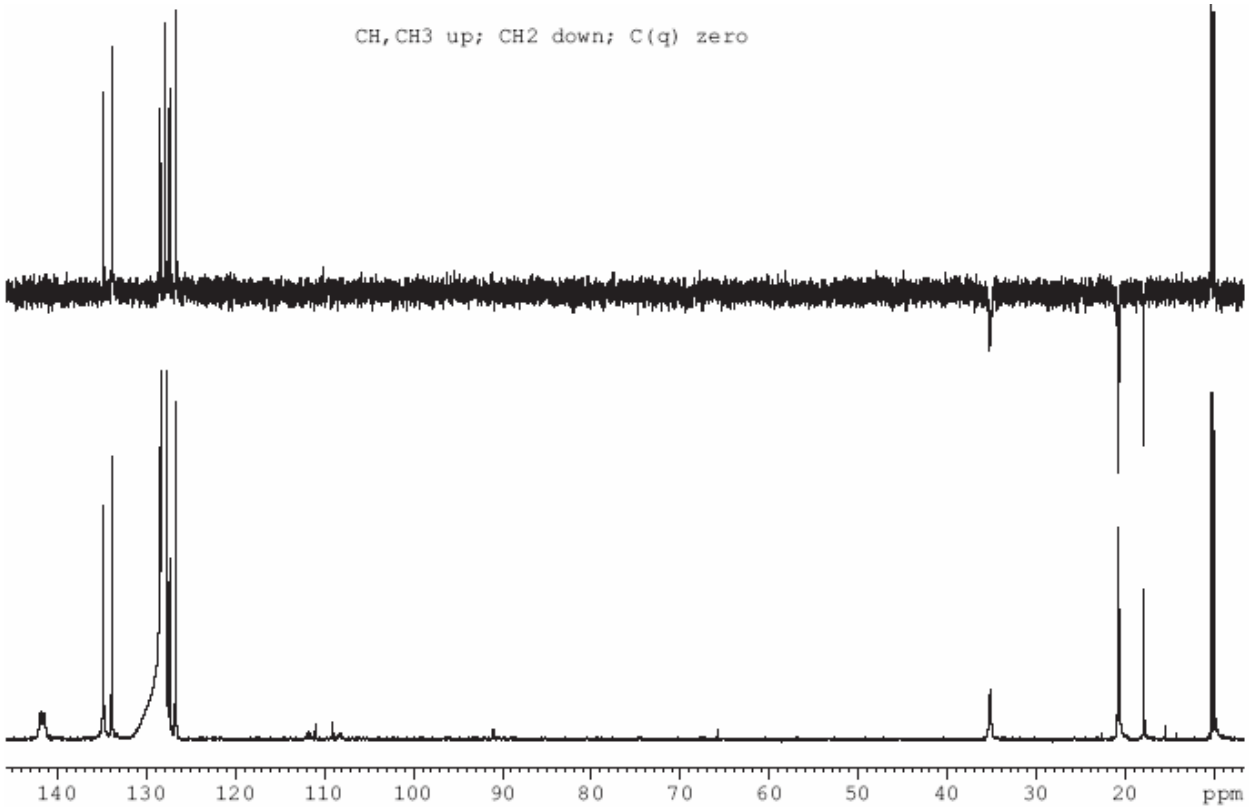

Figure 4S. The ^{13}C DEPT experiment (upper) and "normal" ^{13}C NMR spectrum (bottom) of **5**.

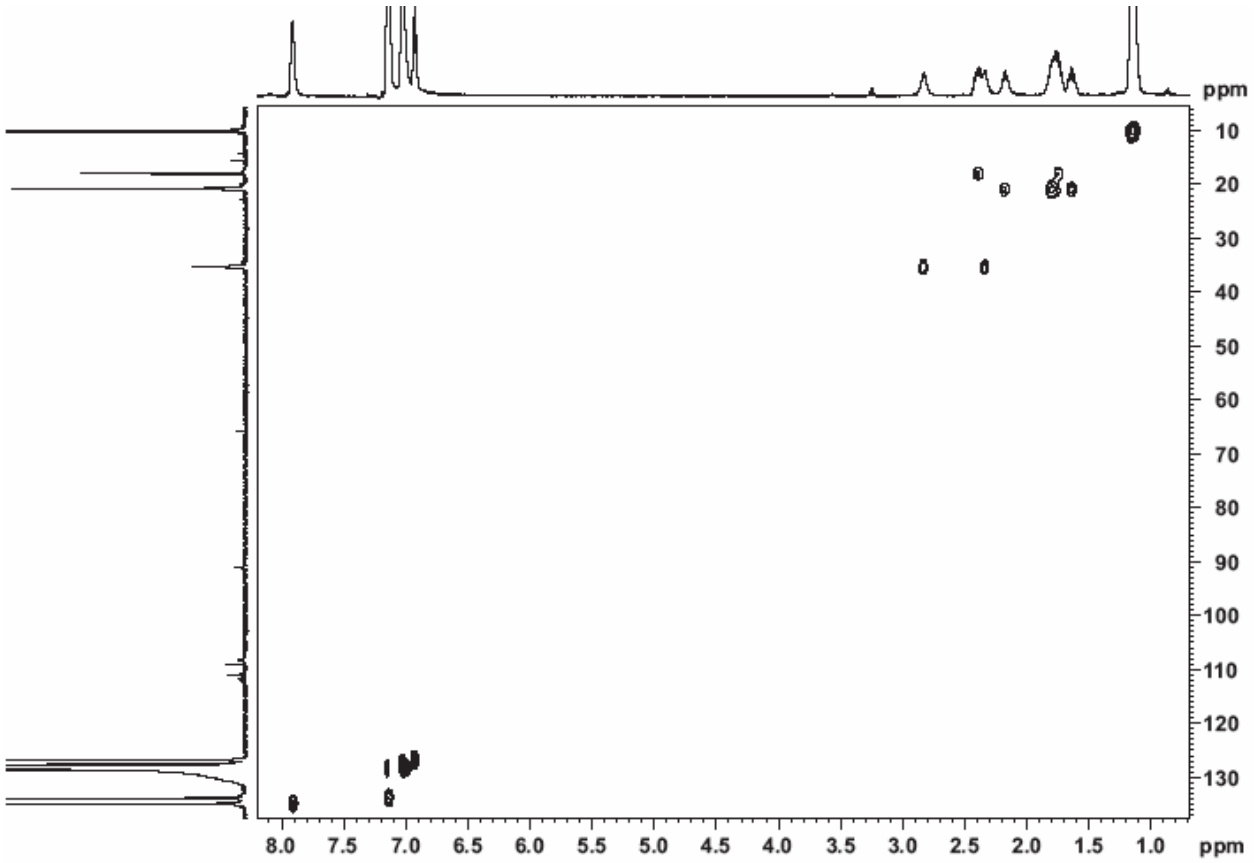

Figure 5S. C – H correlation for **5**.

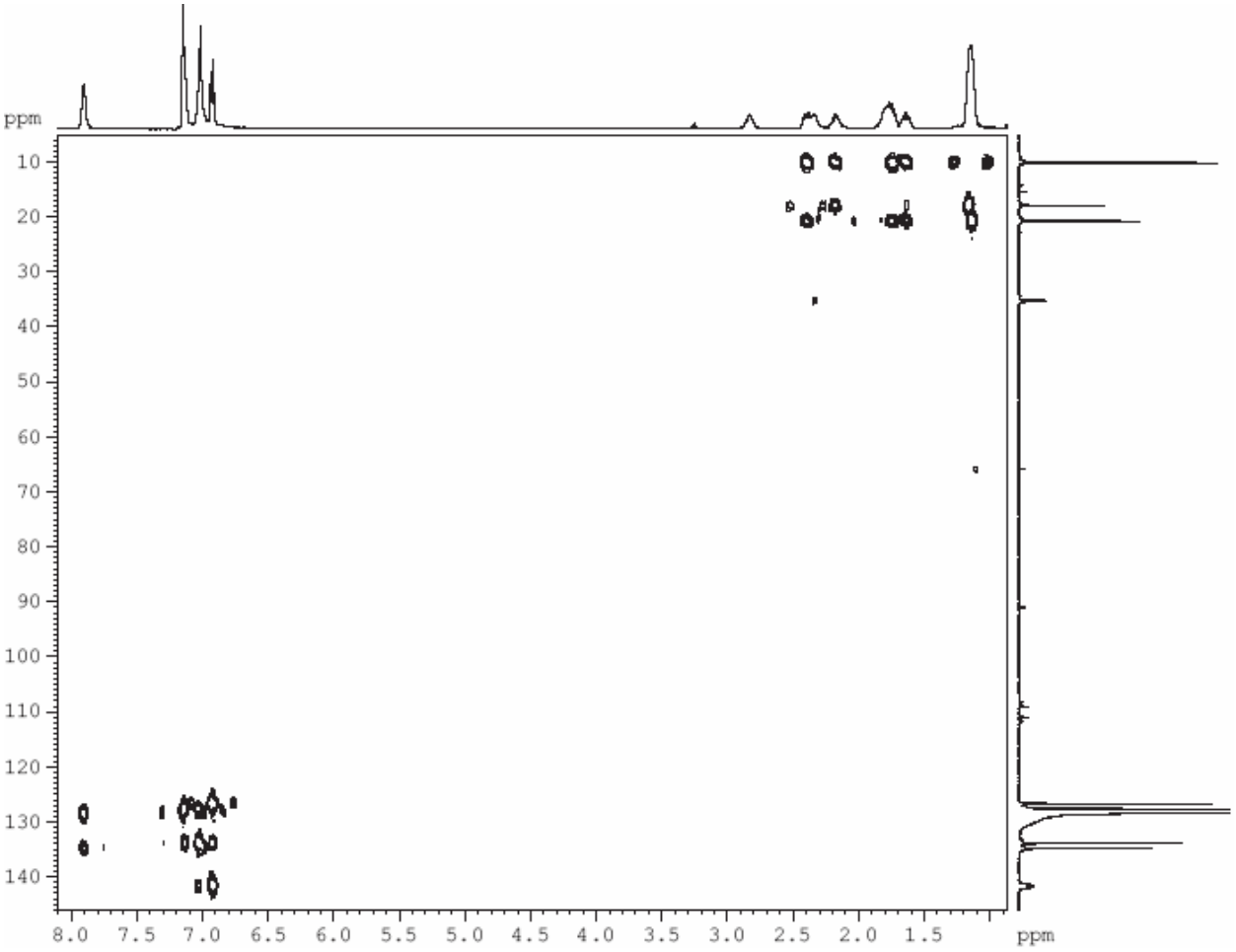

Figure 6S. Long range C – H correlation for **5**.

Cyclic Voltammetry study

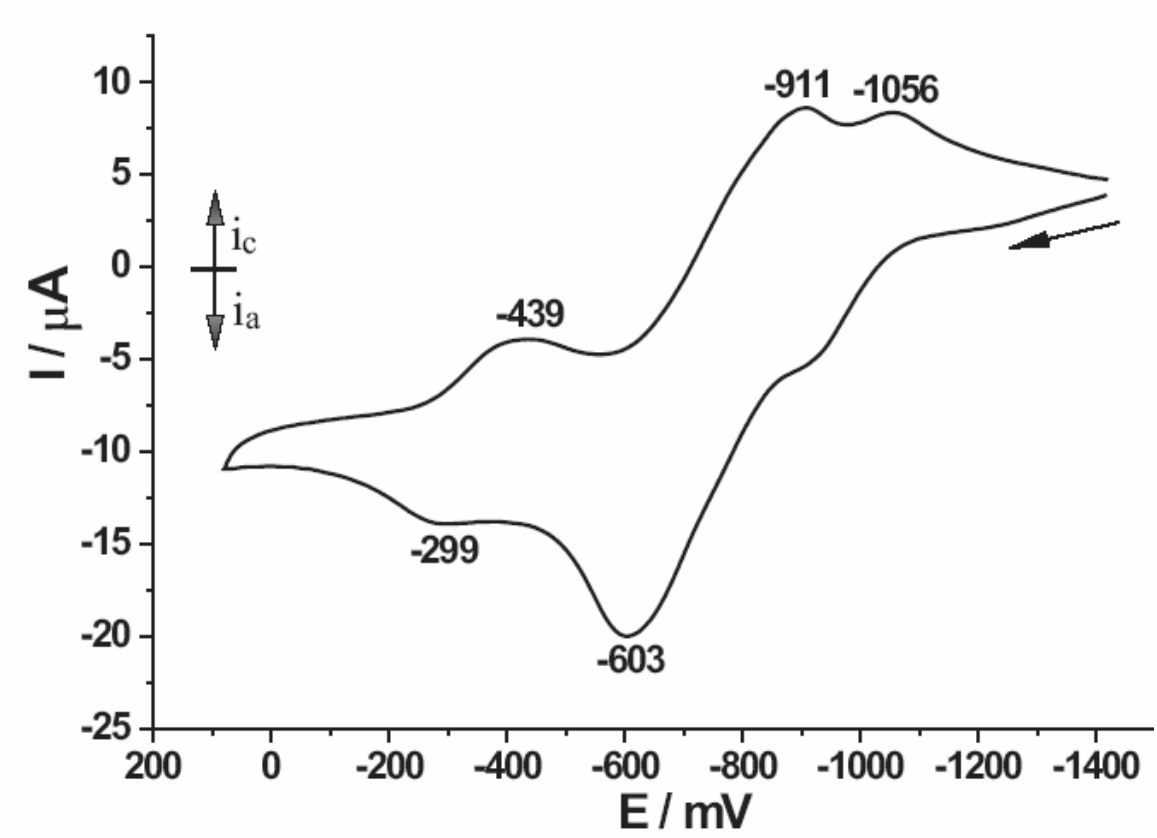

Figure 7S. Cyclic voltammogram for **5** in 0.1M [nBu_4N][PF_6]; Au electrode; E *vs* $Fc^{0/+}$; scan rate = 100 mV/s; 20 ºC; THF.

Table 2S. Summary of Cyclic voltammetry data for **5** in 0.1M [nBu_4N][PF_6]; Au electrode; E *vs* $Fc^{0/+}$; scan rate = 100 mV/s; 20 ºC

Solvent	$E_{1/2\ (ox1)}$ (V)	$E_{1/2\ (ox2)}$ (V) [a]	$E_{1/2\ (ox3)}$ (V) [b]
CH_2Cl_2	-1.04	-0.85	-0.64
THF	-0.98	-0.76	-0.36

[a] For THF solution ox2 is a two electron step. [b] For CH_2Cl_2 solution ox3 is a two electron step.

EPR study

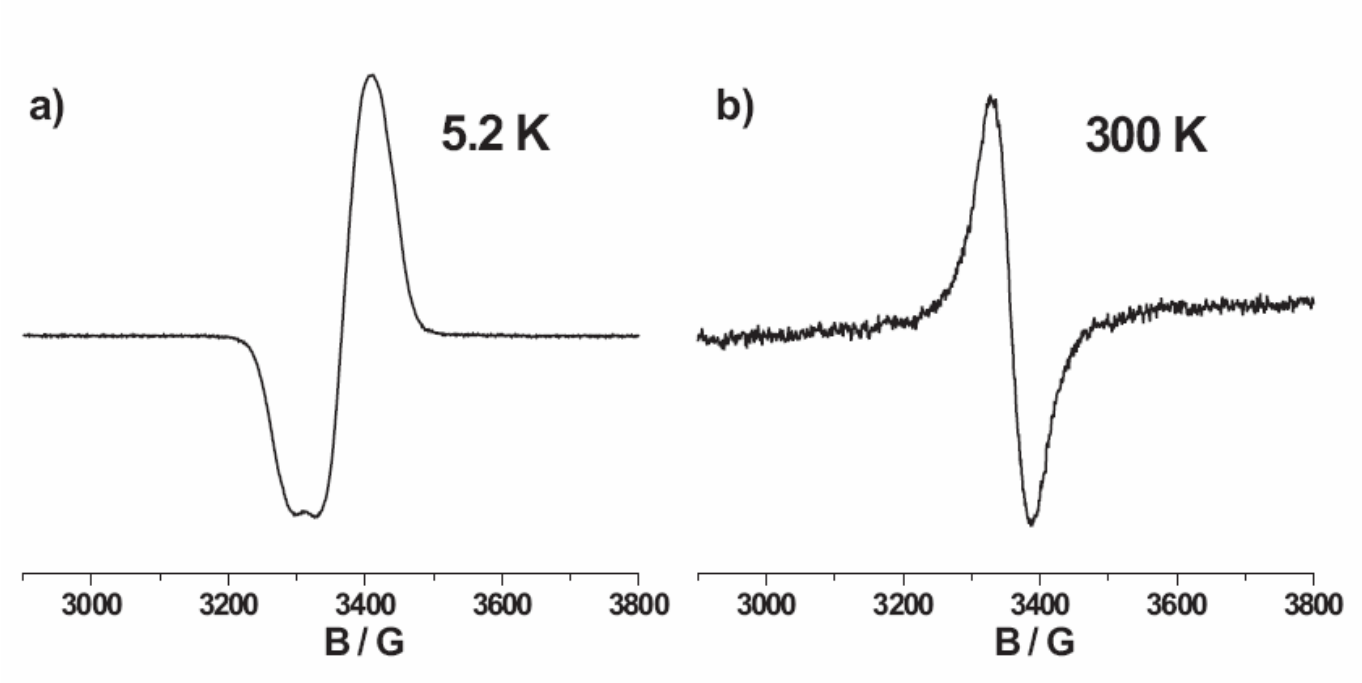

Figure 8S. EPR spectra of a) **5[PF_6]** at 20 K in CH_2Cl_2 glass; b) **5[PF_6]** at 300 K in CH_2Cl_2 solution.

NIR study

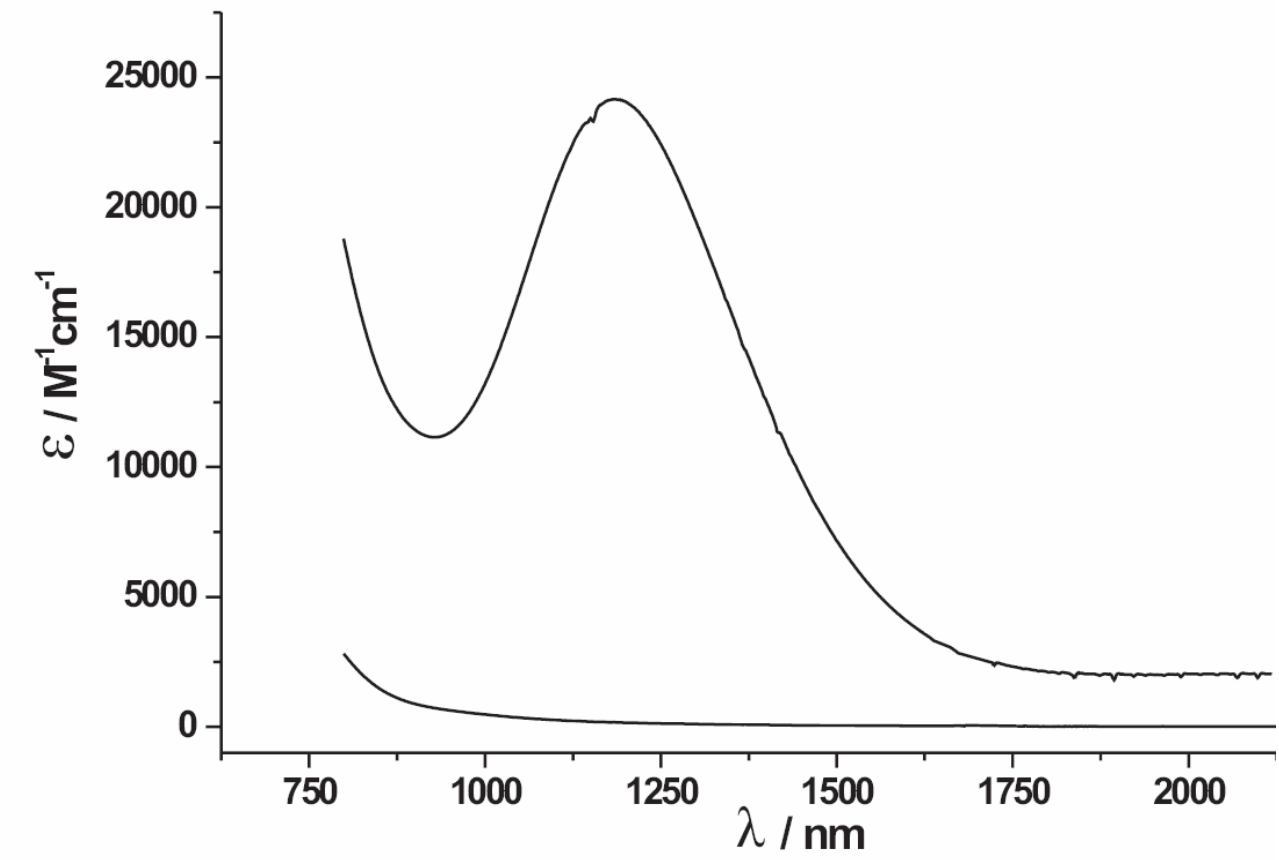

Figure 9S. NIR spectrum of **5[PF_6]** in CH_2Cl_2 solution. The background spectrum of **5** is shown for comparison.

IR study

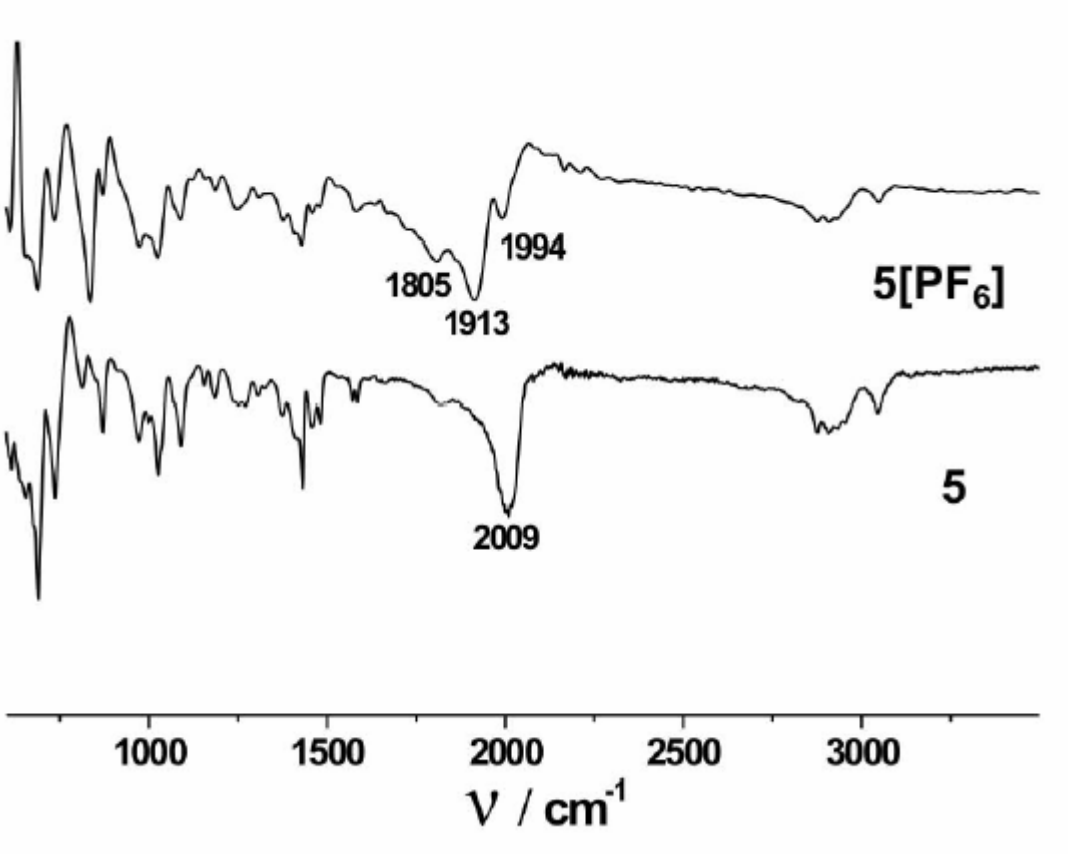

Figure 10S. ν(C_4) absorptions in the IR spectra of **5** and **5[PF_6]** (powder, room temperature).

NIR, EPR and IR study discussion

In contrast to **5**, the mixed-valence complex **5[PF$_6$]** shows a strong Gaussian-shaped band in the NIR spectrum. This band is centered at 1185 nm (8438 cm^{-1}) and has a half-height-width of around 3140 cm^{-1}. These parameters allows to approximate the electronic coupling energy H_{ab} and the reorganization energy λ by the following equations:[11]

$$H_{ab}(cm^{-1}) = [(4.2\times10^{-4})\varepsilon\Delta\bar{\nu}_{1/2}E_{IT}]^{1/2}/d\ ;\ \lambda = E_{IT}$$

where ε is the absorption coefficient in M^{-1}cm^{-1}, $\Delta\nu_{1/2}$ the half-height-width of the absorption band in cm^{-1}, E_{IT} the energy of the band maximum in cm^{-1} and *d* the electron transfer distance in Å. The calculations resulted in a H_{ab} value of 680 cm^{-1}, implying that the electron transfer should be described by an adiabatic regime with a rate constant given by the following equation:[12]

$$k = \nu_n \exp(-\lambda(1-2H_{ab}/\lambda)^2/4k_bT)$$

Taking ν_n in the order of 10^{12} sec^{-1} results in *k* in the order of 10^9 sec^{-1}.

The electron localization was then investigated by EPR. The [Cl(depe)$_2$Fe]$^+$ centers were expected to have a d^5 low spin t_{2g}^5 configuration. Within the frame of the crystal field approximation, compression of an octahedron along the C_4 axis leads to splitting of the $^2T_{2g}$ term into a $^2A_1$ and ^2E term lying higher and lower in energy, respectively. These two levels are then mixed into three Kramers doublets by spin-orbit coupling.[13] The relaxation time in such systems is short, therefore the spectra can be registered only at low temperatures and the g-factor is strongly anisotropic due to a significant orbital component. But, in contrast to the expectations, our system shows relatively sharp signal with g = 2 at both room and liquid helium temperatures, moreover only weak anisotropy was noticed for the resonance in frozen solution.

The lack of a g-factor anisotropy, as well as the appearance of a signal at room temperature could be the result of the partial delocalization of the unpaired electron along the bridge. A conclusion analogous to this was reached after detailed investigations for iron t_{2g}^5 tris-complexes with bidentate sulphur donor ligands, where the lack of g-factor anisotropy could not be explained without the assumption of partial delocalization of the electron into the ligands due to the covalent nature of the bonds.[14]

The full delocalization was finally probed by IR spectroscopy. In symmetry lowered systems with electron exchanges between the metal centers slow on the IR time scale (10^{-13} sec), one can often identify new absorptions forbidden to appear in a symmetrical system.[11] The IR spectra of the complexes **5** and **5[PF$_6$]** are presented in Figure 10S. One absorption attributable to the ν(CC) vibration was found in spectrum of **5**, while three bands were identified in **5[PF$_6$]** spectrum. This difference could be related to the appearance of the ν(CC) band due to the central C≡C bond in the case of **5[PF$_6$]** where the centered symmetry of the molecule is broken on the IR time scale by the iron centers with different electron counts. Consequently, we can speculate that unpaired electron in **5[PF$_6$]** is probably localized in IR time scale.

References

[1] Burt, R. J.; Chatt, J.; Hussain, W.; Leigh, G. J. *J. Organomet. Chem.* **1979**, *182*, 203-206.

[2] Bartik, B.; Dembinski, R.; Bartik, T.; Arif, A. M.; Gladysz J. A. *New J. Chem.* **1997**, *21*, 739-750.

[3] Semenov, S. N.; Blacque, O.; Fox, T.; Venkatesan, K.; Berke, H. *J. Am. Chem. Soc.* **2010**, *132*, 3115 - 3127.

[4] Girolami G. S.; Wilkinson, G.; Galas, A. M. R.; Thorntonpett, M.; Hursthouse, M. B. *J. Chem. Soc. Dalton Trans.* **1985**, 1339-1348.

[5] Oxford Diffraction (2007). Xcalibur CCD system. Oxford Diffraction Ltd, Abingdon, Oxfordshire, England.

[6] R.C. Clark, J. S. Reid, *Acta Cryst.* **1995**, *A51*, 887-897.

[7] *CrysAlisPro* (Versions 1.171.33.34d and 1.171.33.41), Oxford Diffraction Ltd, Abingdon, Oxfordshire, England.

[8] Sheldrick, G. M. *Acta Crystallogr.* **2008**, *A64*, 112-122.

[9] Farrugia, L. J. *J. Appl. Cryst.* **1999**, *32*, 837-838.

[10] Spek, A. L. *J. Appl. Cryst.* **2003**, *36*, 7-13.

[11] a) Demadis, D. D.; Hartshorn, C. M.; Meyer, T. J. *Chem. Rev.* **2001**, *101*, 2655-2685; b) Kaim, W.; Lahiri, G. K. *Angew. Chem. Int. Ed.* **2007**, *46*, 1778-1796.

[12] Sutin, N. *Prog. Inorg. Chem.* **1983**, *30*, 441-498.

[13] DeSimone, R. E.; Drago, R. S. *J. Am. Chem. Soc.* **1970**, *92*, 2343-2352.

[14] Desimone, R. E. *J. Am. Chem. Soc.* **1973**, *95*, 6238-6244.

IV.4. Publication 4

$[W(CO)(dppe)_2]$ Cumulenylidene and Acetylide Complexes Accessed via Stannylated Acetylenes and Butadiynes

*Sergey N. Semenov, Olivier Blacque, Thomas Fox, Koushik Venkatesan, and Heinz Berke**

Department of Inorganic Chemistry, University of Zürich, Winterthurerstrasse 190, 8057 Zürich, Switzerland.

Organometallics **2010**, *29*, 6321-6328.

ORGANOMETALLICS
Article

Organometallics **2010,** *29,* 6321–6328 6321
DOI: 10.1021/om100702x

[W(CO)(dppe)$_2$] Cumulenylidene and Acetylide Complexes Accessed via Stannylated Acetylenes and Butadiynes

Sergey N. Semenov, Olivier Blacque, Thomas Fox, Koushik Venkatesan, and Heinz Berke*

Department of Inorganic Chemistry, University of Zürich, Winterthurerstrasse 190, 8057 Zürich, Switzerland

Received July 16, 2010

The tungsten butatrienylidenes [*cis*-W(CO)(dppe)$_2${C═C═C═C(R)(SnMe$_3$)}] (R = SnMe$_3$ (**2**) and SiMe$_3$ (**3**); dppe = 1,2-bis(diphenylphosphinoethane)) were prepared from the reactions of [*trans*-W(CO)(N$_2$)(dppe)$_2$] (**1**) and the respective butadiynes displaying a 1,4-shift of the respective SnMe$_3$ groups along the butadiyne chains. Stannyl deprotection of **2** with NBu$_4$F·3H$_2$O led to the anionic butadiyne derivative [*trans*-W(CO)(dppe)$_2$(C≡CC≡CH)][NBu$_4$] (**10**). The reaction of **1** with stannylated acetylenes gave the vinylidene derivatives [*cis*-W(CO)(dppe)$_2${C═C(SnMe$_3$)(R)}] (R = Ph (**5**) or SnMe$_3$ (**6**)), which lost a SnMe$_3$ group, yielding W(I) acetylides of the type [*trans*-W(CO)(dppe)$_2$-(C≡CR)] (R = Ph (**7**), SnMe$_3$ (**8**), and SiMe$_3$ (**9**)). They were studied by cyclic voltammetry and EPR spectroscopy.

Introduction

Metallacumulenes [L$_x$M═C(═C)$_n$RR′] possess a high degree of unsaturation, which makes these compounds unique candidates for application as materials with special electronic and NLO (nonlinear optical) properties.[1,2] Related binuclear cumulene complexes revealed a high degree of delocalization of the unpaired electron in mixed valence species.[3,4] While compounds with vinylidenes :C═CRR′ and allenylidenes : C═C═CRR′ as cumulenic ligands are quite common,[1,5] reports on the existence of butatrienylidenes and pentatetraenylidenes of the type [L$_x$M(C═C═C═CRR′)] and [L$_x$M-(═C═C═C═C═CRR′)] are very rare. X-ray diffraction studies of the fairly stable species [Cl(P*i*Pr$_3$)$_2$Ir═C(═C)$_n$(Ph)$_2$] (*n* = 3, 4),[6−8] [Cl(dppe)$_2$Ru(C═C═C═C═CPh$_2$)] (dppe = 1,2-bis-(diphenylphosphinoethane)),[9] [W(CO)$_5${C═C═C═C═C-(NMe$_2$)$_2$}],[10] and [(Cp)(dmpe)Mn{C═C═C═C(SnPh$_3$)$_2$}] (dmpe = 1,2-bis(dimethylphosphinoethane))[11,12] revealed bond length alternation along the cumulenylidene chain. The longest terminal cumulenic chain was found in the C$_7$ compound [M(CO)$_5${C═C═C═C═C═C═C(NMe$_2$)$_2$)}] (M = Cr, W).[13] Other types of group 6 metal centers were also shown to stabilize long-chain cumulenylidenes.[14] Thus, recently C$_4$ tungsten complexes [*cis*-W(CO)(dppe)$_2${C═C═C═C(R)(*p*-C$_6$H$_4$-*t*Bu)}] (R = SnMe$_3$ or H) were reported.[15] The preparation of butatrienylidenes often starts from terminal diynes involving 1,4-H shifts; however 4-H-butatrienylidenes proved to be unstable. We found that topologically related 1,4-SnMe$_3$ shifts may be utilized to circumvent the often too reactive H-substituted cumulenylidenes.

Cationic ruthenium complexes containing a [Ru(C═C═C═C═CRH)]$^+$ fragment were prepared *in situ* (R = H) by Bruce[16] (R ≠ H), Dixneuf,[17] and Winter.[17] They found a variety of typical reactions based on nucleophilic attack at C$_\gamma$ and subsequent cycloaddition. The [2 + 2] addition between the Ru cumulene and butadiyne derivatives led to binuclear

*To whom correspondence should be addressed. E-mail: hberke@aci.uzh.ch.

(1) Bruce, M. I. *Chem. Rev.* **1998**, *98*, 2797.
(2) (a) Bruce, M. I. *Coord. Chem. Rev.* **2004**, *248*, 1603. (b) Cadierno, V.; Gimeno, J. *Chem. Rev.* **2009**, *109*, 3512.
(3) (a) Unseld, D.; Krivykh, V. V.; Heinze, K.; Wild, F.; Artus, G.; Schmalle, H.; Berke, H. *Organometallics* **1999**, *18*, 1525. (b) Venkatesan, K.; Fox, T.; Schmalle, H. W.; Berke, H. *Organometallics* **2005**, *24*, 2834. (c) Rigaut, S.; Massue, J.; Touchard, D.; Fillaut, J. L.; Golhen, S.; Dixneuf, P. H. *Angew. Chem., Int. Ed.* **2002**, *41*, 4513. (d) Rigaut, S.; Le Pichon, L.; Daran, J. C.; Touchard, D.; Dixneuf, P. H. *Chem. Commun.* **2001**, 1206. (e) Rigaut, S.; Olivier, C.; Costuas, K.; Choua, S.; Fadhel, O.; Massue, J.; Turek, P.; Saillard, J. Y.; Dixneuf, P. H.; Touchard, D. *J. Am. Chem. Soc.* **2006**, *128*, 5859.
(4) Venkatesan, K.; Fox, T.; Schmalle, H. W.; Berke, H. *Eur. J. Inorg. Chem.* **2005**, 901.
(5) Bruce, M. I. *Chem. Rev.* **1991**, *91*, 197.
(6) Ilg, K.; Werner, H. *Angew. Chem., Int. Ed.* **2000**, *39*, 1632.
(7) Ilg, K.; Werner, H. *Chem.—Eur. J.* **2002**, *8*, 2812.
(8) (a) Werner, H.; Ilg, K.; Lass, R.; Wolf, J. *J. Organomet. Chem.* **2002**, *661*, 137. (b) Lass, R. W.; Steinert, P.; Wolf, J.; Werner, H. *Chem.—Eur. J.* **1996**, *2*, 19.
(9) Touchard, D.; Haquette, P.; Daridor, A.; Toupet, L.; Dixneuf, P. H. *J. Am. Chem. Soc.* **1994**, *116*, 11157.
(10) (a) Roth, G.; Fischer, H. *Organometallics* **1996**, *15*, 1139. (b) Roth, G.; Fischer, H.; Meyer-Friedrichsen, T.; Heck, J.; Houbrechts, S.; Persoons, A. *Organometallics* **1998**, *17*, 1511.
(11) Venkatesan, K.; Fernandez, F. J.; Blacque, O.; Fox, T.; Alfonso, M.; Schmalle, H. W.; Berke, H. *Chem. Commun.* **2003**, 2006.
(12) Venkatesan, K.; Blacque, O.; Fox, T.; Alfonso, M.; Schmalle, H. W.; Berke, H. *Organometallics* **2004**, *23*, 4661.
(13) Dede, M.; Drexler, M.; Fischer, H. *Organometallics* **2007**, *26*, 4294.
(14) Fischer, H.; Szesni, N. *Coord. Chem. Rev.* **2004**, *248*, 1659.
(15) Semenov, S. N.; Blacque, O.; Fox, T.; Venkatesan, K.; Berke, H. *Angew. Chem., Int. Ed.* **2009**, *48*, 5203.
(16) (a) Bruce, M. I.; Hinterding, P.; Ke, M. Z.; Low, P. J.; Skelton, B. W.; White, A. H. *Chem. Commun.* **1997**, 715. (b) Bruce, M. I.; Hinterding, P.; Low, P. J.; Skelton, B. W.; White, A. H. *J. Chem. Soc., Dalton Trans.* **1998**, 467. (c) Bruce, M. I.; Hinterding, P.; Low, P. J.; Skelton, B. W.; White, A. H. *Chem. Commun.* **1996**, 1009.
(17) (a) Haquette, P.; Touchard, D.; Toupet, L.; Dixneuf, P. *J. Organomet. Chem.* **1998**, *565*, 63. (b) Winter, R. F.; Hornung, F. M. *Organometallics* **1999**, *18*, 4005. (c) Winter, R. F. *Eur. J. Inorg. Chem.* **1999**, 2121. (d) Winter, R. F.; Hornung, F. M. *Organometallics* **1997**, *16*, 4248.

Published on Web 11/15/2010

Scheme 1

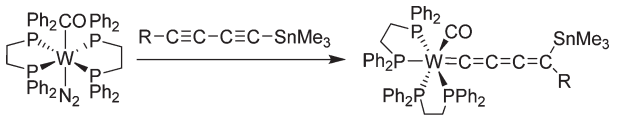

R = $SnMe_3$ (**2**) 72%, $SiMe_3$ (**3**) 62%, *p*-C_6H_4tBu (**4**) 73%

Table 1. IR, NMR, and UV−Vis Data of Complexes 2, 3, and 4

	IR [cm^{-1}]		NMR ^{13}C [ppm]				absorption [nm] (ε/1000 [M^{-1} cm^{-1}])		
	ν (C_4)	ν (CO)	C_α	C_β	C_γ	C_δ	λ_1	λ_2	λ_3
2	1925	1808	249.5	124.8	124.7	46.8	376 (29.6)	466 (4.9)	900 (4.4)
3	1940	1803	254.1	142.4	142.5	49.1	373 (37.4)	468 (5.2)	899 (2.2)
4[a]	1935	1798	267.6	162.6	140.0	70.7	386 (163)	525 (82)	768 (0.7)

[a] Data from ref 15.

complexes possessing a cyclobutene bridge.[18] The related dimerization of tungsten butatrienylidene is another rare example of relatively clean self-coupling.[15] In this work we approached the deprotection of $SnMe_3$-substituted derivatives generating the parent tungsten butadiyne complexes.

On the short chain side there would be tin-substituted vinylidenes, which could undergo chain extension by Stille-type coupling reactions. Up to now mainly tin-substituted manganese vinylidene derivatives were explored,[4,19] which is now extended to tin-substituted tungsten vinylidenes.

Results and Discussion

Synthesis and Structural Studies on Tungstenacumulenes. Butatrienylidene complexes were obtained via primary addition and π binding of 1,4-butadiyne tin derivatives to coordinatively unsaturated electron-rich metal centers. These systems subsequently rearrange to end-on butatrienylidene complexes. For the preparation of tungsten complexes [*trans*-W(CO)-(N_2)(dppe)$_2$] (**1**) was chosen as the metal precursor, offering for ligand exchanges the labile N_2 ligand.[20,21] The four electron-donating dppe ligands were anticipated to create a pronounced preference for "end-on" cumulenylidene ligands via enhanced back-donation, stabilizing the binding of this highly unsaturated ligand.

1 reacts with $Me_3SnC{\equiv}CC{\equiv}CR$ derivatives[15] (Scheme 1) with heating, and repeated removal of N_2 *in vacuo* enabled the binding of the butadiyne ligand accompanied by a 1,4-$SnMe_3$-shift and formation of the butatrienylidene derivative.

The bis-stannylated product [*cis*-W(CO)(dppe)$_2${C=C=C=C(SnMe$_3$)$_2$}] (**2**) was isolated as very air sensitive crystals in 72% yield. A *cis*-position of the diphosphines was indicated in the ^{31}P NMR spectra, showing two doublets of multiplets (J_{P-P} = 100 Hz) originating from coupling with the *trans* phosphorus atoms and two multiplets for the phosphorus atoms located *trans* to CO and *trans* to the C_4 chain. This assignment was confirmed by a COSY experiment. The ^{13}C NMR spectra of **2** showed four resonances for the C_4 cumulenic chain at 249.5 (C_α), 124.9 (C_β), 124.8 (C_γ), and 46.8 ppm (C_δ). All four signals are shifted to high field with respect to the related species [*cis*-W(CO)(dppe)$_2${C=C=C=C(SnMe$_3$)(*p*-C_6H_4tBu)}] (**4**) (Table 1). The ^{119}Sn NMR spectrum of **2** shows Sn−P coupling for the unique signal at −22.5 ppm. A typical ν(C≡O) band is observed at 1786 cm^{-1}, as well as a $\nu(C_4)$ vibration at 1926 cm^{-1}. The position of these bands is similar to those of the previously reported [*cis*-W(CO)(dppe)$_2$(C=CHR)] and [Ir(Cl)(P*i*Pr$_3$)$_2$(C=C=C=CPh$_2$)].[6,7,22]

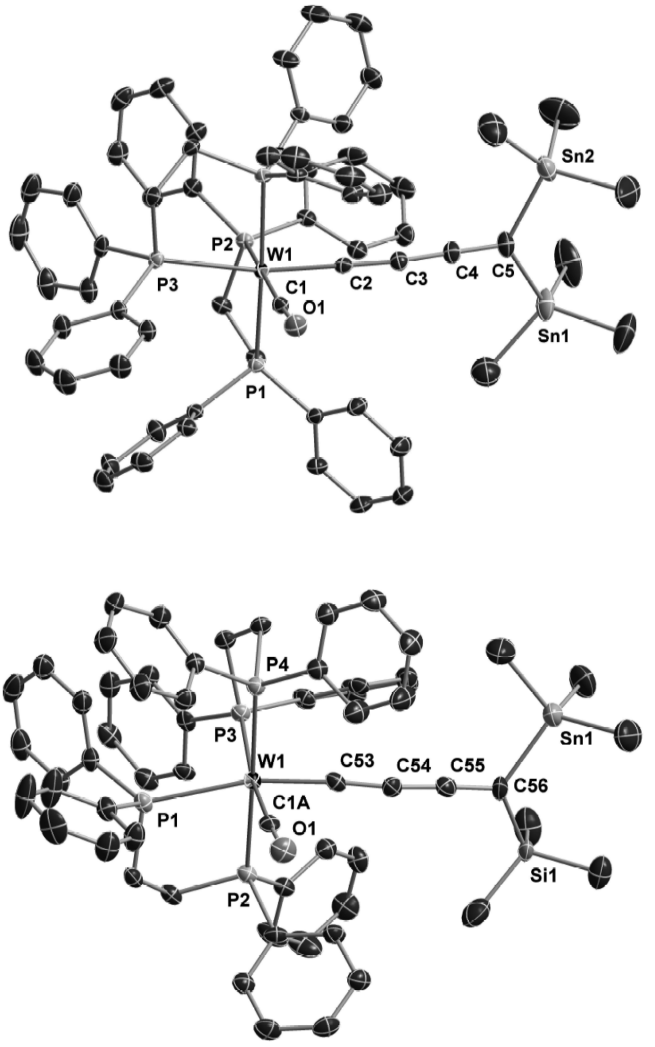

Figure 1. Thermal ellipsoid plots of the structures of **2** (top) and **3** (bottom) (30% probability level). Hydrogen atoms and solvent molecules are omitted for clarity.

The spectroscopically derived structure of **2** was finally confirmed by X-ray structural analysis (Figure 1). Details of the data collection and refinement are presented in Tables 1S and 2S, and selected bond lengths are reported in Table 2.

The unsaturated carbon chain slightly deviates from linearity at C2 with a C1−C2−C3 angle of 170.6°. The lengths of the C2−C3 and C4−C5 double bonds are longer (1.305(5) and 1.307(5) Å) than the internal C3−C4 bond (1.285(5) Å). This behavior is significantly different from the reported Ir−C_4 and Mn−C_4 cumulenic species, where the C_α−C_β and C_γ−C_δ lengths are short and the C_β−C_γ length is longer.[6,11] The W=C bond distance of **2** of 1.937(4) Å is slightly longer than that observed for **4** (1.923(3) Å), presumably indicating weaker

(18) Bruce, M. I.; Ellis, B. G.; Skelton, B. W.; White, A. H. *J. Organomet. Chem.* **2005**, *690*, 1772.
(19) Venkatesan, K.; Blacque, O.; Fox, T.; Alfonso, M.; Schmalle, H. W.; Kheradmandan, S.; Berke, H. *Organometallics* **2005**, *24*, 920.
(20) Ishida, T.; Mizobe, Y.; Tanase, T.; Hidai, M. *J. Organomet. Chem.* **1991**, *409*, 355.
(21) Ishida, T.; Mizobe, Y.; Tanase, T.; Hidai, M. *Chem. Lett.* **1988**, 441.
(22) Nakamura, G.; Harada, Y.; Mizobe, Y.; Hidai, M. *Bull. Chem. Soc. Jpn.* **1996**, *69*, 3305.

Table 2. Selected Average Bond Lengths of Compounds 2−5, 7, and 9[a]

	W−P[b]	W−CO	W−C_α	C_α−C_β	C_β−C_γ	C_γ−C_δ
2	2.5054(6)	1.961(3)	1.937(3)	1.305(4)	1.285(4)	1.307(4)
3[c]	2.505(2)	1.98(1)	1.93(1)	1.31(1)	1.27(1)	1.32(1)
4[d]	2.5205(8)	1.937(3)	1.923(3)	1.306(4)	1.273(4)	1.325(4)
5	2.509(1)	1.940(5)	2.007(4)	1.298(6)		
7	2.4718(5)	2.041(3)	2.207(2)	1.158(3)		
9	2.4783(7)	2.019(4)	2.153(3)	1.204(3)		

[a] Assignment of the bond lengths in the C_4 and C_2 chains according to the following notation: [W]$C_\alpha C_\beta C_\gamma C_\delta$. [b] An average value of the four W−P bonds is presented. [c] An average value for two crystallographically independent molecules of **3** is presented. [d] Data from ref 15.

Scheme 2

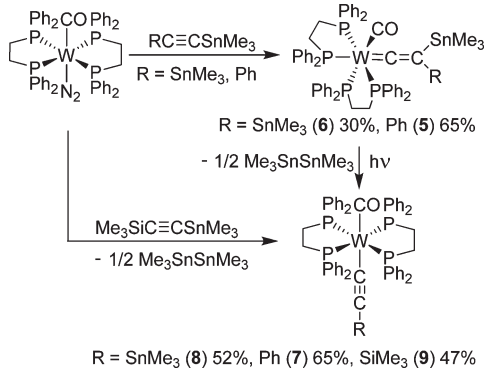

π-acceptor properties of the C4 chain of **2** relative to the one with aromatic substituent.

The stannyl acetylene method was used to access asymmetrically substituted butatrienylidene complexes. Applying **1** in the reaction with $Me_3SnC{\equiv}CC{\equiv}CSiMe_3$, the compound [*cis*-W(CO)(dppe)$_2${C=C=C=C(SnMe$_3$)(SiMe$_3$)}] (**3**) was formed, which could be isolated in 62% yield. Like **2**, **3** revealed *cis*-diphosphines, established via ^{31}P NMR spectroscopy showing four resonances and the expected coupling patterns. The ^{13}C NMR spectra of **3** exhibited butatrienylidene resonances slightly shifted to low field with respect to the bis-trimethyltin-substituted derivative at 254.1 (C_α), 142.4 (C_β), 142.5 (C_γ), and 49.1 ppm (C_δ). In general, the ^{13}C NMR data of the tungsten C_4 cumulenes **2**−**4** turned out to be quite comparable to those of the MnC_4 series except for the C_δ signals, which are located at lower field.[11,12] The ^{119}Sn NMR spectrum of **3** showed a signal similar to **2** at −26.1 ppm. It was simulated using the following ^{119}Sn, ^{31}P coupling constancies: 27.6, 42.3, 44.1, and 59.3 Hz. The crystal structure of **3** was determined from crystals grown from a toluene/pentane mixture. The unit cell contains two independent molecules. The bond alternation of the C_4 chain in the independent molecules was found to be similar to **2**. In both **2** and **3** molecules the W−CO axis is orthogonal to plane of the terminal CSnSn or CSnSi fragment. This could be rationalized on the basis of the idea that the empty p orbital of C_α prefers to be perpendicular to W−CO since it is not concurrent with CO in back-bonding. The double-bond alternation will lead to the observed orientation of the W−CO axis relative to the terminal fragment.

Trimethyltin acetylenes were expected to react in a manner analogous to the diynes, producing via a shift of the stannyl group trimethyltin-substituted vinylidenes. The reaction of **1** with $Me_3SnC{\equiv}CPh$ was carried out under conditions similar to those for **2**, monitoring the progressing reaction by ^{31}P NMR spectroscopy (Scheme 2).

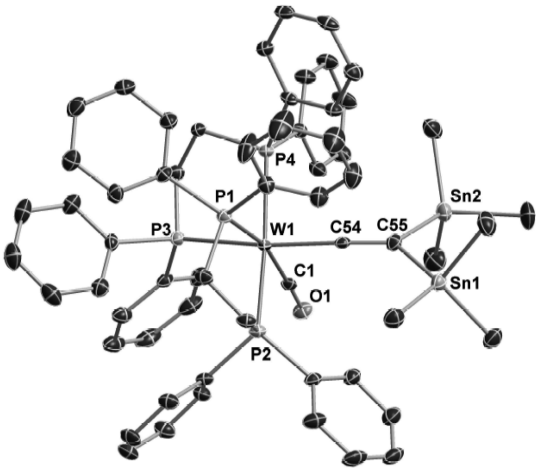

Figure 2. Thermal ellipsoid plot of the structure of **6** (30% probability level). Hydrogen atoms and solvent molecules are omitted for clarity.

The vinylidene complex [*cis*-W(CO)(dppe)$_2${C=C(SnMe$_3$)(Ph)}] (**5**) could eventually be isolated by crystallization from benzene/pentane in the dark. The structure of **5** was fully established by ^{1}H, ^{13}C, and ^{31}P NMR spectroscopy and elemental analysis. The ^{31}P NMR spectrum revealed the tungsten environment to be analogous to **2** and **3** with *cis*-configured diphosphines, and in addition the ^{13}C NMR spectrum of **5** exhibited resonances for the vinylidene unit at 309 (C_α) and 111.6 ppm (C_β), which were comparable to the data of other tungsten vinylidenes.[22,23] The reaction of **1** applying $Me_3SnC{\equiv}CSnMe_3$ afforded the bis-trimethylstannyl-substituted vinylidene complex [*cis*-W(CO)(dppe)$_2${C=C(SnMe$_3$)$_2$}] (**6**) in 30% yield. The structure of **6** was established by spectroscopic methods and confirmed by an X-ray diffraction study (Figure 2).

The [*cis*-W(CO)(dppe)$_2$] substructure of **6** is overall similar to that of **2** and **3**. The W=C bond distance of 2.007(4) Å is longer than that observed for related vinylidene species [cis-W(CO)(dppe)$_2$(C=CHCOOEt)] (1.88(1) Å)[22,24] and is slightly longer than the W=C bond distance in the butatrienylidene complex **2**. This is in line with the theoretical prediction of increasing π-acceptor properties with an increase in the number of cumulenic carbon atoms.[25] The formation of vinylidene derivatives directly from **1** and tin-substituted acetylenes is in contrast to the reactivity of terminal acetylenes, where the required acetylene/vinylidene rearrangement was not accessible; rather the alternative pathways of C−H oxidative additions prevailed.[22]

The reaction of **1** with $Me_3SnC{\equiv}CSiMe_3$ furnished also a vinylidene derivative, which could be detected by NMR in solution, but could not be isolated due to its too low stability. The main product of this reaction was [*trans*-W(CO)(dppe)$_2$(C≡C-SiMe$_3$)] (**9**). In a similar fashion loss of the tin group occurred for **6** and **5**, producing [*trans*-W(CO)(dppe)$_2$(C≡C-SnMe$_3$)] (**8**), phenylacetylide complex [*trans*-W(CO)(dppe)$_2$(C≡CPh)] (**7**), and $Me_3SnSnMe_3$. The yields of **5** and **6** according to Scheme 2 are low, because even in thermally induced reactions they are intermediates on the way to **7** and **8**. Full conversions of **5** and **6** to **7** and **8** could be accomplished by

(23) Birdwhistell, K. R.; Burgmayer, S. J. N.; Templeton, J. L. *J. Am. Chem. Soc.* **1983**, *105*, 7789.
(24) Marrone, A.; Re, N. *Organometallics* **2002**, *21*, 3562.
(25) Re, N.; Sgamellotti, A.; Floriani, C. *Organometallics* **2000**, *19*, 1115.

short periods of UV irradiation. The photolytic activation of the tin-substituted vinylidenes is expected to operate on the same basis as the thermal processes breaking the C−Sn bond with subsequent recombination of the $SnMe_3$ radical to form $Me_3SnSnMe_3$. The remaining radical on the β-carbon atom delocalizes to the tungsten center with structures best described as W(I) acetylide complexes. All three compounds **7**−**9** are paramagnetic d^5 species and are related in the way of their formation to dinuclear tungsten acetylide complexes recently obtained in our group.[15] **7** and **9** were characterized by single-crystal X-ray diffraction analyses (Figure 3 and Supporting Information).

The coordinative environment of the tungsten center in **9** is pseudo-octahedral, composed of a square of phosphorus atoms (*trans* diphosphines) and *trans*-disposed CO and alkynyl ligands. Average W−P distances of 2.472(1) and 2.478(1) Å were found for **7** and **9**, respectively.

We then attempted the deprotection of **2** by treatment with a THF water solution in a similar way to that for **4**;[15] however a complex mixture was obtained that could not be fully unraveled into its components. To gain further insight into this transformation, a low-temperature study of the reaction between **2** and $NBu_4F \cdot 3H_2O$ was initiated and monitored by ^1H and ^{31}P NMR spectroscopy. We found no evidence for the formation of a H-substituted cumulenylidene complex, even at low temperature (−40 °C). Instead two overlapping singlets were detected in the ^{31}P NMR spectrum, remaining at room temperature, but changing in intensities during the course of the reaction. The reaction mixture was evaporated to dryness, and the solid residue was washed with toluene to give an orange powder of complex **10** (Scheme 3). This compound showed a singlet in the ^{31}P NMR spectrum with a chemical shift similar to other complexes with *trans*-disposed dppe ligands and identical to one of the singlets of the VT NMR.[26] The ^{13}C NMR spectrum shows four signals for the C4 carbon atoms at 149.2 (C_α), 98.9 (C_β), 76.8 (C_γ), and 48.7 ppm (C_δ). A DEPT experiment confirmed that C_δ is bonded to one proton. The ^1H NMR spectrum also clearly demonstrated the presence of the $[NBu_4]^+$ cation. On the basis of these data the pseudo-octahedral structure [*trans*-$W(CO)(dppe)_2(C{\equiv}C{-}C{\equiv}CH)][NBu_4]$ (**10**) was proposed, which could be confirmed by an X-ray diffraction analysis (Figure 4). **10** is presumably formed via consecutive destannylation of **2** with [*trans*-$W(CO)(dppe)_2(C{\equiv}CC{\equiv}CSnMe_3)][NBu_4]$ as an intermediate, which was attributed the second singlet appearing in the VT ^{31}P NMR spectra.

Spectroscopic and Electrochemical Properties. The butatrienylidene complexes **2**−**4** were characterized by UV−vis−NIR and CV (cyclic voltammetry) studies. The UV−vis−NIR data are presented in Figure 5.

All three complexes **2**−**4** exhibit three main absorptions. Their intensities decrease with increasing wavelengths (Table 1). The lowest energy transition could be attributed to the HOMO/LUMO transition. The *p*-*t*BuC_6H_4 substituent turns out to be a special case in this series of spectra, because this substituent strongly affects both the position and intensities of the absorptions (Figure 5), while the change of the $SnMe_3$ to a $SiMe_3$ substituent has only little influence on the spectra. As could be seen from the spectra, the band for **4** reveals a strong blue shift and decreases in intensity. This could imply an increase in the HOMO−LUMO gap, which would be consistent with the higher stability of the deprotected complex bearing an aromatic substituent.

CV studies of **2** and **4** revealed irreversible oxidation and reduction processes (see Supporting Information for details).

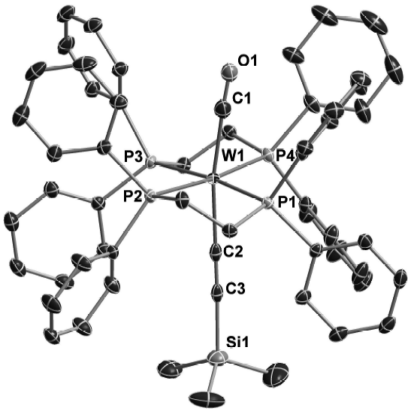

Figure 3. Thermal ellipsoid plot of the structure of **9** (30% probability level). Hydrogen atoms and solvent molecules are omitted for clarity.

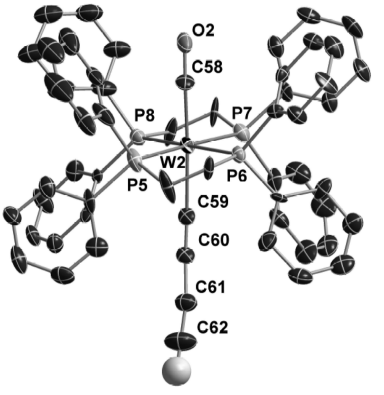

Figure 4. Thermal ellipsoid plot of the structure of the anionic part of **10** (30% probability level). The tetrabutylammonium cation and selected hydrogen atoms are omitted for clarity. Only one of the two crystallographically independent molecules is presented.

Scheme 3

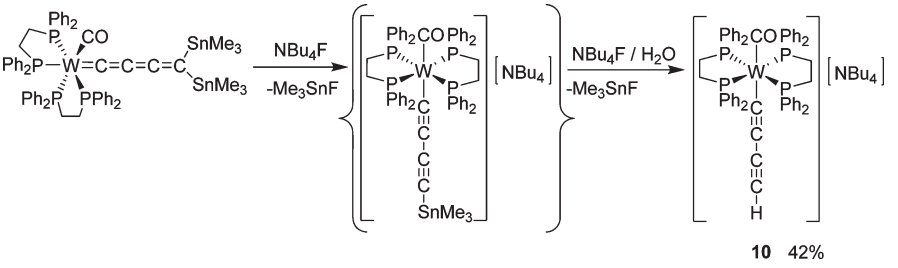

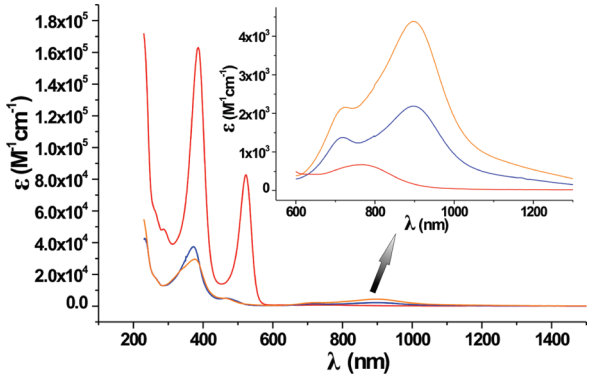

Figure 5. UV−vis−NIR spectra for **2** (orange), **3** (blue), and **4** (red).

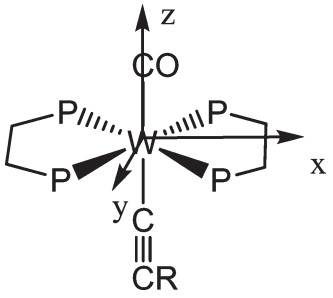

Figure 6. Coordinate system for the interpretation of the CV and EPR data. *x* and *y* are chosen arbitrarily.

Complexes **7**−**9** possess a d^5 configuration. The d_{xy} orbital (see Figure 6 for coordinate system) is expected to be the SOMO. As a result, facile oxidations and reductions were anticipated. The redox properties of **9** were also probed by CV measurements in CH_2Cl_2 and THF solutions (Figures 7 and Supporting Information). They show a fully reversible reduction wave ($E_{1/2} = -1.62$ V vs $Fc^{0/+}$, $i_c/i_a = 1$ in THF; $E_{1/2} = -1.62$ V vs $Fc^{0/+}$, $i_c/i_a = 1.03$ in CH_2Cl_2) and an irreversible oxidation process ($E_{p/2} = -0.869$ V in THF; $E_{p/2} = -0.882$ V in CH_2Cl_2) followed by a reversible oxidation ($E_{1/2} = 0.13$ V, $i_c/i_a = 0.94$ in THF; $E_{1/2} = 0.16$ V, $i_c/i_a = 1.01$ in CH_2Cl_2). The reduction wave probably belongs simply to one electron reduction of **9** to $\mathbf{9}^-$ anion. The irreversibility of the first oxidation wave is not yet understood. The full irreversibility retains up to 2 V/s, suggesting that fast transformation is coupled with oxidation process. This transformation probably does not involve exchange of ligand to solvent because of similarity of behaviors of this wave in THF and CH_2Cl_2.

9 was also investigated by EPR spectroscopy (Figure 8). No signal was observed at room temperature; however at temperatures below 50 K a signal was detected. It is strongly anisotropic with individual *g* factor components ranging from 2.6 to 1.6. The fitting of this spectrum could be carried out approximating the structure of **9** to rhombic symmetry with the *z*-axis in the direction of the acetylide ligand and the *x*- and *y*-axes in the direction of the C_2-axis between the phosphorus atoms (Figure 6).

The spectrum however was modeled with $g_x = 2.57$, $g_y = 2.24$, and $g_z = 1.61$ (Figure 8). The quality of the spectrum did not allow a reliable estimate of the hyperfine coupling of the

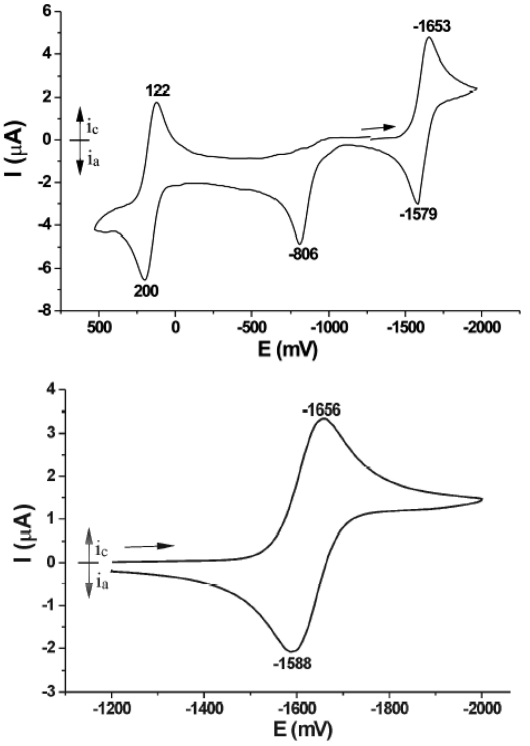

Figure 7. Cyclic voltammogram of **9** in CH_2Cl_2 (top) and in THF (bottom); 0.1 M [nBu$_4$N][PF$_6$]; Au electrode; *E* vs $Fc^{0/+}$; scan rate = 100 mV/s; 20 °C.

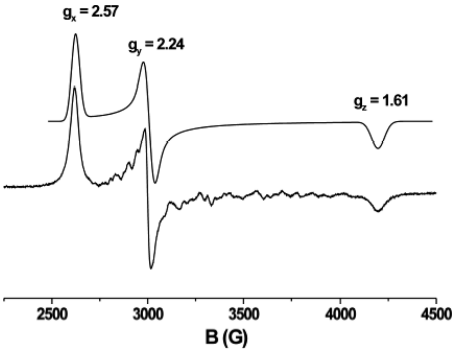

Figure 8. Experimental (bottom) and modeled (top) solid-state EPR spectra of powdered **9** at 30 K.

P nuclei. The obtained values for components of the *g*-factor are in the expected range for d^5 low-spin systems,[27] where two main factors affect the anisotropy of *g*: (a) the splitting of the T_{2g} ground term due to the low symmetry of the coordination sphere and (b) the spin−orbital coupling leading to mixing of these split states. The crystal field in our case is strongly distorted from octahedral symmetry with the π-acceptor interaction as an important factor. Such asymmetry around a 5d metal atom could lead to significant separation of the d_{xy} from d_{xz} and d_{yz} orbitals to give an isotropic signal at g = 2. However, spin−orbital coupling, which can be strong for the heavy metal tungsten, has an opposite influence and would increase the *g* anisotropy. Particularly for d^5 low-spin complexes of group VI metals, such strong *g* anisotropy is not typical. The related [*trans*-M(CO)$_2$(dppm)$_2$]$^+$ (M = Cr, Mo; dppm = 1,2-bis(diphenylphosphinomethane)) have well-resolved EPR

(26) Semenov, S. N.; Blacque, O.; Fox, T.; Venkatesan, K.; Berke, H. *J. Am. Chem. Soc.* **2010**, *132*, 3115.

(27) Rieger, P. H. *Coord. Chem. Rev.* **1994**, *135*, 203.

spectra, while for [*trans*-$W(CO)_2(dppm)_2]^+$ only unclearness of the spectrum was mentioned.[28] The *g* tensor obtained for **9** is less anisotropic than in Ru^{3+} or Os^{3+} tris-bipyridyl complexes, where strong spin−orbital coupling cannot be compensated by strong distortion, and it is then closer to the $[Fe(bipy)_3]^{3+}$ (bipy-2,2′-bipyridyl) values.[29] The EPR experiment indeed confirmed the mixing of d_{xy} with d_{xz} and d_{yz} orbital characters in the [*trans*-$W(CO)(dppe)_2(C{\equiv}C)$] fragment.[15] This would also provide an explanation for the significant antiferromagnetic coupling between such centers in related bridged $W(d^5)(bridge)W(d^5)$ molecules. Electrons in a pure d_{xy} orbital (δ-symmetry) cannot interact with the orbitals of the acetylide ligand, since these are of π-symmetry; however upon mixing with the d_{xz} and d_{yz}, the orbital symmetry restriction is lifted, thereby providing an antiferromagnetic long-distance through-bridge exchange in the dinuclear case.[15]

Conclusion

In conclusion, we have shown that [*trans*-$W(CO)(N_2)(dppe)_2$] is a suitable starting material for the preparation of tungsten butatrienylidene complexes of the type [*cis*-$W(CO)(dppe)_2\{C{=}C{=}C{=}C(SnMe_3)(R)\}$]. We demonstrated that R has a strong influence on the deprotection process and also showed that the bistrimethyltin derivative could be readily destannylated by NBu_4F to give the corresponding butadiyne compound. The UV-vis data revealed that such a difference in stability can be attributed to electronic effects, particularly the higher HOMO/LUMO gap in the case of aryl substitution. The reaction of the N_2 complex with stannylated acetylenes and subsequent removal of the $SnMe_3$ moieties by UV or thermal activation constitutes a new synthetic access to unique [*trans*-$W(CO)(dppe)_2(C{\equiv}CR)$] acetylides. The electronic structures of these complexes were studied by CV and EPR measurements. The accessibility of the butadiyne derivatives and the W(I) acetylide complexes opens up new avenues for the development of binuclear complexes with longer conjugated bridges, i.e., for instance μ-C_8 compounds.

Experimental Section

General Procedures. All the manipulations were carried out under a nitrogen atmosphere using Schlenk techniques or a drybox. Reagent grade benzene, toluene, hexane, pentane, diethyl ether, and tetrahydrofuran were dried and distilled from sodium benzophenone ketyl prior to use. Dichloromethane and acetonitrile were distilled from CaH_2. The literature procedures were used to prepare the following compounds: $Me_3SnC{\equiv}CC{\equiv}CSiMe_3$,[30] [*trans*-$W(CO)(N_2)(dppe)_2$],[20] and [*cis*-$W(CO)(dppe)_2\{C{=}C{=}C{=}C(SnMe_3)(p\text{-}C_6H_4tBu)\}$].[15] $Me_3SnC{\equiv}CC{\equiv}CSnMe_3$ was prepared by a modified literature protocol (see Supporting Information).[31] All other chemicals were used as obtained from commercial suppliers. The IR spectra were obtained on a Bio-Rad FTS-45 instrument and a Bio-Rad Excalibur FTS-3500 instrument. NMR spectra were measured on a Varian Mercury spectrometer at 200 MHz for the ^1H nucleus and at 81 MHz for $^{31}P\{^1H\}$ spectra, on a Varian Gemini-2000 spectrometer at 300 MHz for ^1H spectra and at 75 MHz for $^{13}C\{^1H\}$ spectra, and on Bruker-DRX-500 and Bruker-AV2-500 spectrometers at 500 MHz for ^1H, 125.8 MHz for $^{13}C\{^1H\}$, and 202.5 MHz for $^{31}P\{^1H\}$. Chemical shifts for ^1H and ^{13}C are given in ppm relative to TMS, and those for ^{31}P relative to phosphoric acid. The UV−vis and near-IR spectra were recorded on Varian CARY 50 Scan UV−visible and on Varian CARY 500 Scan UV−visible/near-IR spectrometers. CHN elemental analyses were performed with a LECO CHN-932 microanalyzer. Cyclic voltammograms were obtained with a BAS 100 W voltammetric analyzer equipped with the low-volume cell. The cell was equipped with an Au working and a Pt counter electrode and a nonaqueous reference electrode. All sample solutions (THF or CH_2Cl_2) were approximately 2×10^{-3} M in substrate and 0.1 M in Bu_4NPF_6 and were prepared under nitrogen. Ferrocene was subsequently added, and the calibration of voltammograms recorded. The BAS 100W program was employed for data analysis. X-band EPR spectra were obtained using a Bruker EMX electron spin resonance system (resolution 2048; central field 3400 G; sweep width 3000 G; frequency 9.448 GHz; modulation frequency 100 kHz; modulation amplitude 10 G; time constant 20.48 ms, conversion time 40.96 ms; receiver gain 2.24×10^4). The spectrum was modeled using the SimFonia program (frequency 9.448 GHz; $g_x = 2.57$; $g_x = 2.24$; $g_x = 1.61$; line width *x*-direction 42 G; line width *y*-direction 48 G; line width *y*-direction 68 G).

X-ray Diffraction Studies on 2, 3, 6, 7, 9, and 10. Intensity data for all crystals were collected at 183(2) K on an Oxford Xcalibur diffractometer (4-circle kappa platform, Ruby CCD detector, and a single-wavelength Enhance X-ray source with Mo Kα radiation, $\lambda = 0.71073$ Å)[32] using the CrysAlisPro program.[32] The selected single crystals were mounted using polybutene oil on the top of a glass fiber fixed on a goniometer head and immediately transferred to the diffractometer. The crystal structures were solved with SHELXS-97[33] using direct methods. The structure refinements were performed by full-matrix least-squares on F^2 with SHELXL-97.[33] The program PLATON[34] was used to check the results of the X-ray analyses. All programs used during the crystal structure determination process are included in the WINGX software.[34] CCDC 783485−783490 contain the supplementary crystallographic data (excluding structure factors) for this paper. These data can be obtained free of charge from The Cambridge Crystallographic Data Centre via www.ccdc.cam.ac.uk/data_request/cif.

[*cis*-W(CO)(dppe)$_2${C=C=C=C(SnMe$_3$)$_2$}] (2). [*trans*-$W(CO)(N_2)(dppe)_2$] (100 mg, 0.096 mmol) and $Me_3SnC{\equiv}CC{\equiv}CSnMe_3$ (43 mg, 0.116 mmol) were placed in a Young-Schlenk tube in 10 mL of benzene. Three freeze−pump−thaw cycles were carried out on the resulting solution to remove any dissolved nitrogen. The reaction mixture was heated under vacuum at 60 °C for 5 h. The resulting dark orange solution was concentrated to 1.5 mL *in vacuo* and layered with 10 mL of pentane. Complex **2** was obtained as brown-orange prisms in 10 h. Yield: 95 mg (0.069 mmol, 72%). Single crystals suitable for X-ray diffraction were grown by layering a benzene solution with pentane. Anal. Calcd for $C_{63}H_{66}OP_4Sn_2W$: C, 54.66; H, 4.81. Found: C, 54.92; H, 4.99. IR (cm^{-1}): ν = 1786 (CO), 1808 (CO), 1926 (C_4). ^1H NMR (500 MHz, C_6D_6): δ 8.59 (t, J_{H-H} = 9 Hz, 2H, C_6H_5), 8.54 (t, J_{H-H} = 9 Hz, 2H, C_6H_5), 7.45 (t, J_{H-H} = 8 Hz, 2H, C_6H_5), 7.35−7.25 (m, 5H, C_6H_5), 7.21−6.56 (m, 20H, C_6H_5), 6.38 (t, J_{H-H} = 8 Hz, 1H, C_6H_5), 6.17 (t, J_{H-H} = 8 Hz, 2H, C_6H_5), 3.15−2.88 (m, 2H, CH_2), 2.64 − 2.05 (m, 2H, CH_2), 1.85−1.72 (m, 4H, CH_2), 0.31 (s, 9H, $SnCH_3$ (d, satellite, $^2J_{H-Sn}$ = 52 Hz)). ^{119}Sn NMR (184.6 MHz, C_6D_6): δ −22.5 (m, $SnMe_3$). ^{31}P NMR (81 MHz, C_6D_6): δ 48.8 (m, 1P), 44.9 (m, 1P), 30.0 (m, 1P), 26.8 (m, 1P). ^{13}C NMR (125 MHz, C_6D_6): 249.5 (q, $^2J_{C-P}$ = 11 Hz, Cα), 222.8 (d, $^2J_{C-P}$ = 28 Hz, CO), 144.1

(28) Bond, A. M.; Colton, R.; Jackowski, J. J. *Inorg. Chem.* **1975**, *14*, 2526.
(29) DeSimone, R. E.; Drago, R. S. *J. Am. Chem. Soc.* **1970**, *92*, 2343.
(30) Zheng, Q. L.; Hampel, F.; Gladysz, J. A. *Organometallics* **2004**, *23*, 5896.
(31) Brefort, J. L.; Corriu, R. J. P.; Gerbier, P.; Guerin, C.; Henner, B. J. L.; Jean, A.; Kuhlmann, T.; Garnier, F.; Yassar, A. *Organometallics* **1992**, *11*, 2500.
(32) *Xcalibur CCD System*; Oxford Diffraction Ltd: Abingdon, Oxfordshire, England, 2007.
(33) Sheldrick, G. M. *Acta Crystallogr., Sect. A* **2008**, *64*, 112.
(34) Spek, A. L. *J. Appl. Crystallogr.* **2003**, *36*, 7.

(d, $^1J_{C-P}$ = 28 Hz, ipso-C_6H_5), 142.3 (d, $^1J_{C-P}$ = 29 Hz, ipso-C_6H_5), 140.7 (d, $^1J_{C-P}$ = 25 Hz, ipso-C_6H_5), 139.9 (d, $^1J_{C-P}$ = 46 Hz, ipso-C_6H_5), 139.4 (d, $^1J_{C-P}$ = 45 Hz, ipso-C_6H_5), 137.9 (d, $^1J_{C-P}$ = 25 Hz, ipso-C_6H_5), 136.4 (d, $^1J_{C-P}$ = 28 Hz, ipso-C_6H_5), 134.6 (d, J_{C-P} = 11 Hz, C_6H_5), 133.4 (d, J_{C-P} = 10 Hz, C_6H_5), 133.1 (m, C_6H_5), 132.6 (s, C_6H_5), 132.5 (s, C_6H_5), 132.4 (s, C_6H_5), 132.3 (s, C_6H_5), 131.7 (d, J_{C-P} = 11 Hz, C_6H_5), 131.3 (dd, J_{C-P} = 10 Hz, J_{C-P} = 3 Hz, C_6H_5), 129.1 (dd, J_{C-P} = 18 Hz, J_{C-P} = 2 Hz, C_6H_5), 128.5 (s, C_6H_5), 128.4 (s, C_6H_5), 128.3 (s, C_6H_5), 124.8 (s, Cβ), 124.7 (s, Cγ), 46.8 (s, (d, satellite, $^1J_{C-Sn}$ = 303 Hz) Cδ), 32.5 (m, CH_2), 30.2 (dd, $^1J_{C-P}$ = 23 Hz, $^2J_{C-P}$ = 13 Hz, CH_2), 28.5 (dd, $^1J_{C-P}$ = 23 Hz, $^2J_{C-P}$ = 15 Hz, CH_2), −7.0 (s, (d, satellite, $^1J_{C-Sn}$ = 324 Hz), CH_3).

[*cis*-W(CO)(dppe)$_2${C=C=C=C(SnMe$_3$)(SiMe$_3$)}] (3). An analogous procedure to **2** was followed applying [*trans*-W(CO)(N_2)-(dppe)$_2$] (100 mg, 0.096 mmol) and $Me_3SnC{\equiv}CC{\equiv}CSiMe_3$ (33 mg, 0.116 mmol). Yield: 80 mg (0.062 mmol, 65%). Single crystals suitable for X-ray diffraction were grown by layering a toluene solution with pentane. Anal. Calcd for $C_{63}H_{66}OP_4SnSiW$: C, 58.49; H, 5.14. Found: C, 58.62; H, 5.09. IR (cm^{-1}): ν = 1798 (CO), 1935 (C_4). ^{1}H NMR (500 MHz, C_6D_6): δ 8.48 (t, J_{H-H} = 9 Hz, 2H, C_6H_5), 8.43 (t, J_{H-H} = 9 Hz, 2H, C_6H_5), 7.60 (t, J_{H-H} = 8 Hz, 2H, C_6H_5), 7.35 (t, J_{H-H} = 8 Hz, 2H, C_6H_5), 7.21 (q, J_{H-H} = 8 Hz, 2H, C_6H_5), 7.14−7.09 (m, 10H, C_6H_5), 7.03−6.68 (m, 12H, C_6H_5), 6.62 (t, J_{H-H} = 8 Hz, 4H, C_6H_5), 6.53 (t, J_{H-H} = 7 Hz, 2H, C_6H_5), 6.49 (t, J_{H-H} = 8 Hz, 2H, C_6H_5), 6.06 (t, J_{H-H} = 8 Hz, 2H, C_6H_5), 3.05−2.80 (m, 2H, CH_2), 2.56−2.25 (m, 2H, CH_2), 2.19−1.97 (m, 3H, CH_2), 1.73−1.62 (m, 1H, CH_2), 0.28 (s, 9H, $SiCH_3$), 0.25 (s, (d, satellite, $^2J_{H-Sn}$ = 52 Hz), 9H, $SnCH_3$). ^{119}Sn NMR (184.6 MHz, C_6D_6): δ −26.1 (m, $SnMe_3$). ^{31}P NMR (81 MHz, C_6D_6): δ 48.7 (m, 1P), 44.3 (m, 1P), 29.5 (m, 1P), 26.2 (m, 1P). ^{13}C (125 MHz, C_6D_6): 254.1 (q, $^2J_{C-P}$ = 12 Hz, Cα), 222.5 (d, $^2J_{C-P}$ = 32 Hz, CO), 143.9 (d, $^1J_{C-P}$ = 28 Hz, ipso-C_6H_5), 142.4 (s, Cβ), 142.5 (s, Cγ), 142.1 (d, $^1J_{C-P}$ = 30 Hz, ipso-C_6H_5), 140.4 (d, $^1J_{C-P}$ = 27 Hz, ipso-C_6H_5), 139.8 (d, $^1J_{C-P}$ = 46 Hz, ipso-C_6H_5), 139.2 (d, $^1J_{C-P}$ = 46 Hz, ipso-C_6H_5), 137.9 (dd, $^1J_{C-P}$ = 27 Hz, J_{C-P} = 6 Hz, ipso-C_6H_5), 137.2 (dd, $^1J_{C-P}$ = 27 Hz, J_{C-P} = 3 Hz, ipso-C_6H_5), 136.0 (dd, $^1J_{C-P}$ = 25 Hz, J_{C-P} = 3 Hz, ipso-C_6H_5), 134.7 (d, J_{C-P} = 11 Hz, C_6H_5), 133.4 (d, J_{C-P} = 10 Hz, C_6H_5), 132.5 (d, J_{C-P} = 9 Hz, C_6H_5), 132.5 (d, J_{C-P} = 11 Hz, C_6H_5), 132.4 (d, J_{C-P} = 12 Hz, C_6H_5), 131.8 (d, J_{C-P} = 11 Hz, C_6H_5), 131.4 (dd, J_{C-P} = 10 Hz, J_{C-P} = 4 Hz, C_6H_5), 129.3 (dd, J_{C-P} = 20 Hz, J_{C-P} = 2 Hz, C_6H_5), 128.7 (s, C_6H_5), 128.6 (s, C_6H_5), 128.4 (s, C_6H_5), 49.1 (s, (d, satellite, $^1J_{C-Sn}$ = 290 Hz), Cδ), 32.3 (m, CH_2), 30.4 (dd, $^1J_{C-P}$ = 24 Hz, $^2J_{C-P}$ = 12 Hz, CH_2), 28.3 (dd, $^1J_{C-P}$ = 23 Hz, $^2J_{C-P}$ = 16 Hz, CH_2), 2.0 (s, $SiCH_3$), −7.0 (s, (d, satellite, $^1J_{C-Sn}$ = 310 Hz), $SnCH_3$).

[*cis*-W(CO)(dppe)$_2${C=C(SnMe$_3$)$_2$}] (6). An analogous procedure to **2** was applied starting from [*trans*-W(CO)(N_2)(dppe)$_2$] (20 mg, 0.0193 mmol) and $Me_3SnC{\equiv}CSnMe_3$ (7.4 mg, 0.021 mmol). A higher concentration of **4** and cooling were required to initialize crystallization of **4**. Yield: 8 mg (0.0059 mmol, 30%). Single crystals suitable for X-ray diffraction were grown by layering a benzene solution with pentane. Anal. Calcd for $C_{61}H_{67}OP_4Sn_2W$: C, 53.82; H, 4.96. Found: C, 54.02; H, 4.09. IR (cm^{-1}): ν = 1789 (CO). ^{1}H NMR (500 MHz, C_6D_6): δ 8.48 (t, J = 8 Hz, 2H, C_6H_5), 8.42 (t, J = 8 Hz, 2H, C_6H_5), 8.16 (t, J = 8 Hz, 2H, C_6H_5), 8.00 (t, J = 9 Hz, 2H, C_6H_5), 7.84 (t, J = 7 Hz, 2H, C_6H_5), 7.60 (t, J = 8 Hz, 2H, C_6H_5), 7.42 (t, J = 7 Hz, 2H, C_6H_5), 7.36 (t, J = 8 Hz, 4H, C_6H_5), 7.16 (m, 8H, C_6H_5), 7.00 (m, 8H, C_6H_5), 6.81 (t, J = 7 Hz, 2H, C_6H_5), 6.75 (t, J = 7 Hz, 2H, C_6H_5), 6.23 (m, 4H, C_6H_5), 2.65 (m, 2H, CH_2), 2.29−1.60 (m, 6H, CH_2), 0.28 (s, 18H, $SnCH_3$ (d, satellite, $^2J_{H-Sn}$ = 52 Hz)). ^{119}Sn NMR (184.6 MHz, C_6D_6): δ −32.2 (m, SnMe3). ^{31}P NMR (202 MHz, C_6D_6): δ 42.5 (m, 1P), 38.3 (m, 1P), 28.7 (m, 1P), 26,7 (m, 1P). ^{13}C NMR (125 MHz, C_6D_6): 297.6 (s, Cα), 226.2 (d, $^2J_{C-P}$ = 23 Hz, CO), 144.9 (d, $^1J_{C-P}$ = 34 Hz, ipso-C_6H_5), 142.6 (d, $^1J_{C-P}$ = 27 Hz, ipso-C_6H_5), 141.8 (d, $^1J_{C-P}$ = 27 Hz, ipso-C_6H_5), 141.5 (d, $^1J_{C-P}$ = 34 Hz, ipso-C_6H_5), 141.2 (d, $^1J_{C-P}$ = 27 Hz, ipso-C_6H_5), 140.4 (d, $^1J_{C-P}$ = 22 Hz, ipso-C_6H_5), 140.1 (d, $^1J_{C-P}$ = 18 Hz, ipso-C_6H_5), 138.7 (d, $^1J_{C-P}$ = 34 Hz, ipso-C_6H_5), 134.0 (d, J_{C-P} = 11 Hz, C_6H_5), 133.8 (d, J_{C-P} = 11 Hz, C_6H_5), 133.5 (d, J_{C-P} = 11 Hz, C_6H_5), 133.3 (d, J_{C-P} = 11 Hz, C_6H_5), 132.8 (d, J_{C-P} = 11 Hz, C_6H_5), 131.3 (d, J_{C-P} = 11 Hz, C_6H_5), 131.5 (d, J_{C-P} = 11 Hz, C_6H_5), 131.0 (d, J_{C-P} = 11 Hz, C_6H_5), 129.1 (s, C_6H_5), 128.8 (s, C_6H_5), 128.6 (s, C_6H_5), 128.5 (s, C_6H_5), 127.3 (s, C_6H_5), 127.2 (s, C_6H_5), 127.1 (s, C_6H_5), 90.8 (d, $^3J_{C-P}$ = 15 Hz, Cβ), 32.8 (dd, $^1J_{C-P}$ = 24 Hz, $^2J_{C-P}$ = 16 Hz, CH_2), 29.7 (m, CH_2), 28.1 (dd, $^1J_{C-P}$ = 22 Hz, $^2J_{C-P}$ = 12 Hz, CH_2), −3.2 (s, $SnCH_3$ (d, satellite $^1J_{C-Sn}$ = 313 Hz)).

[*cis*-W(CO)(dppe)$_2${C=C(SnMe$_3$)(Ph)}] (5). An analogous procedure to **2** was followed applying [*trans*-W(CO)(N_2)(dppe)$_2$] (20 mg, 0.0193 mmol) and $PhC{\equiv}CSnMe_3$ (5.6 mg, 0.021 mmol). Yield: 16 mg (0.0125 mmol, 65%). Anal. Calcd for $C_{64}H_{63}OP_4SnW$: C, 60.31; H, 4.98. Found: C, 60.55; H, 5.07. IR (cm^{-1}): ν = 1783 (CO). ^{1}H NMR (500 MHz, THF-d_8): δ 8.17 (t, J_{H-H} = 8 Hz, 2H, C_6H_5), 7.74 (m, 6H, C_6H_5), 7.25−7.00 (m, 25H, C_6H_5), 6.89 (q, J = 8 Hz, 4H, C_6H_5), 6.78 (t, J = 7 Hz, 2H, C_6H_5), 6.68 (t, J = 7 Hz, 2H, C_6H_5), 6.56 (t, J = 7 Hz, 1H, C_6H_5), 6.23 (t, J = 7 Hz, 2H, C_6H_5), 6.17 (t, J = 7 Hz, 2H, C_6H_5), 3.18 (m, 1H, CH_2), 3.18 (m, 1H, CH_2), 2.22−1.62 (m, 6H, CH_2), −0.46 (s, 9H, $SnCH_3$ (d, satellite, $^2J_{H-Sn}$ = 50 Hz)). ^{119}Sn NMR (184.6 MHz, THF-d_8): δ −41.4 (m, $SnMe_3$). ^{31}P NMR (202 MHz, C_6D_6): δ 40.4 (m, 1P), 38.0 (m, 1P), 24.1 (m, 1P), 21.8 (m, 1P). ^{13}C NMR (125 MHz, THF-d_8): 309.1 (dq, $^2J_{C-P(trans)}$ = 20 Hz, $^2J_{C-P(cis)}$ = 10 Hz, Cα), 225.3 (d, $^2J_{C-P}$ = 28 Hz, CO), 151.7 (s, ipso-C_6H_5), 142.2 (d, $^1J_{C-P}$ = 32 Hz, ipso-C_6H_5), 140.4 (d, $^1J_{C-P}$ = 35 Hz, ipso-C_6H_5), 139.1 (d, $^1J_{C-P}$ = 33 Hz, ipso-C_6H_5), 138.6 (s, C_6H_5), 138.4 (d, $^1J_{C-P}$ = 33 Hz, ipso-C_6H_5), 137.9 (d, $^1J_{C-P}$ = 26 Hz, ipso-C_6H_5), 136.0 (s, C_6H_5), 135.9 − 135.7 (m, C_6H_5), 132.1 (d, J_{C-P} = 11 Hz, C_6H_5), 131.5 (d, J_{C-P} = 11 Hz, C_6H_5), 131.3 (d, J_{C-P} = 11 Hz, C_6H_5), 131.0 (d, J_{C-P} = 11 Hz, C_6H_5), 130.5 (d, J_{C-P} = 11 Hz, C_6H_5), 129.6 (d, J_{C-P} = 11 Hz, C_6H_5), 129.4 (d, J_{C-P} = 11 Hz, C_6H_5), 129.3 (d, J_{C-P} = 11 Hz, C_6H_5), 127.2 (s, C_6H_5), 126.7 (s, C_6H_5), 126.4 (s, C_6H_5), 126.3 (s, C_6H_5), 126.0 (s, C_6H_5), 125.9 (s, C_6H_5), 125.8 (s, C_6H_5), 125.6 (s, C_6H_5), 125.5 (s, C_6H_5), 125.4 (s, C_6H_5), 125.3 (s, C_6H_5), 111.6 (d, $^3J_{C-P}$ = 14 Hz, Cβ), 29.8 (dd, $^1J_{C-P}$ = 23 Hz, $^2J_{C-P}$ = 15 Hz, CH_2), 27.3 (m, CH_2), 25.6 (dd, $^1J_{C-P}$ = 25 Hz, $^2J_{C-P}$ = 12 Hz, CH_2), −8.0 (s, $SnCH_3$ (d, satellite $^1J_{C-Sn}$ = 310 Hz)).

[*trans*-W(CO)(dppe)$_2$(C≡CPh)] (7). A solution of **5** (16 mg, 0.0125 mmol) in 0.5 mL of benzene was irradiated with an UV lamp for 5 min. The completeness of the reaction was assured by disappearance of the ^{31}P NMR signals of **5**. The resulting solution was concentrated to 0.3 mL and was layered with pentane to give crystals of **6**. Yield: 16 mg (0.0125 mmol, 65%). Anal. Calcd for $C_{61}H_{54}OP_4W$: C, 65.96; H, 4.90. Found: C, 66.02; H, 5.01. IR (cm^{-1}): ν = 1793 (CO). ^{1}H NMR (200 MHz, THF-d_8): δ 17.3 (br), 13.3 (br), 8.1 (br), 7.1 (br), 6.0 (br), 5.6 (br), 5.4 (br), 0.0 (br).

[*trans*-W(CO)(dppe)$_2$(C≡CSnMe$_3$)] (8). An analogous procedure to that for **7** was followed using [*trans*-W(CO)(N_2)(dppe)$_2$] (50 mg, 0.048 mmol) and $Me_3SnC{\equiv}CSnMe_3$ (18.5 mg, 0.053 mmol). Yield: 30 mg (0.0251 mmol, 52%). Anal. Calcd for $C_{58}H_{58}OP_4SnW$: C, 58.17; H, 4.88. Found: C, 58.49; H, 4.86. IR (cm^{-1}): ν = 1756 (CO). ^{1}H NMR (200 MHz, THF-d_8): δ 13.8 (br), 8.2 (br), 7.0 (br), 6.1 (br), 5.7 (br), 5.2 (br), −1.3 (br).

[*trans*-W(CO)(dppe)$_2$(C≡CSiMe$_3$)] (9). [*trans*-W(CO)(N_2)-(dppe)$_2$] (100 mg, 0.096 mmol) and $Me_3SnC{\equiv}CSiMe_3$ (30 mg, 0.116 mmol) were placed in a Young-Schlenk tube in 6 mL of benzene. Three freeze−pump−thaw cycles was carried out to remove any dissolved nitrogen. The reaction mixture was heated under vacuum to 65 °C for 6 h. The freeze−pump−thaw cycles were repeated twice during the reaction. The resulting yellow solution was irradiated with an UV lamp for 5 min until the ^{31}P NMR signals of the vinylidene derivative disappeared. However, the vinylidene complex turned out to be unstable in this case, and irradiation was not required if the reaction was carried out overnight. Then the reaction mixture was concentrated to 1.5 mL *in vacuo* and layered with 10 mL of pentane. **7** crystallized as red prisms in 10 h. Yield: 50 mg (0.0452 mmol, 47%). Anal. Calcd for $C_{58}H_{58}OP_4SiW$: C, 62.93; H, 5.28. Found: C,

62.80; H, 5.13. IR (cm^{-1}): $\nu = 1756$ (CO). ^1H NMR (200 MHz, THF-d_8): δ 14.1 (br), 8.2 (br), 7.0 (br), 5.8 (br), 5.5 (br), 5.1 (br), 3.1 (br), 0.2 (br).

[*trans*-W(CO)(dppe)$_2$(C≡CC≡CH)][NBu$_4$] (10). A solution of **2** (20 mg, 0.01445 mmol) in 0.5 mL of THF-d_8 was mixed with a solution of $NBu_4F \cdot 3H_2O$ (11 mg, 0.035 mmol) in 0.5 mL of THF-d_8 in a Young-Schlenk tube at −50 °C. Then the reaction mixture was transferred to a precooled NMR spectrometer. The temperature was raised to room temperature in approximately 1 h. The resulting mixture was kept at room temperature for one more hour and evaporated *in vacuo*. The residue was then washed with toluene three times to give **10**. Yield: 8 mg (0.0061 mmol, 42%). (A satisfactory elemental analysis could not be obtained due to thermal instability of this complex.) IR (cm^{-1}): $\nu = 3300$ (≡CH), 2056 (C≡C), 1709 (CO). ^1H NMR (500 MHz, THF-d_8): δ 7.41 (br, 8H, C_6H_5), 7.26 (br, 8H, C_6H_5), 6.93−6.88 (m, 24H, C_6H_5), 3.21 (t, $J_{H-H} = 8.5$ Hz, 8H, NCH_2), 2.38 (m, 4H, CH_2), 2.19 (m, 4H, CH_2), 1.63 (pent, $J_{H-H} = 8$ Hz, 8H, NCH_2CH_2), 1.36 (hex, $J_{H-H} = 7.5$ Hz, 8H, $NCH_2CH_2CH_2$), 1.25 (s, 1H, CH), 1.01 (s, $J_{H-H} = 7$ Hz, 12H $NCH_2CH_2CH_2CH_2$). ^{31}P NMR (81 MHz, C_6D_6): δ 45 br. ^{13}C NMR (125 MHz, CD_2Cl_2): δ 213.1 (m, C_α), 141.7 (br, C_6H_5-ipso), 139.9 (br, C_6H_5-ipso), 135.5 (s, C_6H_5), 134.0 (s, C_6H_5), 129.4 (s, C_6H_5), 126.8 (s, C_6H_5), 86.5 (s, C_β) 36.0 (m, CH_2).

Acknowledgment. Funding from the Swiss National Science Foundation (SNSF) and from the University of Zürich are gratefully acknowledged.

Supporting Information Available: Details of preparation of $Me_3SnC{\equiv}CC{\equiv}CSnMe_3$, CV studies of **2** and **4**, thermal ellipsoid plot for **7**. This material is available free of charge via the Internet at http://pubs.acs.org.

$[W(CO)(dppe)_2]$ Cumulenylidene and Acetylide Complexes Accessed via Stannylated Acetylenes and Butadiynes

Sergey N. Semenov, Olivier Blacque, Thomas Fox, Koushik Venkatesan, and Heinz Berke *

Anorganisch-Chemisches Institut, Universität Zürich, Winterthurestrasse 190, CH-8057 Zürich, Switzerland

Supporting Information

- **Synthesis of $Me_3SnC{\equiv}CC{\equiv}CSnMe_3$**
- **Cyclic voltammetry study of 2**
- **Cyclic voltammetry study of 4**
- **Cyclic voltammetry study of 9**
- **Table S1. Crystallographic data for compounds 2, 3 and 6**
- **Table S2. Crystallographic data for compounds 7, 9 and 10**
- **Thermal ellipsoid plot of 7**

$Me_3SnC{\equiv}CC{\equiv}CSnMe_3$: The $Me_3SiC{\equiv}CC{\equiv}CSiMe_3$ (5.05 g, 26.0 mmol) was solved in 350 mL of dry THF and solution was cooled to -20 °C. A solution of MeLi·LiBr in Ether (38.1 mL, 1.5 M, 57.1 mmol, 2.2 eqv.) was added dropwise. A cooling bath was removed and reaction mixture was left for 4 hours. A white precipitate of Li_2C_4 was formed during this time. A solid Me_3SnCl (11.4 g, 57.1 mmol) was added to suspension of Li_2C_4 in THF and mixture was rotating at room temperature for 1 hour. THF was removed *in vacuo*. Solid residual was extracted by pentane and extract was twice recrystallized from it to give $Me_3SnC{\equiv}CC{\equiv}CSnMe_3$ (8.2 g, 21.9 mmol, 84 %) NMR ^1H (200 MHz, C_6D_6) δ = 0.03 (s, (d, satellite $^2J_{H\text{-}Sn}$ = 60.8 Hz), 18H, $Sn(CH_3)_3$).

Cyclic Voltammetry studies

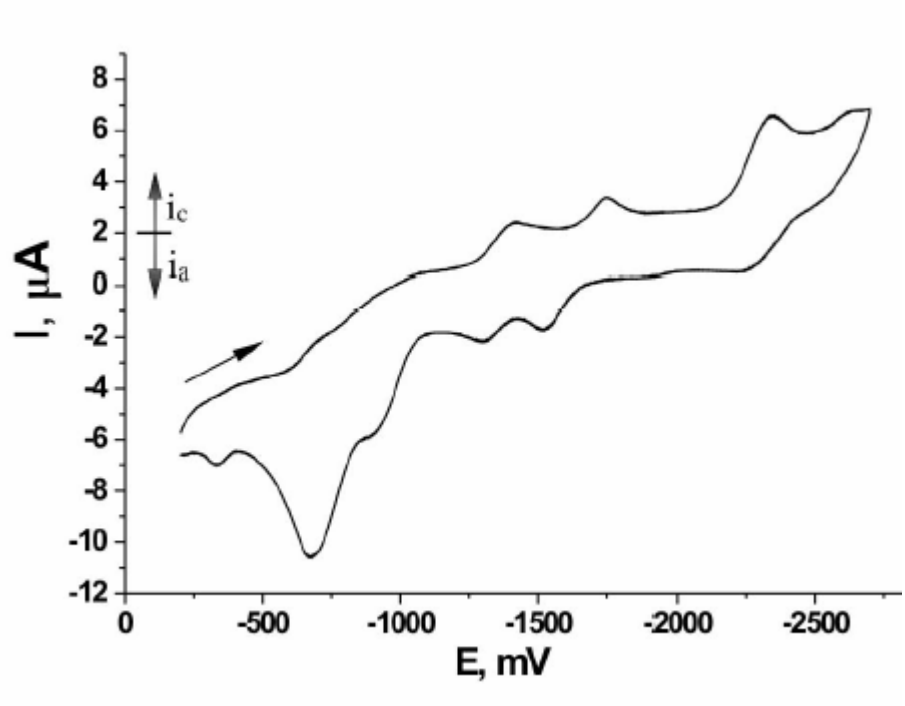

Figure 1S. Cyclic voltammogram for **2** in THF with 0.1M [nBu$_4$N][PF$_6$]; Au electrode; E *vs* $Fc^{0/+}$; scan rate = 100 mV/s; 20 ºC. Separate scans for reduction and oxidation parts show the same position of reduction and oxidation waves.

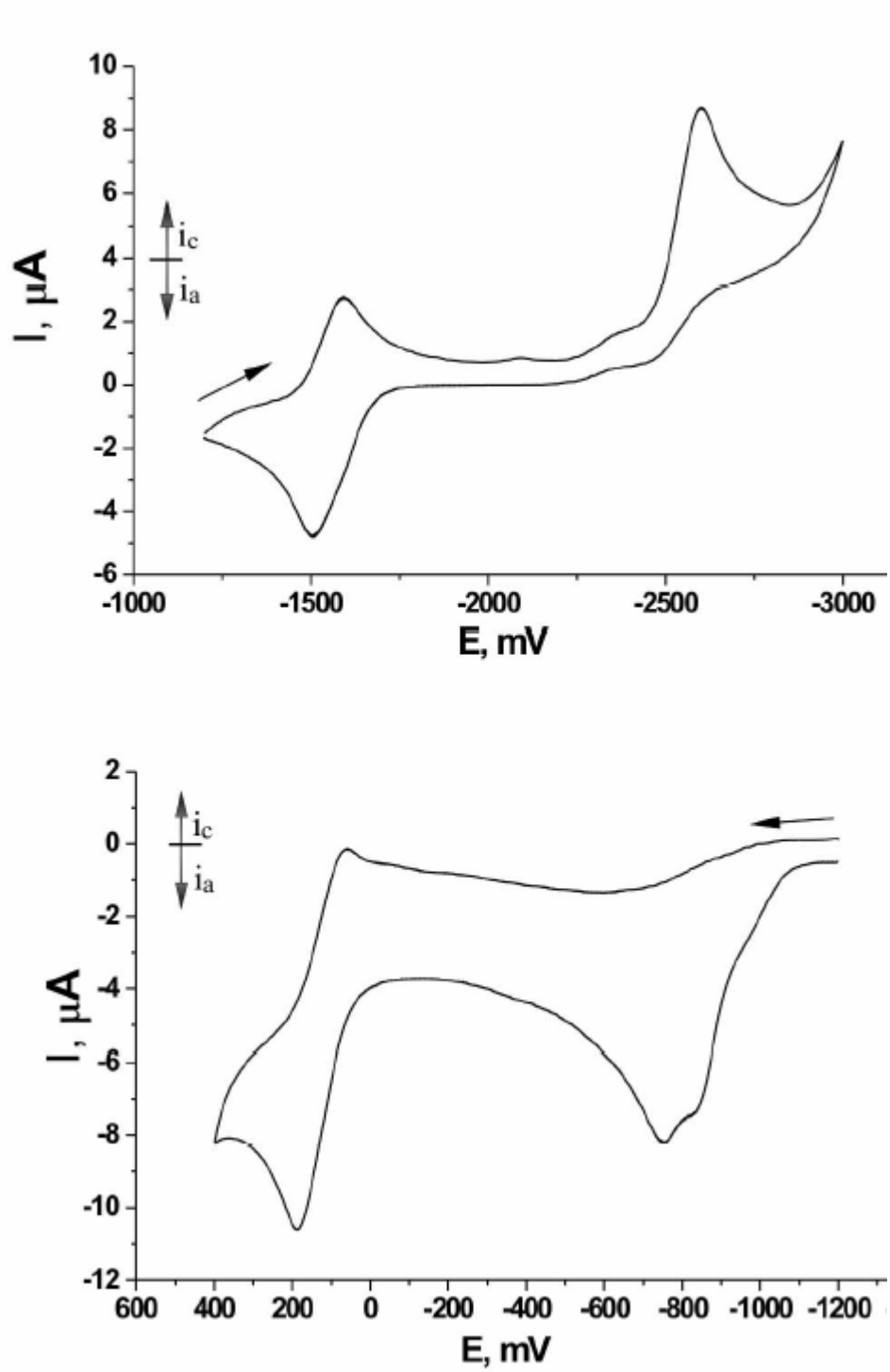

Figure 2S. Cyclic voltammograms for **3** with negative (top) and positive (bottom) direction of scanning in THF; 0.1 M [nBu$_4$N][PF$_6$]; Au electrode; E *vs* $Fc^{0/+}$; scan rate = 100 mV/s; 20 ºC.

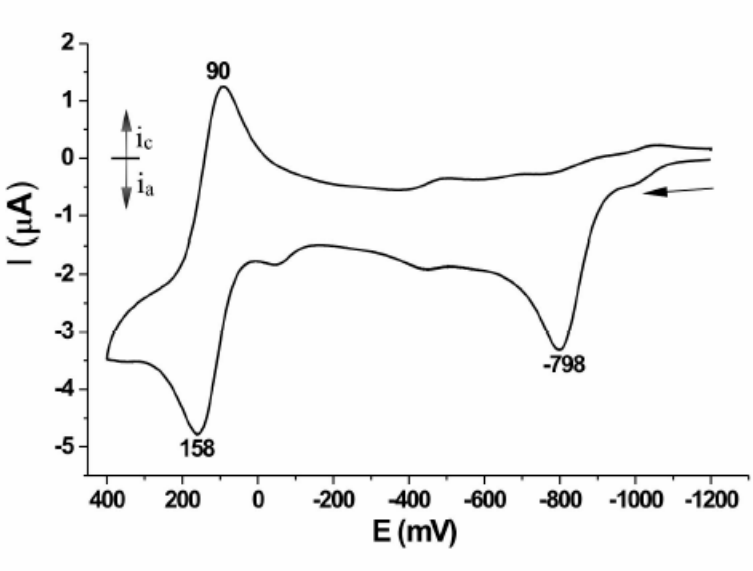

Figure 3S. Cyclic voltammograms for **9** with positive direction of scanning in THF; 0.1 M [nBu$_4$N][PF$_6$]; Au electrode; E *vs* $Fc^{0/+}$; scan rate = 100 mV/s; 20 ºC.

Table 1S. Crystallographic data for compounds **2**, **3** and **6**.

	2	**3**	**6**
empirical formula	$C_{63}H_{66}OP_4Sn_2W$, C_5H_{12}, C_6D_6	$4(C_{63}H_{66}OP_4SiSnW)$, $2.5(C_6H_{14})$, C_6H_6	$C_{61}H_{66}OP_4Sn_2W$, $0.5(C_6H_6)$
formula weight ($g \cdot mol^{-1}$)	1540.57	5468.26	1399.34
temperature (K)	183(2)	183(2)	183(2)
wavelength (Å)	0.71073	0.71073	0.71073
crystal system, space group	monoclinic, $P\,2_1/n$	triclinic, $P\,\bar{1}$	triclinic, $P\,\bar{1}$
a (Å)	21.0584(2)	12.3443(2)	12.0392(3)
b (Å)	12.32370(10)	16.1288(3)	12.1400(3)
c (Å)	26.7046(2)	34.9284(7)	21.6189(5)
α (deg)	90	88.543(1)	102.344(2)
β (deg)	96.937(1)	89.504(1)	102.127(2)
γ (deg)	90	85.639(1)	99.800(2)
volume ($Å^3$)	6879.58(10)	6931.7(2)	2940.26(13)
Z, density (calcd) ($Mg \cdot m^{-3}$)	4, 1.487	1, 1.293	2, 1.581
abs coefficient (mm^{-1})	2.523	2.165	2.943
$F(000)$	3080	2729	1390
crystal size (mm^3)	0.25 x 0.23 x 0.10	0.25 x 0.13 x 0.11	0.17 x 0.13 x 0.08
θ range (deg)	2.4 to 30.5	2.3 to 26.4	2.2 to 30.5
reflections collected	92407	73666	44093
reflections unique	20981 / [R_{int} = 0.0308]	28286 / [R_{int} = 0.0568]	17891 / [R_{int} = 0.0649]
completeness to θ (%)	99.9	99.7	99.6
absorption correction	analytical	analytical	analytical
max/min transmission	0.795 and 0.600	0.826 and 0.687	0.833 and 0.691
data / restraints / parameters	15920 / 6 / 720	16608 / 27 / 1319	12592 / 15 / 643
goodness-of-fit on F^2	1.036	0.999	0.977
final R_1 and wR_2 indices [$I > 2\sigma(I)$]	0.0292, 0.0763	0.0518, 0.1475	0.0481, 0.1036
R_1 and wR_2 indices (all data)	0.0460, 0.0816	0.0972, 0.1573	0.0777, 0.1100

Table 2S. Crystallographic data for compounds **7, 9** and **10**.

	7	**9**	**10**
empirical formula	$C_{61}H_{53}OP_4W$, $2(C_6H_6)$	$C_{58}H_{57}OP_4SiW$	$C_{57}H_{49}OP_4W$, $C_{16}H_{36}N$
formula weight ($g \cdot mol^{-1}$)	1265.97	1105.85	1300.14
temperature (K)	183(2)	183(2)	153(2)
wavelength (Å)	0.71073	0.71073	0.71073
crystal system, space group	triclinic, P -1	triclinic, P -1	triclinic, P -1
a (Å)	11.3842(1)	11.6878(2)	12.2029(9)
b (Å)	15.4538(2)	12.7924(1)	21.5463(9)
c (Å)	17.5602(2)	17.6224(3)	25.0892(12)
α (deg)	97.338(1)	87.9673(13)	77.567(4)
β (deg)	92.873(1)	78.0232(16)	88.606(5)
γ (deg)	104.678(1)	76.5809(13)	89.185(4)
volume ($Å^3$)	2953.08(6)	2506.87(7)	6439.8(6)
Z, density (calcd) ($Mg \cdot m^{-3}$)	2, 1.424	2, 1.465	4, 1.341
abs coefficient (mm^{-1})	2.110	2.496	1.937
F(000)	1290	1122	2688
crystal size (mm^3)	0.33 x 0.29 x 0.13	0.23 x 0.14 x 0.09	0.10 x 0.05 x 0.02
θ range (deg)	2.3 to 30.5	2.3 to 30.5	2.5 to 25.0
reflections collected	112621	66373	45824
reflections unique	18012 / [R_{int} = 0.0405]	15293 / [R_{int} = 0.0373]	22679 / [R_{int} = 0.1113]
completeness to θ (%)	99.9	99.8	99.9
absorption correction	analytical	analytical	analytical
max/min transmission	0.620 and 0.361	0.849 and 0.736	0.962 and 0.868
data / restraints / parameters	15558 / 0 / 712	12394 / 2 / 577	6076 / 511 / 1448
goodness-of-fit on F^2	1.029	1.014	0.619
final R_1 and wR_2 indices [$I > 2\sigma(I)$]	0.0260, 0.0650	0.0307, 0.0772	0.0531, 0.0574
R_1 and wR_2 indices (all data)	0.0334, 0.0684	0.0403, 0.0791	0.2276, 0.0747

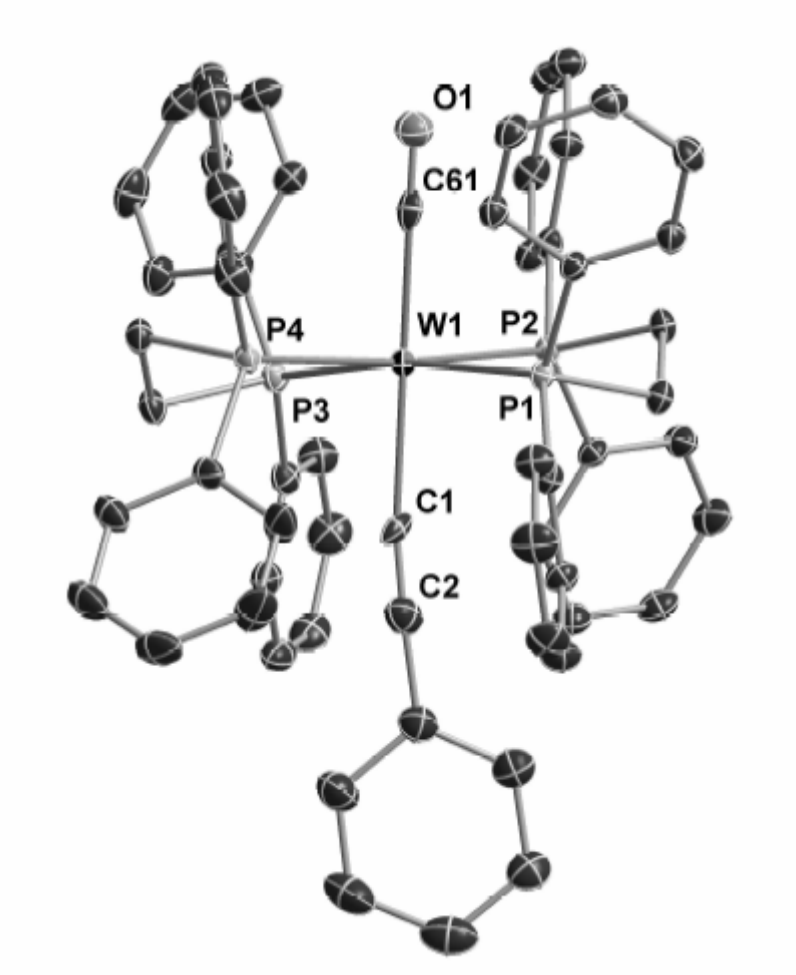

Figure 4S. Thermal ellipsoid plot of **7** (30% probability level). Hydrogen atoms and solvent molecules are omitted for clarity.

V. UNPUBLISHED RESULTS

V.1. Experimental part

V.1.1. General Procedures

All the manipulations were carried out under a nitrogen atmosphere using Schlenk techniques or a drybox. Reagent grade benzene, toluene, hexane, pentane, diethyl ether, and tetrahydrofuran were dried and distilled from sodium benzophenone ketyl prior to use. Dichloromethane and acetonitrile were distilled from CaH_2, and chloroform was dried by P_2O_5. Published procedures were used to prepare the following compounds: $[W(dppe)_2(CO)(N_2)]$,[195] $[I(dppe)_2WC_4W(dppe)_2I]$,[200] $[(OTf)(CO)_2(dppe)WC_4W(CO)_2(dppe)(OTf)]$[200] and $[(Me_3SnC_4)(dppe)_2W(C_4)W(dppe)_2(C_4SnMe_3)]$.[201] Compound *p*-$IC_6H_4SCOtBu$[202] was prepared by procedure analogous to *p*-$IC_6H_4SCOCH_3$.[203] All other chemicals were used as obtained from commercial suppliers. IR spectra were obtained on a Bio-Rad FTS-45 instrument and Bio-Rad Excalibur FTS-3500. NMR spectra were measured on a Varian Mercury spectrometer at 200 MHz for ^1H and 81 MHz for $^{31}P\{^1H\}$, Varian Gemini-2000 spectrometer at 300 MHz for ^1H and 75 MHz for $^{13}C\{^1H\}$, Bruker-AV2-400 spectrometer at 400 MHz for ^1H, 100.6 MHz for $^{13}C\{^1H\}$ and on a Bruker-DRX-500 and AV2-500 spectrometers at 500 MHz for ^1H, 125.8 MHz for $^{13}C\{^1H\}$ and 202.5 MHz for $^{31}P\{^1H\}$. Chemical shifts for ^1H and ^{13}C are given in ppm relative to TMS and those for ^{31}P relative to phosphoric acid. CHN elemental analyses were performed with a LECO CHN-932 microanalyzer.

V.1.2. Synthesis

$Me_3SiC{\equiv}CC{\equiv}C(p\text{-}C_6H_4SCOtBu)$. In a Schlenk flask *p*-$IC_6H_4SCOtBu$ (328 mg, 1 mmol), $Pd(PPh_3)_2Cl_2$ (36 mg, 0.05 mmol) and CuI (10 mg, 0.05 mmol) were mixed in triethylamine (4 mL). HC_4SiMe_3 (150 mg, 1.23 mmol) was added dropwise. The resulting solution was stirred for 12 h. A white fluffy solid precipitated during reaction. The solvent was removed *in vacuo* until the formation of an oily suspension. This residue was extracted with benzene, and the extract was filtered through celite. The solvent was evaporated *in vacuo*. The resulting mixture was chromatographed on silica gel (CH_2Cl_2/hexane 1:5). Recrystallization from hexane gave the pure compound $Me_3SiC{\equiv}CC{\equiv}C(p\text{-}C_6H_4SCOtBu)$. Yield: 212 mg (0.67 mmol, 67%) Anal. Calcd. for $C_{18}H_{22}OSSi$: C, 68.74; H, 7.05. Found: C, 68.55; H, 7.00. ^1H NMR (300 MHz, $CDCl_3$) δ = 7.50 (d, $^3J_{H\text{-}H}$ = 8.7 Hz, 2H, C_6H_4), 7.34 (d, $^3J_{H\text{-}H}$ = 8.1 Hz, 2H, C_6H_4), 1.34 (s, 9H, *t*Bu), 0.27 (s, 9H, $SiMe_3$); ^{13}C (125 MHz, C_6D_6) 201.8 (s, CO), 134.8 (s, C_6H_4), 133.0 (s, C_6H_4), 130.2 (s, ipso-C_6H_4), 122.1 (s, ipso-C_6H_4), 91.5 (s, C≡C), 88.8 (s, C≡C), 76.6 (s, C≡C), 76.3 (s, C≡C), 46.8 (s, $C(CH_3)_3$), 27.0 (s, $C(CH_3)_3$), -0.7 (s, $Si(CH_3)_3$).

HC≡CC≡C(*p*-$C_6H_4SCOtBu$). To a solution of $Me_3SiC{\equiv}CC{\equiv}C(p\text{-}C_6H_4SCOtBu)$ (200 mg, 0.64 mmol) in 1:1 MeOH/THF mixture (2 mL) a solution of CsF (60 mg, 0.79 mmol) in MeOH (1 ml) was added dropwise. The resulting solution was stirred for 1 h. After, the reaction mixture was evaporated and extracted with C_6H_6. The collected extracts were subjected to flash chromatography on silica gel (CH_2Cl_2/hexane 1:1). The first fraction obtained was pure $HC{\equiv}CC{\equiv}C(p\text{-}C_6H_4SCOtBu)$. Yield: 105 mg (0.67 mmol, 68%)[#] ^{1}H NMR (400 MHz, $CDCl_3$) δ = 7.53 (d, $^3J_{H\text{-}H}$ = 8.4 Hz, 2H, C_6H_4), 7.35 (d, $^3J_{H\text{-}H}$ = 8.4 Hz, 2H, C_6H_4), 2.55 (s, 1H, CH), 1.35 (s, 9H, *t*Bu); ^{13}C (100.6 MHz, $CDCl_3$) 203.6 (s, CO), 134.8 (s, C_6H_4), 133.1 (s, C_6H_4), 130.2 (s, ipso-C_6H_4), 121.8 (s, ipso-C_6H_4), 74.8 (s, C≡C), 74.6 (s, C≡C), 71.9 (s, C≡C), 68.0 (s, C≡C), 47.1 (s, $C(CH_3)_3$), 27.4 (s, $C(CH_3)_3$).

[#] Elemental analysis could not be carried out due to a too low stability of compound

$Me_3SnC{\equiv}CC{\equiv}C(p\text{-}C_6H_4SCOtBu)$. To a solution of $HC{\equiv}CC{\equiv}C(p\text{-}C_6H_4SCOtBu)$ (100 mg, 0.41 mmol) in THF (1 mL), a solution of Me_3SnNEt_2 (55 mg, 0.79) in THF (1 mL) was added dropwise at -30 °C. The resulting solution was stirred for 3 h at room temperature. After, the mixture was evaporated and extracted with pentane. Recrystallization from pentane gave the pure compound $Me_3SnC{\equiv}CC{\equiv}C(p\text{-}C_6H_4SCOtBu)$. Yield: 124 mg (0.31 mmol, 75%) Anal. Calcd. for $C_{18}H_{22}OSSn$: C, 53.36; H, 5.47. Found: C, 53.57; H, 5.43. ^{1}H NMR (300 MHz, C_6D_6) δ = 7.19 (d, $^3J_{H\text{-}H}$ = 8.1 Hz, 2H, C_6H_4), 7.09 (d, $^3J_{H\text{-}H}$ = 8.4 Hz, 2H, C_6H_4), 1.12 (s, 9H, *t*Bu), 0.11 (s, (d, satellite, $^2J_{H\text{-}Sn}$ = 60 Hz), 9H, $Sn(CH_3)_3$); ^{13}C (125 MHz, C_6D_6) 201.8 (s, CO), 134.8 (s, C_6H_4), 133.1 (s, C_6H_4), 129.8 (s, ipso-C_6H_4), 122.6 (s, ipso-C_6H_4), 93.3 (s, C≡C), 92.1 (s, C≡C), 76.8 (s, C≡C), 73.9 (s, C≡C), 46.8 (s, $C(CH_3)_3$), 27.0 (s, $C(CH_3)_3$), -8.4 (s, (d, satellite, $^1J_{C\text{-}Sn}$ = 384 Hz), $Sn(CH_3)_3$).

[*cis*-$W(CO)(dppe)_2${C=C=C=C(SnMe$_3$)(*p*-$C_6H_4SCOtBu$)}] (1). [*trans*-$W(CO)(N_2)(dppe)_2$] (150 mg, 0.145 mmol) and $Me_3SnC{\equiv}CC{\equiv}C(p\text{-}C_6H_4SCOtBu)$ (70 mg, 0.174 mmol) were placed in an Young-Schlenk tube in 15 mL benzene. Three freeze-pump-thaw cycles were performed on the resulting solution to remove any dissolved nitrogen. The reaction mixture was heated under vacuum at 55 ºC for 6 h. The resulting dark-red-violet solution was concentrated to 1.5 mL *in vacuo* and layered with 10 mL of pentane. Complex **1** formed as red-violet powder in 10 h. Yield: 161 mg (0.114 mmol, 79%). Anal. Calcd. for $C_{71}H_{71}O_2P_4SSnW$: C, 60.27; H, 5.06. Found: C, 60.50; H, 5.05. IR (cm^{-1}): ν = 1812 (CO), 1941 (C_4), 1695 (CO*t*Bu). NMR ^{1}H (500 MHz, C_6D_6) δ = 8.54 (m, 4H, C_6H_5), 8.75 (t, $J_{H\text{-}H}$ = 8.1 Hz, 2H, C_6H_5), 7.64 (d, $J_{H\text{-}H}$ = 7.6 Hz, 2H, C_6H_4), 7.48 (m, 4H, C_6H_5 + C_6H_4), 7.38 – 6.81 (m, 22H, C_6H_5), 6.74 (m, 4H, C_6H_5), 6.65 (t, $J_{H\text{-}H}$ = 7.3 Hz, 2H, C_6H_5), 6.53 (t, $J_{H\text{-}H}$ = 8.0 Hz, 2H, C_6H_5), 6.13 (t, $J_{H\text{-}H}$ = 7.9 Hz, 2H, C_6H_5), 2.99 (m, 2H, CH_2), 2.43 (m, 2H, CH_2), 2.12 (m, 3H, CH_2), 1.76 (m, 1H, CH_2), 1.30 (s, 9H, $C(CH_3)_3$), 0.39 (s, (d, satellite, $^2J_{H\text{-}Sn}$ = 52 Hz), 9H, $Sn(CH_3)_3$); ^{31}P (81 MHz, C_6D_6) δ = 48.8

(m, 1P), 44.9 (m, 1P), 30.0 (m, 1P), 26.8 (m, 1P); ^{13}C (125 MHz, C_6D_6)$^{\#}$ δ = 266.8 (m, C_α), 222.2 (d, $^2J_{C\text{-}P}$ = 31 Hz, CO), 203.8 (s, *C*O*t*Bu), 142.7 (s, C_6H_5), 142.5 (s, C_6H_5), 141.0 (s, C_6H_5), 140.8 (s, C_6H_5), 140.2 (s, C_6H_5), 139.7 (s, C_β), 139.3 (s, C_6H_5), 139.1 (s, C_6H_5), 138.9 (s, C_6H_5), 138.8 (s, C_6H_5), 138.4 (s, C_6H_5), 138.2 (m, C_6H_5), 136.8 (dd, $^1J_{C\text{-}P}$ = 31 Hz, $J_{C\text{-}P}$ = 5 Hz, ipso-C_6H_5), 136.4 (d, $^1J_{C\text{-}P}$ = 29 Hz, ipso-C_6H_5), 135.3 (s, C_6H_5), 135.1 (s, C_6H_5), 134.1 (d, $^1J_{C\text{-}P}$ = 12 Hz, C_6H_5), 133.9 (d, $^1J_{C\text{-}P}$ = 11 Hz, C_6H_5), 133.2 (d, $^1J_{C\text{-}P}$ = 12 Hz, C_6H_5), 132.8 (d, $^1J_{C\text{-}P}$ = 9 Hz, C_6H_5), 132.6 (s, C_6H_5), 132.5 (s, C_6H_5), 132.4 (s, C_6H_5), 132.3 (s, C_6H_5), 132.2 (d, $^1J_{C\text{-}P}$ = 11 Hz, C_6H_5), 132.0 (s, C_6H_5), 131.5 (s, C_6H_5), 131.4 (s, C_6H_5), 131.3 (s, C_6H_5), 131.2 (s, C_6H_5), 129.9 (s, C_6H_5), 129.7 (s, C_6H_5), 129.5 (s, C_6H_5), 129.4 (s, C_6H_5), 128.7 (s, C_6H_5), 128.6 (s, C_6H_5), 128.5 (s, C_6H_5), 128.4 (s, C_6H_5), 128.3 (s, C_6H_5), 127.3 (s, C_6H_5), 125.6 (s, C_6H_5), 119.7 (s, C_6H_5), 74.0 (s, C_δ), 71.2 (s, C_γ), 31.6 (m, CH_2), 29.4 (m, CH_2), 27.8 (m, CH_2), -8.0 (s, (d, satellite, $^1J_{C\text{-}Sn}$ = 322 Hz), CH_3).

* N = 2 for *ortho* carbons, 3 for *meta* carbons, 4 for *para* carbons.

$^{\#}$ - The differentiation of C_6H_5 and C_6H_4 signals was not possible in this case.

[*cis*-W(CO)(dppe)$_2${C=C=C=C(H)(*p*-C$_6$H$_4$SCO*t*Bu)}] (2). To a THF solution (2 mL) of **1** (40 mg, 0.028 mmol), a 1% solution of water in THF (60 μL) was added. The reaction mixture was stirred for 3 h at room temperature. Conversion was monitored by ^{1}H NMR. The resulting dark-red-violet solution was evaporated to dryness *in vacuo* and extracted with 8 mL of Et_2O. The resulting solution was filtered, concentrated to 1 mL and 8 mL of pentane was added to give **2** as red-violet powder. Yield: 21 mg (0.017 mmol, 61%).$^{\#}$ ^{1}H NMR (200 MHz, C_6D_6) δ = 8.42 – 8.23 (m, 3H, C_6H_5), 7.68 – 6.40 (m, 41H, C_6H_5), 3.74 (pent, $^6J_{H\text{-}P}$ = 4Hz, 1H, =C*H*(p-C_6H_4*t*Bu)), 2.90 – 1.90 (m, 8H, CH_2), 1.18 (s, 9H, *t*Bu); ^{31}P (81 MHz, C_6D_6) δ = 47.6 (m, 1P), 43.7 (m, 1P), 25.2 (m, 1P), 24.6 (m, 1P);

$^{\#}$ Elemental analysis and ^{13}C NMR could not be carried out due to a too low stability of compound

* N = 2 for *orto* carbons, 3 for *meta* carbons, 4 for *para* carbons.

[{*trans*-W(CO)(dppe)$_2$(C≡C−C{=C(H)(*p*-C$_6$H$_4$SCO*t*Bu)})}$_2$] (3). **2** (20 mg, 0.017 mmol) was dissolved in 1 mL of benzene and placed into test-tube. This solution was layered with 5 mL of pentane. The brown crystals of **3** were formed in 24 h. They were washed with benzene and dried *in vacuo* to give pure **3**. Yield: 10 mg (0.004 mmol, 50%). Anal. Calcd. for $C_{136}H_{126}O_4P_8S_2W_2$: C, 65.23; H, 5.07. Found: C, 65.52; H, 5.14. IR (cm^{-1}): ν = 1782 (CO), 1695 (CO*t*Bu). ^{1}H NMR (200 MHz, C_6D_6) δ = 13.87 (br), 12.25 (br), 8.65 (br), 7.91 (br), 6.93 (br), 6.01 (br), 5.70 (br), 2.30 (s, *t*Bu), -6.12 (br, C_6H_5).

[(PhC$_2$)(dppe)$_2$W(C$_4$)W(dppe)$_2$(C$_2$Ph)] (4) The crystalline [I(dppe)$_2$WC$_4$W(dppe)$_2$I] is sparingly soluble in THF and the following procedure was performed to improve its solubility.

[I(dppe)$_2$WC$_4$W(dppe)$_2$I] (200 mg, 0.088 mmol) was dissolved in approximately 20 mL of CH_2Cl_2. This solution was evaporated to dryness in *vacuo* and the residue was dissolved in 5 mL of benzene. The benzene solution was freeze-dried. Amorphous [I(dppe)$_2$WC$_4$W(dppe)$_2$I] (50 mg, 0.022 mmol) was then dissolved in 7.5 mL of THF and mixed with a solution of LiC_2Ph (14.3 mg, 0.133 mmol) in 5 mL of THF. A solution of TlOTf (52 mg, 0.148 mmol) in 7.5 mL of THF was added dropwise to the reaction mixture. The solution turned cloudy at the end of the addition. The reaction was stirred for 6 h at room temperature. The resulting green-yellow solution was evaporated to dryness *in vacuo*. Solid residue was extracted with benzene (3 × 2.5 mL), filtered and again dried *in vacuo*. Resulting mixture was flash chromatographed on Al_2O_3 with benzene as eluent. The first dark green fraction was collected and evaporated. Recrystallization from a mixture of Et_2O and toluene gave crystals of **4** in a few minutes. They were separated from solution and washed with two portions (1 × 1 mL) of Et_2O. Single crystals suitable for X-Ray diffraction were grown by layering acetonitrile over benzene solution of **4**. Yield (23 mg, 0.0106 mmol, 48%) Anal. Calcd. for $C_{126}H_{106}P_8W_2$: C, 67.69; H, 4.78. Found: C, 67.17; H, 4.74. IR (cm^{-1}): ν = 2049 (C≡C). ^{1}H NMR (200 MHz, C_6D_6): δ = 8.12 (br, 16H, C_6H_5), 6.90 (m, 70H, C_6H_5), 6.40 (m, 4H, C_6H_5), 2.83 (br, 8H, CH_2), 2.12 (m, 8H, CH_2). ^{31}P NMR (81 MHz, C_6D_6): δ = 50.4 (s, (d, satellite, $^1J_{P\text{-}W}$ = 267 Hz)); ^{13}C NMR (125 MHz, C_6D_6) δ = 222.1 (m, C_α (WC_4W chain)), 141.2 (m, ipso – C_6H_5), 139.7 (m, ipso – C_6H_5), 137.4 (m, C_α (WC_2Ph)), 135.1 (s, C_6H_5), 133.7 (s, C_6H_5), 133.2 (s, C_6H_5), 120.9 (s, C_6H_5), 129.0 (s, C_6H_5), 128.4 (s, C_6H_5), 127.0 (s, C_6H_5), 124.4 (s, C_6H_5), 119.8 (s, C_β (WC_2Ph)), 92.0 (s, C_β (WC_4W chain)), 35.5 (m, CH_2).

[(Me_3SiC_2)(dppe)$_2$W(C_4)W(dppe)$_2$(C_2SiMe_3)] (5) 5 was obtained analogous to **4** using [I(dppe)$_2$WC$_4$W(dppe)$_2$I] (50 mg, 0.022 mmol) in 7.5 mL of THF, LiC_2SiMe_3 (13.8 mg, 0.133 mmol) in 5 mL of THF and TlOTf (52 mg, 0.148 mmol) in 7.5 ml of THF. The first green fraction eluted with benzene is the desired product. Addition of THF to the eluent allows separation of the second compound, the asymmetrically substituted product. Single crystals suitable for X-Ray diffraction were grown by layering benzene solution with acetonitrile. Yield (22 mg, 0.010 mmol, 45%) Anal. Calcd. for $C_{118}H_{114}P_8Si_2W_2$: C, 64.31; H, 5.21. Found: C, 64.70; H, 5.24. IR (cm^{-1}): ν = 1986 (C≡C). ^{1}H NMR (500 MHz, C_6D_6): δ = 8.02 (br, 16H, C_6H_5), 7.00 (m, 48H, C_6H_5), 6.90 (br, 16H, C_6H_5), 2.86 (m, 8H, CH_2), 2.08 (m, 8H, CH_2), -0.20 (s, 18H, $Si(CH_3)_3$). ^{31}P NMR (81 MHz, C_6D_6): δ = 49.8 (s, (d, satellite, $^1J_{P\text{-}W}$ = 269 Hz)); ^{13}C NMR (125 MHz, C_6D_6)* δ = 161.4 (m, C_α (WC_2Si)), 141.5 (m, C_6H_5 – ipso), 140.1 (m, C_6H_5 – ipso), 135.1 (s, C_6H_5), 133.7 (s, C_6H_5), 129.0 (s, C_6H_5), 127.1 (s, C_6H_5), 125.0 (s, C_β (WC_2Si chain)), 91.0 (s, C_β (WC_4W chain)), 35.5 (m, CH_2), 1.2 (s, $Si(CH_3)_3$).

* - the signal for C_α of the WC_4W chain could not be observed due to low solubility of the compound.

[(*t*BuCOSC$_6$H$_4$C$_4$)(dppe)$_2$W(C$_4$)W(dppe)$_2$(C$_4$C$_6$H$_4$SCO*t*Bu)] (6) A mixture of [(Me$_3$SnC$_4$)(dppe)$_2$W(C$_4$)W(dppe)$_2$(C$_4$SnMe$_3$)] (20 mg, 0.0082 mmol), *p*-IC$_6$H$_4$SCO*t*Bu (7 mg, 0.021 mmol) and [Pd(PPh$_3$)$_4$] (1 mg) in 0.5 mL of THF was placed into a Young-Schlenk tube. The reaction mixture was heated at 60 ^{o}C for 48 h and after the solvent was removed in *vacuo*. The solid residue was recrystallized from Et$_2$O to give **6**. Yield (16 mg, 0.0064 mmol, 78%) Anal. Calcd. for $C_{138}H_{122}O_2P_8S_2W_2$: C, 66.51; H, 4.93. Found: C, 66.30; H, 4.87. IR (cm^{-1}): ν = 2152 (C≡C), 1691 (CO*t*Bu). ^{1}H NMR (200 MHz, C_6D_6): δ = 8.09 (br, 16H, C_6H_5), 7.38 (d, $^3J_{H-H}$ = 8.6 Hz, 4H, C_6H_4), 7.27 (d, $^3J_{H-H}$ = 8.6 Hz, 4H, C_6H_4), 7.01 (m, 48H, C_6H_5), 6.90 (br, 16H, C_6H_5), 2.82 (m, 8H, CH_2), 2.10 (m, 8H, CH_2), 1.13 (s, 18H, C(CH$_3$)$_3$). ^{31}P NMR (81 MHz, C_6D_6): δ = 50.7 (s, (d, satellite, $^1J_{P-W}$ = 273 Hz)); ^{13}C NMR (125 MHz, C_6D_6) δ = 223.9 (m, C_α (WC_4W chain)), 202.4 (s, CO), 145.6 (m, C_α $WC_4C_6H_4$ chain), 140.1 (m, C_6H_5 – ipso), 139.1 (m, C_6H_5 – ipso), 135.0 (s, C_6H_5), 133.1 (s, C_6H_5), 132.6 (s, C_6H_4), 129.1 (s, C_6H_4), 127.1 (s, C_6H_5), 103.8 (s, C_β ($WC_4C_6H_4$ chain)), 91.8 (s, C_β (WC_4W chain)), 81.5 (s, C_γ ($WC_4C_6H_4$ chain)), 68.2 (s, C_δ ($WC_4C_6H_4$ chain)), 46.7 (s, *C*(CH$_3$)$_3$), 35.6 (m, CH_2), 27.1 (s, C(*C*H$_3$)$_3$).

[HW(dppe)$_2$(C$_4$)(dppe)$_2$WH] (7). To a solution of [I(dppe)$_2$WC$_4$W(dppe)$_2$I] (50 mg, 0.022 mmol) in 2.5 mL of THF, 25 μL of 1M solution of Na[BHEt$_3$] in THF was added. The reaction mixture was placed into Young-Schlenk tube and heated at 60 ºC for 1 day. The solvent was removed *in vacuo*. Further 1 mL of benzene was added and freeze dried. The residue was extracted with benzene and was evaporated *in vacuo*. The residue was dissolved in 2 mL of ether and left for 1 day to give green crystals of **7**. Single crystals suitable for X-Ray diffraction were grown by layering a benzene solution with pentane. Yield: 30 mg (0.0149 mmol, 68%). Anal. Calcd. for $C_{108}H_{98}P_8W_2$: C, 64.46; H, 4.91. Found: C, 64.36; H, 4.99. IR (cm^{-1}): ν = 1552 (W–H). ^{1}H NMR (200 MHz, CD_2Cl_2): δ = 7.81 (br, 15H, C_6H_5), 7.23 – 6.75 (m, 65H, C_6H_5), 2.71 – 2.63 (m, 16H, CH_2), -3.79 (pent, 2H, $^2J_{P-H}$ = 28.5 Hz, WH). ^{31}P NMR (81 MHz, C_6D_6): δ = 61.66 ($^1J_{W-P}$ = 278Hz). ^{13}C (125MHz, C_6D_6) δ = 228.9 (m, C_α), 141.7 – 141.6 (m, C_6H_5 – ipso), 134.0 (m, C_6H_5), 133.3 (m, C_6H_5), 128.5 (s, C_6H_5), 127.4 (s, C_6H_5), 92.6 (s, C_β) 37.2 (pent, J_{C-P} = 10.1 Hz, CH_2).

[(PhC$_2$)(CO)$_2$(dppe)WC$_4$W(CO)$_2$(dppe)(C$_2$Ph)](C$_6$H$_6$) (8). 8 mL of a THF solution of LiC$_2$Ph (5.5 mg, 0.051 mmol) were added dropwise to a solution of [(OTf)(CO)$_2$(dppe)WC$_4$W(CO)$_2$(dppe)(OTf)] (40 mg, 0.0246 mmol) in 15 ml of THF at -10 ºC. After stirring the reaction mixture for 20 min, the resulting brown-green solution was evaporated to dryness *in vacuo*. The residue was extracted with benzene frizzed-dried and again extracted with benzene to completely remove LiOTf. Crystallization from benzene/pentane afforded the

desired product. Yield: 12 mg (0.008 mmol, 30%). Single crystals suitable for X-Ray diffraction were grown by layering a benzene solution with pentane. Anal. Calcd. for $C_{82}H_{68}O_4P_4W_2$: C, 61.21; H, 4.26. Found: C, 60.80; H, 4.15. IR (cm^{-1}): 1997 (C≡C), 1974 (CO), 1914 (CO). NMR: ^1H (500 MHz, C_6D_6) δ = 7.87 (t, $^3J_{H-H}$ = 9.0 Hz, 12H, C_6H_5), 7.25 – 7.02 (m, 34H, C_6H_5) 6.95 (d, $^3J_{H-H}$ = 7.0 Hz, 4H, C_6H_5), 2.70 (m, 4H, CH_2), 2.25 (m, 4H, CH_2); ^{31}P (81 MHz, C_6D_6) δ = 37.8 (s, $^1J_{W-P}$ (d, satellite) = 228 Hz); ^{13}C (125 MHz, C_6D_6) δ = 233.7 (t, $^2J_{C-P}$ = 10.0 Hz, C_α WC_4W), 215.8 (dd, $^2J_{C-P(cis)}$ = 6.0 Hz, $^2J_{C-P(trans)}$ = 36.5 Hz, CO), 135.2 (d, $^1J_{C-P}$ = 37.9 Hz, ipso-C_6H_5), 135.0 (d, $^1J_{C-P}$ = 42.7 Hz, ipso–C_6H_5), 133.4 (d, J_{C-P} = 12.3 Hz, C_6H_5), 132.8 (d, J_{C-P} = 12.1 Hz, C_6H_5), 131.5 (s, C_6H_5), 130.5 (s, C_6H_5), 129.8 (s, C_6H_5), 129.1 (s, C_6H_5), 128.5 (d, J_{C-P} = 9.8 Hz, C_6H_5), 125.7 (s, C_6H_5), 125.5 (s, C_6H_5), 121.5 (t, $^3J_{C-P}$ = 3.0 Hz, C_β WC_2Ph), 120.6 (t, $^2J_{C-P}$ = 15.0 Hz, C_α WC_2Ph), 93.2 (t, $^3J_{C-P}$ = 4.0 Hz, C_β WC_4W) 28.7 (dd, $^1J_{C-P}$ = 28.1 Hz, $^2J_{C-P}$ = 12.8 Hz, CH_2).

V.1.3. X-Ray Diffraction Studies on 4, 5, 7 and 8

Data collection for crystals of **4, 5, 7** and **8** were carried out on Oxford Diffraction Xcalibur R diffractometer (4-circle kappa platform, Ruby CCD detector and a single wavelength Enhance X-ray source with MoK_α radiation, λ = 0.71073 Å) at 183(2) K using a cold N_2-gas stream from an Oxford Cryogenic System. Pre-experiment, data collection and data reduction (unit cell determination, intensity data integration and empirical absorption correction) were carried out with the Oxford *CrysAlisPro* software.[204] The structures were solved with the unique data sets using the Patterson method of the program SHELXS-97. The structure refinement was performed with the program SHELXL-97.[205] Non-hydrogen atoms were refined anisotropically by full-matrix least-squares techniques based on F^2. The hydrogen atoms of the organic groups were placed in calculated positions and refined with a riding model with a fixed temperature factor. The program PLATON[206] was used to check the result of the X-ray analysis. Further details on all structures are provided in Tables 5 and 6.

Table 5.

Summary of the X-ray diffraction studies of compounds **4** and **5**.

	4	**5**
empirical formula	$C_{124}H_{106}P_8W_2$	$C_{118}H_{114}P_8Si_2W_2$ 3(C_6H_6)
formula weight ($g \cdot mol^{-1}$)	2211.54	2438.04
temperature (K)	183(2)	183(2)
wavelength (Å)	0.71073	0.71073
crystal system, space group	monoclinic, *P* 2/c	hexagonal, *R* -3c
a (Å)	20.1611(2)	33.8349(1)
b (Å)	13.5663(1)	33.8349(1)

c (Å)	20.688(2)	55.0814(2)
α (deg)	90	90
β (deg)	116.399(1)	90
γ (deg)	90	120
volume ($Å^3$)	5068.4(5)	54609.2(3)
Z, density (calcd) ($Mg·m^{-3}$)	2, 1.449	18, 1.334
abs coefficient (mm^{-1})	2.45	2.068
F(000)	2236	22392
crystal size (mm^3)	0.32 x 0.18 x 0.14	0.40 x 0.31 x 0.23
θ range (deg)	2.3 to 30.5	2.3 to 30.9
reflections collected	101834	332261
reflections unique	15486 [R(int) = 0.080]	15062 [R(int) = 0.056]
completeness to θ (%)	99.9	100.0
absorption correction	analytical	analytical
max/min transmission	0.73 and 0.56	0.79 and 0.54
data / restraints / parameters	15486 / 0 / 604	15062 / 4 / 628
goodness-of-fit on F^2	0.993	1.066
final R_1 and wR_2 indices [$I > 2\sigma(I)$]	0.0335, 0.0849	0.0239, 0.0617
R_1 and wR_2 indices (all data)	0.0477, 0.0889	0.0326, 0.0639
Largest diff. peak and hole (e. $Å^{-3}$)	2.08 / -1.07	1.38 / -0.77

Table 6.

Summary of the X-ray diffraction studies of compounds **7** and **8**.

	7	**8**
empirical formula	$C_{108}H_{98}P_8W_2$	$C_{85}H_{67}O_4P_4W_2$
formula weight ($g·mol^{-1}$)	2011.31	1643.95
temperature (K)	183(2)	183(2)
wavelength (Å)	0.71073	0.71073
crystal system, space group	monoclinic, P 2_1/c	triclinic, P-1
a (Å)	22.7140(1)	12.3979(2)
b (Å)	15.0726(1)	14.7025(3)
c (Å)	27.6260(2)	20.0589(4)
α (deg)	90	96.095(2)
β (deg)	104.692(1)	92.243(2)
γ (deg)	90	100.534(2)
volume ($Å^3$)	9148.8(1)	3568.0(1)
Z, density (calcd) ($Mg·m^{-3}$)	4, 1.460	2, 1.530
abs coefficient (mm^{-1})	2.701	3.363
F(000)	4056	1634

crystal size (mm^3)	0.37 x 0.27 x 0.16	0.17 x 0.08 x 0.07
θ range (deg)	2.3 to 32.6	2.3 to 29.4
reflections collected	185373	38601
reflections unique	33324 [R(int) = 0.0469]	14576 [R(int) = 0.0410]
completeness to θ (%)	100.0	99.8
absorption correction	analytical	multi-scan
max/min transmission	0.710 and 0.510	0.599 and 0.799
data / restraints / parameters	33324 / 0 / 1069	14576 / 22 / 819
goodness-of-fit on F^2	0.972	0.918
final R_1 and wR_2 indices [$I > 2\sigma(I)$]	0.0248, 0.0536	0.0352, 0.0772
R_1 and wR_2 indices (all data)	0.0382, 0.0553	0.0595, 0.0851
Largest diff. peak and hole (e. $Å^{-3}$)	1.95 / -0.69	4.26 / -1.00

V.2. Results and discussion

V.2.1. A cross–conjugated system formula possessing anchor groups

We thought to obtain a cross-conjugated molecule equipped with anchor groups using dimerization of butatrienylidenes developed by our group recently.[207] A subsequent stannylated butadiyne derivative was obtained by a sequence of Sonogashira coupling, deprotection and stannylation (Scheme 1). The usage of CsF in MeOH in the deprotection step is important to avoid hydrolysis of the thioester group. The Et_2NSnMe_3 was used for the stannylation step because the lithiation can't be performed in presence of thioester group.

Scheme 1. Synthesis of $Me_3SnC{\equiv}CC{\equiv}C(p\text{-}C_6H_4SCOtBu)$.

The ligand reacted with [*trans*-W(dppe)$_2$(CO)(N$_2$)] analogous to $Me_3SnC{\equiv}CC{\equiv}C(p\text{-}C_6H_4tBu)$ and formed the butatrienylidene **[*cis*-W(CO)(dppe)$_2${C=C=C=C(SnMe$_3$)(*p*-C$_6$H$_4$SCO*t*Bu)}] (1)** in 79% yield (Scheme 2). It should be mentioned that the presence of potentially reactive thioester group didn't cause any complications during this step. The structure was confirmed by spectroscopic methods and elemental analysis. The ^{31}P NMR spectrum is analogous to the C_6H_4tBu substituted complex and indicates *cis* configuration of dppe ligands. The ^{13}C NMR spectrum is very similar to the **[*cis*-W(CO)(dppe)$_2${C=C=C=C(SnMe$_3$)(*p*-C$_6$H$_4$*t*Bu)}]**. For **1**, typical ν(C≡O) vibrations are observed at 1812 cm^{-1} and $\nu(C_4)$ can be seen at 1941 cm^{-1}. The signal at 1695 cm^{-1} was assigned to thioester ν(C=O) vibration. **1** was deprotected with 1% THF solution of water. The reaction was slightly faster than for the tertbutylphenyl derivative. The resulting derivative **[*cis*-W(CO)(dppe)$_2${C=C=C=C(H)(*p*-C$_6$H$_4$SCO*t*Bu)}] (2)** was

characterized only spectroscopically since the compound was not completely stable and was only an intermediate product in the synthesis of the dimeric molecule. The dimerization of **2** was completely analogous to those of C_6H_4tBu substituted butatrienylidene. It gave the dimer **[{*trans*-W(CO)(dppe)$_2$(C≡C−C{=C(H)(*p*-C$_6$H$_4$SCO*t*Bu)})}$_2$] (3)** in about 50% yield as a brown-red powder. This paramagnetic compound has ^{1}H NMR spectrum analogous to **[{*trans*-W(CO)(dppe)$_2$(C≡C−C{=C(H)(*p*-C$_6$H$_4$*t*Bu)})}$_2$]** confirming structural similarity.

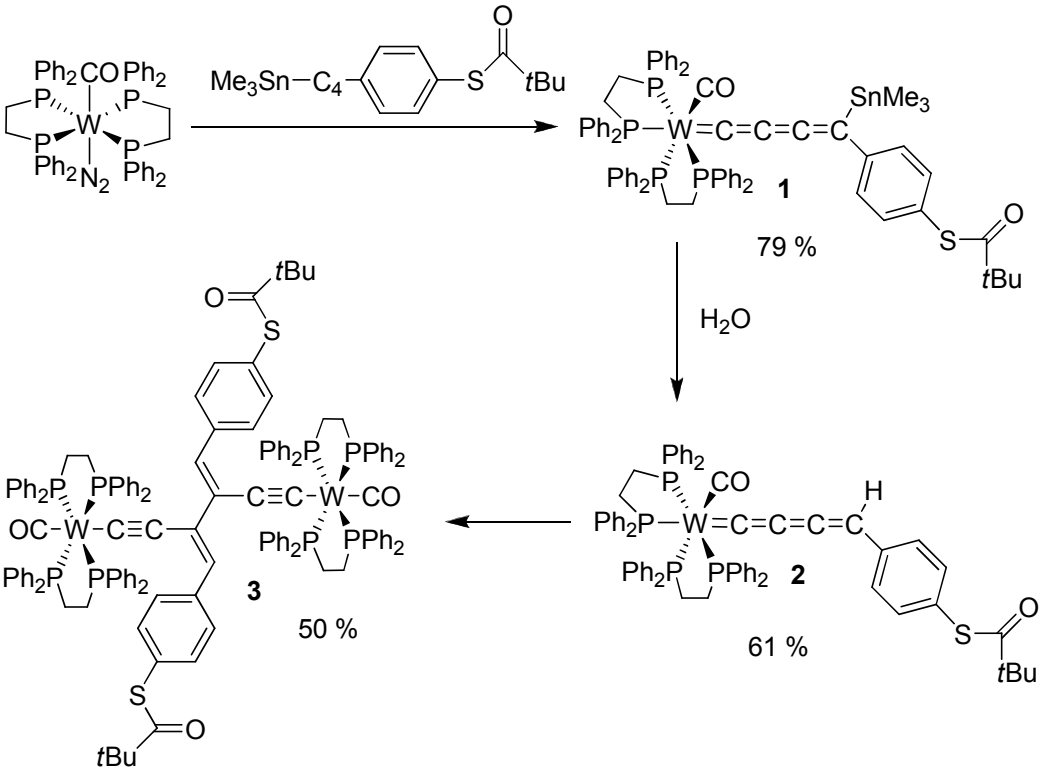

Scheme 2. Reaction path for 1-3.

The signal at 2.3 ppm attributed to the *t*Bu protons in **3** is less shifted from its normal region in comparison to the signal in the C_6H_4tBu derivative due to the longer distance in relation to the magnetic tungsten centers in **3**. Compound **3** is only moderately soluble in THF and CH_2Cl_2 and insoluble in most other common solvents. It is stable at room temperature in solid state and in solution in the absence of air.

V.2.2. Substitution of Iodine in the [I(dppe)$_2$WC$_4$W(dppe)$_2$I]

To functionalize the termini of [I(dppe)$_2$WC$_4$W(dppe)$_2$I], we searched for the conditions to substitute the iodine groups with acetylene type ligands. A quite strong tungsten iodine bond combined with the possibility for *trans*→*cis* rearrangement rendered all standard strategies to be unsuccessful, such as reactions with lithiated and stannylated acetylenes,[134,208] reaction with terminal acetylene in the presence of base and CuI,[154] or sequential iodine abstraction by silver or thallium ions or trimethylsilyl triflate followed by lithium acetylide addition.[179] A successful substitution was archived by a three-fold access of a 1:1 mixture of the lithiated acetylene and

thallium triflate (Scheme 3). The substitution mechanism is unclear; however it probably involves a putative Tl(III) acetylide intermediate due to following facts:

- Metallic thallium is one of the observed reaction products.
- $TlMe_3$ compound reacted with $[I(dppe)_2WC_4W(dppe)_2I]$ resulting in the formation of a mixture of $[(CH_3)(dppe)_2WC_4W(dppe)_2(CH_3)]$ and $[I(dppe)_2WC_4W(dppe)_2(CH_3)]$ as observed by NMR.

The Tl^{III} acetylide is formed by disproportionation of unstable Tl(I) acetylide. Two details are important for this reaction: solutions should be diluted and TlOTf should be in small (about 5%) excess relative to the LiC≡CR component.

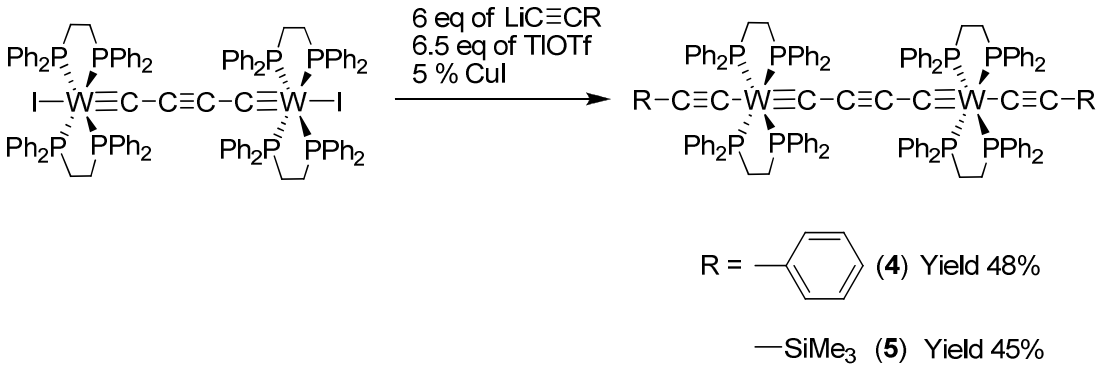

Scheme 3. Synthesis of 4 and 5.

The phenylacetylene was taken as a model substrate for the screening of reaction conditions. Complex **$[(PhC_2)(dppe)_2W(C_4)W(dppe)_2(C_2Ph)]$ (4)** was obtained in 48% yield via the method described above. A singlet resonance in the ^{31}P NMR spectra indicates *trans* configuration of dppe ligands. The ^{13}C spectra of species **4** showed four resonances for the $[C_2WC_4WC_2]$ chain at 222.1 (C≡W), 137.4 (W–C), 119.8 (≡C–Ph) and 92.0 ppm (–C≡C–). The signals of central C_4 fragment are low field shifted relative to complex $[I(dppe)_2WC_4W(dppe)_2I]$ indicating different π-donor properties of I^- and the acetylide ligand. Further, we thought we could obtain the trimethylsilyl acetylene derivative and subsequently deprotect the acetylene groups and those generate reactive terminal groups. The synthesis of complex **$[(Me_3SiC_2)(dppe)_2W(C_4)W(dppe)_2(C_2SiMe_3)]$ (5)** always gave small amounts of the corresponding unsymmetrical compound which could be then separated off by column chromatography on Al_2O_3. The carbon atoms of the central chain turned out to possess NMR chemical shifts almost identical to those in **4**, but signals for the terminal chain carbon atoms are shifted low field (table 7). Unfortunately, **5** was completely unreactive. Strong deprotection reagents such as KOH and NBu_4F did not effect the removal of the trimethylsilyl group. This problem was solved by utilization of trimethylsilyl butadiyne as end group instead of trimethylsilyl acetylene.[201]

Table 7.

Summary of ^{13}C NMR [ppm] data for **4 - 8**.

Compound	C_α	C_β	C_α'[a]	C_β'	C_γ'	C_δ'
4	222.1	92.0	137.4	119.8		
5		91.0	161.4	125.0		
6	223.9	91.8	145.6	103.8	81.5	68.2
7	228.9	92.6				
8	233.7	93.2	120.6	121.5		

[a] '- Indicates that carbon atom belongs to the terminal chain.

The structures of complexes **4** and **5** were confirmed by X-ray diffraction studies (Figure 23 and 24). Both complexes consist of the **[W(dppe)$_2$(C$_4$)(dppe)$_2$W]** fragment capped by acetylene ligands. The structure of the central fragment is essentially similar to those in [I(dppe)$_2$WC$_4$W(dppe)$_2$I].[200] The W–C distances in **4** and **5** are slightly longer than in [I(dppe)$_2$WC$_4$W(dppe)$_2$I] probably due to π-donating properties of I$^-$ in contrast to the weak π-acceptor properties of the acetylide ligand. As in the [I(dppe)$_2$WC$_4$W(dppe)$_2$I] complex, the coordination environment of tungsten centers is distorted from the ideal square pyramide with an angle between the perpendicular of the mean plane (P1, P2, P3, P4) and the W-C axis of about 10^o. The whole [C≡CW≡CC≡CC≡WC≡C] chain possess a totally conjugated system as evident from the bond length analysis affirming alternation of C≡C and W≡C triple and C–C and W–C single bonds (Table 8). The chain is almost linear in the crystal structure of **5**, but in **4** a significant S-type distortion was observed.[148]

Table 8.

Selected bond distances [Å] in crystal structures of **4**, **5, 7** and **8**.

Compound	W–P [a]	W≡C	C–C	C≡C	W–C	C≡C [b]
4	2.4681(7)	1.874(3)	1.373(3)	1.231(5)	2.332(2)	1.076(5)
5	2.4677(6)	1.890(2)	1.351(3)	1.248(4)	2.240(2)	1.195(3)
7 [a]	2.4495(5)	1.876(2)	1.355(2)	1.241(2)		
8 [a]	2.526(1)	1.863(5)	1.375(7)	1.234(7)	2.182(3)	1.179(3)

[a] Average values are presented. [b] C≡C bond from terminal group.

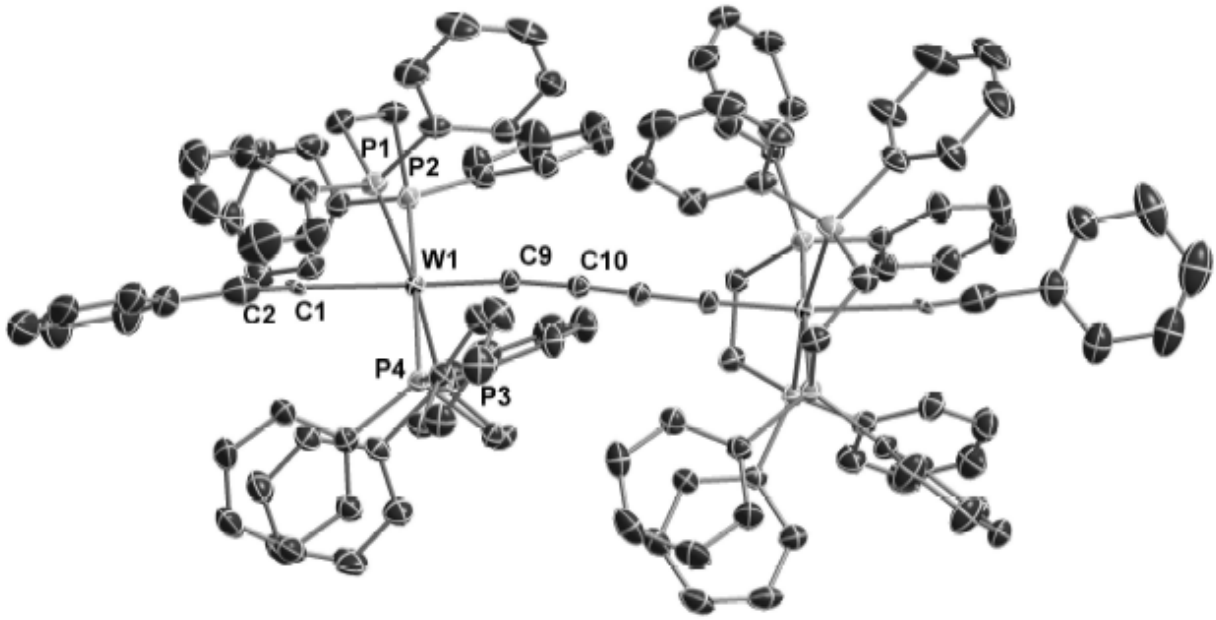

Figure 23. Thermal ellipsoid plot of the structure of 4 (50% probability level).

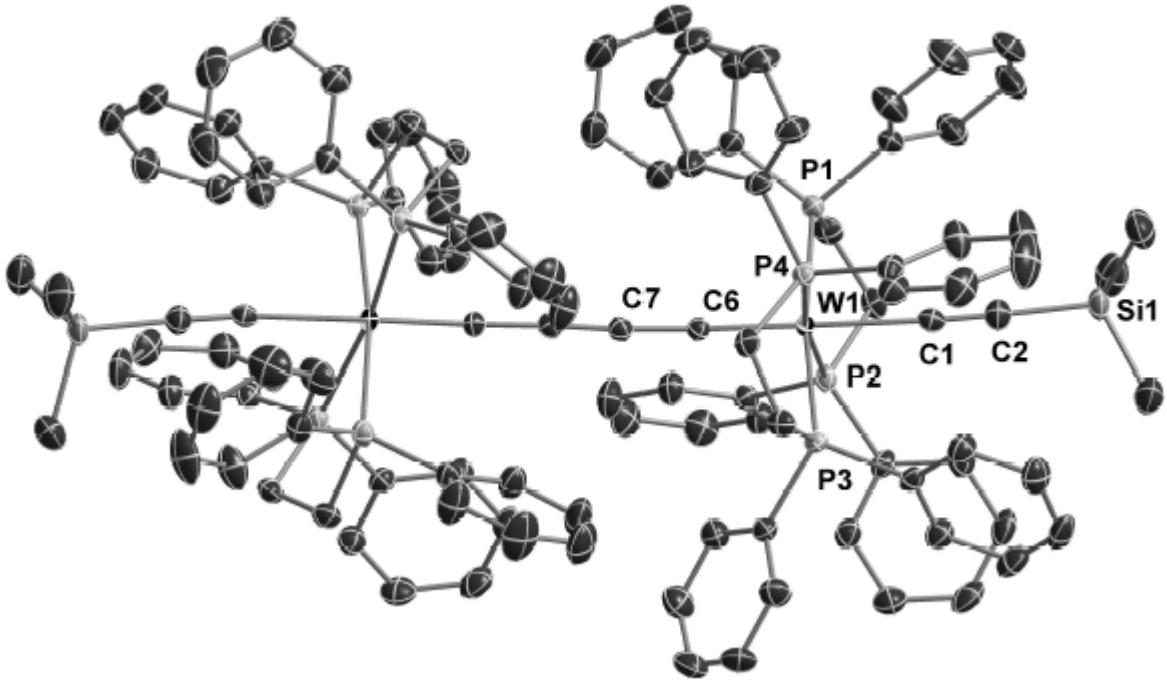

Figure 24. Thermal ellipsoid plot of the structure of 5 (50% probability level).

During the investigation of the reactivity of $[I(dppe)_2WC_4W(dppe)_2I]$, we found that the iodine ligands could be substituted with hydride upon reaction with $Na[BHEt_3]$. Reaction in THF at 60 °C gave **$[HW(dppe)_2(C_4)(dppe)_2WH]$ (7)** as dark-green crystals after recrystallization from ether (Scheme 4). The structure of **7** was established by NMR and IR spectroscopy and by elemental analysis. A hydride signal was observed in the ^1H NMR spectrum as quintet $^2J_{P\text{-}H}$ = 28.5 Hz at -3.79 ppm. Due to the potential high reactivity of the hydride **7**, it could be a promising precursor for derivatization of the **$[W(dppe)_2(C_4)(dppe)_2W]$** fragment‘s terminal sites.

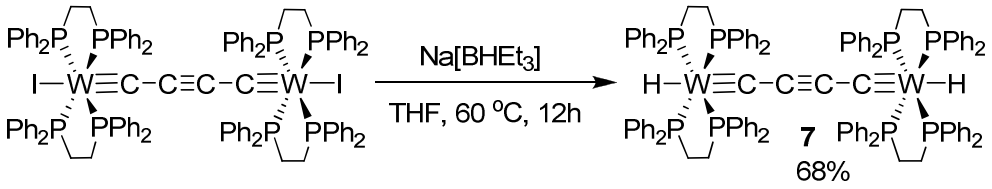

Scheme 4. Synthesis of 7.

The structure of **7** was confirmed by a single crystal X-ray structural analysis (Figure 25). The structure of the hydride **7** is very similar to the iodide. The W–P bonds are however shorter in the hydride complex and [WC_4W] chain shows a bow-shape distortion (cisoid).

The acetylene coupling to CO containing [$(CO)_2$(dppe)$WC_4W(CO)_2$(dppe)] fragment was also archived by triflate substitution (Scheme 5). Complex [$(PhC_2)(CO)_2$(dppe)$WC_4W(CO)_2$(dppe)(C_2Ph)] was fully characterized including crystal structure (Figure 26). Compound is stable at -30 °C in solid state, but decomposes in solution within a few days. This fact in combination with its irreversible electrochemistry made this type of compounds inappropriate for further studies as building blocks in molecular wires.

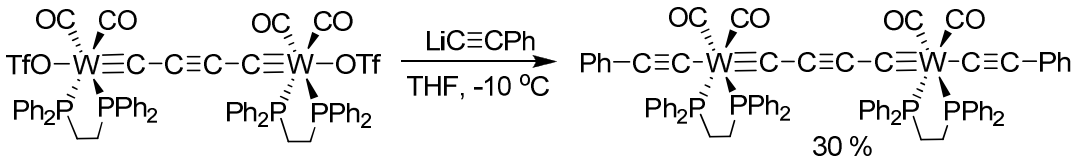

Scheme 5. Synthesis of 8.

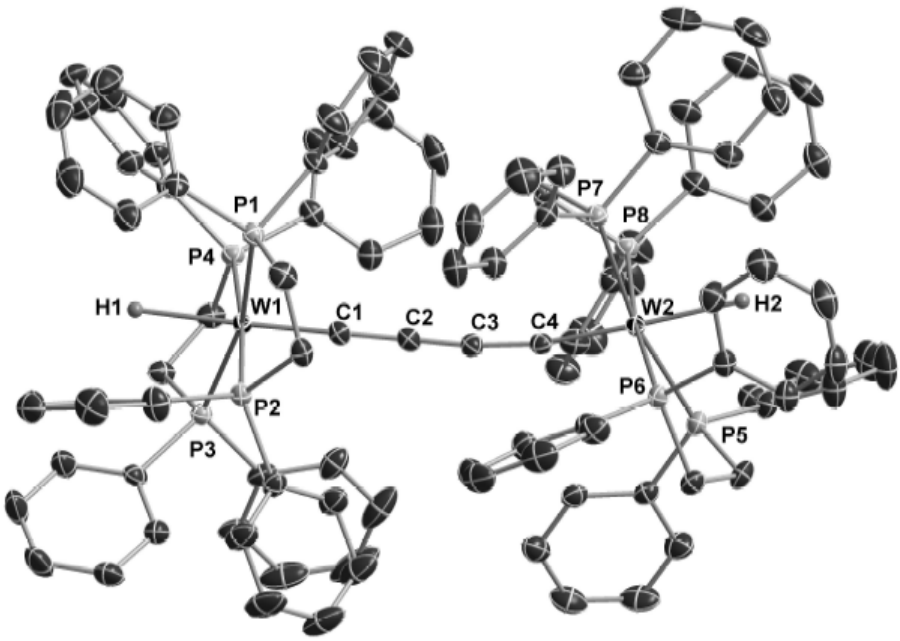

Figure 25. Thermal ellipsoid plot of the structure of 7 (50% probability level).

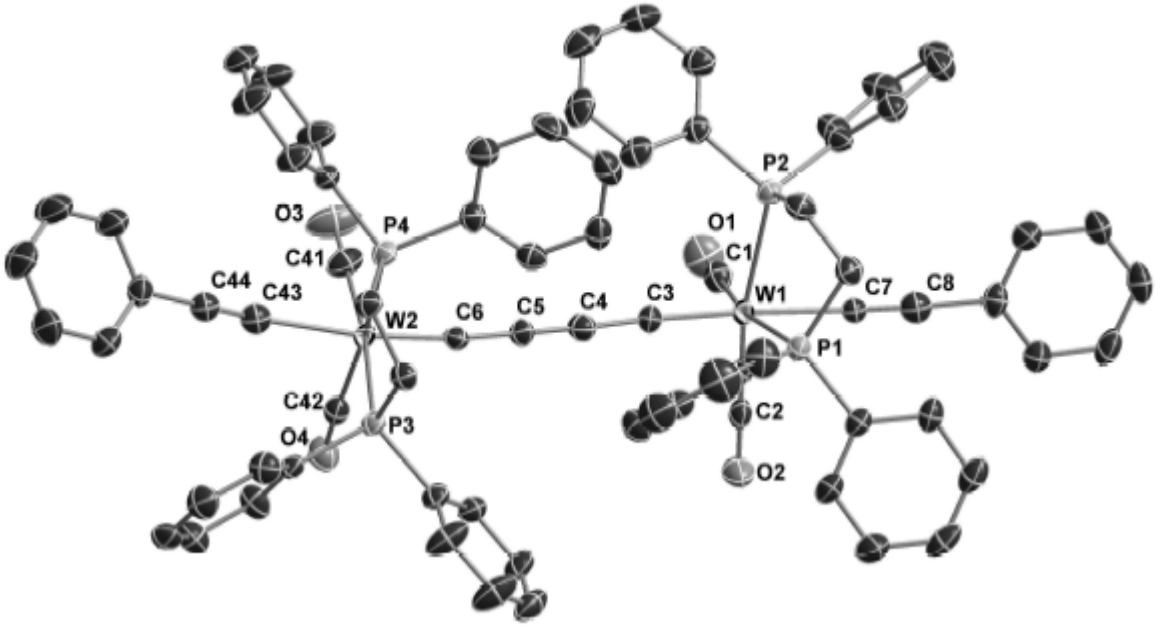

Figure 26. Thermal ellipsoid plot of the structure of 8 (50% probability level).

V.2.3. Linear system with anchor groups

The synthesis of rigid-rod complexes equipped with appropriate anchor groups was one of the main targets of this work. Thiophenol based anchor groups were chosen due to their strong binding affinity to the gold electrodes, as well as due to the possibility for comparison with the published data that mostly consist of a sulfide type contact. The thiopivaloyl group was the first choice due to its lower reactivity compared to the thioacetyl group.

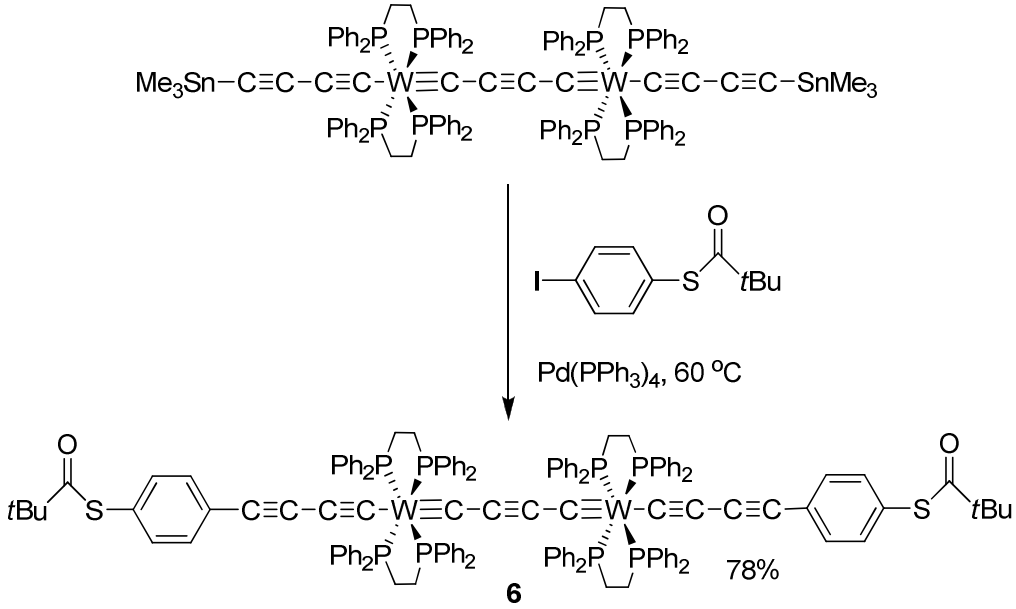

Scheme 6. Synthesis of 6.

Two synthetic strategies were considered. The first strategy was based on a coupling of an acetylene ligand with the tungsten center. The second strategy involves the derivatization of

the precursor, which already bears a tungsten acetylene bond. The general problem of the first approach concerns the difficulties with the deprotonation of $HC_2PhSCOtBu$, which is required for our coupling protocol. The deprotonated compound is unstable because the acetylide anion formed by deprotonation reacts with the thioester group. An alternative possibility was the reaction of the hydride **7** with $HC_2PhSCOtBu$, but acidity of the acetylene was not enough to protonate the hydride.

Two compounds $[(HC_4)(dppe)_2W(C_4)W(dppe)_2(C_4H)]$ and $[(Me_3SnC_4)(dppe)_2W(C_4)W(dppe)_2(C_4SnMe_3)]$ were obtained by us recently, which looked promising in the use as starting materials for the mentioned second approach.[201] The deprotected butadiyne complex was tested in a Sonogashira coupling reaction condition with $IC_6H_4SCOtBu$. The reaction led to many products and several of them were not identified. The stannylated derivative had much more predictable reactivity. Its reaction with $IC_6H_4SCOtBu$ during 48 hour under Stille coupling conditions resulted in the clean formation of the desired product **$[(tBuCOSC_6H_4C_4)(dppe)_2W(C_4)W(dppe)_2(C_4C_6H_4SCOtBu)]$ (6)** in 78 % yield (Scheme 6). Complex **6** was fully characterized. The $C_6H_4SCOtBu$ group shows characteristic signals in the ^1H NMR spectrum as well as characteristic ^{13}C NMR signals at 202.4 (CO), 46.7 ($C(CH_3)_3$) and 27.1 ppm ($C(CH_3)_3$). The chemical shifts of the carbon atoms of the [C≡CC≡CW≡CC≡CC≡WC≡CC≡C] chain are comparable with those of $[(Me_3SiC_4)(dppe)_2W(C_4)W(dppe)_2(C_4SiMe_3)]$. **6** is stable at room temperature in the absence of air.

VI. SUMMARY

For the preparation of tungsten based single molecular conductors various detailed aspects of tungsten organometallic chemistry were explored. The [*trans*-W(dppe)$_2$] fragment was expected to combine stability and suitable electrochemical properties, but there was no synthetic access available, which could be applied for the synthesis of binuclear complexes. In order to develop an efficient synthetic methodology, we had chose two parallel directions: starting from a precursor already possessing [*trans*-W(dppe)$_2$] system or using CO containing precursors [W(dppe)(CO)$_3$L] (L = labile ligand) with consecutive subsequent substitution of CO with dppe.

The [*trans*-W(dppe)$_2$(CO)(N$_2$)] complex seemed to be a promising starting material for our endeavors due to the reversible formation of the pentacoordinated species bearing an open site. We investigated its synthetic potential in more detail and as a result of this study we have found that this complex coordinates stannylated acetylenes and butadiynes, which then undergo 1,2 or 1,4-shift of SnMe$_3$ group to form tungsten vinylidenes and butatrienylidenes (Scheme 7).

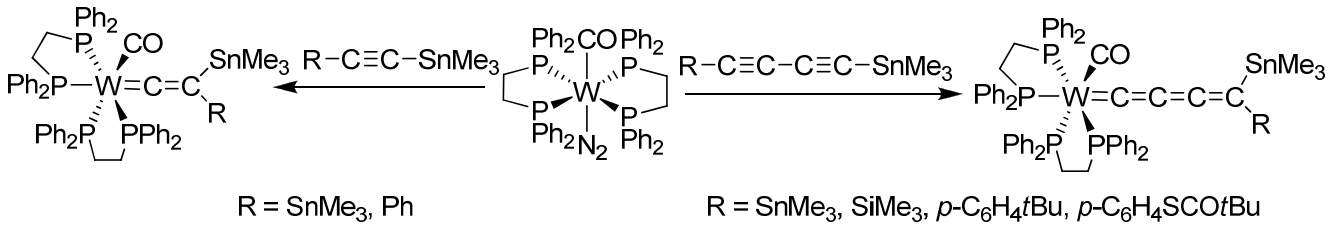

Scheme 7. Formation of vinylidenes and butatrienylidenes.

This synthetic access developed for butatrienylidenes turned out to be very general and was applied to a variety of butadiynes with aromatic or EMe$_3$ (E = Sn, Si) substitutents. The C$_4$ cumulenylidenes was a missing link in the series of tungsten cumulenylidenes with general formula [L$_x$W=C(=C)$_n$RR'] (n = 1, 2, 4). Further more we found that the substituent on the cumulene chain has a strong influence on the stability of deprotected complex. Compounds bearing aromatic substituents were deprotected with the formation of moderately stable H-substituted cumulenylidene complexes, while compounds [*cis*-(CO)(dppe)$_2$W(C=C=C=CRH)] (R = SiMe$_3$, SnMe$_3$ or H) are unstable and the only product that could be characterized was the [*trans*-W(CO)(dppe)$_2$(C≡C-C≡CH)][NBu$_4$] probably formed by destannylation of the cumulenylidene. The stability of [*cis*-(CO)(dppe)$_2$W{C=C=C=C(Ph*t*Bu)(H)}] was sufficiant to allow characterization it by a single crystal X-ray diffraction. It is the first and the only structurally characterized H-substituted butatrienylidene complexes up to now.

The main interest in deprotected cumulenylidenes lies in their potential applications in coupling reactions. We considered coupling of the butatrienylidene complexes as a way to synthesize dinuclear complexes with larger conjugated bridges. Attempts of the oxidative

coupling of [*cis*-(CO)(dppe)$_2$W{C=C=C=C(Ph*t*Bu)(H)}] were however unsuccessful, but we found that it undergoes self-coupling form a dimeric molecule in about 50% yield (Scheme 8). This is the first symmetrical self-coupling reaction of a long cumulenylidenes.

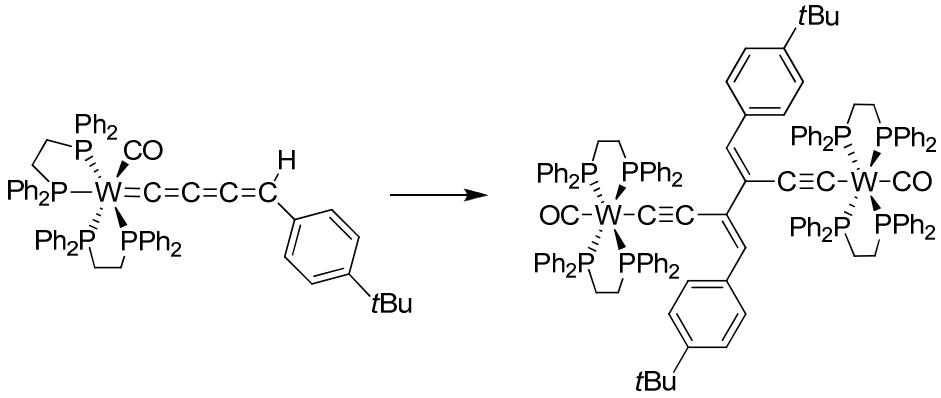

Scheme 8. Dimerization reaction.

The kinetics of the dimerization was studied in detail. It showed a second order kinetics in the substrate concentration suggesting bimolecular rate limiting step, in which the formation of a cyclobutane intermediate was invoked. The dimeric molecule resulting as a product of the coupling is a unique 1,3-diethynyl-butadiene cross-conjugated system.

Surprisingly, the vinylidene complexes were less stable than butatrienylidene derivatives. They loose the $SnMe_3$ group upon UV irradiation resulting in the formation of unique W(I) acetylides (Scheme 9).

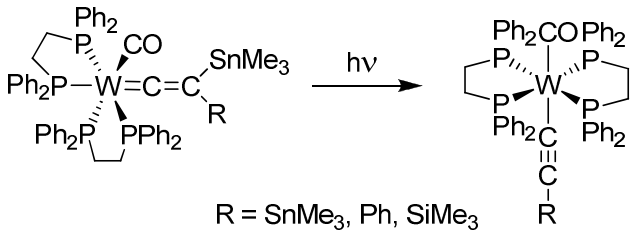

Scheme 9. Formation of W(I) acetylides.

The strategy based on CO containing [*fac*-W(dppe)(CO)$_3$(THF)] precursor was used for the synthesis of C_4 bridged tungsten complexes. A crucial result in this direction was the transformation of the anionic butadiyne bridged complex directly in the neutral carbyne complex (Scheme 10). The reaction was anticipated to involve single electron oxidation steps, loss of CO and coordination of iodide or I^+ transfer at each tungsten center. The synthesis is methodologically unique, because it was based on an oxidative transformation of the polyyne chain to the bis-carbyne bridge. [I(CO)$_2$(dppe)WC$_4$W(dppe)(CO)$_2$I] was very chemically and thermally stable making it a suitable precursor for the development of a subsequent chemistry for the targeted molecular electronics purposes. The stability of the complex probably comes from multiple factors: a strong bonding of tungsten center in low oxidation state with π-acceptor ligands as CO and dppe; stabilization by conjugation in the [WC$_4$W] chain; steric protection by

the bulky dppe ligand and complementary character of π-acceptor carbyne ligand and π-donor I^- ligand ("push-pull" effect in binding).

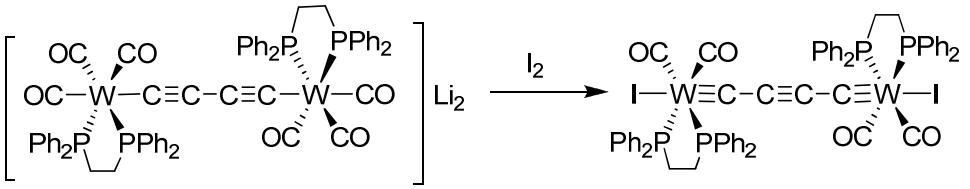

Scheme 10. Formation of C_4 bridged tungsten carbyne.

We were able to synthesize a series of $[X(CO)_2(dppe)WC_4W(dppe)(CO)_2X]$ (X = I, Cl, NCS, OTf) complexes as well as the unsymmetrical complex $[I(CO)_2(dppe)WC_4W(dppe)_2I]$. The analysis of the data showed that axial substituents influences mainly the position of the intense high energy π - π* electronic transition (λ_1), while the equatorial ligands change the position of the low energy d_{xy} - π* transition (λ_2) (Figure 27).

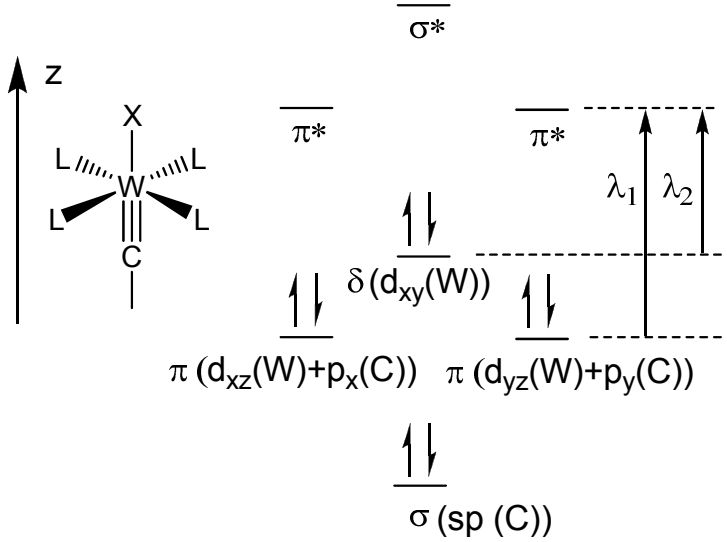

Figure 27. Qualitative molecular orbital diagram for a tungsten carbyne complex of the type discussed.

These observations confirmed the d_{xy} character of the HOMO orbital. Another important conclusion was that the $[C{\equiv}W(dppe)_2I]$ center shows reversible oxidation in contrast to irreversible process for the $[C{\equiv}W(dppe)(CO)_2X]$ centers. This observation motivated us to obtain a symmetrical CO free complex. Compound $[I(dppe)_2WC_4W(dppe)_2I]$ was obtained via heating of $[I(CO)_2(dppe)WC_4W(dppe)(CO)_2I]$ with excess of dppe in 90% yield (Scheme 11).

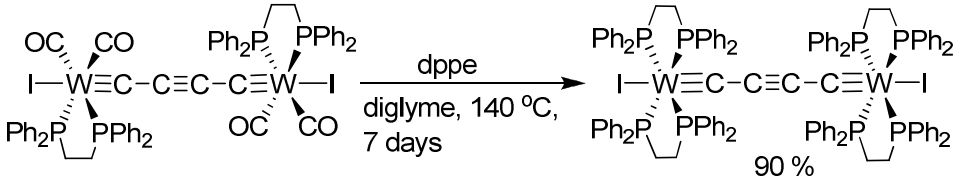

Scheme 11. Synthesis of $[I(dppe)_2WC_4W(dppe)_2I]$.

The overall yield starting from $W(CO)_6$ was about 15 %.

The complex has a high chemical and thermal stability and a reversible electrochemistry for both metal centers. However, in order to make the $[I(dppe)_2WC_4W(dppe)_2I]$ complex close to an ideal building block for the construction of rigid-rod wires, we had to develop a method for the functionalization of the end group.

Published coupling procedures were not successful due to the low reactivity and probably due to the *trans* → *cis* rearrangements of the diphosphines. To overcome these problems, we developed a new method that allows immediate coordination of the acetylide after abstraction of the iodine. It is based on the utilization a mixture of TlOTf and lithium acetylide. This mixture resulted in a Tl(I) acetylide which, slowly disproportionates to the Tl(III) organometallic species and metallic thallium. The reactive form of thallium acetylide is unclear in this case, however we found that $TlMe_3$ substitutes the iodine to the methyl group, which let us speculate that Tl(III) acetylide could be the reactive species. This method can be transferred to a variety of acetylenes, as well as to butadiynes (Scheme 12).

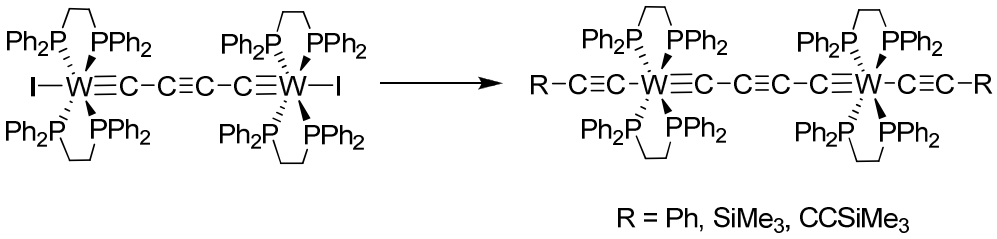

Scheme 12. Iodine substitution reaction.

It is important to mention here that these complexes contain a very rare type of p/d conjugated systems where the metals center formally substitute carbon in acetylene type chains. The acetylene substituted complexes could then be viewed as analogs to decapentayne derivatives and the butadiyne substituted complexes to the tetradecaheptayne derivatives. Both the C_2SiMe_3 and C_4SiMe_3 substituted complexes were tested under different deprotection conditions affirming that the number of acetylene units in the terminal chain has a strong influence on the reactivity of the trimethylsilyl group. The C_2SiMe_3 derivative was resistant to many deprotection conditions, but the trimethylsilyl butadiyne derivative could be deprotected by KOH/MeOH to form a $[(HC_4)(dppe)_2W(C_4)W(dppe)_2(C_4H)]$ molecule which could be stannylated further. A stable central fragment in combination with reactive terminal ends makes these complexes promising building blocks for molecular wires.

The synthesis of linear polynuclear systems is an important task for molecular electronics, because the electron transfer between the remote ends could be then divided to smaller steps of electron hopping between neighboring metal centers. The presence of several redox active centers in such molecules opens real possibilities to control conductance. It was particularly necessary to synthesize system with redox active terminal groups for the study of electronic

communication mediated by new {(C≡C)$_2$[W]≡C(C≡C)C≡[W](C≡C)$_2$} conjugated system. The stannylated block was successfully capped with [Fe(depe)$_2$Cl] to form a tetranuclear complex (Scheme 13).

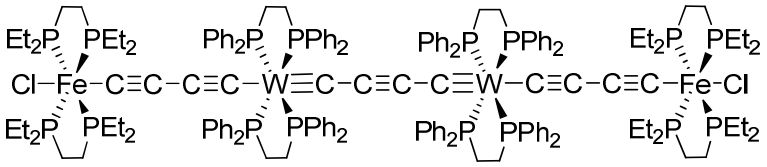

Scheme 13. Structure of tetranuclear complex.

This is the first report of a linear tetranuclear complex consisting of C_n bridges and metal fragments exhibiting reversible redox chemistry until now. It combines unique properties, such as fast electron transfer, reversible oxidation of all four metal centers, presence of terminal reactive sites for further functionalizations, and suitability for surface attachment due to its rigidity and cylindrical shape.

In order to first investigate the efficiency of the electron transfer in the new conjugated systems, we studied our complexes by different appropriate physical methods. The symmetrical binuclear complexes with reversible redox chemistry are optimum molecules for such studies because of the simplified data analysis. Three principally different complexes were studied in detail: the dinuclear molecules with [W(dppe)$_2$(CO)] groups, the [I(dppe)$_2$WC$_4$W(dppe)$_2$I] complex and the tetranuclear species. The interactions supported by new 2,3-diethynylbutadiene and ditungstenatetradecaheptayne π-conjugated bridge systems were studied in this work. Although the but-2-yn-1,4-diylidyne system was investigated by CV before, a comprehensive study was carried out during this work.

Investigations were carried out in the following way. A complex in an initial oxidation state was investigated by CV. These studies provided information about the accessible oxidation states and about conditions required for the access to the MV complex. The separation of the redox waves gave a qualitative assessment of the electronic interaction. The MV complex was then studied by NIR spectroscopy and the data were analyzed using the Hush approximation. A special attention should be paid to the case of Class III systems, which should be analyzed in a different way. Main parameters extracted from NIR studies were the electron coupling integral H_{AB} and the reorganization parameter λ. In combination with EPR and IR studies, these values could be used to estimate the electron transfer rate between the terminal centers. Two points are important and should be considered: (i) The H_{AB} should not be too large. In other words, the complex should have two minima in the ground state; (ii) Value of H_{AB} identifies the type of (adiabatic or nonadiabatic) electron transfer and consequently determines the type of equation used for calculations.

Finally, the magnetic exchange integral is extracted from magnetization studies of the biradical form. In the end we obtain a complete view of the interaction from electrochemical, spectroscopic and magnetic studies. Most important parameters are summarized in table 9.

Table 9.

Summary of study of electronic interaction in obtained complexes.

Compound	ΔE [V], (K_c)	H_{AB} [cm^{-1}]	J [cm^{-1}]
[{*trans*-W(CO)(dppe)$_2$(C≡C−C{=C(H)(*p*-C_6H_4*t*Bu)})}$_2$]	0.15 (400)	-	21
[I(dppe)$_2$WC_4W(dppe)$_2$I]	0.29 (7.5×10^4)	250	160
[Cl(depe)$_2$Fe(C_4)(dppe)$_2$WC_4W(dppe)$_2$(C_4)Fe(depe)$_2$Cl]	0.19 (1500)	680	-

As could be seen from this table the cross-conjugated molecule has a weak interaction between tungsten centers. To understand the results of the electronic interaction studies we have to consider at least two qualitative assessment factors: degree of conjugation in the bridge and interaction of the bridge with the metals HOMO orbital. In the dimer molecule, the HOMO of the metal center is probably the d_{xy} orbital, but we have shown by EPR that those orbital is mixed with d_{zy} and d_{zx} orbital character. This mixing should provide sufficient coupling of the [*trans*-W(CO)(dppe)$_2$] fragment with the acetylide ligand. The reason for the weak communication in the dimeric molecule is probably due to the reduced electron delocalization in the 2,3-diethynyl-butadiene system.

A contrasting situation is observed in the biscarbyne [W]≡C(C≡C)C≡[W] arrangement. The conjugation in the C_4 chain is strong here, as well as the delocalization; however the HOMO of the metal centres is the energetically well separated d_{xy} orbital, which has δ symmetry and is orthogonally arranged to the π-symmetry orbitals of the bridge. Interaction between them is forbidden for in an ideal case. [I(dppe)$_2$WC_4W(dppe)$_2$I] was found to possess however a strong distortion from D_{4d} symmetry. In addition the heavy metal tungsten center and the iodine atoms induce mixing of orbitals by spin-orbital coupling. As a result, a interaction of medium strength was observed in the biscarbyne system (class II). This complex represents a good example of a system where the study of the MV complex could be not be directly related to molecular conductivity. The studies are related only to the interaction between orbitals bearing unpaired electron and do not stress the effect of the fully conjugated molecular π-orbitals of the [W]≡C(C≡C)C≡[W] chain.

The study of the tetranuclear complex supports previous considerations about the possibility of an electron transfer through the metal-organic polyyne π-system. This complex consists of {(C≡C)$_2$[W]≡C(C≡C)C≡[W](C≡C)$_2$} unit capped by iron groups. It allows the study of electronic interaction between the iron centres via this new type of conjugated system. The

oxidation processes for the two iron centres are well separated even if the Fe ··· Fe distance is about 24 Å. MV complex shows a very strong NIR absorption indicating a significant H_{AB}. The fully conjugated chain and the appropriate interaction of the iron d-orbitals with the acetylide type ligands favours good overall interaction in this system. Finally, we can conclude that ditungstenapolyynes could efficiently mediate electron communication over long distances, but are much more stable than the pure organic polyynes.

As could be seen from the physical studies, the ditungstenatetradecaheptayne system is the most promising candidate for single electron conductance studies. The 1,3-diethynyl-butadiene system doesn't show strong communication between the metal centers but is interesting due to its cross-conjugation effect.

The [{*trans*-W(CO)(dppe)$_2$(C≡C−C{=C(H)(*p*-C$_6$H$_4$SCO*t*Bu)})$_2$] molecule with anchor groups was obtained by a protocol similar to the *t*-butyl derivatives (Scheme 14). The compound is unique for fundamental studies of single molecule conductance. Since the metal fragments are not on the conducting chain, tungsten centers should not directly influence the detected current. However, it was recently shown that the side chain strongly influences the current through the main chain. It would be interesting to investigate the possibility to control current through the butadiene chain by change of the oxidation state of tungsten. Another unique property of this molecule is the presence of the two antiferromagnetically coupled magnetic centers. It opens new possibilities to study Kondo resonance in single molecules, particularly important information could probably be extracted by measurements of conductance at above and below Neel temperature.

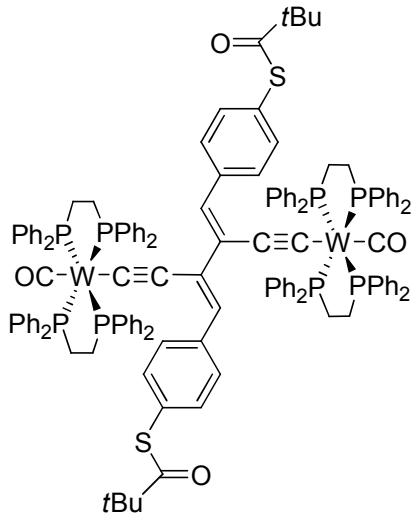

Scheme 14. Structure of [{trans-W(CO)(dppe)$_2$(C≡C−C{=C(H)(p-C$_6$H$_4$SCOtBu)})$_2$].

To obtain molecule based on {(C≡C)$_2$[W]≡C(C≡C)C≡[W](C≡C)$_2$} system and suitable for conductance measurements, we used Stille coupling conditions between the stannylated

precursor $[(Me_3SnC_4)(dppe)_2W(C_4)W(dppe)_2(C_4SnMe_3)]$ and *p*-$IC_6H_4SCOtBu$. The resulting complex is drawn out below (Scheme 15).

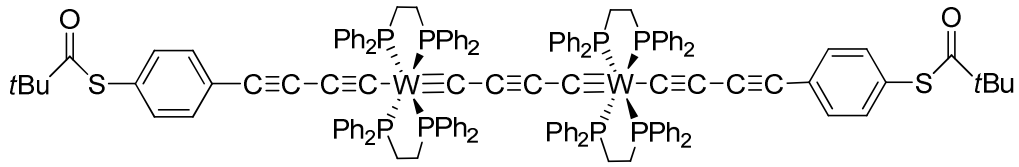

Scheme 15. Structure of $[(tBuCOSC_6H_4C_4)(dppe)_2W(C_4)W(dppe)_2(C_4C_6H_4SCOtBu)]$

This compound should be a good candidate for single molecular studies because of stability at room temperature, solubility in solvents such as THF and CH_2Cl_2 and in addition the theoretical treatment of results that are expected to be simplified by the quite high symmetry of the system. Due to the unique electronic structure of the bridge, such molecule could combine direct tunneling through the conjugated π-system with electron hopping between d_{xy} orbitals (Figure 28). Another interesting aspect could be the control of a low voltage tunneling current through the π-system by removing the electron from the d_{xy} orbital.

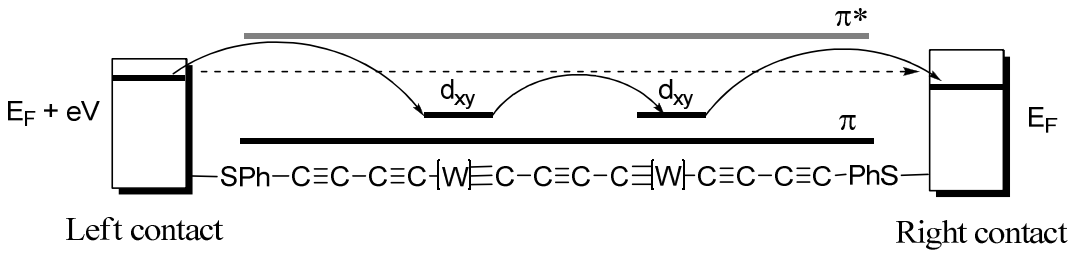

Figure 28. Schematic representation of possible conductance mechanisms through $\{(C\equiv C)_2[W]\equiv C(C\equiv C)C\equiv[W](C\equiv C)_2\}$ system *(A dashed arrow represents tunnelling process, solid arrows show hopping steps, black lines represents occupied orbitals and grey line shows unoccupied orbital).*

The work on the synthesis of analogous molecule with thioacetyl anchor groups is currently in progress. The conductances of these molecules are expected to be studied in collaboration with IBM research laboratory in Zurich in the near future.

In conclusion, as could be seen from this summary, the work has contributed to the fields of metal-organic chemistry in general, the physics of electronic interactions in MV complexes and to the synthesis of compounds for single molecular studies.

VII. CONCLUSIONS

1. The chemistry of tungsten C_4 cumulenylidenes was explored. It was shown that:
   - Tungsten butatrienylidenes can be obtained from stannylated butadiyne precursors and [*trans*-$W(dppe)_2(CO)(N_2)$];
   - aromatic substitutents on C_4 chain stabilize H-substituted cumulenylidenes;
   - H-substituted butatrienylidenes undergo self-coupling reaction with the formation of complex containing 2,3-diethynyl-butadiene cross-conjugated system.
2. Investigations of tungsten C_4 bridged biscarbyne complexes showed that:
   - they could be obtained by oxidation of butadiyne bridged precursors;
   - the fully dppe substituted complex $[I(dppe)_2WC_4W(dppe)_2I]$ showed an optimum combination of stability and electrochemical properties;
   - the iodine ligands in this complex can be substituted with acetylide ligands by thallium activated reactions.
3. The building block $[(Me_3SiC_4)(dppe)_2W(C_4)W(dppe)_2(C_4SiMe_3)]$ allowed in combination with the chemical inertness of the metal fragment, to have reversible redox properties and selectively reactive terminal groups. It was used for synthesis of:
   - a deprotected metalorganic polyyne $[(HC_4)(dppe)_2W(C_4)W(dppe)_2(C_4H)]$ which showed much higher stability than the parent polyynes $H(C{\equiv}C)_nH$ with $n > 4$;
   - a linear tetranuclear complex $[Cl(depe)_2Fe(C_4)(dppe)_2WC_4W(dppe)_2(C_4)Fe(depe)_2Cl]$ with unique electrochemical and photophysical properties.
4. The interaction between metal centers was studied for three complexes with different types of conjugated systems which are presented in the picture below:

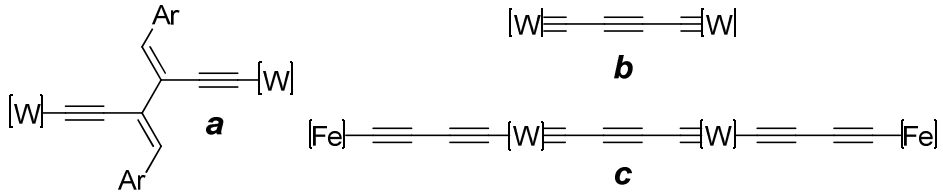

   These studies showed that:
   - system ***a*** provided only weak interactions between the tungsten centers probably due to low electron delocalization in the 1,3-diethynyl-butadiene bridge;
   - system ***b*** has only moderate interaction of the highest occupied metal centered orbitals due to the orthogonality of δ type d_{xy} orbitals and the π type orbitals of the bridge;
   - system ***c*** mediates strong communication between iron centers over 24 Å distance.

5. Suitable for single molecule conductance measurements molecules with skeletons ***a*** [{*trans*-$W(CO)(dppe)_2(C{\equiv}C{-}C\{{=}C(H)(p\text{-}C_6H_4SCO\textit{t}Bu)\}\})\}_2$] and ***c*** [$(\textit{t}BuCOSC_6H_4C_4)(dppe)_2W(C_4)W(dppe)_2(C_4C_6H_4SCO\textit{t}Bu)$] were obtained.

VIII. REFERENCES

(1) Joachim, C.; Gimzewski, J. K.; Aviram, A. *Nature* **2000**, *408*, 541-548.

(2) Chen, F.; Hihath, J.; Huang, Z. F.; Li, X. L.; Tao, N. J. *Annu. Rev. Phys. Chem.* **2007**, *58*, 535-564.

(3) Tao, N. J. *J. Mat. Chem.* **2005**, *15*, 3260-3263.

(4) James, D. K.; Tour, J. M. *Chem. Mater.* **2004**, *16*, 4423-4435.

(5) McCreery, R. L.; Bergren, A. J. *Adv. Mater.* **2009**, *21*, 4303-4322.

(6) Muller, C. J.; Vleeming, B. J.; Reed, M. A.; Lamba, J. J. S.; Hara, R.; Jones, L.; Tour, J. M. *Nanotechnology* **1996**, *7*, 409-411.

(7) Xu, B. Q.; Tao, N. J. J. *Science* **2003**, *301*, 1221-1223.

(8) Haiss, W.; Wang, C. S.; Grace, I.; Batsanov, A. S.; Schiffrin, D. J.; Higgins, S. J.; Bryce, M. R.; Lambert, C. J.; Nichols, R. J. *Nature Mater.* **2006**, *5*, 995-1002.

(9) He, J.; Sankey, O.; Lee, M.; Tao, N. J.; Li, X. L.; Lindsay, S. *Faraday Discuss.* **2006**, *131*, 145-154.

(10) Reed, M. A.; Zhou, C.; Muller, C. J.; Burgin, T. P.; Tour, J. M. *Science* **1997**, *278*, 252-254.

(11) Moreland, J.; Ekin, J. W. *J Appl. Phys.* **1985**, *58*, 3888-3895.

(12) Muller, C. J.; Vanruitenbeek, J. M.; Dejongh, L. J. *Phys. Rev. Lett.* **1992**, *69*, 140-143.

(13) Lortscher, E.; Ciszek, J. W.; Tour, J.; Riel, H. *Small* **2006**, *2*, 973-977.

(14) Lortscher, E.; Weber, H. B.; Riel, H. *Phys. Rev. Lett.* **2007**, *98*, 176807/1-176807/4.

(15) Reichert, J.; Ochs, R.; Beckmann, D.; Weber, H. B.; Mayor, M.; von Lohneysen, H. *Phys. Rev. Lett.* **2002**, *88*, 176804/1-176804/4.

(16) Huang, Z. F.; Chen, F.; Bennett, P. A.; Tao, N. J. *J. Am. Chem. Soc.* **2007**, *129*, 13225-13231.

(17) Tour, J. M.; Rawlett, A. M.; Kozaki, M.; Yao, Y. X.; Jagessar, R. C.; Dirk, S. M.; Price, D. W.; Reed, M. A.; Zhou, C. W.; Chen, J.; Wang, W. Y.; Campbell, I. *Chem. Eur. J.* **2001**, *7*, 5118-5134.

(18) Stapleton, J. J.; Harder, P.; Daniel, T. A.; Reinard, M. D.; Yao, Y. X.; Price, D. W.; Tour, J. M.; Allara, D. L. *Langmuir* **2003**, *19*, 8245-8255.

(19) Chen, F.; Li, X. L.; Hihath, J.; Huang, Z. F.; Tao, N. J. *J. Am. Chem. Soc.* **2006**, *128*, 15874-15881.

(20) Stuhr-Hansen, N.; Sorensen, J. K.; Moth-Poulsen, K.; Christensen, J. B.; Bjornholm, T.; Nielsen, M. B. *Tetrahedron* **2005**, *61*, 12288-12295.

(21) Vonlanthen, D.; Mishchenko, A.; Elbing, M.; Neuburger, M.; Wandlowski, T.; Mayor, M. *Angew. Chem. Int. Ed.* **2009**, *48*, 8886-8890.

(22) Ko, C. H.; Huang, M. J.; Fu, M. D.; Chen, C. H. *J. Am. Chem. Soc.* **2010**, *132*, 756-764.

(23) Fu, M. D.; Chen, W. P.; Lu, H. C.; Kuo, C. T.; Tseng, W. H.; Chen, C. H. *J. Phys. Chem. C* **2007**, *111*, 11450-11455.

(24) Han, W. H.; Durantini, E. N.; Moore, T. A.; Moore, A. L.; Gust, D.; Rez, P.; Leatherman, G.; Seely, G. R.; Tao, N. J.; Lindsay, S. M. *J. Phys. Chem. B* **1997**, *101*, 10719-10725.

(25) Han, W. H.; Li, S. M.; Lindsay, S. M.; Gust, D.; Moore, T. A.; Moore, A. L. *Langmuir* **1996**, *12*, 5742-5744.

(26) Hing, Y.; Park, T.-H.; Venkatramani, R.; Keinan, S.; Beratan, D. N.; Therien, M. J.; Borguet, E. *J. Am. Chem. Soc.* **2010**, *132,* 7946-7956.

(27) Park, Y. S.; Whalley, A. C.; Kamenetska, M.; Steigerwald, M. L.; Hybertsen, M. S.; Nuckolls, C.; Venkataraman, L. *J. Am. Chem. Soc.* **2007**, *129*, 15768-15769.

(28) Martin, C. A.; Ding, D.; Sorensen, J. K.; Bjornholm, T.; van Ruitenbeek, J. M.; van der Zant, H. S. J. *J. Am. Chem. Soc.* **2008**, *130*, 13198-13199.

(29) Angelici, R. J.; Lazar, M. *Inorg. Chem.* **2008**, *47*, 9155-9165.

(30) Kiguchi, M.; Miura, S.; Hara, K.; Sawamura, M.; Murakoshi, K. *Appl. Phys. Lett.* **2006**, *89*, 213104/1-213104/3.

(31) Chen, J.; Calvet, L. C.; Reed, M. A.; Carr, D. W.; Grubisha, D. S.; Bennett, D. W. *Chem. Phys. Lett.* **1999**, *313*, 741-748.

(32) Wang, C. S.; Batsanov, A. S.; Bryce, M. R.; Martin, S.; Nichols, R. J.; Higgins, S. J.; Garcia-Suarez, V. M.; Lambert, C. J. *J. Am. Chem. Soc.* **2009**, *131*, 15647-15654.

(33) Tsutsui, M.; Taniguchi, M.; Kawai, T. *J. Am. Chem. Soc.* **2009**, *131*, 10552-10556.

(34) Getty, S. A.; Engtrakul, C.; Wang, L.; Liu, R.; Ke, S. H.; Baranger, H. U.; Yang, W.; Fuhrer, M. S.; Sita, L. R. *Phys. Rev. B* **2005**, *71*, 241401/1-241401/4.

(35) Ratner, M. A.; Davis, B.; Kemp, M.; Mujica, V.; Roitberg, A.; Yaliraki, S. *Molecular Electronics: Science and Technology* **1998**, *852*, 22-37.

(36) Nitzan, A.; Ratner, M. A. *Science* **2003**, *300*, 1384-1389.

(37) Joachim, C.; Ratner, M. A. *Nanotechnology* **2004**, *15*, 1065-1075.

(38) Galperin, M.; Ratner, M. A.; Nitzan, A.; Troisi, A. *Science* **2008**, *319*, 1056-1060.

(39) Tao, N. J. *Nature Nanotechnol.* **2006**, *1*, 173-181.

(40) Salomon, A.; Cahen, D.; Lindsay, S.; Tomfohr, J.; Engelkes, V. B.; Frisbie, C. D. *Adv. Mater.* **2003**, *15*, 1881-1890.

(41) Magoga, M.; Joachim, C. *Phys. Rev. B* **1997**, *56*, 4722-4729.

(42) Chen, F.; Tao, N. J. *Acc. Chem. Res.* **2009**, *42*, 429-438.

(43) Kim, W. Y.; Kim, K. S. *Acc. Chem. Res.* **2010**, *43*, 111-120.

(44) Ratner, M. *Materials Today* **2002**, 20-27.

(45) Wang, W. Y.; Lee, T.; Reed, M. A. *Phys. Rev. B* **2003**, *68*, 035416/1-035416/7.

(46) Chen, J.; Reed, M. A.; Dirk, S. M.; Price, D. W.; Rawlett, A. M.; Tour, J.; Grubisha, D. S.; Bennett, D. W. In *Molecular Nanoelectronics*; Reed, M. A., Lee, T., Eds.; American Scientific Publishers: 2003.

(47) Huang, Z. F.; Xu, B. Q.; Chen, Y. C.; Di Ventra, M.; Tao, N. J. *Nano Lett.* **2006**, *6*, 1240-1244.

(48) Yu, L. H.; Keane, Z. K.; Ciszek, J. W.; Cheng, L.; Stewart, M. P.; Tour, J. M.; Natelson, D. *Phys. Rev. Lett.* **2004**, *93*, 266802/1-266802/4.

(49) Hipps, K. W.; Mazur, U. *J. Phys. Chem. B* **2000**, *104*, 4707-4710.

(50) Landauer, R. *Ibm Journal of Research and Development* **1957**, *1*, 223-231.

(51) Haiss, W.; van Zalinge, H.; Bethell, D.; Ulstrup, J.; Schiffrin, D. J.; Nichols, R. J. *Faraday Discuss.* **2006**, *131*, 253-264.

(52) Li, X. L.; He, J.; Hihath, J.; Xu, B. Q.; Lindsay, S. M.; Tao, N. J. *J. Am. Chem. Soc.* **2006**, *128*, 2135-2141.

(53) Quek, S. Y.; Choi, H. J.; Louie, S. G.; Neaton, J. B. *Nano Lett.* **2009**, *9*, 3949-3953.

(54) Venkataraman, L.; Klare, J. E.; Nuckolls, C.; Hybertsen, M. S.; Steigerwald, M. L. *Nature* **2006**, *442*, 904-907.

(55) He, J.; Chen, F.; Li, J.; Sankey, O. F.; Terazono, Y.; Herrero, C.; Gust, D.; Moore, T. A.; Moore, A. L.; Lindsay, S. M. *J. Am. Chem. Soc.* **2005**, *127*, 1384-1385.

(56) Segal, D.; Nitzan, A.; Ratner, M.; Davis, W. B. *J. Phys. Chem. B* **2000**, *104*, 2790-2793.

(57) Wang, W. Y.; Lee, T.; Reed, M. A. *Rep. Prog. Phys.* **2005**, *68*, 523-544.

(58) Lu, Q.; Liu, K.; Zhang, H. M.; Du, Z. B.; Wang, X. H.; Wang, F. S. *ACS Nano* **2009**, *3*, 3861-3868.

(59) Li, X. L.; Hihath, J.; Chen, F.; Masuda, T.; Zang, L.; Tao, N. J. *J. Am. Chem. Soc.* **2007**, *129*, 11535-11542.

(60) Sedghi, G.; Sawada, K.; Esdaile, L. J.; Hoffmann, M.; Anderson, H. L.; Bethell, D.; Haiss, W.; Higgins, S. J.; Nichols, R. J. *J. Am. Chem. Soc.* **2008**, *130*, 8582-8583.

(61) Selzer, Y.; Cabassi, M. A.; Mayer, T. S.; Allara, D. L. *J. Am. Chem. Soc.* **2004**, *126*, 4052-4053.

(62) Gorman, C. B.; Carroll, R. L.; Fuierer, R. R. *Langmuir* **2001**, *17*, 6923-6930.

(63) Tao, N. J. *Phys. Rev. Lett.* **1996**, *76*, 4066-4069.

(64) Lin, H. W.; Wang, X. H.; Zhao, X. J.; Li, J.; Wang, F. S. *Synth. Met.* **2003**, *135*, 239-240.

(65) Mayor, M.; von Hanisch, C.; Weber, H. B.; Reichert, J.; Beckmann, D. *Angew. Chem. Int. Ed.* **2002**, *41*, 1183-1186.

(66) Schull, T. L.; Kushmerick, J. G.; Patterson, C. H.; George, C.; Moore, M. H.; Pollack, S. K.; Shashidhar, R. *J. Am. Chem. Soc.* **2003**, *125*, 3202-3203.

(67) Liang, W. J.; Shores, M. P.; Bockrath, M.; Long, J. R.; Park, H. *Nature* **2002**, *417*, 725-729.

(68) Park, J.; Pasupathy, A. N.; Goldsmith, J. I.; Chang, C.; Yaish, Y.; Petta, J. R.; Rinkoski, M.; Sethna, J. P.; Abruna, H. D.; McEuen, P. L.; Ralph, D. C. *Nature* **2002**, *417*, 722-725.

(69) Xiao, X. Y.; Brune, D.; He, J.; Lindsay, S.; Gorman, C. B.; Tao, N. J. *Chem. Phys.* **2006**, *326*, 138-143.

(70) Liu, K.; Wang, X. H.; Wang, F. S. *ACS Nano* **2008**, *2*, 2315-2323.

(71) Ruben, M.; Landa, A.; Lortscher, E.; Riel, H.; Mayor, M.; Gorls, H.; Weber, H. B.; Arnold, A.; Evers, F. *Small* **2008**, *4*, 2229-2235.

(72) Tuccitto, N.; Ferri, V.; Cavazzini, M.; Quici, S.; Zhavnerko, G.; Licciardello, A.; Rampi, M. A. *Nature Mater.* **2009**, *8*, 41-46.

(73) Kim, B.; Beebe, J. M.; Olivier, C.; Rigaut, S.; Touchard, D.; Kushmerick, J. G.; Zhu, X. Y.; Frisbie, C. D. *J. Phys. Chem. C* **2007**, *111*, 7521-7526.

(74) Aviram, A.; Roland, P. *Molecular Electronics: Science and Technology* **1998**, *852*, 339-348.

(75) Renz, M.; Theilacker, K.; Lambert, C.; Kaupp, M. *J. Am. Chem. Soc.* **2009**, *131*, 16292-16302.

(76) Demadis, D. D.; Hartshorn, C. M.; Meyer, T. J. *Chem. Rev.* **2001**, *101*, 2655-2685.

(77) Kaim, W.; Klein, A.; Glockle, M. *Acc. Chem. Res.* **2000**, *33*, 755-763.

(78) Paul, F.; Lapinte, C. *Coord. Chem. Rev.* **1998**, *178-180*, 431-509.

(79) Richardson, D. E.; Taube, H. *Coord. Chem. Rev.* **1984**, *60*, 107-129.

(80) Ward, M. D.; McCleverty, J. A. *Dalton Trans.* **2002**, 275-288.

(81) Astruc, D. *Acc. Chem. Res.* **1997**, *30*, 383-391.

(82) Ward, M. D. *Chem. Soc. Rev.* **1995**, 121-134.

(83) Benniston, A. C. *Chem. Soc. Rev.* **2004**, *33*, 573-578.

(84) Barlow, S.; O'Hare, D. *Chem. Rev.* **1997**, *97*, 637-669.

(85) Kaim, W.; Lahiri, G. K. *Angew. Chem. Int. Ed.* **2007**, *46*, 1778-1796.

(86) Creutz, C.; Taube, H. *J. Am. Chem. Soc.* **1969**, *91*, 3988-3989.

(87) Lay, P. A.; Magnuson, R. H.; Taube, H. *Inorg. Chem.* **1988**, *27*, 2364-2371.

(88) Creutz, C.; Taube, H. *J. Am. Chem. Soc.* **1973**, *95*, 1086-1094.

(89) Hush, N. S. *Prog. Inorg. Chem.* **1967**, *8*, 391-444.

(90) Brunschwig, B. S.; Sutin, N. *Coord. Chem. Rev.* **1999**, *187*, 233-254.

(91) Sutin, N. *Prog. Inorg. Chem.* **1983**, *30*, 441-498.

(92) Murrell, J. N. *J. Am. Chem. Soc.* **1959**, *81*, 5037-5043.

(93) Salaymeh, F.; Berhane, S.; Yusof, R.; de la Rosa, R.; Fung, E. Y.; Matamoros, R.; Lau, K. W.; Zheng, Q.; Kober, E. M.; Curtis, J. C. *Inorg. Chem.* **1993**, *32*, 3895-3908.

(94) Christensenand, P. A.; Hamnett, A. *Techniques and Mechanisms in Electrochemistry* Blackie Academic & Professional, An Imprint Of Chapman & Hall Glasgow 1994.

(95) Geiger, W. E. *Organometallics* **2007**, *26*, 5738-5765.

(96) Kissinger, P. T.; Helneman, W. R. *J. Chem. Educ.* **1983**, *60*, 702-706.

(97) Mabbott, G. A. *J. Chem. Educ.* **1983**, *60*, 697-702.

(98) Palaniappan, V.; Singru, R. M.; Agarwala, U. C. *Inorg. Chem.* **1988**, *27*, 181-187.

(99) Ernst, S.; Kasack, V.; Kaim, W. *Inorg. Chem.* **1988**, *27*, 1146-1148.

(100) Barriere, F.; Geiger, W. E. *J. Am. Chem. Soc.* **2006**, *128*, 3980-3989.

(101) Geiger, W. E.; Barriere, F. *Acc. Chem. Res.* **2010**, *43,* 1030-1039.

(102) Demadis, K. D.; El-Samanody, E. S.; Coia, G. M.; Meyer, T. J. *J. Am. Chem. Soc.* **1999**, *121*, 535-544.

(103) Drago, R. S. *Physical methods in chemistry (Russian translation)*; Mir: Moscow, 1981.

(104) Brady, M.; Weng, W. Q.; Zhou, Y. L.; Seyler, J. W.; Amoroso, A. J.; Arif, A. M.; Bohme, M.; Frenking, G.; Gladysz, J. A. *J. Am. Chem. Soc.* **1997**, *119*, 775-788.

(105) Thompson, A. M. W. C.; Gatteschi, D.; McCleverty, J. A.; Navas, J. A.; Rentschler, E.; Ward, M. D. *Inorg. Chem.* **1996**, *35*, 2701-2703.

(106) Ung, V. A.; Thompson, A. M. W. C.; Bardwell, D. A.; Gatteschi, D.; Jeffery, J. C.; McCleverty, J. A.; Totti, F.; Ward, M. D. *Inorg. Chem.* **1997**, *36*, 3447-3454.

(107) Stobie, K. M.; Bell, Z. R.; Munhoven, T. W.; Maher, P. J.; McCleverty, J. A.; Ward, M. D.; McInnes, E. J. L.; Totti, F.; Gatteschi, D. *Dalton Trans.* **2003**, 36-45.

(108) McCleverty, J. A.; Ward, M. D. *Acc. Chem. Res.* **1998**, *31*, 842-851.

(109) Robin, M. B.; Day, P. *Adv. Inorg. Chem. Radiochem.* **1967**, *10*, 247-422.

(110) Sutton, J. E.; Taube, H. *Inorg. Chem.* **1981**, *20*, 3125-3134.

(111) Kasack, V.; Kaim, W.; Binder, H.; Jordanov, J.; Roth, E. *Inorg. Chem.* **1995**, *34*, 1924-1933.

(112) Scheiring, T.; Kaim, W.; Olabe, J. A.; Parise, A. R.; Fiedler, J. *Inorg. Chim. Acta* **2000**, *300*, 125-130.

(113) Marcus, R. A. *Rev. Mod. Phys.* **1993**, *65*, 599-610.

(114) Bartik, B.; Dembinski, R.; Bartik, T.; Arif, A. M.; Gladysz, J. A. *New J. Chem.* **1997**, *21*, 739-750.

(115) Bartik, T.; Bartik, B.; Brady, M.; Dembinski, R.; Gladysz, J. A. *Angew. Chem. Int. Ed. Engl.* **1996**, *35*, 414-417.

(116) Bartik, T.; Weng, W. Q.; Ramsden, J. A.; Szafert, S.; Falloon, S. B.; Arif, A. M.; Gladysz, J. A. *J. Am. Chem. Soc.* **1998**, *120*, 11071-11081.

(117) Dembinski, R.; Bartik, T.; Bartik, B.; Jaeger, M.; Gladysz, J. A. *J. Am. Chem. Soc.* **2000**, *122*, 810-822.

(118) Herrmann, C.; Neugebauer, J.; Gladysz, J. A.; Reiher, M. *Inorg. Chem.* **2005**, *44*, 6174-6182.

(119) Horn, C. R.; Gladysz, J. A. *Eur. J. Inorg. Chem.* **2003**, 2211-2218.

(120) Jiao, H. J.; Costuas, K.; Gladysz, J. A.; Halet, J. F.; Guillemot, M.; Toupet, L.; Paul, F.; Lapinte, C. *J. Am. Chem. Soc.* **2003**, *125*, 9511-9522.

(121) Paul, F.; Meyer, W. E.; Toupet, L.; Jiao, H. J.; Gladysz, J. A.; Lapinte, C. *J. Am. Chem. Soc.* **2000**, *122*, 9405-9414.

(122) Weng, W. G.; Bartik, T.; Gladysz, J. A. *Angew. Chem. Int. Ed. Engl.* **1994**, *33*, 2199-2202.

(123) Zhou, Y. L.; Seyler, J. W.; Weng, W. Q.; Arif, A. M.; Gladysz, J. A. *J. Am. Chem. Soc.* **1993**, *115*, 8509-8510.

(124) Ramsden, J. A.; Weng, W. Q.; Arif, A. M.; Gladysz, J. A. *J. Am. Chem. Soc.* **1992**, *114*, 5890-5891.

(125) Lenarvor, N.; Toupet, L.; Lapinte, C. *J. Am. Chem. Soc.* **1995**, *117*, 7129-7138.

(126) Coat, F.; Lapinte, C. *Organometallics* **1996**, *15*, 477-479.

(127) Ibn Ghazala, S.; Paul, F.; Toupet, L.; Roisnel, T.; Hapiot, P.; Lapinte, C. *J. Am. Chem. Soc.* **2006**, *128*, 2463-2476.

(128) Coat, F.; Paul, F.; Lapinte, C.; Toupet, L.; Costuas, K.; Halet, J. F. *J. Organomet. Chem.* **2003**, *683*, 368-378.

(129) Justaud, F.; Argouarch, G.; Ibn Ghazala, S.; Toupet, L.; Paul, F.; Lapinte, C. *Organometallics* **2008**, *27*, 4260-4264.

(130) Tanaka, Y.; Shaw-Taberlet, J. A.; Justaud, F.; Cador, O.; Roisnel, T.; Akita, M.; Hamon, J. R.; Lapinte, C. *Organometallics* **2009**, *28*, 4656-4669.

(131) Sakurai, A.; Akita, M.; Moro-oka, Y. *Organometallics* **1999**, *18*, 3241-3244.

(132) Akita, M.; Tanaka, Y.; Naitoh, C.; Ozawa, T.; Hayashi, N.; Takeshita, M.; Inagaki, A.; Chung, M. C. *Organometallics* **2006**, *25*, 5261-5275.

(133) Akita, M.; Chung, M. C.; Sakurai, A.; Sugimoto, S.; Terada, M.; Tanaka, M.; Morooka, Y. *Organometallics* **1997**, *16*, 4882-4888.

(134) Kheradmandan, S.; Heinze, K.; Schmalle, H. W.; Berke, H. *Angew. Chem. Int. Ed.* **1999**, *38*, 2270-2273.

(135) Venkatesan, K.; Fox, T.; Schmalle, H. W.; Berke, H. *Organometallics* **2005**, *24*, 2834-2847.

(136) Fernandez, F. J.; Blacque, O.; Alfonso, M.; Berke, H. *Chem. Commun.* **2001**, 1266-1267.

(137) Bruce, M. I.; Low, P. J.; Costuas, K.; Halet, J. F.; Best, S. P.; Heath, G. A. *J. Am. Chem. Soc.* **2000**, *122*, 1949-1962.

(138) Antonova, A. B.; Bruce, M. I.; Elis, B. G.; Gaudio, M.; Humphrey, P. A.; Jevric, M.; Melino, G.; Nicholson, B. K.; Perkins, G. J.; Skelton, B. W.; Stapleton, B.; White, A. H.; Zaitseva, N. N. *Chem. Commun.* **2004**, 960-961.

(139) Rigaut, S.; Le Pichon, L.; Daran, J. C.; Touchard, D.; Dixneuf, P. H. *Chem. Commun.* **2001**, 1206-1207.

(140) Rigaut, S.; Massue, J.; Touchard, D.; Fillaut, J. L.; Golhen, S.; Dixneuf, P. H. *Angew. Chem. Int. Ed.* **2002**, *41*, 4513-4517.

(141) Rigaut, S.; Perruchon, J.; Le Pichon, L.; Touchard, D.; Dixneuf, P. H. *J. Organomet. Chem.* **2003**, *670*, 37-44.

(142) Qi, H.; Gupta, A.; Noll, B. C.; Snider, G. L.; Lu, Y. H.; Lent, C.; Fehlner, T. P. *J. Am. Chem. Soc.* **2005**, *127*, 15218-15227.

(143) Woodworth, B. E.; White, P. S.; Templeton, J. L. *J. Am. Chem. Soc.* **1997**, *119*, 828-829.

(144) Woodworth, B. E.; White, P. S.; Templeton, J. L. *J. Am. Chem. Soc.* **1998**, *120*, 9028-9033.

(145) Sun, J.; Shaner, S. E.; Jones, M. K.; O'Hanlon, D. C.; Mugridge, J. S.; Hopkins, M. D. *Inorg. Chem.* **2010**, *49*, 1687-1698.

(146) Kheradmandan, S.; Venkatesan, K.; Blacque, O.; Schmalle, H. W.; Berke, H. *Chem. Eur. J.* **2004**, *10*, 4872-4885.

(147) Re, N.; Sgamellotti, A.; Floriani, C. *Organometallics* **2000**, *19*, 1115-1122.

(148) Szafert, S.; Gladysz, J. A. *Chem. Rev.* **2003**, *103*, 4175-4206.

(149) Zhuravlev, F.; Gladysz, J. A. *Chem. Eur. J.* **2004**, *10*, 6510-6522.

(150) Chung, M. C.; Gu, X. H.; Etzenhouser, B. A.; Spuches, A. M.; Rye, P. T.; Seetharaman, S. K.; Rose, D. J.; Zubieta, J.; Sponsler, M. B. *Organometallics* **2003**, *22*, 3485-3494.

(151) Frohnapfel, D. S.; Woodworth, B. E.; Thorp, H. H.; Templeton, J. L. *J. Phys. Chem. A* **1998**, *102*, 5665-5669.

(152) Bruce, M. I.; Costuas, K.; Davin, T.; Halet, J. F.; Kramarczuk, K. A.; Low, P. J.; Nicholson, B. K.; Perkins, G. J.; Roberts, R. L.; Skelton, B. W.; Smith, M. E.; White, A. H. *Dalton Trans.* **2007**, 5387-5399.

(153) Liang, M.; Maatta, E. A. *Inorg. Chem.* **1992**, *31*, 953-956.

(154) Bruce, M. I.; Ke, M. Z.; Low, P. J. *Chem. Commun.* **1996**, 2405-2406.

(155) Roberts, R. L.; Puschmann, H.; Howard, J. A. K.; Yamamoto, J. H.; Carty, A. J.; Low, P. J. *Dalton Trans.* **2003**, 1099-1105.

(156) Dewhurst, R. D.; Hill, A. F.; Willis, A. C. *Organometallics* **2005**, *24*, 3043-3046.

(157) Dewhurst, R. D.; Hill, A. F.; Smith, M. K. *Organometallics* **2005**, *24*, 5576-5580.

(158) Dewhurst, R. D.; Hill, A. F.; Willis, A. C. *Organometallics* **2009**, *28*, 4735-4740.

(159) Dewhurst, R. D.; Hill, A. F.; Rae, A. D.; Willis, A. C. *Organometallics* **2005**, *24*, 4703-4706.

(160) Crause, C.; Gorls, H.; Lotz, S. *Dalton Trans.* **2005**, 1649-1657.

(161) Ipaktshi, J.; Munz, F. *Eur. J. Inorg. Chem.* **2006**, 2078-2082.

(162) Wagner, N. L.; Laib, F. E.; Bennett, D. W. *Inorg. Chem. Commun.* **2000**, *3*, 87-90.

(163) Hu, J. S.; Sun, J. B.; Hopkins, M. D.; Rosenbaum, T. F. *J. Phys. Condens. Matter* **2006**, *18*, 10837-10841.

(164) Filippou, A. C.; Schnakenburg, G.; Philippopoulos, A. I.; Weidemann, N. *Angew. Chem. Int. Ed.* **2005**, *44*, 5979-5985.

(165) Hills, A.; Hughes, D. L.; Kashef, N.; Lemos, M. A. N. D. A.; Pombeiro, A. J. L.; Richards, R. L. *J. Chem. Soc., Dalton Trans.* **1992**, 1775-1782.

(166) Hills, A.; Hughes, D. L.; Kashef, N.; Richards, R. L.; Lemos, M. A. N. D. A.; Pombeiro, A. J. L. *J. Organomet. Chem.* **1988**, *350*, C4-C7.

(167) Nakamura, G.; Harada, Y.; Mizobe, Y.; Hidai, M. *Bull. Chem. Soc. Jpn.* **1996**, *69*, 3305-3315.

(168) Birdwhistell, K. R.; Burgmayer, S. J. N.; Templeton, J. L. *J. Am. Chem. Soc.* **1983**, *105*, 7789-7790.

(169) Birdwhistell, K. R.; Tonker, T. L.; Templeton, J. L. *J. Am. Chem. Soc.* **1985**, *107*, 4474-4483.

(170) Roth, G.; Fischer, H. *Organometallics* **1996**, *15*, 1139-1145.

(171) Dede, M.; Drexler, M.; Fischer, H. *Organometallics* **2007**, *26*, 4294-4299.

(172) Fischer, H.; Szesni, N. *Coord. Chem. Rev.* **2004**, *248*, 1659-1677.

(173) Birdwhistell, K. R.; Templeton, J. L. *Organometallics* **1985**, *4*, 2062-2064.

(174) Feng, S. G.; White, P. S.; Templeton, J. L. *J. Am. Chem. Soc.* **1992**, *114*, 2951-2960.

(175) Schlientz, W. J.; Ruff, J. K. *J. Chem. Soc. A* **1971**, 1139-1140.

(176) Bruce, M. I.; Smith, M. E.; Skelton, B. W.; White, A. H. *J. Organomet. Chem.* **2001**, *637-639*, 484-499.

(177) Viola, E.; Lo Sterzo, C.; Crescenzi, R.; Frachey, G. *J. Organomet. Chem.* **1995**, *493*, C9-C13.

(178) Holmes, S. J.; Schrock, R. R.; Churchill, M. R.; Wasserman, H. J. *Organometallics* **1984**, *3*, 476-484.

(179) Manna, J.; Geib, S. J.; Hopkins, M. D. *J. Am. Chem. Soc.* **1992**, *114*, 9199-9200.

(180) John, K. D.; Hopkins, M. D. *Chem. Commun.* **1999**, 589-590.

(181) Pollagi, T. P.; Geib, S. J.; Hopkins, M. D. *J. Am. Chem. Soc.* **1994**, *116*, 6051-6052.

(182) Brison, H. A.; Pollagi, T. P.; Stoner, T. C.; Geib, S. J.; Hopkins, M. D. *Chem. Commun.* **1997**, 1263-1264.

(183) Stevenson, M. A.; Hopkins, M. D. *Organometallics* **1997**, *16*, 3572-3573.

(184) Mcdermott, G. A.; Dorries, A. M.; Mayr, A. *Organometallics* **1987**, *6*, 925-931.

(185) Yu, M. P. Y.; Cheung, K. K.; Mayr, A. *J. Chem. Soc.: Dalton Trans.* **1998**, 2373-2378.

(186) Bannwart, E.; Jacobsen, H.; Furno, F.; Berke, H. *Organometallics* **2000**, *19*, 3605-3619.

(187) Furno, F.; Fox, T.; Schmalle, H. W.; Berke, H. *Organometallics* **2000**, *19*, 3620-3630.

(188) Fischer, E. O.; Kalder, H. J.; Kohler, F. H. *J. Organomet. Chem.* **1974**, *81*, C23-C27.

(189) Schwenzer, B.; Schleu, J.; Burzlaff, N.; Karl, C.; Fischer, H. *J. Organomet. Chem.* **2002**, *641*, 134-141.

(190) Holmes, S. J.; Clark, D. N.; Turner, H. W.; Schrock, R. R. *J. Am. Chem. Soc.* **1982**, *104*, 6322-6329.

(191) Atagi, L. M.; Critchlow, S. C.; Mayer, J. M. *J. Am. Chem. Soc.* **1992**, *114*, 1483-1484.

(192) Chatt, J.; Pearman, A. J.; Richards, R. L. *Nature* **1975**, *253*, 39-40.

(193) Dilworth, J. R.; Richards, R. L. *Inorg. Synth.* **1990**, *28*, 33-43.

(194) Ishida, T.; Mizobe, Y.; Tanase, T.; Hidai, M. *Chem. Lett.* **1988**, 441-444.

(195) Ishida, T.; Mizobe, Y.; Tanase, T.; Hidai, M. *J. Organomet. Chem.* **1991**, *409*, 355-365.

(196) Birdwhistell, K. R.; Dema, A. C.; Li, X.; Lukehart, C. M.; Owen, M. D. *Inorg. Synth.* **1992**, *29*, 141-146.

(197) Enriquez, A. E.; White, P. S.; Templeton, J. L. *J. Am. Chem. Soc.* **2001**, *123*, 4992-5002.

(198) Desmond, T.; Lalor, F. J.; Ferguson, G.; Parvez, M. *J. Chem. Soc.: Chem. Commun.* **1983**, 457-459.

(199) Yu, M. P. Y.; Yam, V. W. W.; Cheung, K. K.; Mayr, A. *J. Organomet. Chem.* **2006**, *691*, 4514-4531.

(200) Semenov, S. N.; Blacque, O.; Fox, T.; Venkatesan, K.; Berke, H. *J. Am. Chem. Soc.* **2010**, *132*, 3115-3127.

(201) Semenov, S. N.; Taghipourian, S. F.; Blacque, O.; Fox, T.; Venkatesan, K.; Berke, H. *J. Am. Chem. Soc.* **2010**, *132*, 7584-7585.

(202) Li, Y. *unpublished results*.

(203) Hortholary, C.; Coudret, C. *J. Org. Chem.* **2003**, *68*, 2167-2174.

(204) Version 1.171.32.5 ed.; Oxford Diffraction Ltd: Abingdon, Oxfordshire, England.

(205) Sheldrick, G. M. *Acta Crystallogr.* **2008**, *A64*, 112-122.

(206) Spek, A. L. *J. Appl. Cryst.* **2003**, *36*, 7-13.

(207) Semenov, S. N.; Blacque, O.; Fox, T.; Venkatesan, K.; Berke, H. *Angew. Chem. Int. Ed.* **2009**, *48*, 5203-5206.

(208) Fritz, T.; Schmalle, H. W.; Blacque, O.; Venkatesan, K.; Berke, H. *Z. Anorg. Allg. Chem.* **2009**, *635*, 1391-1401.

APPENDIX

List of prepared metal complexes

Acetylide complexes

[*trans*-W(CO)(dppe)$_2$(C≡CPh)]

[*trans*-W(CO)(dppe)$_2$(C≡CSnMe$_3$)]

[*trans*-W(CO)(dppe)$_2$(C≡CSiMe$_3$)]

[*trans*-W(CO)(dppe)$_2$(C≡CC≡CH)][NBu$_4$]

[{*trans*-W(CO)(dppe)$_2$(C≡CC{=C(H)(C$_4$H$_6$*t*Bu)})}$_2$]

[IW(CO)$_3$(dppe)(C≡CPh)]

[{*trans*-W(CO)(dppe)$_2$(C≡CC{=C(H)(*p*-C$_6$H$_4$SCO*t*Bu)})}$_2$]

Li$_2$[(CO)$_3$(dppe)WC≡CC≡CW(CO)$_3$(dppe)]

Cumulenylidene complexes

[*cis*-W(CO)(dppe)$_2${C=C=C=C(SnMe$_3$)$_2$}]

[*cis*-W(CO)(dppe)$_2${C=C=C=C(SnMe$_3$)(SiMe$_3$)}]

[*cis*-W(CO)(dppe)$_2${C=C(SnMe$_3$)$_2$}]

[*cis*-W(CO)(dppe)$_2${C=C(SnMe$_3$)(Ph)}]

[*cis*-W(CO)(dppe)$_2${C=C=C=C(SnMe$_3$)(*p*-C$_6$H$_4$*t*Bu)}]

[*cis*-W(CO)(dppe)$_2${C=C=C=C(H)(*p*-C$_6$H$_4$*t*Bu)}]

[*cis*-W(CO)(dppe)$_2${C=C=C=C(SnMe$_3$)(*p*-C$_6$H$_4$SCO*t*Bu)}]

[*cis*-W(CO)(dppe)$_2${C=C=C=C(H)(*p*-C$_6$H$_4$SCO*t*Bu)}]

Carbyne complexes

[I(CO)$_2$(dppe)W≡CC≡CC≡W(CO)$_2$(dppe)I]

[Cl(CO)$_2$(dppe)W≡CC≡CC≡W(CO)$_2$(dppe)Cl]

[(SCN)(CO)$_2$(dppe)W≡CC≡CC≡W(CO)$_2$(dppe)(NCS)]

[(TfO)(CO)$_2$(dppe)W≡CC≡CC≡W(CO)$_2$(dppe)(OTf)]

[I(dppe)$_2$W≡CC≡CC≡W(dppe)$_2$I]

[I(dppe)$_2$W≡CC≡CC≡W(dppe)$_2$I][PF$_6$]

[I(dppe)$_2$W≡CC≡CC≡W(dppe)$_2$I][PF$_6$]$_2$

[I(dppe)$_2$W≡CC≡CC≡W(dppe)(CO)$_2$I]

[I(dppe)$_2$W≡CC≡CC≡W(dppe)(CO)$_2$I][PF$_6$]

[H(dppe)$_2$W≡CC≡CC≡W(dppe)$_2$H]

[I(CO)$_2$(dppe)W≡CC(CH$_3$)=C(CH$_3$)C≡W(CO)$_2$(dppe)I]

[$Cl(CO)_2(dppe)W{\equiv}CC(CH_3){=}C(CH_3)C{\equiv}W(CO)_2(dppe)Cl$]

[$(Me_3SiC{\equiv}CC{\equiv}C)(dppe)_2W{\equiv}CC{\equiv}CC{\equiv}W(dppe)_2(C{\equiv}CC{\equiv}CSiMe_3)$]

[$(HC{\equiv}CC{\equiv}C)(dppe)_2W{\equiv}CC{\equiv}CC{\equiv}W(dppe)_2(C{\equiv}CC{\equiv}CH)$]

[$(Me_3SnC{\equiv}CC{\equiv}C)(dppe)_2W{\equiv}CC{\equiv}CC{\equiv}W(dppe)_2(C{\equiv}CC{\equiv}CSnMe_3)$]

[$Cl(depe)_2Fe(C{\equiv}CC{\equiv}C)(dppe)_2W{\equiv}CC{\equiv}CC{\equiv}W(dppe)_2(C{\equiv}CC{\equiv}C)Fe(depe)_2Cl$]

[$Cl(depe)_2Fe(C{\equiv}CC{\equiv}C)(dppe)_2W{\equiv}CC{\equiv}CC{\equiv}W(dppe)_2(C{\equiv}CC{\equiv}C)Fe(depe)_2Cl][PF_6$]

[$(t\text{BuCOSC}_6H_4C{\equiv}CC{\equiv}C)(dppe)_2W{\equiv}CC{\equiv}CC{\equiv}W(dppe)_2(C{\equiv}CC{\equiv}CC_6H_4SCOt\text{Bu})$]

[$(PhC{\equiv}C)(dppe)_2W{\equiv}CC{\equiv}CC{\equiv}W(dppe)_2(C{\equiv}CPh)$]

[$(Me_3SiC{\equiv}C)(dppe)_2W{\equiv}CC{\equiv}CC{\equiv}W(dppe)_2(C{\equiv}CSiMe_3)$]

Abstract

The work is devoted to the synthesis and study of tungsten based conjugated molecules for potential applications in molecular electronics. Metal containing molecular conductors are important target for studies because the introduction of the metal center could lead to enhanced conductivity and provides more possibilities to control electric current by redox switching and switch of spin states in comparison with pure organic molecules. However, introduction of metal in conducting molecules very often causes undesirable decrease in the chemical and thermal stability. The [*trans*-W(dppe)$_2$] (1,2-Bis(diphenylphosphinoethane)) fragment was expected to combine stability and suitable electrochemical properties. The conjugated molecules based on such fragment were target of this study.

During this work tungsten butatrienylidenes and vinylidenes were synthesized. We found that H-substituted butatrienylidenes could be separated in the solid state, however dimerize in the solution forming complex containing a 2,3-diethynyl-butadiene cross-conjugated system. We developed novel synthetic access to the fully dppe substituted C_4 - bridged biscarbyne complex [I(dppe)$_2$WC$_4$W(dppe)$_2$I] with an optimum combination of stability and electrochemical properties. The iodine ligands in this complex was substituted with butadiyne ligands by thallium activated reactions forming compounds with unique p/d conjugated system directly involving metal orbitals into the conjugation.

The studies of electronic interaction between metal centers in MV complexes showed that: 1,3-diethynyl-butadiene system provided only weak interactions between the tungsten centers probably due to low electron delocalization in the bridge; biscarbyne system has only moderate interaction of the highest occupied metal centered orbitals due to the orthogonality of the δ type d_{xy} orbitals and the π type orbitals of the bridge; {(C≡C)$_2$[W]≡C(C≡C)C≡[W](C≡C)$_2$} system mediates strong communication between iron centers over 24 Å distance.

On the basis of the physical studies, we concluded that the ditungstenatetradecaheptayne system is the most promising candidate for single electron conductance studies. The 2,3-diethynyl-butadiene system did not show strong communication between the metal centers but is interesting due to its cross-conjugation effect. To study such type of complexes on the molecular level compounds suitable for single molecule conductance measurements [{trans-W(CO)(dppe)$_2$(C≡C−C{=C(H)(p-C$_6$H$_4$SCO*t*Bu)})$_2$] and [(*t*BuCOSC$_6$H$_4$C$_4$)(dppe)$_2$W(C$_4$)W(dppe)$_2$(C$_4$C$_6$H$_4$SCO*t*Bu)] were obtained.

Overall, the work has contributed to the fields of metal-organic chemistry, the physics of electronic interaction in mixed-valence complexes and to the synthesis of compounds for single molecular studies.

Zusammenfassung

Die vorliegende Arbeit behandelt die Synthese und Untersuchung von konjugierten wolframhaltigen Systemen, die Anwendungen in der Molekularelektronik finden können. Das Interesse an den molekularen metallhaltigen Stromleitern lag im auf ihre höhere Leitfähigkeit im Vergleich zu rein organischen Molekülen, und war ausserdem durch die Möglichkeit, die Stromstärke durch die Oxidationsstufe und Spinzustände zu kontrollieren, gegeben. Der Einbau von Metallzentren lührt oft zur unerwünschten Herabsetzung der thermischen und chemischen Stabilität der Moleküle. Deshalb ist die Auswahl des metallischen Zentrums kritisch zu bewerten. Unter Berücksichtigung aller Aspekte wurde in dieser Arbeit Wolfram als metallisches Zentrum mit einer Phosphorliganden umgebung gewählt.

Im Laufe der experimentellen Arbeiten wurden zum ersten Mal C_4-Cummulenylidene min Wolfram zentren synthetisiert. Es wurde festgestellt, dass die monosubstituierten Derivate dieses Typs im Festkörper relativ stabil sind, während sie in Lösung dimerisiere unter Bildung eines 2,3-Diethinylbuta-1,3-dien Komplexes [{*trans*-W(CO)(dppe)$_2$(C≡C−C{=C(H)(*p*-C$_6$H$_4$*t*Bu)})}$_2$]. Eine neue Synthesemethode für die C_4-Dicarbin, Einheiten ermöglichte es, einen chemisch inerten Komplex [I(dppe)$_2$WC$_4$W(dppe)$_2$I] mit reversibler Oxidations/Reduktions beiden Zentren charakteristischen herzustellen. Durch Substitution der terminalen Iodatome durch Acetylen-Liganden konnten die neuen Verbindungen isoliert werden, die einen einzigartigen Typ von π-System (mit unmittelbarer Teilnahme der d-Metallorbitale an der Konjugation) besitzen.

Die Untersuchung der Elektronenwechselwirkung in Komplexen mit gemischter Wertigkeit (Valenz), welche als Derivate der obengenannten konjugierten Systeme angesehen werden konnen, hat gezeigt, dass die verbrückende 2,3-Ethinylbuta-1,3-dien-Gruppe eine schwache Wechselwirkung zwischen den Wolframzentren ermöglicht. Eine stärkere Wechselwirkung wurde in Dicarbinkomplexen beobachtet, während Komplexe mit {(C≡C)$_2$[W]≡C(C≡C)C≡[W](C≡C)$_2$}- Polyin-System die stärkste Wechselwirkung zwischen terminalen Gruppen zeigten.

Auf Grund der erhaltenen Daten lässt sich die Schlussfolgerung treffen, das die Systeme, die 2,3-ethinylbuta-1,3-dien-Ligand bzw. Diwolframpolyine enthalten, vom grössten praktischen und fundamentalen Interesse sind. Erstere auf grund der Kreuzkonjugation und letztere wegen der hohen Effektivität als molekulare Leiter für die elektronischen Wechselwirkung, gekoppelt mit hoher Stabilität. Für die Untersuchung dieser molekularen Systeme wurden die entsprechenden Komplexe mit terminalen Thiopivalat-Gruppen [{*trans*-W(CO)(dppe)$_2$(C≡C−C{=C(H)(*p*-C$_6$H$_4$SCO*t*Bu)})}$_2$] und

[(*t*BuCOSC$_6$H$_4$C$_4$)(dppe)$_2$W(C$_4$)W(dppe)$_2$(C$_4$C$_6$H$_4$SCO*t*Bu)] synthetisiert, welche für die Bindung an Mikro-Goldelektroden notwendig sind.

Zusammenfassend lässt sich sagen, dass diese Ergebnisse wesentlich zur metallorganischen Wolframchemie, sowie zur Untersuchung der Elektronenwechselwirkung in Komplexen mit gemischter Wertigkeit (Valenz) und neuen Typen von Brückengruppen beitragen. Die einzigartigen Verbindungen für die Untersuchungen der physikalischen Eigenschaften auf molekularen Niveau und einzigartig.

CURRICULUM VITAE

Mr. Sergey N. Semenov

Institute of Inorganic Chemistry, University of Zürich, Winterthurerstr. 190

8057 Zürich, Switzerland

Tel. (+41) 44-6354696; Email: semenov@aci.uzh.ch

1. CHRONOLOGY

1.1 Birthplace and Date; Nationality: 20.06.1984 in Podolsk, Moscow region, USSR; Russian.

1.2 Education

School	Location	Subject	Dates	Degree
University of Zürich	Zürich, Switzerland	Organometallic Chemistry	2006 – 2010	Ph.D. (with honors)
Moscow State University	Moscow, Russia	Chemistry (with inorganic chemistry specialization)	2001 – 2006	M.S. (with honors)

1.3 Professional positions

Position	University	Location	Department	Dates
Teaching/Research assistant	University of Zürich	Zürich, Switzerland	Institute of Inorganic Chemistry	2006 – 2010
Visiting Scientist	University of Camerino	Camerino, Italy	Chemistry	2006 (August)
Research assistant	Moscow State University	Moscow, Russia	Chemistry	2002 – 2006
Teacher in the "School for Young chemists"	Moscow State University	Moscow, Russia	Chemistry	2005 – 2006

2. RESEARCH

2.1 Master Thesis

Title: "Terbium and Europium complexes with new 4-acylpyrazolones: synthesis, structure and luminescent properties."

Supervisor: Assoc. Prof. Dr. Andrey Drozdov, Moscow State University, Moscow, Russia

Description: This work has been focused on the Rare Earth Metals (REM) complexes with β-diketones and, particularly, acylpyrazolones as organic ligands. In particular: (i) Reactions of Europium and Terbium acylpyrazolonates with different ancillary ligands such as bipyridyl's, phenanthrolines, phosphine oxides; (ii) Bis-acylpyrazolones as ligands for multinuclear supramolecular systems. (iii) Luminescent spectroscopy for Europium and Terbium complexes.

2.2 Doctoral Work

Title: "Development Of Conjugated Mono- And Polynuclear Tungsten Organometallic Complexes For Potential Application In Molecular Electronics"

Supervisor: Prof. Dr. Heinz Berke, University of Zürich, Zürich, Switzerland

Description: The main directions in this research are: (i) Design of long conjugated molecules based on binuclear C4 – bridged tungsten carbynes; (ii) Chemistry of tungsten C4 cumulenes; (iii) Electron transfer in Mixed-Valence complexes (iv) Design of metalorganic molecules suitable for single molecular conductance measurements.

2.3 Research interests

Rare Earth Metals (REM) complexes with β-diketones; Supramolecular assembles from metal ions and polydentate ligands; Luminescent properties of Lanthanides complexes

High energetic materials

Acetylenes and longer polyynes chemistry

Tungsten metalorganic chemistry (mainly acetylides, cumulenes and carbynes)

Mixed-Valence complexes; Electron transfer in single molecule; Molecular electronics

Crystallography

3. PROFESSIONAL EXPERIENCE

3.1 Experimental skills

Synthetic organic chemistry

Metalorganic synthesis in inert atmosphere (Schlenk and Glove-Box techniques)

Handling and interpreting data from the following instruments: Single crystal diffractometer (including structure solution); IR – spectrometers; NMR – spectrometers (Varian and Bruker); Luminescent spectrometer; UV-Vis spectrometer; EPR spectrometer; SQUID magnetometer; Electrochemistry system (Cyclic Voltammetry technique). Responsible for Electrochemical, EPR and SQUID measurements in Prof. H. Berke group.

3.2 Writing experience

Writing of research articles

Writing of research grant proposals

4. PROFESSIONAL ACTIVITIES

Reviewer**:** *Dalton Transactions* and *Crystal Engineering Communications* (2008-present) in regular order, *Journal of Materials Chemistry*, *Physical Chemistry Chemical Physics* and *Journal of Molecular Structure* in single instances.

5. THEACHING

Teacher in chemistry in the "School for Young chemists" (12-14 years old pupils).

Supervisor of course works in inorganic chemistry of 1st year students in Moscow State University

Assistant in Inorganic chemistry laboratory course 1 in University of Zürich

Supervisor of projects in Inorganic chemistry laboratory course 2 in University of Zürich

6. AWARDS and RESEARCH GRANTS

6.1 Research Grants

Forschungskredit 2008 research grant for 11 month financial support from University of Zürich. Project: "Tungsten Organometallic Chemistry for Potential Molecular Electronics Applications".

6.2 Awards

Third award at Samsung idea contest 2005, Moscow, Russia

Grant for talented students, Ph.D. students and young scientists of Lomonosov Moscow State University 2006, for cycle of articles "Terbium and Europium complexes with new 4-acylpyrazolones: synthesis, structure and luminescent properties"

7. LANGUAGES

Russian (native), English.

8. LIST OF PUBLICATIONS

1. **Sergey N. Semenov**, Olivier Blacque, Thomas Fox, Koushik Venkatesan, Heinz Berke "[W(CO)(dppe)$_2$] Cumulenylidene and Acetylide Complexes Accessed via Stannylated Acetylenes and Butadiynes" // *Available online in Organometallics*.
2. **Sergey N. Semenov**, Shiva F. Taghipourian, Olivier Blacque, Thomas Fox, Koushik Venkatesan, Heinz Berke "An Iron Capped Metalorganic Polyyne {[Fe](C≡C)$_2$[W]≡CC≡CC≡[W](C≡C)$_2$[Fe]}" // *J. Am. Chem. Soc.,* **2010**, *132*, 7584-7585.
3. **Sergey N. Semenov**, Olivier Blacque, Thomas Fox, Koushik Venkatesan, Heinz Berke "Electronic Communication in Dinuclear C_4-Bridged Tungsten Complexes" // *J. Am. Chem. Soc.,* **2010**, 132, 3115-3127.
4. **Sergey N. Semenov**, Olivier Blacque, Thomas Fox, Koushik Venkatesan, Heinz Berke "Self-Coupling of a 4-H-Butatrienylidene Tungsten Complex" // *Angew. Chem., Int. Ed.* **2009**, 48, 5203-5206.
5. Oxana Kotova, **Sergey Semenov**, Svetlana Eliseeva, Sergey Troyanov, Konstantin Lyssenko, Natalia Kuzmina "New Helical Zinc Complexes with Schiff Base Derivatives of β -Diketonates or β -Keto Esters and Ethylenediamine" // *Eur. J. Inorg. Chem.*, **2009**, 23, 3467-3474.
6. **Sergey N. Semenov**,***** Andrey Yu. Rogachev, Svetlana V. Eliseeva, Claudio Pettinari, Fabio Marchetti, Andrey A. Drozdov, Sergey I. Troyanov "First Direct Assembly of Molecular Helical Complexes into Coordination Polymer" // *Chem. Commun.,* **2008**, 1992-1994.
7. Svetlana V. Eliseeva, Oxana V. Kotova, Frédéric Gumy, **Sergey N. Semenov**, Vadim G. Kessler, Leonid S. Lepnev, Jean-Claude G. Bünzli, Natalia P. Kuzmina "Role of the Ancillary Ligand N,N-Dimethylaminoethanol in the Sensitization of Eu^{III} And Tb^{III} Luminescence In Dimeric β-Diketonates" // *J. Phys. Chem. A*, **2008**, 112, 3614-3626.
8. **Sergey N. Semenov**,***** Andrey Yu. Rogachev, Svetlana V. Eliseeva, Yury A. Belousov, Andrey A. Drozdov, Sergey I. Troyanov "5-nitroaminotetrazole as Building Block for Extended Network Structures: Syntheses and Crystal Structures of a Number of Heavy Metal Derivatives" // *Polyhedron*, **2007**, 26, 4899-4907.
9. Claudio Pettinari, Fabio Marchetti, Riccardo Pettinari, Paolo Natanti, Andrey Drozdov, **Sergey Semenov**, Sergey I. Troyanov, Vladislav Zolin "Syntheses, Spectroscopic Characterization and X-Ray Structural Studies of Lanthanide Complexes with Adamantyl Substituted 4-Acylpyrazol-5-One" // *Inorg. Chem. Acta.*, **2006**, 359, 4063-4070.
10. Claudio Pettinari, Fabio Marchetti, Riccardo Pettinari, Andrey Drozdov, **Sergey Semenov**, Sergey I. Troyanov, Vladislav Zolin "A New Rare-Earth Metal Acylpyrazolonate

Containing the Zundel Ion $H_5O_2^+$ Stabilized by Strong Hydrogen Bonding" // *Inorg. Chem. Commun.*, **2006**, 9, 634-637.

11. **Sergey N. Semenov**,* Egor Yu. Maltsev, Ivan G. Timokhin, Sergey I. Troyanov, Andrey A. Drozdov "The Crystal Structure of Two Hydrated Tin Chlorides $SnCl_4 \cdot 2H_2O$ And $SnCl_4 \cdot 3H_2O$" // *Mend. Commun.*, **2005**, 205-207.

12. Claudio Pettinari, Riccardo Pettinari, Fabio Marchetti, Andrey Drozdov, Ivan Timokhin, **Sergey Semenov**, Sergey I. Troyanov "The Role of Reaction Medium on the Coordination Environment of Terbium in Complexes with 4-Acylpyrazol-5-Ones" // *Inorg. Chem. Commun.*, **2003**, 6, 1423-1425.

* - indicating corresponding author

Symposium/Conference participation:

1. Fall Meeting of the Swiss Chemical Society, 16 September, 2010, Zurich, Switzerland, oral presentation.

2. Gordon Research Conference on Electron Donor-Acceptor interactions, 8 - 13 August, 2010, Newport, USA, poster presentation.

3. Fall Meeting of the Swiss Chemical Society, 4 September, 2009, Lausanne, Switzerland, poster presentation.

4. XVIII EuCheMS Conference on Organometallic Chemistry, 22 - 25 June, 2009, Göteborg, Sweden, poster presentation.

5. XVII EuCheMS Conference on Organometallic Chemistry, 1 – 6 September, 2007, Sofia, Bulgaria, poster presentation.

6. 6^{th} International conference on f-elements, 4 – 9 September, 2006, Wroclaw, Poland, poster presentation.

7. IV National Crystallographic conference, 25 – 30 June, 2006, Chernogolovka, Russia, poster presentation.